A SUMO-dependent step during establishment of Sister Chromatid Cohesion

Seba Almedawar

Dipòsit Legal: L.1319-2013
http://hdl.handle.net/10803/123807

Doctoral thesis:

A SUMO-dependent step during establishment of Sister Chromatid Cohesion

Seba Almedawar
IRBlleida, Udl
25.07.2013

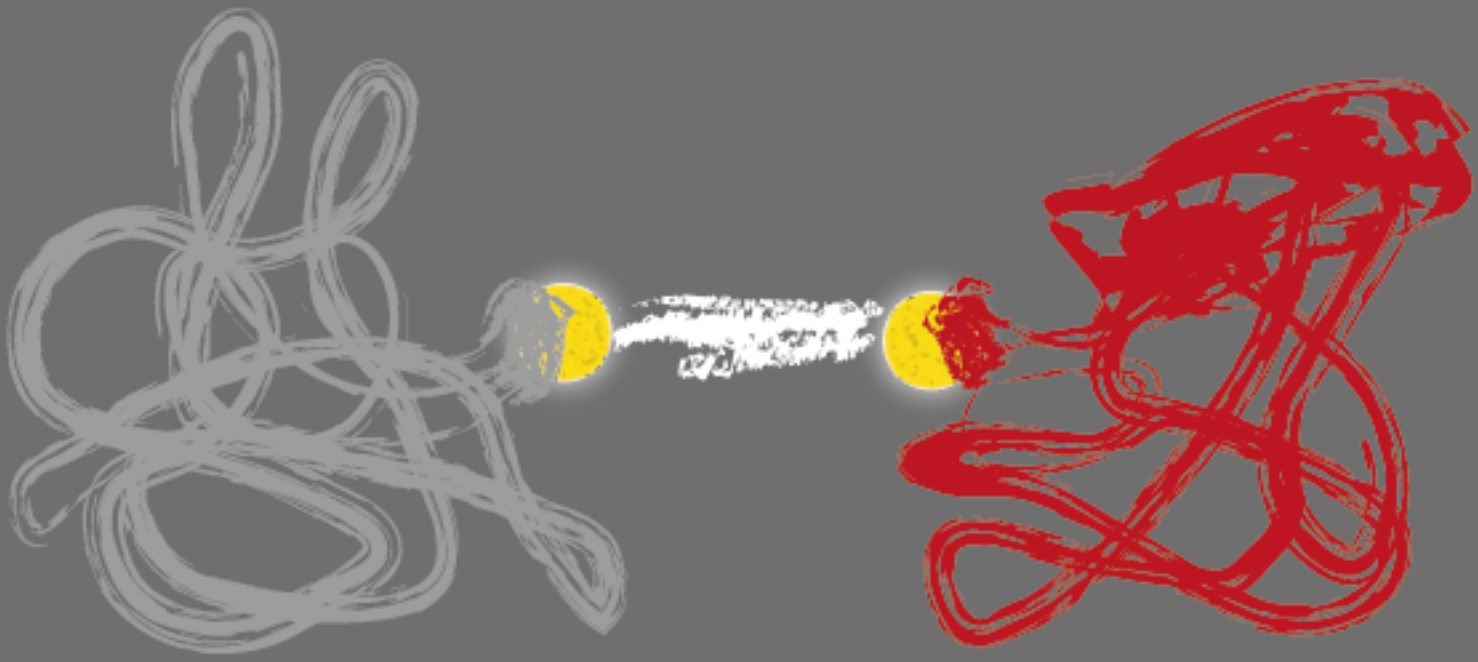

A SUMO-dependent step during establishment of Sister Chromatid Cohesion

Seba Almedawar

PhD Thesis, UdL

Lleida 2013

PhD thesis supervised by Jordi Torres Rosell and presented by Seba Almedawar to obtain the doctor title from the University of Lleida (UdL)

"No body said it was easy, no one ever said it would be so hard…I am going back to the start"

The Scientist

Coldplay

Acknowledgments

I would like to thank all current members of the CYC group including Jordi Torres, Neus Colomina, Irene Pociño, Marta Rafel, Sonia Rius, Eloi Gari, and Paco Ferrezuelo; and previous members of the CYC group especially Marti Aldea and Carme Gallego for their support and friendship.

I would also like to thank our collaborators in MRC (London) and in CNRS (Montpellier).

No words can explain my gratitude towards my family in Lebanon, to whom I dedicate this work.

Finally and most importantly, I would like to thank my husband Amarante for believing in me and for his support in good and bad times.

List of Tables

List of Supplementary Tables

List of Figures

All the experimental results in this thesis have been obtained in the cell cycle lab except:

Figure 35,36 was done in CNRS (Montpellier) by Seba Almedawar, Mireille Tittle-Elmer and Armelle Lengronne

Figure 37 was done in MRC (London) by Alexandra McAleenan and Luis Aragon.

Introduction

Materials and Methods

Results

Discussion

Abbreviations

ABC: ATP Binding Cassette

APC: Anaphase Promoting Complex

ATP: Adenosine Tri-phosphate

CDK: Cyclin Dependent Kinase

CoIP: Coimmunoprecipitation

DDR: DNA Damage Repair

DI: Damage induced

DSB: Double Strand Break

DNA: Deoxyribonucleic acid

HR: Homologous Recombination

HU: Hydroxyurea

I.P: Immunoprecipitation

IR: Ionizing Irradiation

MMS: methyl methanesulfonate

NBD: Nucleotide Binding Domain

NHEJ: Non Homologous End Joining

P.D: Pull-Down

SCC: Sister Chromatid Cohesion

SCR: Sister Chromatid Recombination

SENP: Sentrin specific Protease

SIM/SBM: SUMO Interacting Motif/ SUMO Binding Motif

SMC: Structural Maintenance of Chromosomes

ssDNA: Single stranded DNA

STUbL: SUMO-Targeted Ubiquitin Ligase

SUMO: Small Ubiquitin Like Modifiers

UD: Ulp Domain

ULP: Ubiquitin like protein protease

UV: Ultra Violet

Index

"...and the strangest thing was waiting for that bell to ring, it was the strangest start..."

The hardest part, Coldplay

Summary

I. Summary

Cohesin rings composed of the Smc1, Smc3, Scc1 and Scc3 proteins topologically bind to DNA, keeping pairs of sister chromatids together from the time of DNA replication until the onset of anaphase. This feature, known as Sister Chromatid Cohesion (SCC), allows the biorientation of chromosomes on the mitotic spindle, and their subsequent segregation. Sister Chromatid Cohesion also has other roles, such as enabling repair of DNA damage through homologous recombination. Thus, it is not surprising that cohesin is subjected to multiple levels of control during the cell cycle by different regulatory factors and post-translational modifications. For example, acetylation of the Smc3 subunit is required to prevent the opening of cohesin rings, keeping them stably bound to chromatin. Alterations in the cohesin molecule itself and/or its regulation may lead to the development of serious pathologies and can contribute to tumor progression.

In this study, we describe the sumoylation of cohesin as a new post-translational modification required for Sister Chromatid Cohesion in *Saccharomyces cerevisiae*. Sumoylation of cohesin is partially dependent on the Nse2 SUMO ligase and the Smc5/6 complex. All subunits of the cohesin complex are sumoylated *in vivo* during DNA replication, after the formation of cohesin rings and their recruitment onto chromatin, in a process dependent on the binding of ATP to the SMC subunits, and independent of Smc3 acetylation.

In order to alter the sumoylation status of cohesin rings and to identify its functional relevance, we designed a new approach to remove SUMO from all cohesin subunits, based on the fusion of the SUMO peptidase domain of Ulp1 (UD) to the Scc1 protein. Scc1-UD fusions are properly incorporated into cohesin rings, loaded onto chromatin and located along yeast chromosomes. However, desumoylation of cohesin

rings prevents Sister Chromatid Cohesion, arresting cells in G2/M and causing the loss of cell viability. These effects are due to the activity of the SUMO peptidase domain rather than structural problems in the Scc1-UD fusion, since mutation of the catalytic site in the UD restores cohesion and cell viability. Parallel experiments suggest that sumoylation of cohesin might have similar functions in human cells.

Surprisingly, cohesin rings remain acetylated in the absence of sumoylation. Current models propose that cohesin rings are stably locked once they are acetylated. Therefore, it is likely that in the absence of sumoylation cohesin encircles a single chromatid. Consequently, we propose that sumoylation of cohesin is required during DNA replication to entrap the two sister chromatids inside its ring structure.

I.1. **Resumen**

Los anillos de cohesina, formados por las proteínas Smc1, SMC3, Scc1 y Scc3, se unen topológicamente al DNA, manteniendo las parejas de cromátidas hermanas unidas desde la duplicación del DNA hasta el comienzo de la anafase. Esta función, conocida como Cohesión entre Cromátidas Hermanas, permite la biorientación de los cromosomas en el huso mitótico y, posteriormente, su correcta segregación. Se trata por lo tanto de una función fundamental para la vida. La cohesión entre cromátidas hermanas también tiene otras funciones, como favorecer la reparación del daño en el DNA a través de recombinación homóloga. Es por estos motivos que la cohesina está sometida a varios niveles de regulación a lo largo del ciclo celular, a través de diferentes factores reguladores y modificaciones post-traduccionales. Por ejemplo, la acetilación de la subunidad Smc3 es necesaria para que los anillos se mantengan establemente unidos a cromatina. Alteraciones en la molécula de cohesina y/o en su regulación pueden provocar el desarrollo de patologías y contribuir a la progresión tumoral.

En este estudio, describimos la sumoilación de la cohesina como una nueva modificación post-traduccional necesaria para la cohesión en *Saccharomyces cerevisiae*. La sumoilación de la cohesina depende, en parte, de la SUMO ligasa Nse2 y de un complejo Smc5/6 plenamente funcional. Todas las subunidades del complejo cohesina se sumoilan *in vivo* durante la replicación del ADN, después de la formación de los anillos de cohesina y de su reclutamiento en cromatina, en un proceso dependiente de la unión de ATP a las subunidades SMC, e independiente de la acetilación de Smc3.

Con el fin de alterar el estado de sumoilación de los anillos de cohesina e identificar la relevancia funcional de esta modificación, hemos diseñado una nueva aproximación experimental que permite eliminar SUMO de todas las proteínas del complejo, basado en la fusión del dominio SUMO peptidasa de Ulp1 (UD) a la proteína Scc1. Las fusiones Scc1-UD se incorporan a los anillos de cohesina, se cargan en la

cromatina y se localizan adecuadamente sobre los cromosomas de levadura. Sin embargo, la desumoilación de los anillos de cohesina impide la cohesión entre las cromátidas hermanas, deteniendo el ciclo celular en G2/M y provocando la pérdida de viabilidad de las células. Estos efectos son debidos a la actividad del dominio SUMO peptidasa, y no a problemas estructurales en la proteína de fusión Scc1-UD, ya que la mutación puntual del centro catalítico de UD restaura la cohesión y la viabilidad celular. Experimentos en paralelo sugieren que la sumoilació de la cohesina podría tener funciones similares en células humanas.

Sorprendentemente, los anillos de cohesina continúan acetilados en ausencia de sumoilación. Dado que los modelos actuales proponen que los anillos se cierran establemente al ser acetilados, es probable que en ausencia de sumoilación la cohesina se cierre en torno a una sola cromátida. En consecuencia, proponemos que la sumoilación de la cohesina sería necesaria durante la replicación del ADN para atrapar las dos cromátidas hermanas de forma estable en el interior del anillo.

I.2. **Resum**

Els anells de cohesina, formats per les proteïnes Smc1, Smc3, Scc1 i Scc3, s'uneixen topològicament al DNA, mantenint les parelles de cromàtides germanes unides des de la duplicació del DNA fins al començament de l'anafase. Aquesta funció, coneguda com a Cohesió entre Cromàtides Germanes, permet la biorientació dels cromosomes en el fus mitòtic i, posteriorment, la seva correcta segregació. Es tracta per tant d'una funció fonamental per a la vida. La cohesió entre cromàtides germanes també té altres funcions, com ara afavorir la reparació del dany en el DNA a través de recombinació homòloga. És per aquests motius que la cohesina està sotmesa a diferents nivells de regulació al llarg del cicle cel·lular, a través de diversos factors reguladors i modificacions post-traduccionals. Per exemple, l'acetilació de la subunitat Smc3 és necessària per a que els anells es mantinguin establement units a cromatina. Alteracions en la molècula de cohesina o en la seva regulació poden provocar el desenvolupament de patologies i contribuir en la progressió tumoral.

En aquest estudi, descrivim la sumoilació de la cohesina com una nova modificació post-traduccional necessària per la cohesió en *Saccharomyces cerevisiae*. La sumoilació de la cohesina depèn, en part, de la SUMO lligasa Nse2 i d'un complex Smc5/6 plenament funcional. Totes les subunitats del complex cohesina es sumoilen *in vivo* durant la replicació del DNA, després de la formació dels anells de cohesina i del seu reclutament a cromatina, en un procés depenent de la unió d'ATP a les subunitats SMC, i independent de l'acetilació de Smc3.

Per tal d'alterar l'estat de sumoilació dels anells de cohesina i identificar la rellevància funcional d'aquesta modificació, hem dissenyat un nou sistema experimental que permet eliminar SUMO de totes les proteïnes del complex, basat en la fusió del domini SUMO peptidasa de Ulp1 (UD) a la proteïna Scc1. Les fusions Scc1-UD s'incorporen als anells de cohesina, es carreguen en la cromatina i es localitzen

adequadament sobre els cromosomes de llevat. Tanmateix, la desumoilació dels anells de cohesina bloqueja la cohesió entre les cromàtides germanes, aturant el cicle cel·lular en G2/M i provocant la pèrdua de viabilitat de les cèl·lules. Aquests efectes són deguts a l'activitat del domini SUMO peptidasa, i no a problemes estructurals en la proteïna de fusió Scc1-UD, ja que la mutació puntual del centre catalític de UD restaura la cohesió i la viabilitat cel·lular. Experiments en paral·lel suggereixen que la sumoilació de la cohesina podria tenir funcions similars en cèl·lules humanes.

Sorprenentment, els anells de cohesina continuen acetilats en absència de sumoilació. Donat que els models actuals proposen que els anells es tanquen de forma estable en ser acetilats, és probable que en absència de sumoilació la cohesina encercli una sola cromàtida. Per tant, proposem que la sumoilació de la cohesina seria necessària durant la replicació del DNA per atrapar les dues cromàtides germanes de forma estable en l'interior de l'anell.

"…I'd rather be a coma than a full stop…"

Coldplay

Introduction

II. Introduction

The word “Cell” comes from the latin word “Cella” which means small room (Simpson 1977). The size of living eukaryotic cells can range from 10 microns, which is the diameter of budding yeast *Saccharomyces cerevisiae* (Pelczar, Chan et al. 1993), to around 30 microns, the diameter of human keratinocytes (Sun, Green 1976), and up to 1300 microns, the diameter of *Xenopus laevis* frog oocytes (Dumont 1972). Scientists have always been amazed by the ability of such small compartments to enclose large molecular structures such as chromosomes (up to 2 meters if extended), which contain the genetic material that has to be duplicated during DNA replication, and then divided with high fidelity to daughter cells (Bak, Zeuthen et al. 1977). Chromosomes undergo abrupt transformations, that range from the “ball of string” appearance to the amazing emergence of defined duplicated chromosomes (sister chromatids), held together by some sort of a glue (sister chromatid cohesion), in the middle of the cell. This state is changed by the sudden loss of this glue, which leads to the proper segregation of chromosomes towards the opposite poles of the cell. The fidelity of chromosomes segregation is essential to transfer the genetic material to the daughter cells and to ensure the continuity of the organism. Any defects in this process are deleterious and can lead to diseases such as cancer and/or death. The glue that holds sister chromatids from the time of DNA replication until the time when sister chromatids separate is now known as cohesin (Michaelis, Ciosk et al. 1997, Guacci, Koshland et al. 1997). This protein belongs to a recently discovered family of chromosomal enzyme complexes called structural maintenance of chromosomes (SMC), which also include condensin (Hirano, Kobayashi et al. 1997), and Smc5/6 complex (Lehmann 2005). These complexes are remarkably involved in almost all aspects of chromosomal transformations, and are regulated by the cell cycle so that such transformations are finely tuned with the rest of events leading to nuclear and cell division.

II.1. **The cell cycle**

Nucleated cells destined to grow and reproduce, have to go through a cyclic process that includes growth, DNA duplication, nuclear division (mitosis) and cellular division (cytokinesis). During interphase cells take their time to grow (G1 and G2), replicate their DNA (S phase), repair DNA damage, and make sure that cells are ready to divide in the proceeding stage (M phase). M phase is composed of two major events mitosis and cytokinesis. During mitosis sister chromatids are attached to microtubules coming from opposite poles of the spindle, and are aligned in the middle of the cell forming the metaphase plate. Once all sister chromatids are correctly bi-oriented, sister chromatid cohesion is destroyed resulting in their separation and retraction towards the opposite ends of the cell during anaphase. Mitosis ends with nuclear cleavage (telophase), and is followed by cytokinesis, which results in two daughter cells each with identical chromosome number to that of the original cell.

To ensure the correct order of events, the cell contains a complex regulatory network called the cell cycle control system. Cyclin dependent kinases (Cdks) are the central components of this system, which catalyze the covalent attachment of phosphate groups derived from ATP to protein substrates. Cdks are activated by binding to different cyclins, which trigger different cell cycle events. The different cyclin/Cdk complexes can be classified into G1/Cdk, G1-S/Cdk, S/Cdk, and M/Cdk. Each cyclin/Cdk complex promotes the activation of the next in sequence, thus ensuring that the cycle progresses in an orderly manner. The cell cycle control system drives progression through the cell cycle at regulatory transitions called checkpoints. The first is called Start or G1/S checkpoint. When conditions are ideal for cell proliferation, the levels of G1/S cyclin increase, which promotes the formation of G1-S/Cdk complexes. These complexes activate S/Cdk, resulting in phosphorylation of proteins that initiate DNA replication.

Eventually, G1/S and S/Cdk complexes promote the activation of M/Cdk complexes, which drive progression through the second major checkpoint at the entry into mitosis (G2/M checkpoint). M/Cdk complexes phosphorylate proteins that promote spindle assembly, bringing the cell to metaphase. Progression through the last checkpoint (Spindle assembly checkpoint) at the metaphase to anaphase transition, occurs when M/Cdk stimulate the anaphase promoting complex (APC) which causes the proteolytic destruction of cyclins to close the cell cycle. In addition, APC triggers anaphase by destruction of a protein called securin. If the conditions are not appropriate for cell proliferation, cells arrest cell cycle progression at these checkpoints until they are satisfied and the conditions are favorable again to continue. Arrest at the early stages of the cell cycle occurs at the start checkpoint by inhibiting the activation of S/Cdks. Similarly, failure to complete DNA replication blocks entry into mitosis by inhibiting M/Cdk activation. The proteolytic activity of the APC is also inhibited at the metaphase to anaphase transition when there is a delay in the spindle assembly, which prevents sister chromatid segregation until the spindle is ready (Morgan 2007, Peters 2006).

II.2. **DNA Damage Response (DDR)**

Checkpoints act as surveillance mechanisms not only during unperturbed cell cycle conditions but also under DNA damage conditions where a block in cell cycle progression is required to avoid replication and segregation of damaged DNA, and to activate DNA repair mechanisms.

There are two main DNA damage checkpoint kinases, ATM and ATR (Tel1 and Mec1 in budding yeast), which are activated by the presence of a DSB (Double strand break) and single stranded DNA (ssDNA) respectively. These kinases initiate signaling pathways that inhibit cell cycle progression and stimulate the expression of large numbers of proteins involved in DNA repair and other kinases such as Chk1 (Jazayeri, Falck et al. 2006).

Exposure to ionizing irradiation (IR) leads to the most deleterious type of DNA damage, namely DSB formation. DSB can be repaired by either homologous recombination (HR) during stages of the cell cycle, when the sister chromatid is available, and the CDK activity is high (between S phase and mitosis); or by non-homologous end joining (NHEJ), when CDK activity is low, and the sister chromatid is still not available for recombinational repair, mainly during G1 (Ira, Pellicioli et al. 2004).

When CDK activity is high, the MRX complex (Mre11/Rad50/Xrs2) is recruited to DSBs, which facilitates recruitment of the DNA damage checkpoint kinase ATM and promotes resection leading to ssDNA overhangs. ATM phosphorylates downstream targets, such as H2A histone, which promotes recruitment of more proteins involved in the damage repair pathway. Next, replication protein A (RPA) coating of ssDNA activates the kinase ATR. As a result, RPA is replaced by Rad51 with the help of Rad52 leading to the formation of presynaptic filaments. This initiates strand invasion of the homologous region forming a D-loop, which is extended by DNA synthesis. Double holiday junction intermediates arise when the second DSB end is captured. These intermediates have to be resolved for complete repair by the action of resolvases (nucleases that cleave and resolve the junctions) or dissolvases (a helicase-topoisomerase III pair capable to remodel the junction into a substrate for topoisomerase-mediated disentanglement). ATR and ATM also phosphorylate downstream targets that block cell cycle progression until damage is repaired (Branzei, Foiani 2005, Branzei, Foiani 2008, Wu, Hickson 2003).

If DNA damage causes DSB during DNA replication (intra-S phase damage), the replication fork stalls at the site of the lesion, and thus, these checkpoint kinases are additionally required to phosphorylate down stream targets that inhibit origin of replication firing and stabilize the replication fork, which prevents fork collapse and allows fork restart. Damage repair and fork restart depend on template switch (TS) with

the sister chromatid in an error free manner similar to homologous recombination (Branzei, Foiani 2005).

Replication forks can also stall due to natural replication fork barriers or slow replication zones, a phenomenon known as replicative stress. Replicative stress can be also provoked externally by adding hydroxyurea (HU), which inhibits ribonucleotide reductase (RNR), and thus, depletes the dNTP pool (Slater 1973). In this case ATR checkpoint kinase is activated due to exposure to RPA coated ssDNA, which phosphorylates downstream targets leading to cell cycle arrest, inhibition of origin firing, and stabilization of the replication fork until the stress is relieved, and conditions are available for fork restart (Branzei, Foiani 2005).

Alkylating agents, such as methyl methanesulfonate (MMS), methylate certain reactive sites on some bases such as guanine, which might mispair with thymine during DNA synthesis. Repair of such damage requires base excision repair (BER) to remove the damaged base; the undamaged complementary strand is used as template to restore the sequence (Wyatt, Pittman 2006). Other sources of DNA damage include exposure to UV (ultraviolet) light, which causes the covalent crosslinking of adjacent pyrimidine bases producing dimers. These pyrimidine dimers block DNA replication because the replication machinery cannot tell which bases to insert opposite the dimer. Repair of such damage is done by the nucleotide excision repair (NER) pathway, which removes a short stretch of the damaged strand; the undamaged strand is then used as a template to restore the sequence (Lehoczky, McHugh et al. 2007). While strong UV damage induces accumulation of ssDNA and ATR activation, methylated bases do not normally activate the DNA damage checkpoint kinases, as long as the replication fork does not encounter these modified bases, or any of the repair intermediates (Wyatt, Pittman 2006).

II.3. **SMC complexes**

SMC complexes are highly conserved proteins from bacteria to humans, highlighting their importance in chromosome organization and dynamics (Cobbe, Heck 2004). In eukaryotes there are three SMC complexes: cohesin, condensin, and Smc5/6 (Figure 1, Table 1). At the heart of each complex there are two Smc subunits that heterodimerize to form a V shaped molecule, which associates with other regulatory non-smc subunits to shape the whole complex. Each Smc subunit is formed of self-folded anti-parallel coiled-coil, that at one end has an heterodimerization domain commonly referred to as the hinge domain (Figure 1A) (Melby, Ciampaglio et al. 1998). At the other end, each Smc subunit possesses an ATP binding cassette-like (ABC) head domain. ATP binding brings the two heads from each subunit together, while its hydrolysis drives them apart, a feature that has been proposed to allow SMC complexes to dynamically associate with chromosomes (Hirano, Hirano 2004). The core subunits of cohesin are Smc1 and Smc3 (Figure 1C, Table 1), which associate with the Scc1/Mcd1/Rad21 kleisin protein (Sonoda, Matsusaka et al. 2001), and to heat repeat-containing Scc3/SA (Losada, Yokochi et al. 2000, Toth, Ciosk et al. 1999, Kueng, Hegemann et al. 2006) to form the whole complex. Other less stabely associated, but equally important, subunits include Pds5 (Hartman, Stead et al. 2000, Losada, Yokochi et al. 2005, Panizza, Tanaka et al. 2000, Toth, Ciosk et al. 1999), and Rad61/ Wapl (Kueng, Hegemann et al. 2006, Sutani, Kawaguchi et al. 2009).

In humans there are two condensin complexes, I and II, while in *S. cerevisiae* there is only one condensin complex homologous to condensin I. The core subunits of condensin are Smc2 and Smc4 (Figure 1D), which associate in *S. cerevisiae* with Brn1 (kleisin), Ycs4 and Ycg1 (Ono, Losada et al. 2003, Freeman, Aragon-Alcaide et al. 2000).

Smc5 and Smc6 associate with 6 non-SMC elements (Nse1-6), including a kleisin subunit (Nse4), an heterodimeric ubiquitin ligase (Nse1-Nse3) and a SUMO ligase (Nse2), to form the more recently described Smc5/6 complex (Figure 1B) (Zhao, Blobel 2005, Lehmann 2005, Pebernard, Wohlschlegel et al. 2006, Pebernard, McDonald et al. 2004, Stephan, Kliszczak et al. 2011).

Although SMC complexes share sequence and structure similarities, probably because they derive from a common ancestor (Cobbe, Heck 2004), each complex differs in the way it interacts with DNA and the modifications that it brings upon (Nasmyth, Haering 2005). Cohesin's main function is to hold sister chromatids during DNA replication until the onset of anaphase, which is important for proper chromosome bi-orientation and segregation (Nasmyth, Haering 2009), while that of condensin is to condense and resolve chromosomes which prevents them from getting tangled up during segregation (Renshaw, Ward et al. 2010). Unlike cohesin and condensin, little is known about the Smc5/6 complex. Clearly however, it is essential for DNA damage repair, and sister chromatid resolution during anaphase (Bermudez-Lopez, Ceschia et al. 2010). However different, the collective role of these complexes is to ensure proper replication of chromosomes, maintenance, and their equal segregation to the new daughter cells (Nasmyth, Haering 2005).

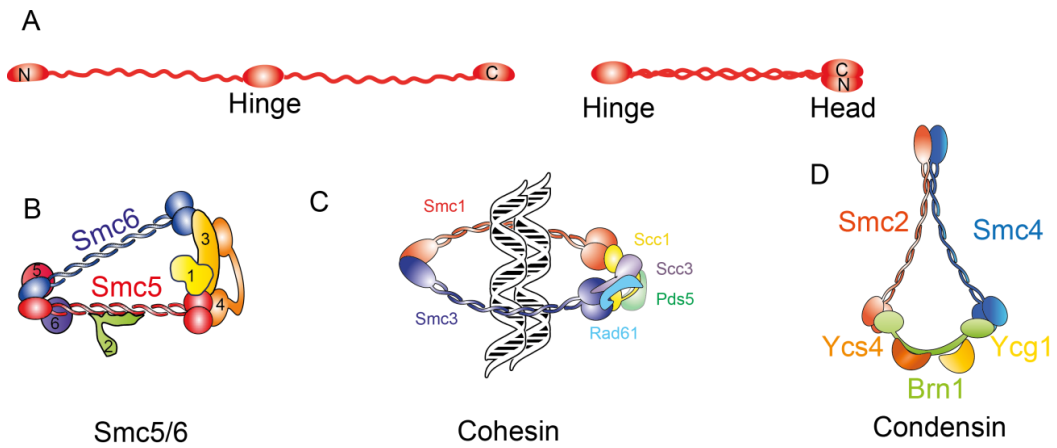

Figure 1. SMC Complexes in *S. cerevisiae*. (A) Each SMC complex is formed of self-folded anti-parallel coild-coils that contain at one end the ATP-binding cassette (head domain) and a dimerization domain at the other end (hinge domain). (B) Smc5/6 complex. Nse1-6 subunits, labeled 1 to 6, are shown complexed with Smc5 and Smc6 (Zhao, Blobel 2005, Lehmann 2005, Pebernard, Wohlschlegel et al. 2006, Pebernard, McDonald et al. 2004, Stephan, Kliszczak et al. 2011). (C) The core subunits of cohesin are Smc1 and Smc3, which associate with Scc1 kleisin protein, to heat repeat-containing Scc3, and to other less stabely associated proteins, which include Pds5, Rad61 (Haering, Lowe et al. 2002, Kulemzina, Schumacher et al. 2012, Chatterjee, Zakian et al. 2013). The complex has been proposed to embrace replicated sister chromatids. (D) The condensin complex is formed of Smc2 and Smc4, which associate with Brn1 (kleisin), Ycs4 and Ycg1 (Piazza, Haering et al. 2013). The illustration depicts the open ring structure of cohesin as opposed to the more closed lollipop structure of condensin as observed in (Anderson, Losada et al. 2002).

II.4. **Cohesin:**

II.4.1. **Structure and composition in *S. cerevisiae***

Detailed studies of cohesin ring structure have shown that Smc1 binds stably, through its NBD, to the C- terminal of an essential α-kleisin protein called Scc1/Mcd1. This interaction is a prerequisite for the binding of its N-terminal domain to the NBD of Smc3, and thus, for tripartite ring formation.

This sequential interaction with Smc1 first, and then Smc3, ensures that only one Scc1 molecule can interact with each Smc1/3 heterodimer (Haering, Lowe et al. 2002, Haering, Schoffnegger et al. 2004). Moreover, it alters the structure of the NBD in favorable position for ATP binding and hydrolysis, which has been shown to be sandwiched between the two NBDs of Smc1 and Smc3 (Arumugam, Nishino et al. 2006).

Scc3 is another non-SMC subunit that associates stably with the C-terminal part of Scc1, while Pds5 is a heat-repeat containing subunit that binds to Scc3, and associates less stably with the N-terminal part of Scc1 in an Scc3 independent manner (Kulemzina, Schumacher et al. 2012). Scc3 and Pds5 are both essential and they were first identified as genes that, when mutated, result in sister chromatid cohesion (SCC) defects (Toth, Ciosk et al. 1999, Hartman, Stead et al. 2000).

Table 1. Components of the cohesin complex in *S. cerevisiae* and Humans.

	S. cerevisiae	Humans
SMC proteins	Smc1	Smc1A (Mitosis) , Smc1B (Meiosis)
	Smc3	Smc3
α-kleisin	Scc1/Mcd1 (Mitosis), Rec8 (Meiosis)	Rad21(Mitosis), Rec8 (Meiosis)
Regulatory Subunits	Scc3	SA1/SA2
	Rad61	Wapl
	Pds5	Pds5A/B
		sororin
	Sgo1(Meiosis only)	Sgo1
Loading Complex	Scc2	Nipbl
	Scc4	Mau2
Acetyl Transferase	Eco1	Esco1/2
Deacetylase	Hos1	HDAC8

Two key proteins that do not stably bind to cohesin, but are nevertheless crucial for its regulation, are the essential acetyl transferase Eco1/Ctf7, and the non-essential Rad61. Eco1/Ctf7 is responsible for Smc3 and Scc1 acetylation (Ivanov, Schleiffer et al. 2002, Heidinger-Pauli, Unal et al. 2009). Rad61 interacts stably with the N-terminal part of Pds5 and less stably with Scc3 (Chan, Roig et al. 2012, Gruber, Arumugam et al. 2006, Kulemzina, Schumacher et al. 2012). It also interacts with Smc3 ATPase domain and may modulate the ATPase activity of the cohesin complex (Chatterjee, Zakian et al. 2013).

Based on electron micrographs of the cohesin complex in humans (Figure 8A), the ring structure has been shown to have a wide angle at the hinge (around 88°) and a kink in the coiled coil region of around 102° (Anderson, Losada et al. 2002). Other micrographs of cohesin in *S. cerevisiae* have shown that the ring can adapt foldback structures where the hinge and the head domain might interact (Gruber, Arumugam et al. 2006). The 40 nm diameter of the ring shaped cohesin molecule quickly lead to the proposal that it traps DNA inside thereby providing SCC (Haering, Lowe et al. 2002,

Ivanov, Nasmyth 2005). Later on, it was shown that cohesin binds to chromatin topologically (Haering, Farcas et al. 2008). However, whether one ring traps both sister chromatids, referred to as the ring model (Figure 2A), or two rings trap sisters individually and then interact through Scc3 to establish SCC (Handcuff Model) (Figure 2B), is not really known (Nasmyth, Haering 2009).

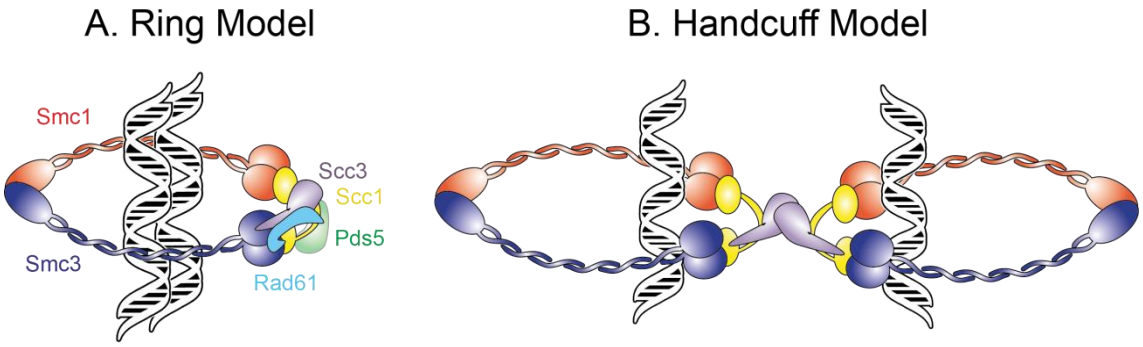

Figure 2. Cohesin models for sister chromatids coentrapment. (A) The ring Model: One ring traps both sister chromatids (Haering, Farcas et al. 2008). (B) Handcuff model: Two cohesin rings might entrap sister chromatids individually, which are then brought together through Scc3 (Zhang, Pati 2009).

II.4.2. **The cohesin ring cycle in *S. cerevisiae***

II.4.2.1. **Loading:**

According to the ring model, the cohesin ring is assembled before its loading to unreplicated DNA in late G1 (Haering, Lowe et al. 2002) (Figure 3 and Figure 4A). The loading requires ATP binding and hydrolysis, and it depends on the Scc2/Scc4 loading complex, which recruits the cohesin ring to substrate chromatin (Ciosk, Shirayama et al. 2000). It has been hypothesized that the Scc2/4 complex, Scc3, and kinetochore proteins at the centromeres facilitate interaction of ATP engaged NBDs with closed Smc1/3 hinges through fold-back structure formation. Subsequently, ATP hydrolysis drives the disengagement of NBDs, what could open the hinges allowing entry of the unreplicated chromatin fiber. Entrapment occurs when Smc1/3 hinges re-associate

through the free energy of hinge-dimerization which does not require ATP (Hu, Itoh et al. 2011). After loading, the cohesin ring relocates to places of convergent transcription, origins of replications, and pericentromeric regions. This relocation is essential to move cohesin away from the Scc2/4 loading complex, which might destabilize it by stimulating the NBD ATPase activity (Hu, Itoh et al. 2011, Lengronne, Katou et al. 2004).

Unlike the replication apparatus, the transcription machinery is too large to pass through the ring. Thus, the relocation of cohesin between converging intergenes could be attributed to transcription, which pushes cohesin while it translocates along the DNA until it meets another converging transcription machinery. The topological association between cohesin and chromatin explains the ability of cohesin to slide along chromatin and relocate (Ivanov, Nasmyth 2005).

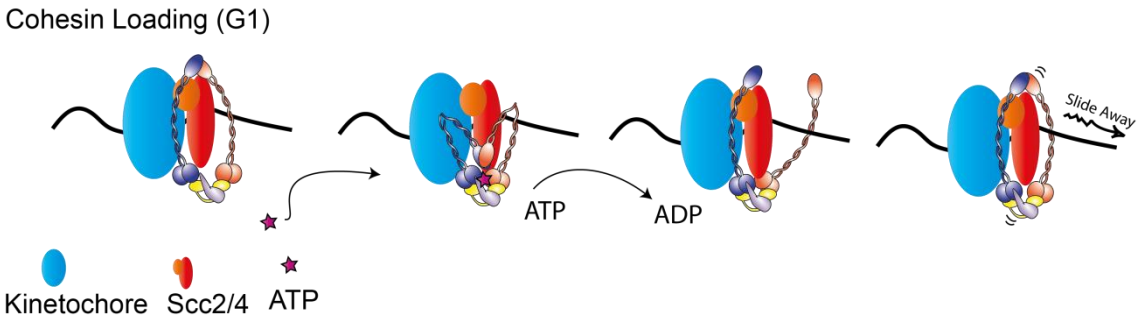

Figure 3 Cohesin loading in G1. Scc2/4 complex, Scc3, and kinetochore proteins facilitate interaction of ATP engaged NBDs with closed Smc1/3 hinges through fold-back structure formation. Subsequently, ATP hydrolysis drives the disengagement of NBDs, which opens the hinges allowing entry of the unreplicated chromatin fiber. Entrapment occurs when Smc1/3 hinges re-associates through the free energy of hinge-dimerization which does not require ATP (Hu, Itoh et al. 2011). After loading, the cohesin ring relocates to places of convergent transcription, origins of replications, and pericentromeric regions (Hu, Itoh et al. 2011, Lengronne, Katou et al. 2004).

II.4.2.2. **Establishment of sister chromatid cohesion**

It has been proposed that the binding of cohesin to unreplicated chromatin is unstable due to the antiestablishment complex (described below) (Lopez-Serra, Lengronne et al. 2013), what leads to its release through the newly described release

gate present at the Scc1-Smc3 interface (Figure 4A) (Buheitel, Stemmann 2013, Chan, Roig et al. 2012). During passage of the replication fork cohesin coentraps newly replicated sister chromatids (Figure 4B), and cohesin complexes with short residence time on chromatin are converted to ones with higher half life when two lysine residues, namely K112 and K113, within the Smc3 head domain are acetylated by EcoI (Lengronne, McIntyre et al. 2006, Rolef Ben-Shahar, Heeger et al. 2008).

Smc3 acetylation is essential for SCC, and thus, e*co1*Δ *is lethal*. Certain mutations in *SCC3*, *PDS5*, and *RAD61* reverse the lethality of *eco1*Δ, what proves the existence of an antiestablishment complex, formed by the interaction of Scc3, Pds5 and Rad61. Upon Eco1 dependent acetylation of Smc3 cohesin rings counteract the antiestablishment activity thereby becoming cohesive (tightly shut), (Figure 4C). In the absence of Smc3 acetylation, the antiestablishment complex would release cohesin through the exit gate at the Scc1-Smc3 interface leading to precocious loss of SCC (Figure 4D) (Rowland, Roig et al. 2009).

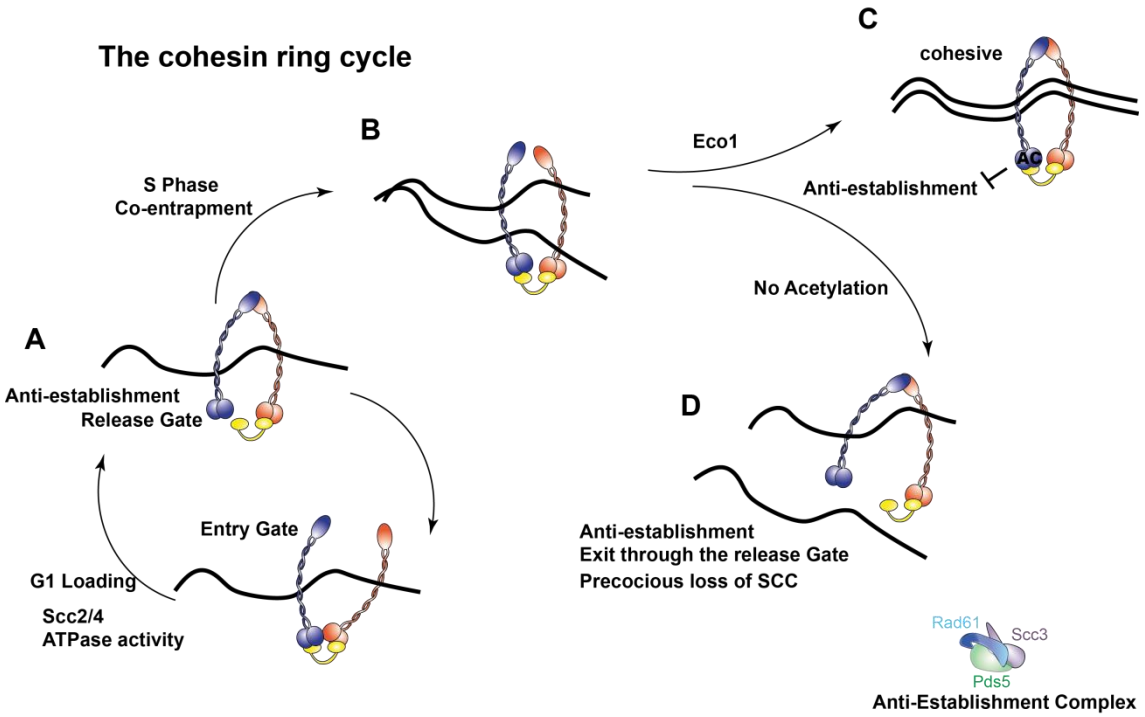

Figure 4. The cohesin ring cycle. (A) Cohesin is loaded onto chromatin during the G1 phase of the cell cycle through the entry gate located at the hinge domain. The binding of cohesin to unreplicated chromatin is unstable due to the antiestablishment complex, what leads to its release through the release gate present at the Scc1-Smc3 interface. (B) Cohesin co-entraps newly replicated sister chromatid by an unknown mechanism. (C) Cohesin ring becomes cohesive (tightly shut) upon Eco1 dependent acetylation of Smc3, which counteracts the antiestablishment activity. (D) In the absence of acetylation, the antiestablishment complex releases cohesin from sister chromatids leading to precocious loss of SCC**.**

The mechanism of sister chromatids coentrapment is not really known. However, It has been suggested that passage of the replisome forces the hinge to reopen, and once again fold to interact with the NBD of Smc3. This interaction would stimulate acetylation of Smc3 K112 and K113 by EcoI (Figure 5). After passage the hinge recloses allowing co-entrapment of the two newly replicated sister chromatids (Lengronne, McIntyre et al. 2006, Kurze, Michie et al. 2011). It is not known whether reopening and closing the ring requires a new ATP-binding/hydrolysis cycle, and if so, how is this coordinated with acetylation, taking into consideration that the acetylation sites are close to Smc3's ATP-binding pocket. Alternatively, cohesin can be loaded to already replicated sister chromatids, a model that is yet to be explored experimentally (Kurze, Michie et al. 2011).

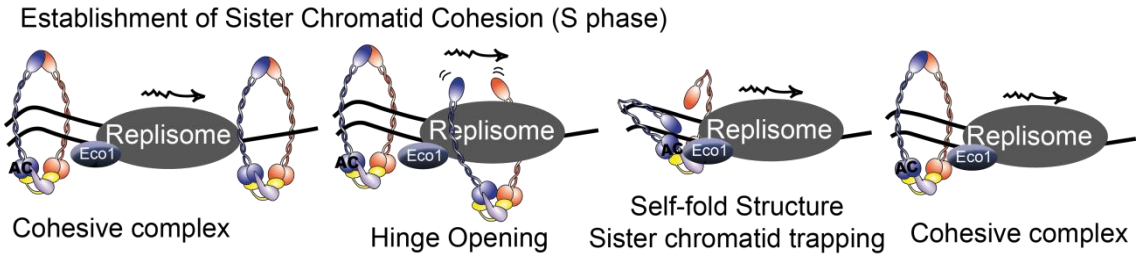

Figure 5. Cohesin coentrapment of newly replicated sister chromatids. Passage of the replisome forces the hinge to reopen, and once again fold to interact with the NBD of Smc3. This interaction stimulates acetylation of Smc3 K112 and K113 by EcoI. After passage the hinge recloses allowing co-entrapment of the two newly replicated sister chromatids (Lengronne, McIntyre et al. 2006, Kurze, Michie et al. 2011)

There are many other factors that may be important for establishment of SCC. One of these factors is Proliferating cell nuclear antigen (PCNA), which is a homotrimeric protein that acts as a sliding clamp on DNA, and recruits a variety of proteins involved in replication, recombination, or DNA damage repair (Hoege, Pfander et al. 2002). $RFC^{ctf18/Dcc1/Ctf8}$ proteins are required for PCNA association with the replication fork and contribute to SCC. PCNA, in return, binds Eco1 through its N-terminal motif thus recruiting it to the replication fork, and potentially bringing it in close proximity to cohesin (Moldovan, Pfander et al. 2006). Other factors involved in replication, such as Ctf4, Tof1, Csm3, Chl1 and Mrc1 also contribute to cohesion establishment, and facilitate cohesin acetylation (Borges, Smith et al. 2013).

II.4.2.3. **Cohesin release and chromosome segregation**

Cohesion established during S phase is maintained during G2 and until the onset of anaphase to prevent premature separation of sister chromatids due to the pulling forces of microtubules on kinetochores. The tension created between sister chromatids by cohesin and the pulling forces of the microtubules enable chromosome biorientation. This tension will eventually be removed by cleavage and opening of cohesin rings at anaphase onset. Cleavage of cohesin rings is promoted by activation of the APC/Cd20 ubiquitin ligase once all chromosomes are properly bioriented, a process that is supervised by the spindle checkpoint.

Cohesin rings are cleaved by a protease known as separase, which recognizes a specific sequence on the Scc1 subunit (Ciosk, Zachariae et al. 1998). Prior to anaphase, separase (Esp1), is inhibited by the chaperone securin (Pds1). However, at the onset of anaphase, and once APC/Cdc20 is activated, securin is targeted for degradation by the ubiquitin system leading to separase release and activation (Morgan 2007, Peters 2006). In addition, Scc1 is phosphorylated by the Polo Kinase Plk, which is required for efficient cleavage by separase (Alexandru, Uhlmann et al. 2001) (Figure 6A).

Cleavage of the Scc1 subunit triggers Smc3 deacetylation by Hos1 (Figure 6B). Importantly, Smc3 molecules that fail to be deacetylated in *hos1*Δ background are not able to establish SCC during the next cell cycle, which means that *de novo* acetylation of Smc3 during S phase is required for establishment of SCC (Beckouet, Hu et al. 2010).

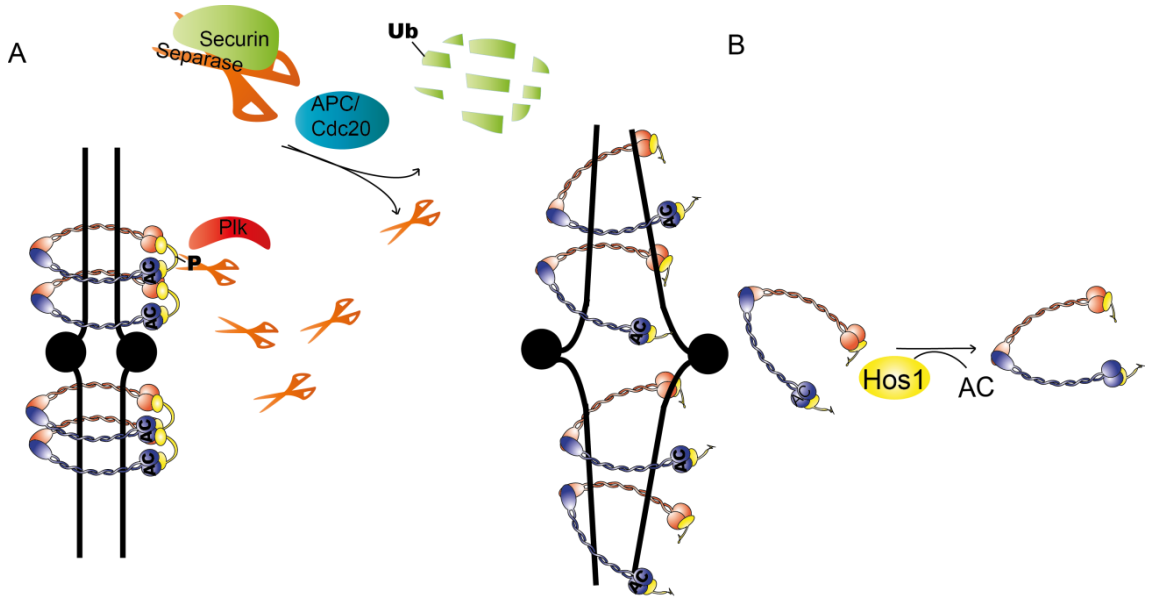

Figure 6. Cohesin release in *S. cerevisiae*. (A) At the onset of anaphase, APC/Cdc20 targets securin to degradation by the ubiquitin system leading to separase release and activation. Scc1 phosphorylation by Plk is required for efficient cleavage by separase. (B) After cleavage, Hos1 deacetylates Smc3 so that it can be reused in the next cell cycle.

II.4.3. **Beyond cohesin: resolution and segregation of chromosomes**

Apart from cohesin release, topoisomerase II contributes to SC resolution by removing most of the tangles between SC that form during DNA replication (catenation) in a process termed “decatenation”. Topoisomerase II decatenates DNA strands that cross one another by creating a DSB in one strand, passing the unbroken strand through this break, and finally resealing it.

The action of topoisomerase II is coordinated and occurs in parallel with chromosome condensation, carried out mainly by condensin through axial chromosome

compaction (Carter, Sjogren 2012, Nitiss 2009). *In vitro* studies suggest that condensin induces positive supercoiling in the mitotic chromosome, thereby exposing intermolecular catenanes to Top2 action (Baxter, Sen et al. 2011). An earlier study showed that chromosome recoiling by condensin induces removal of residual cohesin during anaphase by reinforcing the physical separation of sister chromatids (Renshaw, Ward et al. 2010).

II.4.4. **Damage induced cohesion**

Cohesin rings loaded onto chromatin outside S phase are not acetylated. Therefore, they are not cohesive, and are thus discharged by the action of the antiestablishment complex (Chan, Roig et al. 2012). However, the presence of DSBs during G2/M causes *de novo* cohesin loading and establishment both at the break site and genome wide on normal cohesin binding sites, a phenomenon known as damage induced (DI) cohesion (Figure 7). DI cohesion maintains the physical proximity of the sister chromatids, and thus, favors repair by sister chromatid recombination (SCR) over other types of repair (Unal, Arbel-Eden et al. 2004, Unal, Heidinger-Pauli et al. 2007, Strom, Karlsson et al. 2007).

Mec1 and Tel1 dependent phosphorylation of histone H2A is required for cohesin binding, which is enabled by Mre11 protein and Scc2/4 loading complex (Unal, Arbel-Eden et al. 2004). In striking contraposition to the pivotal role played by Smc3 acetylation, it has been suggested that the main acetylation target for establishment during DNA repair is Scc1. The Chk1 kinase would phosphorylate Scc1 on S83 to allow Eco1-mediated acetylation of Scc1 at residues K84 and K210 for establishment of DI cohesion (Heidinger-Pauli, Unal et al. 2009, McAleenan, Cordon-Preciado et al. 2012). Although mutation of K84 and K210 certainly supports this hypothesis, it has not been possible to demonstrate their *in vivo* acetylation yet. While cohesin would be maintained at proximal regions to ensure recombinational repair with sister chromatid, it has been

recently shown that separase would mediate dissociation of cohesin at the break site to allow the access of the resection machinery (McAleenan, Clemente-Blanco et al. 2013).

Cohesin is also required for proper repair of stalled forks and for fork restart. Replication fork may stall due to natural replication barriers or to external agents such as replication inhibitors or base modification. It has been shown that cohesin is enriched at early replication origins after HU treatment in a Rad50 dependent manner, what would promote recovery by maintaining a conformation that favors recombination dependent fork restart (Tittel-Elmer, Lengronne et al. 2012).

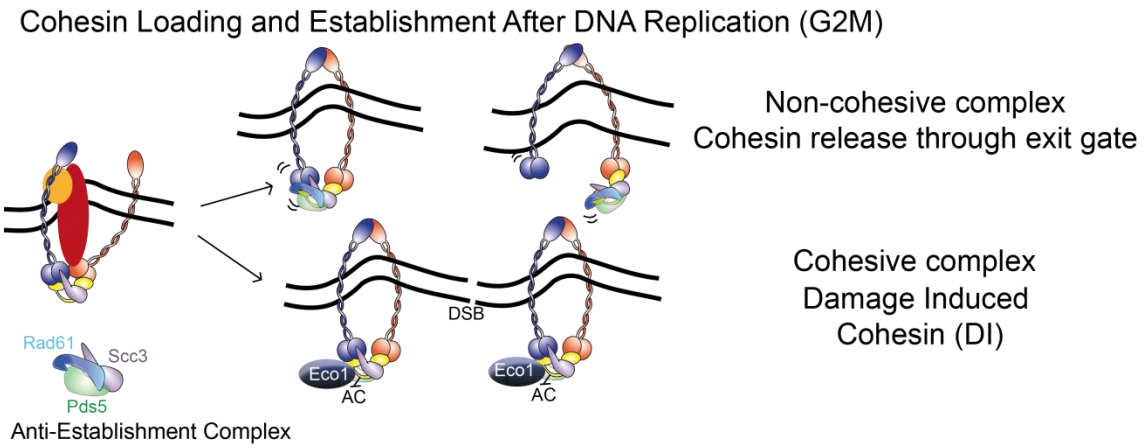

Figure 7. Damage induced cohesion. Cohesin rings loaded to chromatin outside S phase do not get acetylated and thus do not establish SCC under physiological conditions due to their release by the action of the antiestablishment complex through opening of the Smc3/Scc1 interface (Chan, Roig et al. 2012). However, the presence of DNA DSBs during G2/M causes de novo cohesin loading and establishment not only at domains flanking the break site, but also across the whole genome, a phenomenon known as damage induced (DI) cohesion. Phosphorylation of residue S83 of Scc1 by the Chk1 kinase activates Eco1-mediated acetylation of Scc1 at residues K84 and K210, which is required for establishment of SCC (Heidinger-Pauli, Unal et al. 2009, McAleenan, Cordon-Preciado et al. 2012).

II.4.5. **Other roles of cohesin in budding yeast**

Cohesin is responsible for mono-orientation of sister kinetochores during meiosis I and bi-orientation of dyad chromosomes during meiosis II. These functions are achieved by replacing Scc1/Rad21 with a meiosis-specific version (Rec8), which is also

responsible for meiotic DSB repair using non-sister chromatids (Bannister, Reinholdt et al. 2004, Goldstein 1981). Cohesin is important for some aspects of transcription regulation too, such as restricting the spread of silencing at the silent mating-type loci (Gullerova, Proudfoot 2008, Donze, Adams et al. 1999). Finally, cohesin is required for chromosome condensation, since *mcd1-ts* and *eco1-ts* mutants display defects in chromosome condensation (Guacci, Koshland et al. 1997, Skibbens, Corson et al. 1999). Smc3 acetyl-mimicking mutant *smc3R113Q* and *rad61*Δ partially restore condensation defects seen in *eco1-ts* mutants, pointing out the importance of cohesin regulation by Eco1 and Rad61 in chromosome condensation and segregation (Lopez-Serra, Lengronne et al. 2013, Guacci, Koshland 2011).

II.4.6. **Cohesin in Humans: Structure and regulation**

The basic composition and structure of the cohesin complex is be conserved in evolution. Smc1, Smc3, and Rad21 constitute the core structure of the ring in human cells (Figure 8B and Table 1)(McKay, Troelstra et al. 1996, Schmiesing, Ball et al. 1998). On the other hand, there are two human homologues of budding yeast Scc3: SA1, which mediates telomere cohesion, and SA2, which is responsible for centromere cohesion, and both are required for arm cohesion. Importantly, SA1 and SA2 do not coexist in the same cohesin complex (Losada, Yokochi et al. 2000, Canudas, Smith 2009). Two Pds5 proteins with overlapping functions have been identified in humans, namely Pds5A and Pds5B (Losada, Yokochi et al. 2005). Other regulatory proteins of the cohesin complex include Esco1 and Esco2 (homologues of Eco1), which are both required for Smc3 acetylation. Wapl (homologue of Rad61) is another regulatory protein, which interacts with Pds5 and SA through its FGF motives (Shintomi, Hirano 2010). Finally, sister chromatid cohesion in humans requires the participation of sororin, a cohesin factor that apparently does not have a counterpart in yeast (Whelan, Kreidl et al. 2012).

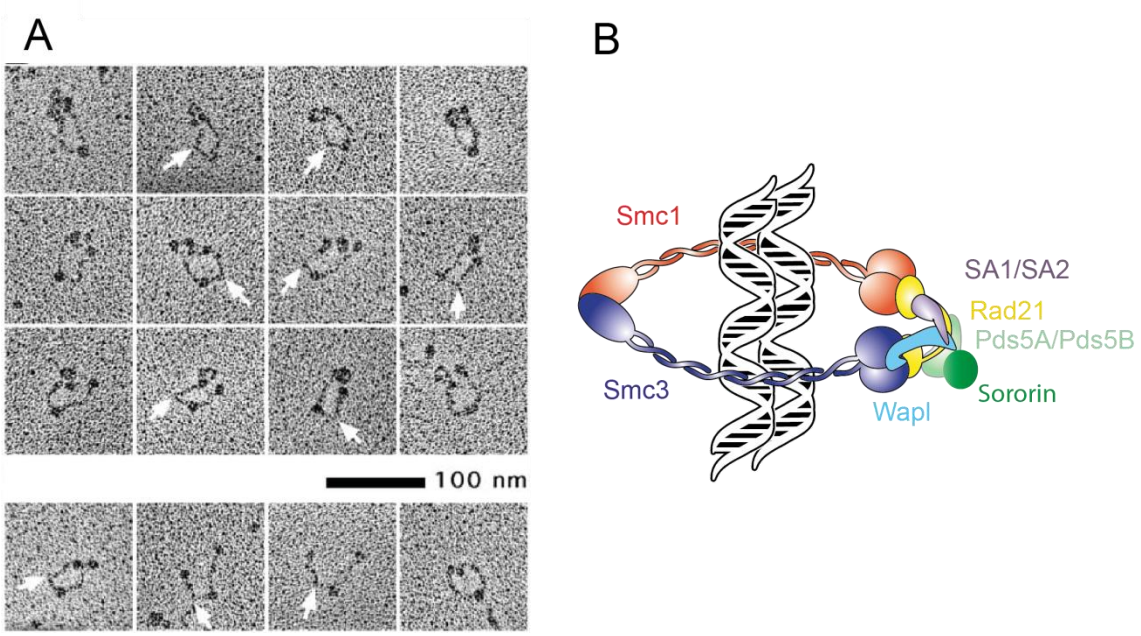

Figure 8. Structure of the cohesin ring in humans. (A) Different conformations of the cohesin ring shown by electron micrographs. Arrows point at the kink seen in this complex (Anderson, Losada et al. 2002). (B) The structure of cohesin in humans is very similar to that in *S. cerevisiae* with few differences. Mainly, Scc3 in *S. cerevisiae* has two homologs in humans SA1and SA2 which do not coexist in the same cohesin complex. Pds5 has also two homologues in humans, Pds5A and Pds5B. Homologues of regulatory proteins have also been identified, which include; Esco1 and Esco2 (homologs of Eco1), and Wapl (homolog of Rad61). Sororin is the only subunit identified in humans that, so far, has no known homolog in *S. cerevisiae*.

Although cohesin has a fundamental role in mitotic and meiotic cycles, it is also expressed in non-cycling cells, suggesting it may have other roles beyond SCC. Other evidence suggests important functions in gene regulation through global organization of chromatin architecture. For example, cohesin is a key regulator of long-range enhancer-promoter interactions by formation of chromatin loops (Figure 9) (Hadjur, Williams et al. 2009). Besides, it may facilitate the V(D)J recombination of immunoglobulin genes (Degner, Wong et al. 2009).

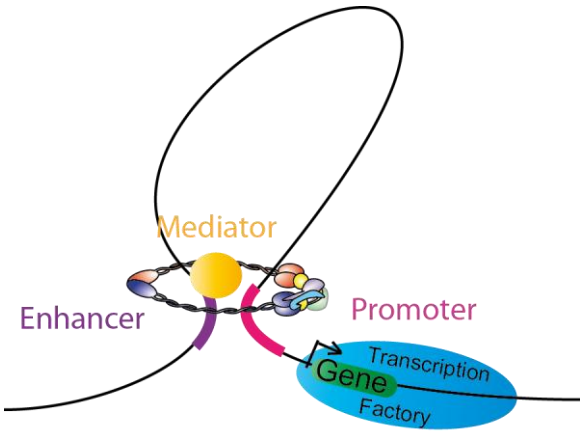

Figure 9. Cohesin as a key regulator of long range enhancer-promoter interactions. cohesin stabilizes enhancer-promoter interactions by creating chromatin loops (Hadjur, Williams et al. 2009)

Loading of cohesin depends on Nipbl/Mau2 loading complex (homologue of Scc2/4) (Watrin, Schleiffer et al. 2006, Krantz, McCallum et al. 2004). Smc3 acetylation is not sufficient for SCC, which also requires recruitment of sororin to counteract the antiestablishment activity of Wapl (Figure 10A). Sororin contains an FGF motif that allows its interaction with Pds5, thus competing with Wapl (Remeseiro, Losada 2012, Nishiyama, Ladurner et al. 2010).

Differently to budding yeast, cohesin release takes place in two steps in mammalian cells. During the first step, called the “prophase pathway”, SA2 and sororin are phosphorylated by Plk1 and Cdk1 respectively, what disrupts the Pds5-Soronin interaction and favors that of Wapl, leading to cohesin removal from chromosome arms (Shintomi, Hirano 2010) (Figure 10B). At this stage, the centromeric cohesion is still required for bipolar attachment, and is protected from mitotic kinases by Sgo1-PP2A complex (Liu, Rankin et al. 2012). Cohesin release during the prophase pathway involves opening of the Smc3-Scc1 gate (Buheitel, Stemmann 2013). Once the chromosomes are bi-oriented and the spindle assembly checkpoint is satisfied, separase cleaves Rad21, thereby removing the remnant centromeric cohesin and triggering chromosome segregation (Figure 10C). In human cells, separase is additionally inhibited by Cdk1 cyclin B dependent phosphorylation. Therefore, activation of separase does not

only depend on securin destruction by the APC/Cdc20, but also on cyclin B destruction and concomitant Cdk1 inactivation (Huang, Hatcher et al. 2005). Finally, Smc3 is deacetylated by HDAC8 after Rad21 cleavage, allowing its reuse in the next cell cycle (Deardorff, Bando et al. 2012).

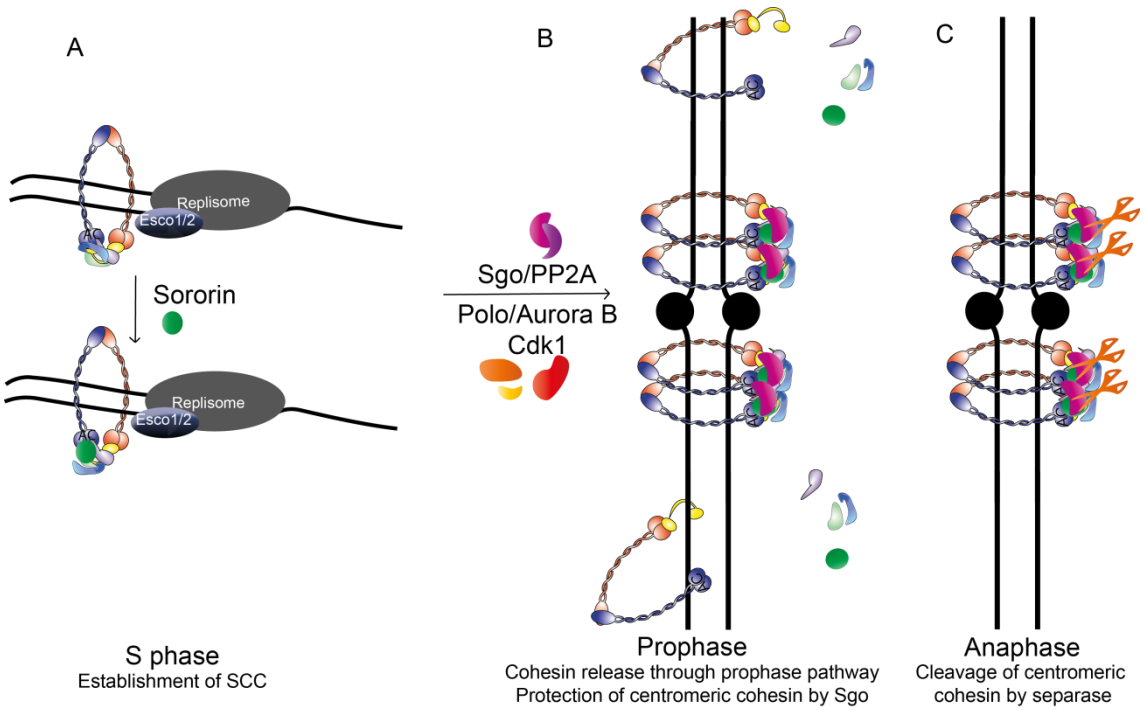

Figure 10. Establishment of sister chromatid cohesion in humans, and the two step release of cohesin. (A) Establishment of SCC in humans requires binding of sororin to stabilize cohesin. (B) The prophase pathway. The antiestablishment activity of Wapl destabilizes the ring causing its release by opening of the Smc3-Scc1 gate. SA2 and sororin are phosphorylated by Polo/Aurora B and Cdk1 respectively, what disrupts the Pds5-Soronin interaction; this leads to cohesin removal from chromosome arms. Centromeric cohesion is protected by Sgo1-PP2A complex from mitotic kinases and Wapl(Liu, Rankin et al. 2012)(Liu, Rankin et al. 2012)(Liu, Rankin et al. 2012)(Liu, Rankin et al. 2012)(Liu, Rankin et al. 2012)(Liu, Rankin et al. 2012)(Liu, Rankin et al. 2012). (C) In anaphase, Rad21 is cleaved by separase which removes centromeric cohesin for proper segregation.

II.4.7. **Involvement in disease: cohesinopathies and cancer**

Mutations in cohesin subunits, or its regulators are responsible for two main developmental syndromes in humans collectively referred to as cohesinopathies (Figure 11).

Cornelia de Lange Syndrome (CdLS) is the most common cohesinopathy (1:10,000). 65% of CdLS cases are caused by dominantly inherited mutations in the *NIPBL* gene, which causes the more severe phenotype. These mutations, which include heterozygous truncations or non-sense mutations, seem to be haplo-insufficient with 15-30% decrease sufficient to give rise to CdLS phenotype. Some mutations interfere with NipbI interaction with Mau2, or other proteins. More importantly, there are no obvious chromosome segregation deficiencies, indicating that developmental defects in CdLS might be attributed to cohesin functions in gene regulation. CdLS patients are normally small in size and have arched eyebrows, thin upper lip, long eyelashes, hirsutism, an upturned nose, synophrysptosis, a long philtrum, and micrognathia (Figure 11B). Additional severe developmental anomalies include upper limb truncations or limb differences (Jackson et al., 1993). Neurodevelopmental delay and highly variable mental retardation are also observed in all CDLS patients. A milder phenotype is caused by heterozygous missense mutations in *SMC1* and *SMC3* which account for about 5% of CdLS cases. An even milder phenotype is seen with *RAD21* heterozygous deletions and missense mutations. However, lymphoblastoid cell lines from patients with *RAD21* mutations exhibit radiation sensitivity (Horsfield, Print et al. 2012).

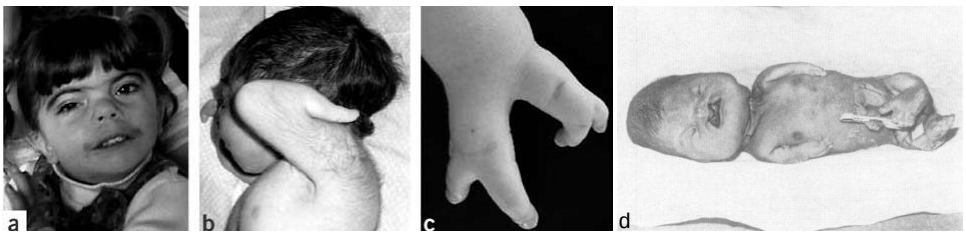

Figure 11. Phenotype of individuals with cohesinopathies. (a) A child with CdLS showing characteristic facial features. (**b**,**c**) CDLs patient with upper limb abnormalities and hirsutism of the back. a, b, and c are taken from (Krantz, McCallum et al. 2004) (d) Photograph of a newborn baby with RBS. The baby died 17 minutes after delivery. This photos is taken from (Mann, Fitzsimmons et al. 1982).

Robert's syndrome (RBS) (Figure 11A) is another less common, although severe, cohesinopathy. A less severe variant of this syndrome is SC phocomelia. RBS is characterized by multiple craniofacial abnormalities, limb malformations, growth deficiency, and mental retardation. Severely affected fetuses normally do not fully develop, or dye just after birth. While in the variant type, individuals normally get to adulthood. The syndrome is caused by homozygous recessive mutations in the *ESCO2* gene. Unlike cells from CDLS, cells from RBS patients show precocious loss of SCC, micronuclei formation, aneuploidy, lagging chromosomes, and mitotic defects (Horsfield, Print et al. 2012).

Chromosome instability and aneuploidy seen in many cancer types has been attributed to mutations in cohesin subunits affecting cohesin's main function in sister chromatid cohesion. One such example is colorectal cancer, where mutations within *SMC1*, *SMC3* and *NIPBL* have been identified. These mutations lead to decreased cohesin gene expression resulting in premature loss of SCC and increased chromosome instability, which contribute to the pathogenesis of this cancer. Overexpression of *SMC3* and *RAD21* in cancer cell lines has also been reported. For example, *SMC3* is overexpressed in human colon cancer cell lines (Xu, Tomaszewski et al. 2011).

Other human cancers can emerge from mutations that affect the role of cohesin in the regulation of gene transcription, or DNA damage repair through homologous recombination, which could lead to emergence of oncogenic chromosomal aberrations, deletions, inversions and translocations (Xu, Tomaszewski et al. 2011).

II.5. **Sumoylation**

Some subunits of the SMC complexes have been identified as potential targets of SUMO modification by proteomic screens (Wohlschlegel, Johnson et al. 2004, Denison, Rudner et al. 2005). Sumoylation is a reversible post-translational modification where

SUMO proteins (Small Ubiquitin like MOdifiers) are covalently conjugated to lysine residue(s) within target proteins (Johnson, Schwienhorst et al. 1997, Kamitani, Nguyen et al. 1997). The name comes from the resemblance seen between the three dimensional structure and the biochemistry of conjugation in both ubiquitin and SUMOpathways, which proceed through an enzymatic cascade of E1 activating enzyme, E2 conjugase, and an E3 ligase (Johnson 2004) (Figure 12, Table 2). However, these enzymes do not overlap between the two processes. Moreover, although they might seem similar, SUMO and ubiquitin differ in many aspects, which include amino acid sequence (less than 20% identity) and surface charge (Bayer, Arndt et al. 1998). Sumoylation is mostly used to direct localization of its targets (Matunis, Coutavas et al. 1996), modify their interactions with other proteins (Mahajan, Delphin et al. 1997), or mark them for, or protect them from, degradation by the ubiquitin system (Hoege, Pfander et al. 2002).

SUMO conjugates are usually low abundant and short-lived. The highly dynamic nature of this process is due to SUMO-specific proteases, which actively remove SUMO from the target protein. This has led to the proposal that the rate of desumoylation is much faster than that of sumoylation. Strikingly, the effect of this modification on cellular functions seems to be dramatic compared to the levels of sumoylation seen for its targets (Mukhopadhyay, Dasso 2007).

Proteomic studies have identified more than 1000 proteins as potential SUMO targets in budding yeast. Known targets localize predominantly in the nucleus. However, some targets are found in other cellular locations including the cytoplasm, the ER, the mitochondria, and the plasma membrane. Potential targets identified by these proteomic studies include proteins involved in DNA metabolism, including replication, repair, transcriptional activators and repressors, and factors involved in chromatin remodeling. Other known SUMO targeted processes are metabolic pathways, RNA-related

processes, protein translation and folding, and cell division (Wohlschlegel, Johnson et al. 2004, Denison, Rudner et al. 2005, Zhao, Kwon et al. 2004, Panse, Hardeland et al. 2004). Many of these proteins have been validated as true targets *in vivo*, and their modification by SUMO is relevant in processes such as transcription (Sapetschnig, Rischitor et al. 2002), DNA repair (Psakhye, Jentsch 2012, Dou, Huang et al. 2011), mitotic chromosome structure and segregation (Wan, Subramonian et al. 2012, Alexandru, Uhlmann et al. 2001, Stead, Aguilar et al. 2003, Bachant, Alcasabas et al. 2002).

Given the broad array of cellular functions affected by sumoylation, SUMO proteins, as well as SUMO enzymes, are highly conserved throughout the eukaryotic kingdome. Both SUMO and Ubc9 are essential in *S. cerevisiae* and in mammals (Johnson, Blobel 1997, Dieckhoff, Bolte et al. 2004, Nacerddine, Lehembre et al. 2005). In *S. cerevisiae*, there is only one SUMO protein, which is coded by the *SMT3* gene, and is conjugated either individually or in chains to target proteins (Johnson, Schwienhorst et al. 1997). In human cells there are four SUMO proteins: SUMO1-4 (Saitoh, Hinchey 2000, Guo, Li et al. 2004). SUMO1-3 are ubiquitously expressed, while SUMO4 expression is restricted to the spleen lymph node and kidney, and it is not clear whether it is processed to its mature form, or if it participates in formation of SUMO conjugates *in vivo* (Owerbach, McKay et al. 2005, Melchior 2000). The mature form of SUMO1 shares 50% identity with SUMO2 and 3. In addition, SUMO1 has non-redundant targets with SUMO2 and 3. On the other hand, SUMO2 and 3 share 97% similarity (Saitoh, Hinchey 2000). Moreover, they are both involved in forming poly-SUMO chains, and have redundant functions in the cell (Tatham, Jaffray et al. 2001). The ability to form SUMO chains is due to the presence of a conserved lysine residue in the N-terminal amino acid stretch found in SUMO proteins (Tatham, Jaffray et al. 2001). In budding yeast formation of these chains is not essential for vegetative growth. However, it is required for

synaptonemal complex assembly important for completion of meiotic chromosome segregation (Cheng, Lo et al. 2006). In addition, SUMO chains are required for the maintenance of normal higher-order chromatin structure and transcriptional repression of environmental stress response genes in budding yeast (Srikumar, Lewicki et al. 2013).

Table 2. SUMO Proteins and Enzymes in *S. cerevisiae* and humans.

	Humans	S. cerevisiae
SUMO	SUMO1-4	Smt3P
E1 Activating enzyme	Uba2+AosI	Uba2+AosI
E2 Conjugase	Ubc9	Ubc9
E3 Ligase	PIASI PIAS3 PIASxα PIASyβ Mms21/Nse2	Siz1 Siz2 Mms21/Nse2
SUMO peptidase	SENP1-3, SENP5-7	Ulp1,Ulp2

II.5.1. **The SUMO conjugation pathway**

Before SUMO is conjugated to target proteins, it undergoes a post-translational maturation step which is catalyzed by the hydrolysis activity of the SUMO proteases Ulp/SENP (Ubiquitin Like protein Protease (*S. cerevisiae*)/ Sentrin specific Proteases (human)). The protease cleaves the residues after the conserved 'GG' sequence within the C-terminal of the SUMO precursor, which reveals this di-glycine motif (Mukhopadhyay, Dasso 2007). The N-terminal glycine residue in the mature form of SUMO then forms a thioester linkage with the heterodimer activating enzyme complex formed of Uba2 and Aos1 in an ATP dependent manner resulting in SUMO activation (Johnson, Schwienhorst et al. 1997). The thioester linkage is then transferred to the conjugating enzyme (Ubc9), which acts together with SUMO ligases to form a covalent bond between the terminal di-glycine motif of SUMO and an ε-amino group of the lysine residue within the target protein (Johnson, Blobel 1997) (Figure 12).

The majority of SUMO ligases contain an SP-RING motif essential for their function (Hochstrasser 2001). PIAS (protein inhibitor of activated STAT) proteins in humans (Palvimo 2007), Siz (SAP and miz-finger domain) proteins in budding yeast (Johnson, Gupta 2001, Takahashi, Kahyo et al. 2001), and Nse2 (part of the Smc5/6 complex) in both species, contain this SP-RING. Siz1, Siz2 and Nse2 are the only known mitotic ligases is budding yeast. SP-RING ligases simultaneously bind to Ubc9 and the target protein, bringing the three players in a favorable position for SUMO transfer (Hochstrasser 2001, Song, Durrin et al. 2004). In *S. cerevisiae* Siz1 and Siz2 are responsible for most SUMO conjugation (Takahashi, Kahyo et al. 2001, Johnson, Gupta 2001), while Nse2 has few specific targets, which include the Smc5/6 complex itself, and Yku70 (Zhao, Blobel 2005, Potts, Yu 2005). *siz1*Δ*siz2*Δ double mutants are viable, while Nse2 is essential for vegetative growth and DNA repair (Zhao, Blobel 2005).

Unlike ubquitylation, where a ubiquitin E3 ligase is always required, SUMO E1 and Ubc9 alone are able to sumoylated many substrates *in vitro*, without the need for an E3 SUMO ligase. However, in some cases the presence of an E3 SUMO ligase increases sumoylation efficiency and substrate specificity (Johnson, Blobel 1997, Zhao, Blobel 2005).

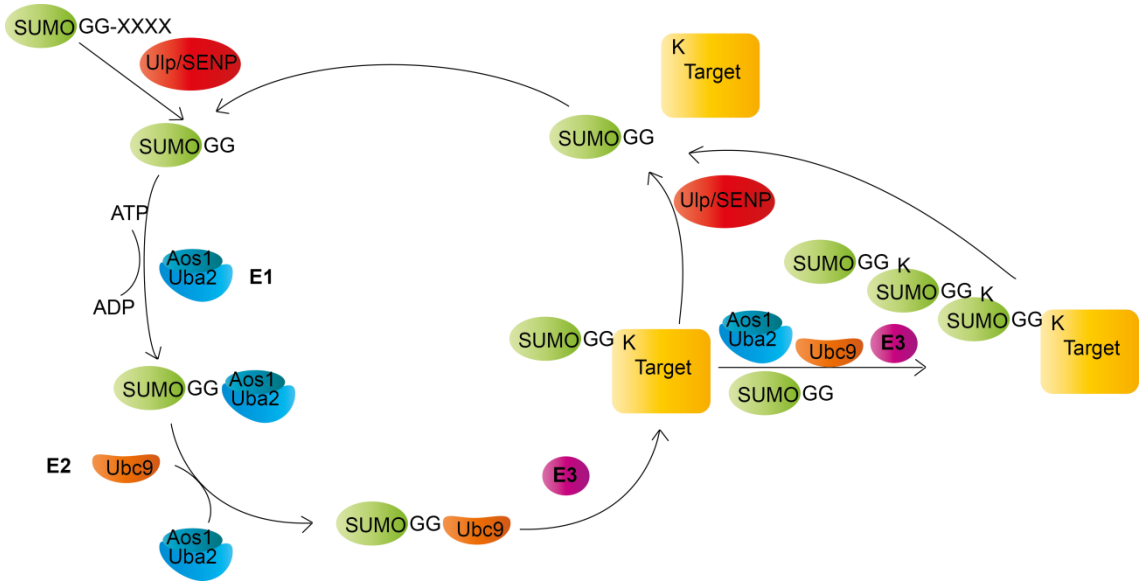

Figure 12. SUMO conjugation and deconjugation pathway. Before SUMO is conjugated to target proteins, it undergoes a post-translational maturation step which is catalyzed by the hydrolysis activity of the SUMO proteases Ulp/SENP. The protease cleaves the residues after the conserved 'GG' region within the C-terminal of the SUMO precursor, which reveals this diglycine motif. These glycine residues then form a thioester linkage with heterodimer activating enzyme (Uba2) in an ATP dependent manner resulting in SUMO activation. The thioester linkage is then transferred to the conjugating enzyme (Ubc9), which acts together with SUMO ligases to form a covalent bond between the terminal di-glycine residues of SUMO and ε-amino group of the lysine residue within the target protein. Deconjugation of SUMO by SUMO proteases (Ulp/SENP) is essential to ensure the reversible nature of SUMO conjugation. Cleavage of SUMO from the target protein occurs at the scissile isopeptide bond.

II.5.1.1. **Nse2 E3 SUMO ligase and Smc5/6 complex**

Nse2 is an E3 SUMO ligase that belongs to the Smc5/6 complex, which is essential in *S. cerevisiae*. Smc5/6 is recruited to DSBs and is required for HR dependent DNA damage repair. In addition, Smc5/6 complex is enriched at repetitive rDNA, telomeric sequences, and at discrete sites along chromosome arms in a length dependent manner (Kegel, Betts-Lindroos et al. 2011, Lindroos, Strom et al. 2006). It has been shown that Smc5/6 is required for maintenance and proper segregation of the rDNA (Torres-Rosell, Machin et al. 2005, Torres-Rosell, Sunjevaric et al. 2007), and for proper resolution of SC linkages during mitosis (Bermudez-Lopez, Ceschia et al. 2010). This complex is composed of the core subunits Smc5 and Smc6 (Figure 1A) (Zhao,

Blobel 2005), and is associated with other regulatory non-SMC subunits Nse1-6. Nse4 is a kleisin protein that binds to the head domains of Smc5. Nse1 and Nse3 interact with each other and with Nse4 (Palecek, Vidot et al. 2006). Nse1 has a ubiquitin ligase ring domain and its ubiquitin ligase activity is only gained when associated with Nse3 (Doyle, Gao et al. 2010). Nse5 and Nse6 bind to the hinge domain (Duan, Yang et al. 2009, Palecek, Vidot et al. 2006). Nse2 is formed of two domains; an Smc5 binding domain, which resides in the N terminal of Nse2, and a SUMO ligase domain in the C-terminal of Nse2 (Figure 13A). In the absence of DNA damage, the SUMO ligase activity is not essential for survival. However, deleting the entire *NSE2* gene is lethal in *S. cerevisiae*, which suggests that Nse2 might have other roles that do not involve its SUMO ligase activity. Nse2 binds to the coiled-coils of Smc5 in a site where a bend of 165° has been observed (Figure 13C). Mutations that disrupt binding of Nse2 (Figure 13B) to Smc5 are inviable (Duan, Sarangi et al. 2009).

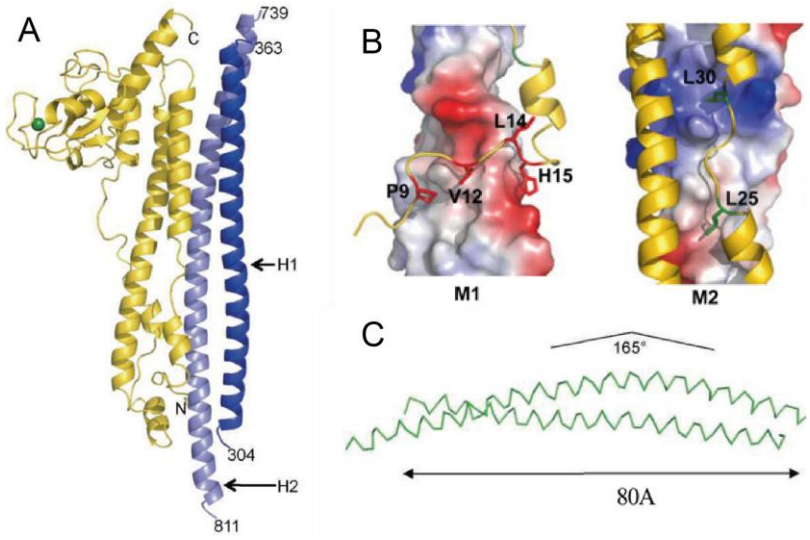

Figure 13. Structure of Nse2 in complex with the coiled-coil region of Smc5. (A) Nse2 is shown in gold and the coiled-coil regions of Smc5 are shown in blue. (B) M1 and M2 mutations that abolish interaction between Nse2 and Smc5 are colored in red and green respectively. (C) The arm region of Smc5 exhibits a moderate curvature (Duan, Sarangi et al. 2009).

II.5.2. **SUMO deconjugation**

Deconjugation of SUMO by SUMO proteases (Ulp/SENP) is essential to ensure the reversible nature of SUMO conjugation. Cleavage of SUMO from the target protein occurs at the scissile isopeptide bond (Figure 12). Ulp/SENP proteases contain a conserved catalytic domain in the C terminal region referred to as Ulp1 domain (UD), which is necessary and sufficient to promote SUMO deconjugation *in vitro* (Mossessova, Lima 2000). In addition to the catalytic domain, Ulp/SENPs possess an N-terminal domain that shares no similarity between the different proteases, and is required for subcellular localization and substrate specificity (Lima, Reverter 2008).

In *S. cerevisiae*, there are two SUMO proteases; Ulp1 and Ulp2/Smt4. Ulp1 is associated with the nuclear envelope, while Ulp2 is predominantly nuclear. Ulp1 is responsible for SUMO maturation, it is essential for cell viability and for cell cycle progression through G2/M phase (Li, Hochstrasser 1999). On the other hand, Ulp2 is not essential for vegetative growth, but it is required for disassembly of poly-SUMO chains (Bylebyl, Belichenko et al. 2003). Although *ulp2* mutants are viable, they grow poorly, and exhibit chromosome segregation defects (Mossessova, Lima 2000).

In humans there are six different SUMO specific proteases; SENP1, SENP2, SENP3, SENP5, SENP6, and SENP7. SENP1 and SENP2 are most closely related to each other and are more efficient in catalyzing SUMO deconjugation over processing. SENP1 has no preference for specific SUMO isoforms. However, SENP2 shows a slight preference for SUMO2/3. SENP1 and 2 are very similar to the budding yeast Ulp1 and they both localize to the nuclear envelop (Mukhopadhyay, Dasso 2007). SENP3 and 5 are also similar to Ulp1, but they localize to the nucleolus, and they have a preference for SUMO2/3 deconjugation and processing (Mukhopadhyay, Dasso 2007). SENP6 and 7

are similar to budding yeast Ulp2 in that they are found in the nucleoplasm, and have a strong preference for disassembly of SUMO2/3 polymeric chains (Lima, Reverter 2008).

II.5.3. **Functional outcomes of SUMO modification**

As with other post-translational modifications, several lysines within the same protein can be conjugated to SUMO. The multiple sumoylation sites might be functionally redundant, as occurs in many recombinational proteins (Psakhye, Jentsch 2012), or might have specific functions, as is the case for PCNA (Hoege, Pfander et al. 2002). Sometimes, sumoylated lysines can lie within a signature motif, which is useful for predicting candidate lysines. This motif is defined by the amino acid sequence ψKxE/D, where x is any amino acid and ψ is a hydrophobic amino acid, which can be valine, isoleucine, or leucine. During SUMO conjugation, the target lysine is localized to the catalytic pocket of Ubc9, while the other amino acids interact with the surface of Ubc9 (Bernier-Villamor, Sampson et al. 2002). However, in many other cases, as seen for the modification of K164 in PCNA, sumoylation can also occur at lysines that are not present within a Ubc9-consensus sequence (Hoege, Pfander et al. 2002).

The effect of sumoylation on its targets is specific and can influence their interactions with other proteins or DNA in a positive or negative manner. This can be because covalent binding of SUMO can mask binding sites within the sumoylated protein, which will cause decrease in the ability of this protein to interact with other proteins or DNA, as noted in some transcription repressors (Zheng, Yang 2004). On the other hand, sumoylation can add an additional binding interface by allowing the target protein to interact with other proteins, that bind to SUMO non-covalently through their SUMO interacting/binding motifs SIM/SBM. For example, in *S. cerevisiae*, sumoylated PCNA attracts the anti-recombinogenic SIM-containing DNA helicase Srs2 to replication forks to prevent unnecessary recombination events during S phase by interacting with Rad51 and disrupting formation of Rad51 filaments. Upon replication fork stalling, due to

DNA lesions, PCNA is monoubiquitylated at the same lysine residue K164, which is promoted by it previous sumoylation. Other modifications such as acetylation can compete with sumoylation for acceptor lysines within target proteins, which might serve to regulate it (Stankovic-Valentin, Deltour et al. 2007, Hoege, Pfander et al. 2002). In addition, phosphorylation of the same target can enhance or down-regulate sumoylation due to enhanced interaction with Ubc9, or masking of sumoylation site respectively (Hietakangas, Anckar et al. 2006).

A part from promoting new interactions, sumoylation may induce a conformational change in the target protein. For instance, thymine DNA glycosylase (TDG) is a DNA mismatch repair enzyme that is sumoylated, but at the same time binds non-covalently to SUMO, which induces a conformational change. This conformational change is required for the release of TDG from DNA after base excision (Hardeland, Steinacher et al. 2002).

In other cases, sumoylation can affect the localization of the target protein. For example, RanGAP1 is localized to the cytoplasm in human cells during interphase. However, sumoylated RanGAP1 localizes it to the NPC, where it interacts with RanBP2 to form the RRSU complex. This complex is localized to kinetochores and mitotic spindles during mitosis (Matunis, Coutavas et al. 1996).

II.5.4. **Sumoylation and Genome integrity**

Mutation or depletion of sumoylation enzymes results in failure to repair damaged genome, what highlights the importance of SUMO-mediated response in protecting genome integrity, and in modulating DNA repair. It has been proposed that sumoylation-based response to DNA damage occurs in parallel to phosphorylation-based damage response and is required for efficient repair and maintenance (Cremona, Sarangi et al. 2012).

Many DNA repair proteins become sumoylated in response to DNA damage. For example, Rad52 and Yku70, which regulate HR and NHEJ respectively, are sumoylated. Sumoylation of Rad52 protects it from proteasomal degradation, and regulates ribosomal DNA recombinational repair (Sacher, Pfander et al. 2006, Zhao, Blobel 2005, Torres-Rosell, Sunjevaric et al. 2007). As mentioned previously, PCNA sumoylation and ubiquitylation cooperate to control the response to replication-blocking lesions during S phase (Hoege, Pfander et al. 2002, Parker, Ulrich 2012). Other proteins involved in homologous recombination repair pathway in response to DNA damage are also regulated by sumoylation in a Siz2 dependent manner; such as Rad9, Mrc1, Mec1, and Tel1 (Psakhye, Jentsch 2012, Cremona, Sarangi et al. 2012).

Ubc9 is known to play a key role in genome integrity, specially by preventing the accumulation of X-shaped DNA at damaged replication forks. This DNA repair function of Ubc9 requires the Nse2 SUMO ligase (Branzei, Sollier et al. 2006). In fact, *nse2* mutant is the only E3 mutant in budding yeast that is sensitive to DNA damage, indicating that the Nse2-branch of the SUMO pathway plays a prominent role in DNA repair. Nse2-dependent sumoylation is most probably required to trigger removal of recombination intermediates (Bermudez-Lopez, Ceschia et al. 2010, Chavez, George et al. 2010). However, the real targets at this stage are still not known (Zhao, Blobel 2005).

II.5.5. **Sumoylation and SMC complexes**

Over the past years, several proteomic studies have identified the Smc complexes as potential targets of SUMO modification (Wohlschlegel, Johnson et al. 2004, Denison, Rudner et al. 2005). Although *in vivo* sumoylation was detected for various subunits of the SMC complexes, the physiological role of this modification is still not clear. In *S. cerevisiae* Pds5 is has been proposed to be sumoylated in a Siz1 dependent manner, starting in S phase until the onset of mitosis. Defects seen in *pds5* thermosensitive alleles are suppressed by Ulp2 overexpression. Thus, it has been

proposed that Pds5 sumoylation disrupts the interaction between Pds5 and cohesin, which leads to cohesin destabilization and release (Stead, Aguilar et al. 2003). Moreover, Nse2 dependent sumoylation of Smc1, Smc3, Smc2, and Smc5 was shown in nocodazole arrested *S. cerevisiae* cells. It has been suggested that sumoylated SMC complexes cooperate with topoisomerases in rDNA maintenance (Takahashi, Dulev et al. 2008). In addition, sumoylation of human Rad21 and Sa2, was also shown to depend on Nse2 *in vitro* (Potts, Porteus et al. 2006). Furthermore, sumoylation of Ycs4 subunit of condensin was also detected *in vivo* in *S. cerevisiae*. It seems that Cdc14p promotes sumoylation of Ycs4 during anaphase, which allows condensin's localization to rDNA (D'Amours, Stegmeier et al. 2004). Finally, sumoylation of Smc5 and Nse2 was demonstrated *in vivo* using *S. cerevisiae* as a model. It has been suggested that the Smc5/6 complex facilitates sumoylation of Nse2 targets by localizing it to the target site (Zhao, Blobel 2005).

II.5.6. **Methods to study sumoylation**

The study of protein sumoylation faces two main challenges that stem from the characteristics of the sumoylation process. First, only a small fraction of a given protein is sumoylated for a short period of time. Second, the highly active peptidases are normally controlled by the cell by confining them to certain cell compartments, such as; the nuclear pore. However, upon cell disruption these peptidase are released, and rapidly desumoylate proteins, which might lead to failure of detection of SUMO conjugates. In order to solve these problems several approaches can be followed separately or in combination. First, purification of SUMO conjugates is normally done under denaturing conditions (such as 8M urea). This helps in various aspects, which include; restricting the activity of the peptidases; and eliminating proteins that are bound non-covalently to SUMO through SIM. The use of protease inhibitors, specially cysteine-dependent proteases like N-ethylmaleimide (NEM), and others like PMSF is also

recommended. A second approach would be to purify the SUMO conjugates after conditional inactivation of Ulp peptidases (Sacher, Pfander et al. 2005).

"...every siren is a symphony,
every teardrop is a waterfall..."

Coldplay

Objectives

III. Objectives

- Determine whether cohesin is sumoylated *in vivo* under physiological conditions.
- Identify the molecular requirements of cohesin sumoylation.
- Develop a model, which uses Ulp1 Domain (UD) fusion to Scc1 protein to down-regulate sumoylation of the whole complex, and thus, characterize the role of sumoylation in cohesin function.
- Study the phenotype of cohesin desumoylation in human cells.

"…Just because I'm losing, doesn't mean I'm lost, doesn't mean I'll stop, doesn't mean I'll cross…"

Lost, Coldplay

Materials and Methods

IV. Materials and Methods

IV.1. Construction of yeast strains

Epitope tagging of genes and deletions was performed as described (Goldstein, McCusker 1999, Janke, Magiera et al. 2004, Alexandru, Uhlmann et al. 2001). Lists of the strains, plasmids, and primers used in this study are provided in Supplementary Table 2, Supplementary Table 3, and Supplementary Table 4. All PCRs were done using GeneAmp PCR system 2700 from Applied BioSystems. The polymerase "Expand high fidelity" from Roche was used for epitope tagging and deletions of genes. To check gene integrations in yeast one of these two methods were used; colony PCR or genomic DNA extraction (Promega) followed by PCR using SupraTherm DNA polymerase (Gene Craft).

IV.1.1. Yeast competent cells preparation and transformation

Optical density was always measured with Jenway 6300 spectrophotometer at 600 nm (OD_{600}) before collecting cells. For preparation of yeast competent cells, 50 ml of exponentially growing cells (OD_{600} 0.8-1) were collected and washed first with Milli-Q water and then with sorbitol buffer (100mM LiOAc, 10mM Tris-HCl pH 8, 1mM EDTA/NaOH pH 8, 1M Sorbitol). After washing, the pellet was resuspended with 360 µl sorbitol buffer and 40 µl of denatured carrier DNA (Salmon sperm DNA, Gibco BRL).

Next, 50 µl aliquots were directly used for transformation, or stored at -80°C. The amount of DNA used for transformation varied depending on the target homology in the case of PCR transformation, or on the concentration of DNA in the case of plasmids. Commonly, for centromere or multicopy plasmid transformation 1- 5 µl of plasmid DNA (100ng- 5µg) was added to 10 µl of competent cells, while for transformation of integrative vectors 10 µl of digested plasmid DNA (≈5µg) were added to 50 µl of cells. In the case of PCR transformation, 10µl of DNA (≈50µg) were used if

the target homology was low (40bp), while 3-4µl were used for targets with higher homology (>150bp). Next, PEG buffer (100mM LiOAc, 10mM Tris-HCl pH 8, 1mM EDTA/NaOH pH 8, 40% PEG) was added to the transformation tube and incubated at room temperature for 30 minutes. Then, heat shock was done at 42°C for 15 minutes after adding DMSO to 10%. Finally, the transformation buffer was removed after spinning at 2400 rpm for 5 minutes, and cells were resuspended with Milli-Q water and plated on the appropriate selection medium.

For transformations that require expression of drug resistance genes before platting, cells were incubated at room temperature with non-selective medium for 2-4 hours before plating.

IV.1.2. **Colony PCR from yeast**

A yeast colony was resuspended in 15 µl of Milli-Q (Millipore) water and patched in appropriate selection plate. Next, a small spoon of glass beads (SIGMA) was added, and cells were boiled at 95°C for 2 minutes. Then, cells were broken for 30 seconds at power 5.5 using the FastPrep (FP120, Bio101 Thermosavant). Finally, after spinning at 10 krpm for 1 min, 2 µl of supernatant were taken for the PCR reaction.

IV.2. **Gene cloning and plasmid construction**

PCR purification was done using QIAquick PCR purification kit from Qiagen. Dephosphorylation and ligation were done using the Rapid DNA Dephos & Ligation Kit from Roche. Site-directed mutagenesis was performed using the Quickchange mutagenesis kit from Agilent Technologies. Plasmid extraction was done using GenElute Plasmid Miniprep Kit (SIGMA). Newly constructed plasmids were checked by either plasmid jet preps and restriction digestion, or *E.coli* colony PCR. Detection of DNA was done by loading on D-1 low EEO agarose (CONDA) gel prepared with the running buffer 1XTAE (from 50X; Tris-HCL, EDTA-Na2 pH 8.5). DNA was then stained

by incubating the agarose gel for 15 minutes in ethidium bromide bath with a final concentration of 0.5 µg/ml. Detection was done by exposing the gel to UV light source (Alpha Inno Tech), image capture by Olympus camera, and analysis with AlphaDigiDoc software.

The Scc1-UD fusions were made by cloning the Ulp1 SUMO-peptidase domain (amino acids 418 to 621) next to the 3xHA epitope into the multi-copy vector pYES2. The *SCC1* open reading frame was cloned N-terminally of the 3xHA linker. The fusions were then transferred to the integrative vector YIplac211 by PCR and recombination cloning in *recA+ E. coli* cells (MC1061). Replacement of the *GAL* promoter by the *SCC1* promoter was done recombinational cloning in MC1061 using two PCRs: one containing the yeast *SCC1* promoter (1.1 Kb) flanked by 40 nucleotide sequences homologous to the ends of a second PCR, performed on the YIplac211 plasmids to remove the *GAL* promoter.

NSE2-3HA was amplified from yeast genomic DNA with 5'-HindIII-Nse2 promoter and 3'-SacI -3HA, and cloned in to HindIII-SacI sites in pRS315. M1 and M2 single and double mutations on Nse2 were done by site-directed mutagenesis.

IV.2.1. ***E.coli*** **competent cells preparation and transformation**

DH5α

For plasmid transformation, 50 µl of Subcloning Efficiency™ DH5α™ Competent Cells from Invitrogen were thawed on ice and 1-5 µl of DNA were added with gentle mixing. Next, they were incubated on ice for 30 minutes, at 42°C for 20 seconds (heat shock) and on ice again for 2 minutes. 1 ml of prewarmed LB was added to the transformation tube, and cells were then incubated at 37°C for one hour to allow expression of the antibiotic (ampicillin) resistance gene. After incubation, cells were pelleted at 6000 rpm for 5 minutes, and 950 µl of the supernatant was removed, while the pellet was resuspended with the 50 µl left and plated on LB-Ampicillin plate.

MC1061

For MC1061 competent cells preparation, cells were grown overnight in LB at 37°C. The next day, 1 ml of the culture was diluted in 100 ml of LB and left to reach OD_{600} 0.2-0.4 at 37°C. Next, cells were collected by centrifugation at 3200 rpm for 10 minutes at 4°C, and resuspended with 50 ml of ice cold 0.1 M CaCl2, and then left on ice for 2 hours. Then, cells were collected as before and resuspended with 10 ml of ice cold 0.1 M CaCl2 and 10% glycerol. After leaving on ice for 30 minutes cells were aliquoted (100 µl/aliquot) and stored at -80°C. MC1061 cells were mainly used for plasmid construction through recombination. This was done by transforming 10 µl of vector plus insert DNAs per 100 µl of competent cells. Transformation of the vector alone or the insert alone was used as background control. Special care was taken that the molar concentration of the insert was at least twice as that of the vector. The transformation procedure was the same as that described for DH5α cells, except for the heat shock step, which was done for 2 minutes at 42°C.

IV.2.2. **Colony PCR from *E. coli***

Colonies were picked with toothpicks and swirled into 25 µl of Milli-Q water. The same toothpick was used to make a patch on LB-Ampicillin plate. The suspended colonies were then boiled for 2 minutes, and centrifuged at 13000 rpm for 2 minutes. 20 µl of the supernatant were transferred to a new tube, from which 1 µl was used as template for the PCR. This procedure allows rapid screening for the presence of the insert in its correct orientation.

IV.2.3. **Jet preps**

Colonies that were previously picked on LB-Ampicillin plate were resuspended in 500 µl of LB-Ampicillin liquid medium and then pelleted by centrifugation for 30 seconds at 13000 rpm. Next, 50 µl of BT (2% Triton X-100/NaOH pH 12.4) were added to the pellet without resuspension. Then, 50 µl of phenol/chloroform were added and

the tubes where shaken vigorously for 30 seconds. After centrifugation for 5 minutes at 13000 rpm, 5 µl were combined with loading buffer (5X FLB, 100 µg/ml RNAse). To analyze with restriction digestion, 40 µl of the supernatant were taken and chromatin was precipitated by adding 4 µl of 2% acetic acid 4 µl of 3 M NaOAc pH 8, and 100 µl of ethanol, and centrifugation at 13000 rpm for 5 minutes. The pellet was then washed with 1 ml 70% ethanol, and resuspended with10 µl Milli-Q water. 5 µl of the resuspended chromatin was used in 10 µl digestion reaction. The digested plasmids were combined with loading buffer (5X FLB, 100 µg/ml RNAse) and loaded into an agarose gel along with the undigested ones.

IV.3. **Growth media**

Yeast cells were grown in YP (Yeast extract, peptone) supplemented with different sugars (2%), glucose, galactose and raffinose. A final concentration of 200 µg/ml of genetecin (DUCHEFA), 300 µg/ml of hygromycin B (SIGMA), and 200 µg/ml of nourseothricin (Werner BioAgents) antibiotics, was used to select for gene tagging and deletions that confer antibiotic resistance. SC medium (YNB, drop-out) was used to select for plasmid auxotrophies, which include; Tryptophan (40 µg/ml), Leucine (120 µg/ml), Histidine (20 µg/ml) and Uracil (20 µg/ml). LB was used to grow bacterial *E.coli* DH5α and MC1061. A final concentration of 50 µg/ml of Ampicillin (ROCHE) was added to select for cloned plasmids.

IV.4. **Mating, sporulation, and tetrad dissection**

MATa and MATα strains were crossed on YPD plates, and the appearance of zygotes was checked under the light microscope after 4 hours of incubation at 30°C. Diploids were then streaked and isolated on selective media, and after 2 days, big colonies were crossed against haploid MATa and MATα strains to exclude haploid colonies.

Sporulation was done by growing cells in YPD supplemented with the auxotrophies; uracil, tryptophan, and adenine for 2-3 days, then the culture was diluted to OD_{600} 1 in sporulation medium containing potassium acetate (1%) and the auxotrophies (10X less concentrated). The observation of tetrads under light microscope was normally seen in 2-3 days.

For tetrad dissection, cells were treated with β-glucoronidase/Arylsulfatase (Roche) as follows; 1 ml of the culture was collected and resuspended in 12 ml tube with 0.5 ml Milli-Q water. Then, 12 µl of β-glucoronidase/Arylsulfatase were added to the resuspended tetrads, and the tube was incubated at 30°C for 30 minutes in horizontal position. Next, the enzyme was inactivated by diluting the reaction to 5 ml with Milli-Q water. Tetrads were collected by spinning for 10 minutes at 1000 rpm without break, and then resuspended with 0.5 ml Milli-Q water. Finally, 10 µl were added as a drop on YPD plate in an inclined position, so that the drop could extend vertically. Tetrad dissection was done using the dissection microscope MSM400 from Singer Instruments.

IV.5. **FACS (Fluorescence activated cell sorting):**

Propidium iodide (PI) staining

FACS tubes with 1 ml of 100% ethanol were prepared prior to sample collection. 333 µl of culture were added to the FACS tube and incubated for 1 hour and up to two weeks at 4°C. After incubation, cells were collected by spinning at 2500 rpm for 5 minutes, and the pellet was resuspended with 1XSCC buffer from 20X stock (3M NaCl, 3M Na_3citrate pH 7) + RNAse (200 µg/ml), and incubated overnight at 50°C. The next day 1XSSC+ Proteinase K (100 µg/ml) were added and cells were incubated at 50°Cfor one hour. Finally, 1XSCC+PI (3 µg/ml) were added and cells were incubated at room temperature for at least 60 minutes.

FACS reading and analysis

Before reading with BD FACSCanto II, cells were sonicated for 10 seconds at power 8 with SoniPrep 150. The cytometer was normally set to read 20,000 events at a slow rate. FSC was set to 357, SSC to 418, and PE to 709. Analysis was done using the program WinMDI^{TM}.

IV.6. **Metaphase cohesion assay**

Exponentially growing wild- type or *scc1-73* cells, carrying a chromosome tag on centromere 5 (tet operators, tet repressor-YFP), were arrested in G1 using 10^{-8} M alpha factor (Genscript). Once arrested, the *GAL* promoter was switched on to allow expression of the *SCC1* fusions, and the temperature was shifted to 36ºC to inactivate the *scc1-73* allele. After 30 minutes, cells were released into a synchronous cell cycle at 36ºC by washing twice with YP galactose and resuspended with YP galactose containing pronase (0.1 mg/ml, SIGMA) and 1% DMSO. Next, budding was monitored and nocodazole (SIGMA) was added to a final concentration of 7,5 µg/ml once budding starts (45 minutes later) for metaphase block (Figure 14).

To tag centromere V with tet operators, we transformed a plasmid that contains tet operators after restriction digestion (*SpeI*) to a site that is 1.4 Kb away from the centromere. This plasmid has been previously described in and we have kindly received it from this lab pT271. pCJ097 plasmid, expressing Tet repressor-YFP, was received from Elmar Schiebel's lab and described in (Janke, Ortiz et al. 2002). To integrate this plasmid in the *ADE* locus the plasmid was digested with *StuI*. Wild-type (Y CCG8946) and *scc1-73* (Y CCG9151) strains carrying tet operators next to centromere IV were obtained from Luis Aragon's lab.

Similarly, wild-type or *scc1-73* cells carrying a chromosome tag on centromere 4 or 5, and expressing *SCC1* fusions from the *SCC1* promoter, were arrested in G1.

Cultures were then shifted to 37ºC to inactivate *scc1-73* temperature sensitive allele. 30 min later, cells were released into a synchronous cell cycle at 37ºC as described in the previous paragraph except that the washes were done with YPD instead of YP galactose. Next, cells were arrested in metaphase with nocodazole and observed microscopically for centromere cohesion.

Binding sites for Scc1 were found near the silent loci, and coinciding with the boundary elements in the case of silenced mating-type loci *HMR*. To check SCC in the *HMR* locus when cohesin sumoylation is absent, we transformed *SCC1*, *SCC1-UD* to *scc1-73* cells, where the *HMR* locus, containing an origin of replication, was tagged with lac-GFP and flanked by loxP sites. Expression of the Cre recombinases from the *GAL* promoter leads to excision of the locus producing two chromatin circles that remain associated with one another in wild-type cells but loose cohesion in *scc1-73* cells (Chang, Wu et al. 2005). Cells were arrested in G1, and then, once arrested, galactose was added to express the *SCC1* constructs and the HO recombinase, and the temperature was shifted to 37ºC to inactivate the *scc1-73* allele. 30 min later, cells were released into a synchronous cell cycle at 37ºC, arrested in metaphase with nocodazole and observed microscopically for *HMR* cohesion.

To check whether the same defects in SCC at the *HMR* locus are also seen in *nse2*Δ*C* cells, we transformed this allele to cells that have lac-GFP tag on *HMR* and we scored for metaphase cohesion as before. To check whether the same defects in SCC at the *HMR* locus are also seen in *smc6-9* cells, we transformed this allele to cells that have lac-GFP tag on *HMR* and we scored for metaphase cohesion as before.

To monitor microscopically how cells that lack cohesin sumoylation progress throughout the cell cycle we arrested *scc1-73 thermosensitive* cells that overexpress *SCC1* and *SCC1-UD* from the *GAL* promoter and tet operators on centromere V in G1 by α factor. Then, we released them at non permissive temperatures into a

synchronous cell cycle and we added galactose to induce the *GAL* promoter. Then, we took samples every 15 minutes for analysis by FACS and fluorescence microscopy.

Cells carrying GFP or YFP chromosome tags were analyzed by fluorescence microscopy after DNA staining. DNA was stained using 4,6,-Diamidino-2-phenylindole (DAPI) at 1 µg/ml final concentration in the presence of mounting solution and 0,4% Triton X-100 to permeabilize cells. For fluorescence microscopy, a series of z-focal plane images were collected with a DP30 monochrome camera mounted on an upright BX51 Olympus fluorescence microscope (Figure 15). Synchronic cultures were routinely checked by FACS analysis.

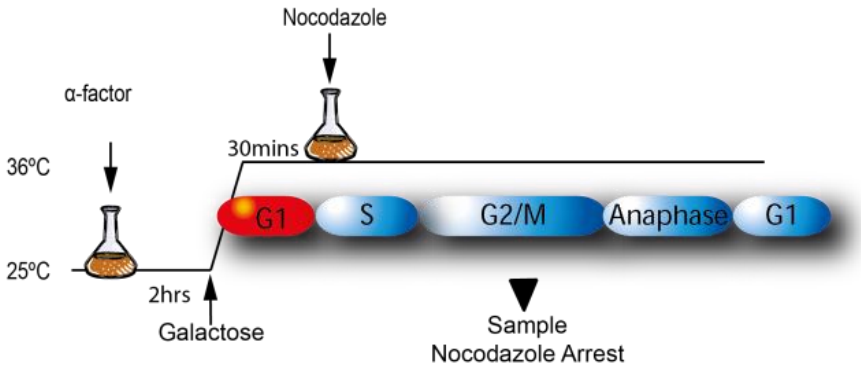

Figure 14. Metaphase cohesion assay. Wild-type or *scc1-73* cells carrying a chromosome tag on centromere 5 were arrested in G1. Once arrested, the *GAL* promoter was switched on to allow expression of the indicated *SCC1* fusions, and the culture shifted to 36ºC to inactivate the *scc1-73* allele. After 30 minutes, cells were released into a synchronous cell cycle at 36ºC, arrested in metaphase with nocodazole and observed microscopically for centromere cohesion.

IV.7. Down-regulation of the endogenous copy of *SCC1* by the auxin-based induced degron (AID) system

Indole-3-acetic acid (IAA) belongs to a family of plant hormones called auxins, which control gene expression during many aspects of growth and development. IAA binds to the F-box transport inhibitor response 1 (TIR1) protein and promotes the interaction of the E3 ubiquitin ligase SCF-TIR1 and the IAA transcription repressors (AUX/IAA). SCF-TIR1 recruits an E2 ubiquitin conjugating enzyme that then

polyubiquitylates AUX/IAAs resulting in rapid degradation of the latter by the proteasome.

Budding yeast lack the auxin response but share the SCF degradation pathway. Transforming the AID system to *S. cerevisiae* enables rapid depletion of a protein of interest in the presence of auxin, which allows the generation of efficient conditional mutants of essential proteins (Figure 15). To induce degradation of Scc1, the 'aid' degron IAA17 (*Arabidopsis thaliana*) was amplified from pSM409 (hygromycin resistance) or pSM411 (nurseothrycin resistance with Scc1 S2/S3 primers, and recombined in yeast with the C-terminal of *SCC1*. In addition, pNC1854 (HIS3 marker) or pNHK53 (URA3 marker), carrying OsTIR1 (*Oryza sativa*) expressed under the *ADH1* promoter and tagged with 9xmyc, were digested with BsiwI or StuI respectively to be integrated in the yeast genome (Nishimura, Fukagawa et al. 2009).

The final concentration of IAA in liquid and solid YPD medium was 1000 µM. For exponentially growing cultures, auxin was added at around OD_{600} 0.4 and cells were collected 2 hours afterwards. To study cell cycle progression of strains carrying Scc1-UD fusion in Scc1-AID background by FACS analysis, auxin was added once cells were arrested in G1 with the alpha factor. Then, 30 minutes after auxin addition, cells were released by adding pronase, and samples were taken every 10 minutes for 200 minutes. To check acetylation levels of Smc3 in strains carrying Scc1-UD fusion in Scc1-aid background, auxin was added once cells were arrested in G1 with the alpha factor. Then, 30 minutes after auxin addition, cells with released by washing the alpha factor off. Once released (in 30 minutes), nocodazole was added and cells were collected 90 minutes afterwards.

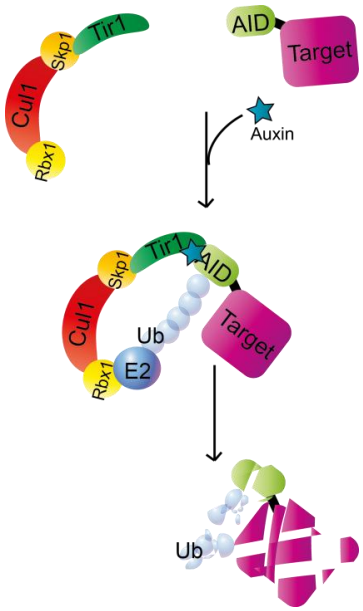

Figure 15. Schematic illustration of the degron system. Budding yeast lack the auxin response but share the SCF degradation pathway (Skp1, Cul1, Rtx1). Auxin binding to TIR1 promotes the interaction between TIR1 and the aid degron of the target protein. SCF-TIR1 acts as an E3 ubiquitin ligase to recruit an E2 ligase resulting in polyubiquitylation of the aid degron. Finally, the target is degraded by the proteasome (Nishimura, Fukagawa et al. 2009).

IV.8. **Serial dilution and replica plating of yeast cells**

First, around one colony was resuspended in 400 µl of the appropriate growth medium. Then, the OD_{600} was measured and cells were diluted in 200 µl to OD_{600} 0.3 inside 96 well plate. Four 10X serial dilutions or five 5X serial dilutions were made by carrying 20 µl from the first dilution to the next and throwing away the last 20 µl, or by carrying 40 µl respectively. Replica plating on different media was done by 48 pin stamp.

IV.9. **Generation time measurement**

Cells were grown overnight in YP plus raffinose. The next day, cultures were diluted to the same OD_{600} and split in to two; in one of the two the sugar raffinose was substituted with galactose to allow the expression of the fusions under the *GAL* promoter. The OD_{600} was measured every hour for 8 hours. The ln of the OD_{600} was calculated in an excel table and plotted on a graph as a function of time. The slope was

used to calculate the generation time by dividing the natural logarithm of 2 ln(2) over the slope.

IV.10. **Protein Techniques**

IV.10.1. **Post-alkaline extraction**

Post-alkaline extraction was mainly used to check correct tagging of transformation colonies. Yeast cells, obtained from colony patches on plates, were resuspended in 200 µl 0.1 M NaOH, and incubated for 5 minutes at room temperature. After incubation, the alkaline supernatant was removed by spinning at 13.000 rpm for 15 seconds, and the pellets were resuspended with 1XSSR and boiled at 95°C for protein elution. Next, samples were loaded on SDS-PAGE gels and analyzed by western blot. 4XSS (20% sucrose, 0.05% bromophenol blue, 0.1% NaAZ) and 4X SR (8%SDS in 0.5 M Tris-HCl pH 6.8) are used at equal volumes, along with 2% β-mercaptoethanol, to prepare the loading buffer 2XSSR.

IV.10.2. **Urea extraction**

Urea extraction was mainly used to quantitatively check the levels of expression of proteins. 10 ODs of exponentially growing cultures were collected and processed by adding 30 µl of 5 M urea and boiling at 95°C for 2 minutes. Next, two small spatulefull of glass beads were added, and cells were broken using the FastPrep for 30 seconds power 6. Then, 100 µl of 1XSR were added and cell extracts were boiled at 95°C for 2 minutes.

Finally, the protein extracts in the supernatant were obtained after centrifugation at high speed for 5 minutes. Protein concentration was checked using BIO-RAD Micro DC protein assay. Equal concentrations of proteins were loaded on SDS-PAGE gels after boiling at 95°C with loading buffer (1XSS and 2% 2-β-mercaptoethanol) for 2 minutes.

IV.10.3. **Pull-Down**

SUMO Pull-Down

SUMO pull-down analysis was done on strains that contain N-terminal 6hi-FLAG (HF) tag on *SMT3* (SUMO). Histidine tags have affinity to nickel, and thus SUMO conjugated proteins were retained using nickel beads (Figure 16).

Strains with no HF tag on *SMT3* were used to discard unspecific binding to nickel beads. On the other hand, strains with no tag on cohesin subunits were used as negative controls, to discard unspecific bands that do not correspond to the proteins under investigation.

200 ODs of exponentially growing cultures were collected and processed either directly or stored at -80°C. In some cases, pellets were taken from cells that were arrested in G1, and then released into a synchronous cell cycle to monitor accumulation of SUMO conjugates throughout the cell cycle. Progression throughout the cell cycle was monitored by FACS.

Cells were mechanically broken for 40 seconds power 6 at room temperature with glass beads under denaturing conditions using buffer A (8M Urea, 100mM NaH2PO4, 10mM Tris-HCl, 0.05% Tween-20, pH 8 with 1X protease inhibitors PIA 100X in Milli-Q (leupeptin, antipain, chymostain, aprotinin), PIB 200X in ethanol (TPCK, pepstain), PMSF 200X in ethanol (phenyl methyl sulfonyl fluoride)).

The supernatant was separated from the glass beads and cell debris by centrifugation at 4°C. 17 µl of the protein extract was saved to check protein concentration and to be used as input, and the rest (1 ml) was combined with 50µl nickel beads (Ni-NTA Agarose, Qiagen) in the presence of 15 mM imidazole.

After 2 hours of incubation on the rotor at 4°C, the beads were washed at room temperature three times (10 minutes each) with buffer A containing 2mM imidazole, and three times with buffer C (8M Urea, 100mM NaH2PO4, 10mM Tris-HCl, 0.05% Tween-20 pH 6,3).

For elution, 25 µl and 15 µl of 2XSSR were added to the beads and the protein extract respectively. SUMO pull downs were loaded in SDS-PAGE gels next to protein extracts to confirm the slower mobility of SUMO conjugates with respect to the unmodified protein. The antibodies used for detection of SUMO-conjugated proteins were anti-HA and anti-myc (Supplementary Table 1). Membranes were reproved with anti-FLAG or anti-SUMO to control the amount of SUMO pulled down.

PCNA Pull-Down

PCNA pull-down analysis was done on strains that contained 6His-myc tag on *POL30* (PCNA). The pull-down procedure was the same as above. Detection of sumoylated PCNA was done using anti-myc and anti-SUMO (Supplementary Table 1).

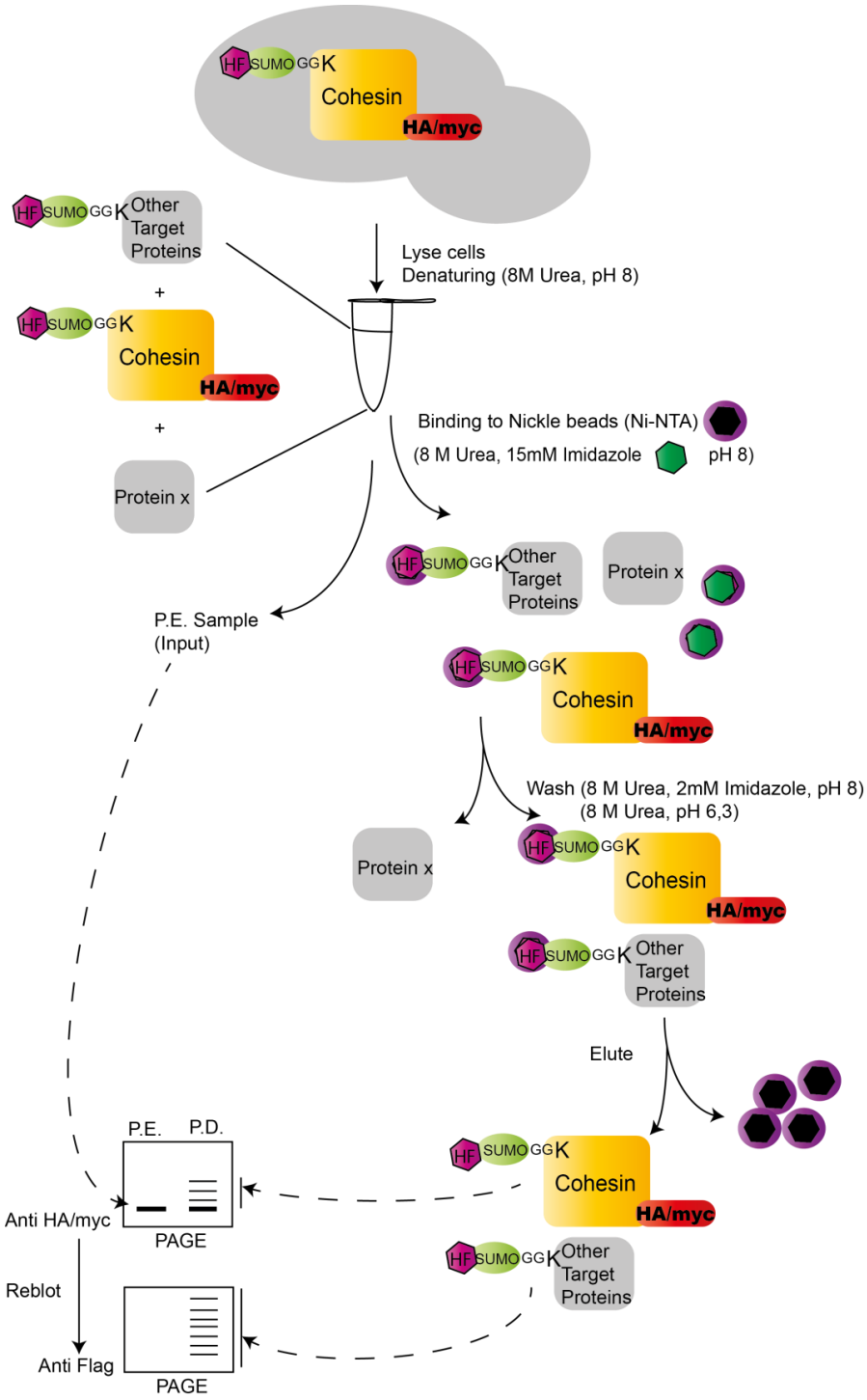

Figure 16. Schematic representation of the SUMO pull-down experiment. SUMO pull down analysis was done on strains that contain N-terminal 6HIS-FLAG tag on SMT3 (SUMO), and a myc or HA tag on the protein under investigation, in this case cohesin subunits. Histidine has affinity to nickel, and thus SUMO conjugated proteins were retained using nickel beads, and then eluted under high concentrations of imidazole, which competes with Histidine for nickel binding. HF: 6xHis-Flag, P.D. Pull Down, P.E. Protein Extract, PAGE: Poly Acrylamide Gel Electrophoresis.

IV.10.4. **Protein Immunoprecipitation**

Pellets of 100 ODs were collected and processed either directly or stored at -80°C. Cells were mechanically broken for 40 seconds power 6 at room temperature with glass beads under non-denaturing conditions using buffer EBX (50mM HEPES/KOH pH 7.5, 100 mM KCl, 2.5 mM MgCl2, 0.25% Triton X-100, 0.5 mM DTT, protease inhibitors PIA, PIB, PMSF, protease cocktail tablet EDTA free from Roche), or buffer A that has higher salt concentration (50mM HEPES/NaOH, 150 mM KCl, 1.5 mM MgCl2, 0.5% Triton X-100, 0.5 mM DTT, protease inhibitors PIA, PIB, PMSF, protease cocktail tablet EDTA free from Roche and 25XPPI (25 mM Sodium Floride, 25 mM β-glycerophosphate, 25mM EGTA, 125 mM sodium pyrophosphate)). Sodium butyrate (SIGMA) was added to protein extracts during purification of acetylated Smc3.

17 µl of the protein extract was saved to check protein concentration and to be used as input, while the rest (0.5 ml) was combined with 50µl beads. myc-tagged proteins were immunoprecipitated using anti-myc antibodies (9E10;Roche) coupled to protein G Dynabeads (Invitrogen). Washing of the beads and binding to the antibody was done using 0.1 M phosphate buffer pH 8 with 0.01% Tween-20. HA-tagged proteins were immunoprecipitated using anti-HA Affinity matrix (Roche).

After 2 hours of incubation on the rotor at 4°C, the beads were washed five times for 5 minutes with IPP150 buffer (100mM Tris-HCL, 150 mM NaCl, 0.1% Triton X-100). Proteins were eluted from HA beads by adding 25 µl 2XSSR and boiling for 5 minutes at 95°C. Elution from the magnetic beads was done by incubating the beads with 1XSR at 70°C for 10 minutes, and then the supernatant was boiled at 95°C with loading buffer (1XSS and 2% 2-β-mercaptoethanol) for two minutes.

The immunoprecipitated proteins were loaded together with the input in SDS-PAGE, and detected using western blot analysis. The antibodies used for western blot analysis were anti-HA, anti-myc, and anti-acetyl lysine (Supplementary Table 1).

IV.10.5. **Chromatin Binding Assay**

Pellets of 15 OD_{600} were collected and resuspended with 1ml of prespheroplast buffer (100mM PIPES/KOH pH 9.4, 10mM DTT, 0.1% sodium azide), then incubated at room temperature for 10 minutes.

After spinning at 2000 rpm for 3 minutes, the supernatant was decanted and cells were resuspended with the spheroplast buffer (50 mM Kpi, 0.6 M sorbitol, 10 mM DTT, 50 mm KH_2PO_4/K_2HPO_4 pH 7.5, Zymoliase 100T 0.03 mM), and incubated at 37°C with occasional mixing until the OD_{600} of a 1:100 dilution of the cell suspension (in water) dropped to <10% of the value before digestion (around 10 minutes).

After centrifugation at 1200 rpm for 5 minutes, sphereoplasts were washed with 1 ml of ice-chilled wash buffer (100 mM KCl, 50 mM HEPES/KOH pH 7.5, 2.5 mM $MgCl_2$, and 0.4 M Sorbitol), pelleted at 1200 rpm for 5 minutes at 4°C, and resuspended in an equal pellet volume (~50 µl) of extraction buffer EB (100 mM KCl, 50 mM HEPES-KOH pH 7.5, 2.5 mM $MgCl_2$, 10 mM DTT, and protease inhibitors PMSF, PIA, PIB, and protease cocktail tablet EDTA free from Roche).

Next, spheroplasts were lysed by adding Triton X-100 to 0.25% and incubating on ice for 5 minutes with gentle mixing. 1 µl was saved to measure protein concentration (BIO-RAD). Then the suspension was split in two tubes (40 µl each) one corresponding to the whole cell extract (WCE) and the other was underlayered with 100 µl EBXS (EB, Triton X-100 0.25%, 30% sucrose) and spun at 12,000 rpm for 10 min at 4°C to separate the chromatin and supernatant fractions. After centrifugation, 40 µl of the yellowish part of the supernatant were transferred to a new tube (SN), and the

chromatin pellet was washed with 100 µl EBX, and finally, resuspended with 40 µl EBX (CP).

For elution, the three fractions (WCE, SN, CP) were boiled at 95°C for 3 minutes with 40 µl of 2XSSR, and centrifuged at 10,000 rpm for 1 min before loading to SDS-PAGE gels for western blot analysis.

IV.10.6. **ChIP-On-CHIP**

IV.10.6.1. **Extract preparation**

Cultures were grown exponentially in YPD. 100 mls of $8x10^6$ cells/ml were collected after they were fixed overnight with a final concentration of 1% formaldehyde at 4°C. Extracts were processed for ChIP-on-chip analysis as described in (lengronne et al., 2004) with some modifications. In brief, after cell breakage using Multi-Beads Shoker (MB400, YASUI KIKAI, Osaka), and sonication using Bioruptor TM NEXT GEN, the cell extracts were combined with magnetic beads (protein A Dynabeads) coupled to anti-HA Mouse monoclonal antibody (HAF7, Santa cruz). A total of 40 µl of the supernatant was saved to be used as microarray control (Input). After elution, the immunoprecipitates and the supernatant (saved previously) were incubated for 6 hours at 65°C to reverse cross-link. For DNA cleanup a Proteinase K solution containing TE pH 8, and Glycogen were added to the immunoprecipitated chromatin and the supernatant and kept at 37°C for 2 hours. The clean-up was followed by two phenol/chloroform DNA extractions using Phase Lock Gel Kit (5 prime). Extracted chromatin was then precipitated with 200mM NaCl and 100% ethanol overnight at -20°C. The precipitated chromatin pellet was resuspended in TE with RnaseA and incubated at 37°C for one hour. Chromatin was purified with Qiagen purification Kit minelute.

IV.10.6.2. **DNA Amplification**

The Input DNA and the Immunoprecipitated DNA were Amplified using the Genomeplex Whole Genome amplification kit (WGA2). However the first step which is the Random fragmentation step was skipped. OmniPlex library preparation was done as described in the Kit. In the last step (Whole Genome Amplification) dUTP was included in the reaction mixture in order to incorporate dUTP in the Amplified DNA. This modification is important for the following step, namely “Fragmentation of Double stranded DNA” which was done according to Affymetrix recommendations using the GeneChip® WT Double stranded DNA Terminal Labeling Kit (PN900812). The labeling step was also done using the same kit.

IV.10.6.3. **Array Hybridization, Staining and Scanning:**

For hybridization of the labeled target on arrays, we prepared the hybridization cocktail using GeneChip® Hybridization, Wash and Stain Kit (P/N 900720). Then the cocktails were hybridized to the GeneChip *S. cerevisiae* Tiling 1.0R Array. The labeled immunoprecipitated DNA and Input DNA were both hybridized on two separate arrays. The staining and washing steps were done in the affymetrix service center in Montpellier using the GeneChip® Fluidics Station following the Affymetrix® Chromatin Immunoprecipitation Assay Protocol, available on affymetrix website. Array Scanning was also done in the affymetrix service center using GeneChip® Scanner 3000 7G.

IV.10.6.4. **Data Analysis**

A two sample comparison analysis was carried out using Affymetrix Tiling Analysis software version 1.1.02 to obtain signal (log2) and p-values(-10log10). The signal intensities were normalized on each array separately to 100. The bandwidth for probe analysis was chosen to be 300. The intensities were calculated from perfect match probes (PM) only, and a one sided upper test was chosen. P-values greater than the chosen threshold (1e-005) were used for interval analysis with a maximum

gap of 80 and a minimum run of 40. Details of the algorithms used for the computation of these values are available in the affymetrix website.

Graphical maps which show the signal log ratio across *S. cerevisiae* chromosomes, were generated using the Integrated Genome Browser software (IGB version 5.3).

For generating average profiles, the signal files were transformed to text files and then averages were calculated based on reference bed files for centromeres, origins of replication, and ORFs using a homemade program.

IV.10.7. **Cohesin ChIP-q PCR at DSB**

IV.10.7.1. **Induction of DSBs.**

DSBs were induced in strains containing stably integrated *GAL10::HO.* Centromeric plasmids that express *SCC1*, *SCC1-UD* and *SCC1-UBC9* form the *GAL* promoter were transformed to this background. Strains were grown until they reached mid-log phase in a small volume of appropriate dropout media with glucose, then diluted into YP lactate or YP raffinose overnight. Once mid-log phase had been reached again, expression of both HO and *SCC1* constructs was induced by adding galactose to a final concentration of 2% for 6 hours.

IV.10.7.2. **Chromatin Immunoprecipitation (ChIP).**

For ChIP analysis, 50ml of culture (at OD_{600}~0.5) was fixed with formaldehyde (final concentration 1.42%) for 15 minutes at room temperature. The formaldehyde was quenched with glycine (final concentration 125 mM) for 5 minutes at room temperature and the cells harvested by centrifugation (4000 rpm, 2 minutes). The pellet was washed with PBS, transferred to a screw cap tube, and snap frozen in liquid nitrogen. Pellets were stored at -80°C.

Pellets were resuspended in 100 µl IP buffer (150 mM NaCl, 50 mM Tris-HCl (pH 7.5), 5 mM EDTA, NP-40 (0.5% v/v), Triton X-100 (1.0% v/v)) containing PMSF (final concentration 1mM) and Complete protease inhibitor cocktail (Roche), and 500µl glass beads were added. Cells were lysed by two 20s cycles, power 6.5 in a FastPrep FP120 (BIO 101) machine, with 5 minutes on ice in between cycles. 300 µl IP buffer containing PMSF and protease inhibitors was then added. Tubes were pierced with a hot needle and placed on top of fresh eppendorfs and spun (1000rpm, 2 minutes) to collect lysate minus glass beads. Samples were pelleted (13000rpm, 1 minute, 4°C). The nuclear pellet was resuspended thoroughly in 1 ml IP buffer containing PMSF and protease inhibitors.

The chromatin was sonicated for 1 hour (15s ON 15s OFF at high power at 4°C) (Diagenode Biorupter). At this point, sonicated chromatin could be stored at -80°C. 120µl (30% of sample) was taken for input and 400µl for IP. After clarification (13000rpm, 1 minute) input DNA was precipitated from the supernatant by the addition of KaOAc to a final concentration of 0.3M and 2.75 volumes of ethanol. The mixture was incubated at -20°C for 2 hours/overnight, then spun (13000rpm, 5 minutes) and the supernatant discarded. 100µl 10% (w/v) Chelex 100 suspension was added to the dried pellet and the sample boiled for 20 minutes. The supernatant was cleaned using the PCR purification kit (Qiagen) according to the manufacturer's instructions, and the DNA eluted in 250µl water. DNA was stored at -20°C.

2µg α-HA antibody (Roche) was added to 400µl chromatin for the IP, and the samples were incubated in an ultrasonic water bath for 30 min at 4°C. After clarification (13000rpm, 2 minutes, 4°C) the supernatant was added to 100µl of a 50:50 slurry of Protein A and Protein G beads (Roche), which had been pre-equilibrated in IP buffer. The sample and beads were incubated for 2 hours/overnight on a rotating platform at 4°C.

The beads were then washed 3 times in IP buffer, and then 250µl 10% (w/v) Chelex 100 suspension added and the sample boiled for 20 minutes. After spinning down (13000rpm, 1 minute) the supernatant was transferred into a fresh tube and stored at -20°C.

IV.10.7.3. **Real-time PCR.**

PCR reactions were performed using the Sensimix NoRef Kit (Quantance). Reactions were carried out according to the manufacturer's instructions in a total volume of 20µl containing 3µl Input or IP DNA and oligonucleotide primer pairs (final concentration 1.5µM). Amplification was performed in a DNA Engine Opticon2 thermal cycler and analyzed using Opticon software (MJ Research) or in a Bio-Rad C1000 thermal cycler in conjunction with the Bio-Rad CFX96 Real-time-system and analyzed using CFX manager (Bio-Rad). The primers used for the analysis of the HO-break at the MAT locus are shown in Supplementary Table 4. The melting curve of each primer pair was analyzed to confirm the absence of contaminant PCR products.

IV.10.8. Western Blot

The running gel was prepared at different percentages from 30% acrylamide/Bis-acrylamide with 0.375 M Tris-HCl pH 8.8, 0.1% SDS, 0.08% Ammonium persulfate, and 0.1% TEMED. 5% stacking gel was prepared from 30% acrylamide/ Bis-acrylamide, with 0.125 M Tris-HCl pH 6.8, 0.1% SDS, 0.066% Ammonium persulfate, and 0.1% TEMED. After loading, proteins were allowed to migrate at 20 mA/gel for around 90 minutes. The Mini-PROTEAN® Tetra cell for handcast gels and PowerPac™ HC power supply along with casting stands, casting frames, and glass plates from BIO-RAD were used.

PVDF membrane (Millipore) was prepared by wetting with methanol then rehydrating with water and then transfer buffer. 20% methanol transfer buffer was used for transfer small proteins while 10% was used for larger ones. The gel and the

membrane were assembled with transfer paper (GE Health care) as directed in the Semi-Dry transfer machine TE 77 (Pharmacia Bioteq), and proteins were transferred at 60 mA/gel for one hour.

Blocking was done with 5% milk TBST (20 mM Tris-HCl, 125 mM NaCl, 0.1% Tween-20) for one hour at room temperature. The primary antibody was added and left for 2 hours at room temperature or overnight at 4°C. The antibodies used for western blot analysis are shown in (Supplementary Table 1). The membrane was washed three times with TBST for 5 minutes each, and then incubated with the secondary antibody in 0.025% milk TBST for one hour at room temperature. After washing three times with TBST, the membrane was incubated with Immobilon Western AP Substrate from Millipore for 5 minutes. The signal was detected using ChemiDoc™ MP gel imaging system from BIO-RAD.

IV.11. **Methods used to transfer the UD fusion model to human cell lines**

IV.11.1. **Gene Cloning and Plasmid construction**

4HA-UD from the human SUMO peptidase (SENP1) was cloned in the C-terminus of human *SCC1* (*RAD21*) found in the vector CMV-FLAG-GFP-RAD21. On the newly made vector, human *RAD21* was substituted by mouse *RAD21* using the restriction sites BsrGI and NotI (pCB2383). To obtain mouse *RAD21* vector without *UD* (*SENP1*), *UD* was removed by digesting the vector with SpeI (pCB2389). SENP1 active site C603 was mutated to Serine by site directed mutagenesis (pCB2411).

Human Rad21 siRNA was designed as described in (Guillou, Ibarra et al. 2010) and ordered from Thermo scientific as follows;

Target sequence: NNGGUGAAAAUGGCAUUACGG

Sense sequence: GGUGAAAAUGGCAUUACGGdtdt

Antisense sequence: CCGUAAUGCCAUUUUCACCdtdt

This siRNA is highly specific to human Rad21 as it contains four amino acid differences with Rad21 from mouse species *Mus musculus* used in this study.

IV.11.2. **Growth media of cell lines and culture conditions**

Human Embryonic Kidney 293 cells with T antigen of SV40 (HEK293-T) cells, were kindly provided by Dr. Joan X. Comella. This cell line has been broadly used to monitor protein expression and cell cycle events.

Cells were maintained at 37°C in humidified atmosphere of 5% CO2 in Dulbecco's modified Eagle medium (DMEM) from PAA Laboratories supplemented with 2 mM L-glutamine, 20 Units/ml penicillin, 20mg/ml streptomycin and 10% (vol/vol) fetal calf serum from GIBCO. I will refer to supplemented DMEM as DMEM/S.

Culture dishes used to plate cells were precoated with collagen 10 µg/ml (BD Biosciences) prepared in 0.02 N glacial acetic acid. Every 2-3 days when the confluence level reaches 80% cells were either transfected and the next day processed for western blot analysis, immunofluorescence, FACS, or Immunoprecipitation; or divided again.

To divide the cells, DMEM/S was aspirated and cells were washed with prewarmed 1XPBS (prepared from 10X PBS; 0.58MNa2HPO4, 0.17 M NaH2PO4.H20, 0.68 M NaCl). Then, cells were left with trypsin for 1-2 minutes and then rapidly inactivated by adding DMEM/S again. Next, cells were centrifuged at 1000 rpm for 5 minutes and then resuspended with DMEM medium. Cells were counted in a neubauer chamber and seeded at 40% density.

For example, for transfecting cells used for protein Immunoprecipitation, around 150x 10^4 cells were seeded in 100 mm/ 60 cm^2 dish in a final volume of 10 ml

DMEM/S. However, if transfected cells were to be used for FACS analysis, 50x 10^4 cells were seeded in 60 mm/ 20 cm^2 dish in a final volume of 4 ml DMEM/S. On the other hand, 50x 10^3 cells, were seeded in 16 mm/ 2 cm^2 wells in a final volume of 500 µl DMEM/S, for immunofluorescence and western blot analysis. In most cases, cells were seeded one day before transfection and processed one day afterwards.

IV.11.3. **Transfection of cell lines**

For transfection of HEK293Tcells with vector DNA, lipofectamine and PEI (Polyethyleneimine) were used depending on the amount of cells transfected. In general, PEI was used for experiments that needed bigger amount of cells (FACS and Immunoprecipitation), while lipofectamine was used for smaller cultures needed for Immunofluorescence, or western blot analysis. HiPerFect transfection reagent from QIAGEN was used for transfection of human Rad21 siRNA.

For transfection using lipofectamine, DMEM/S was removed and cells were washed with prewarmed Opti-MEM (GIBCO). For transfection in 16mm wells 0.5 µg of DNA was added to 50 µl of Opti-MEM, and 1 µl of lipofectamine was added to 50 µl of Opti-MEM. Then they were both combined and incubated at room temperature for 20 minutes. The mixture was added to the cells, and 100 µl of Opti-MEM was added on top, and cells were left in the incubator for 15 minutes. Finally, Opti-MEM was removed and replaced with DMEM/S and cells were left for expression during 20-24 hours in the incubator.

For transfection using PEI, DMEM/S was also removed and cells were washed with prewarmed Opti-MEM (GIBCO). For 60 mm plates, 8 µg total DNA in 500µl Opti-MEM and 80 µl PEI in 420 µl Opti-MEM were combined, vortexed immediately at half power (1800 rpm) for 2-5 sec and incubated at room temperature for 10 minutes. For 100 mm plates 24 µg total DNA in 1500 µl Opti-MEM and 240 µl PEI in 1260 µl Opti-

MEM were mixed. Next, the mixture was added first to the plate, and then 1.5 ml or 4 ml of Opti-MEM were added to 60 mm or 100 mm plates respectively, and were incubated for 1 hour at 37°C. Finally, Opti-MEM was removed and replaced with DMEM/S and cells were left for expression during 20-24 hours in the incubator.

Transfection of siRNA was done by reverse transfection. 120 ng of human *RAD21* siRNA was added to 100 µl of DMEM (final concentration of siRNA used was 100 nM in 600 µl), and 3 µl of HiPerFect transfection reagent from QIAGEN was added. The mixture was incubated for 5-10 minutes at room temperature. Meanwhile, cells were diluted in 500 µl of DMEM/S to have $60x10^4$ cells, and transferred to 16 mm dish. The siRNA mixture was added soon afterwards and mixed gently with the cells by swirling the plate. Finally, cells were left to settle in the incubator for 24-48 hours.

Cotransfection of siRNA and Vector DNA was done by reverse transfection. DNA-RNAi molecule-Lipofectamine complexes were prepared as follows. First, 0.25 µl Lipofectamine was diluted in 25 µl Opti-MEM, mixed gently and incubated for 5 minutes at room temperature. At the same time, 2.5 µl of 10 µM siRNA, and 0.5 µg of vector DNA were diluted in 25 µl Opti-MEM, mixed gently, and incubated for 5 minutes at room temperature in the final culture well without the cells. After the 5-minute incubation, the diluted Lipofectamine was added to the wells with the diluted siRNA and DNA molecules, mixed gently and incubated for 15 minutes at room temperature to allow complex formation to occur. Meanwhile, cells were diluted to $20x10^3$ in 100 µl DMEM and added to the wells containing the siRNA, DNA and lipofectamine mixture after the 15 minutes incubation. Cells were mixed gently in the wells by swirling and incubated for 24-48 hours.

IV.11.4. **Live cell imaging and Immunofluorescence of Rad21 in cell lines**

HEK293T cells were seeded and transfected as described earlier. Cells were washed with cold PBS, fixed with 4% paraformaldehyde for 20 minutes at 4°C, and then washed with cold PBS. Next, cells were treated with cold methanol (-20°C) for 2 minutes, and then washed twice with cold PBS. 5% of BSA (Bovine Serum Albumin) in 1XPBS were added for blocking during 30 minutes, and then cells were incubated with the primary antibody (anti-GFP, Table 3), diluted with BS (1:200), for 2 hours. The secondary antibody, also diluted with BS (1:500), was added after washing the excess primary with PBS three times, and incubated for 1 hour. Finally, cells were washed and mounted with the solution containing 0.5 µg/ml Hoestch (SIGMA) and slow fade (Molecular Probes).

All the images were taken using the inverted microscope Olympus IX71 with the 20X and 40X objectives. Images were taken with the DP controller program analyzed using DP controller software.

IV.11.5. **Rad21 Immunoprecipitation in HEK293T cells**

HEK293T cells were seeded and transfected as described earlier. Cells were washed with 10 ml prewarmed PBS (37°C), and then collected with 1 ml PBS using the cell scraper to lift the cells from the dish. Then, cells were centrifuged in the cold for 2 minutes at 2000 rpm, and the supernatant was discarded and replaced with 500 µl of breaking buffer (20 mM HEPES, 100 mM KCl, 2 mM MgCl2, 0.2 mM EDTA, 0.1% Tween-20, PIA, PIB, PMSF, 5 mM sodium orthovanadate). The pellet was resuspended, and cells were broken with Glass Tenbroek Tissue Grinder. 15 µl of the whole cell extract were mixed with 2XSSR and boiled at 95°C for 2 minutes. The rest of the extract was centrifuged at high speed for 5 minutes at 4°C. 15 µl of the supernatant were saved for western blot analysis, while the rest of the supernatant was combined with 50 µl of HA beads (previously washed with the breaking buffer). After 2 hours of

incubation in the orbital roller at 4°C, the beads were washed with the breaking buffer twice for 5 minutes and twice for 10 minutes, and proteins were finally eluted with 30 µl 2XSSR at 95°C for 5 minutes, and then, centrifuged at full speed for 1 minute before loading into SDS-PAGE gel.

IV.11.6. **Total protein extraction from human cell lines**

HEK293T cells were seeded and transfected as described earlier. DMEM was removed and cells were washed with 500 µl PBS, collected with 75 µl 1XSR using cell scraper (SIGMA), and boiled at 95°C for 2 minutes. Next, the cell extract was sonicated for 5 seconds at power 8, and finally, boiled with 1XSS and 1% β-mercaptoethanol at 95°C for 2 minutes.

IV.11.7. **FACS HEK293Tcells**

Cells were harvested by trypsinization. Next, pellets were washed by spinning at 500-1000 rpm for 3-2 minutes with ice cold 1ml PBS, and then, transferred to a FACS tube containing 1 ml of 70% ethanol with vortexing to avoid formation of cell aggregates. Samples were fixed at -20°C for at least 30 minutes. Then, they were washed twice with PBS, and incubated at 37°C with PBS plus PI (50 µg/ml), and RNAse A (50 µg/ml) for 30 minutes. After incubation, samples were vortexed and analyzed by flow citometry. Analysis of the FACS profile was done using ModFItLT V3.2 (win32) software.

"...When you try your best, but you don't succeed, When you get what you want, but not what you need, When you feel so tired, but you can't sleep, Stuck in reverse..."

Fix you, Coldplay

Results

V. Results

V.1. Cohesin sumoylation is required for establishment of SCC in *S. cerevisiae*

Proteomic studies have identified cohesin subunits as potential targets of sumoylation (Denison, Rudner et al. 2005, (Panse, Hardeland et al. 2004). Moreover, sumoylation of Smc1 and Smc3 was shown in nocodazole arrested *S. cerevisiae* cells (Takahashi, Dulev et al. 2008). In addition, human Rad21 sumoylation has been reported *in vitro* (Potts, Yu 2005). However, the physiological significance of this modification in cohesin regulation has not been elucidated yet. Thus, we started by checking whether cohesin is sumoylated *in vivo* under physiological conditions.

V.1.1. Cohesin is sumoylated *in vivo*

Due to the highly dynamic nature of sumoylation, a small fraction of a given protein is sumoylated for a short period of time (Johnson 2004), and thus, the chances of detecting cohesin sumoylation *in vivo* without further purification measurements are low.

In a first attempt to detect Scc1 sumoylation *in vivo*, we tagged Scc1 with the 18xmyc epitope in wild-type and *ubc9-1* thermosensetive cells. Ubc9 is the only SUMO conjugase in yeast (Johnson, Blobel 1997), and thus, after heat inactivation of this thermosensitive allele, bands that correspond to SUMO modified forms of Scc1 should disappear. Overexposure of western blots from extracts of Scc1-18myc tagged yeast cells, revelaed a few slow mobility forms of Scc1 that disappear in extracts from *ubc9-1* cells, suggesting that they correspond to SUMO conjugated forms of Scc1. These SUMO conjugates accumulate in a Ubc9 dependent manner after treatment with the DNA-damaging agent MMS (0,01%) (Figure 17A), suggesting that Scc1 sumoylation might be required during DNA damage repair.

Now that we had seen that cohesin is sumoylated *in vivo*, we decided to use a pull down approach to enrich for these modified forms. In order to purify SUMO conjugated forms of cohesin, pull-down experiments were performed under denaturing conditions, and in the presence of protease inhibitors to inhibit the highly active SUMO peptidases. Exponentially growing cells that have a 6xhis-Flag (HF) N-terminal tag on *SMT4* (SUMO gene), and a 9xmyc epitope on cohesin subunits were collected and processed for pull-down analysis. The protein extracts and the purified extracts were loaded in parallel in polyacrylamide gel electrophoresis (PAGE) to differentiate the unmodified form of the protein from the SUMO conjugated forms, which appear as bands of slower mobility when analyzed by western blot.

Pull-down experiments show that both the core (Scc1, Scc3, Smc1, and Smc3) and the more loosely associated (Pds5) subunits of the cohesin complex are sumoylated (Figure 17B). Sumoylation of Pds5 seems to be the highest among the five subunits, followed by Scc1, while the levels of sumoylation of Smc1, Smc3, and Scc3 are similar. The pull-down was reprobed with α-Flag as a control for the total amount of SUMO conjugated proteins pulled down, which seems to be equal in this case.

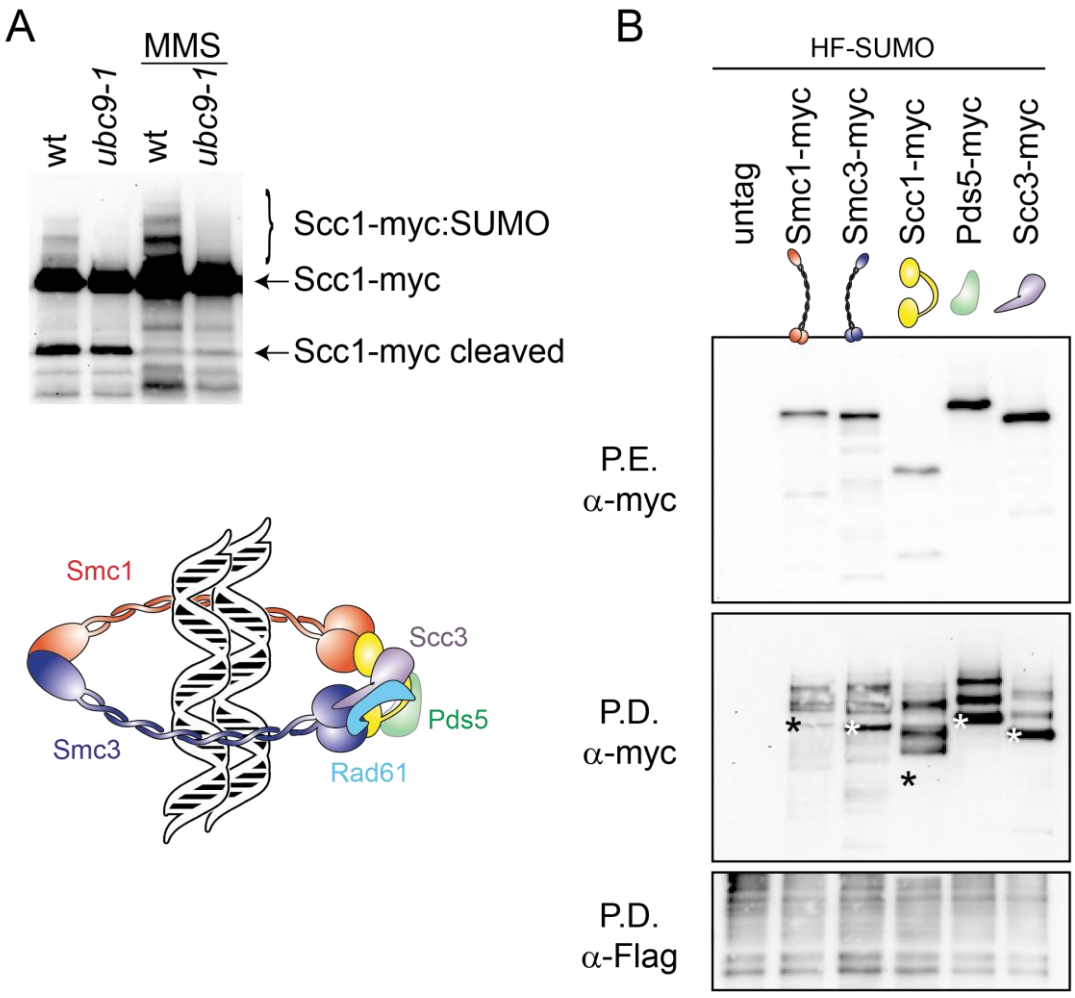

Figure 17. Cohesin is sumoylated *in vivo*. (A) Protein extracts from wild-type (Y355) and *ubc9-1* (YTR692) mutant cells expressing *SCC1-18myc* were run in SDS-PAGE and probed with anti-myc after performing a western blot. Note the slower mobility forms of Scc1 in wt extracts, which are absent in extracts from *ubc9-1* cells, and are inducible by the DNA-damaging agent MMS (0,01%). **(B) Analysis of sumoylation of different subunits of the cohesin complex.** 6His-Flag (HF) tagged SUMO was pulled down (P.D.) under denaturing conditions from yeast protein extracts (P.E.). Samples were prepared from strains expressing the indicated 9xmyc-tagged versions of cohesin subunits at their endogenous locus (YTR907, YSM1992, YSM1996, YSM1734, YSM1736, and YSM1193). Note the appearance of slower mobility forms of cohesin subunits in the pull-down, indicative of modification by SUMO. Sumoylation of Pds5 seems to be the highest among the five subunits, followed by Scc1, while the levels of sumoylation of Smc1, Smc3, and Scc3 are similar. The gray asterisk marks the unsumoylated form. The pull-down is reproved with α-Flag as a control for the total amount of SUMO conjugated proteins pulled down, which seem to be equal in this pull-down.

To check whether sumoylation of other cohesin subunits is up-regulated in response to DNA damage, wild-type cells that express Scc1-18xmyc, Smc1-18xmyc, Smc3-18xmyc and HF:SUMO were grown exponentially and then MMS was added to a

final concentration of 0.01%. Samples were collected before and after MMS addition, and were processed for pull-down analysis. As seen in Figure 18, similar to Scc1, sumoylation of Smc1 and Smc3 is also up-regulated in response to DNA damage, suggesting that sumoylation of the cohesin complex might be required for DNA repair.

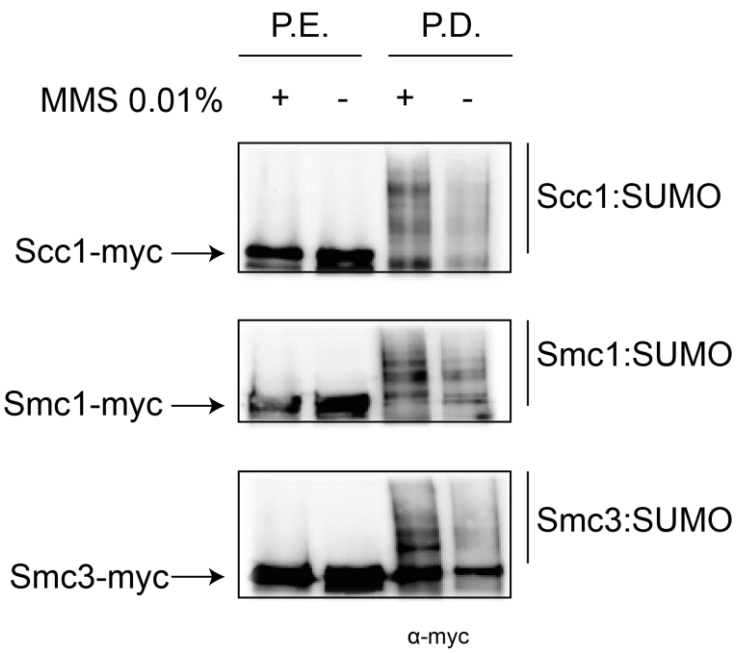

Figure 18. Sumoylation of cohesin is up-regulated in response to DNA damage. Exponentially growing cultures that express HF-SUMO, Scc1-18xmyc (YMB586), Smc1-18xmyc (YSM1992), and Smc3-18xmyc (YMB748) were treated with 0.01% MMS for two hours, and samples were collected before and after MMS treatment and processed for pull-down analysis. Note that sumoylation of the three basic subunits of cohesin (Smc1, Smc3, and Scc1) is up-regulated in response to DNA damage.

V.1.2. **Cohesin sumoylation peaks during DNA replication**

Cohesin is cell cycle regulated (Nasmyth, Haering 2009). Thus, to check whether cohesin sumoylation changes during cell cycle progression, we arrested cells that express Scc1-18xmyc in G1, and then released them in to a synchronous cell cycle at 25°C. Samples were taken for FACS and western blot analysis. Scc1 sumoylation starts at time 30 minutes after G1 release and is maximal at 45-60 minutes, which corresponds to replicating cells as seen by the FACS profile. The levels of sumoylation start to decline again as cells accumulate 2N DNA content, and decrease drastically at 90 minutes,

when cells enter anaphase (Figure 19A). The membrane was stained with coomassie, which serves as a loading control for the total amount of protein loaded. Scc1 is expressed at the G1/S boundary and is degraded after anaphase onset (Nasmyth, Haering 2009). The pattern of sumoylation is coincident with the accumulation and degradation of Scc1 observed during the cell cycle, and thus, changes in Scc1 sumoylation could stem from changes in the levels of Scc1 protein.

To check this possibility, we decided to analyze Smc1 sumoylation, but this time Smc1 sumo conjugates were purified by SUMO pull-down. To this end, cells expressing HF-SUMO and Smc1-9xmyc were arrested in G1 and released into a synchronous cell cycle at 30°C. As seen in Figure 19B Smc1 sumoylation peaks shortly after G1 release at 30°C, coincident with DNA replication (36-54 minutes), and goes down again when cells enter anaphase (72 minutes). At 90 minutes sumoylation peaks again as cells enter the next cell cycle. Thus, both Smc1 and Scc1 become SUMO targets during S phase, which suggest that cohesin sumoylation is required during DNA replication. The levels of Smc1 sumoylation in exponentially growing cells are similar to those seen during S phase. The pull-down was reproved with α-Flag to control the total amount of sumo conjugated proteins pulled down. However, since sumoylation levels are variable throughout the cell cycle, reaching maximum levels during mitosis (Wan, Subramonian et al. 2012), α-Flag blot is not useful in this case as a pull-down control, but it confirms that at 72 minutes cells were actually in mitosis.

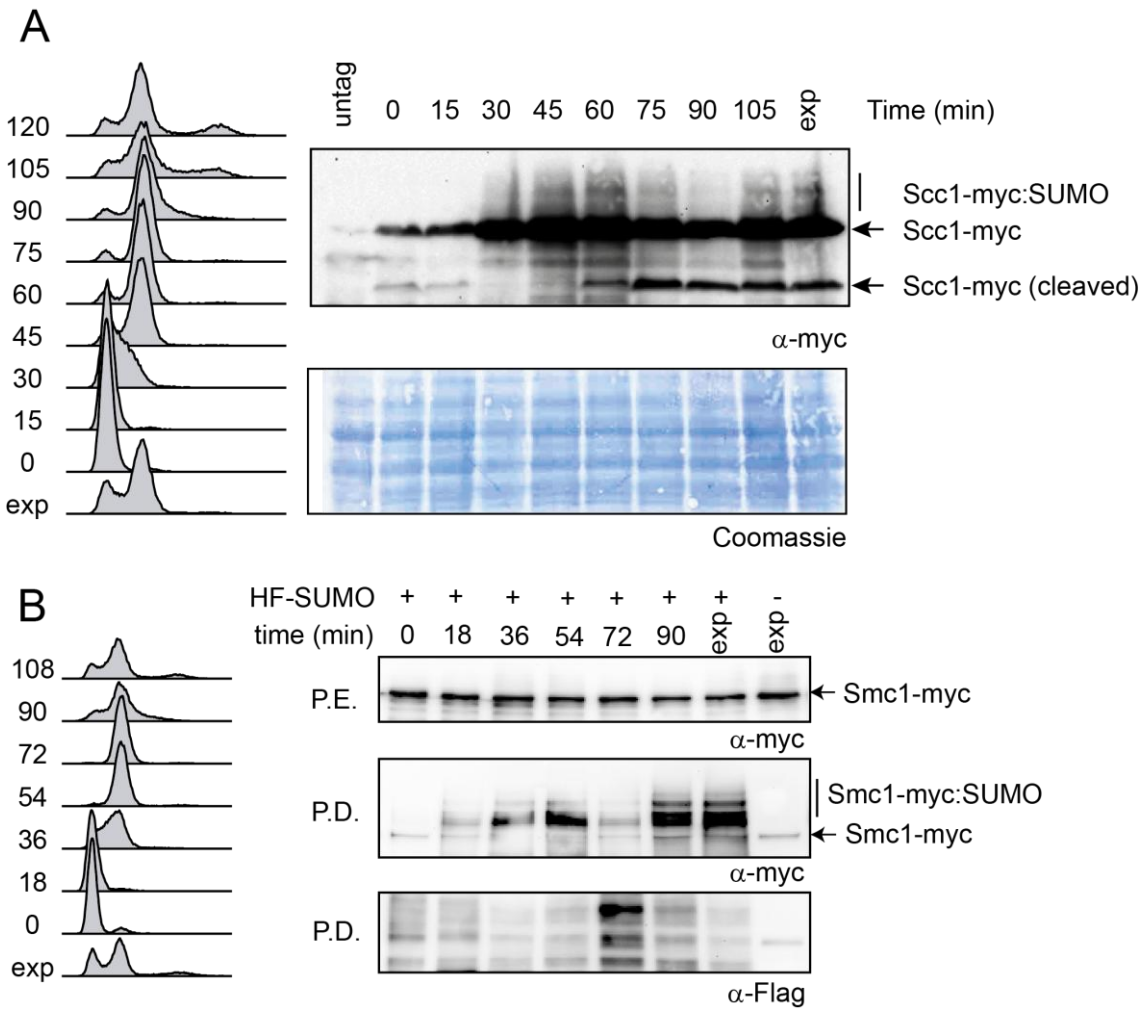

Figure 19. Cohesin sumoylation peaks during DNA replication. (A) Exponentially growing wild-type cells carrying an 18myc C-terminal epitope tag on Scc1 (Y355) were arrested in G1 and released into a synchronous cell cycle at 25ºC. Samples were taken at the indicated times for FACS and western blot analysis. Note the appearance of slower mobility forms of Scc1-18myc at times 30-60 minutes (coincident with DNA replication) and their decrease at times 75-90 minutes (when the anaphase-dependent cleavage of Scc1 starts to accumulate). The membrane was stained with coomassie as a loading control for the total amount of proteins. **(B)** An HF-SUMO Smc1-9myc strain (YSM1994) was arrested in G1 with alpha factor, and then released into a synchronous cell cycle. Samples were taken for FACS and SUMO pull-down analysis at regular intervals. Note that Smc1 is not sumoylated in G1, reaches a maximum during DNA replication, and drops as cells reach 2N DNA content. The levels of Smc1 sumoylation in exponentially growing cells are similar to those seen during S phase. The pull-down was reprobed with α-Flag to control the total amount of sumo conjugated proteins pulled down. However, since sumoylation levels are variable throughout the cell cycle, reaching maximum levels during mitosis (Wan, Subramonian et al. 2012), α-Flag blot is not useful as a pull-down control, but it confirms that at 72 minutes cells were actually in mitosis. Note also that the maximum and minimum values for Scc1 sumoylation in (A) are slightly delayed with respect to those shown for Smc1 in (B) due to the different temperatures used in both experiments. The untagged strain used in (A) and (B) is YTR907. exp, exponentially growing cells.

V.1.3. **Molecular requirements of cohesin sumoylation**

V.1.3.1. **Sumoylation of different cohesin subunits depends variably on E3 ligases**

There are three mitotic SUMO E3 ligases in budding yeast: Siz1 and Siz2, which facilitate sumoylation of most of the target proteins in the cell, and Nse2, which is part of the Smc5/6 complex, and has few known specific targets. SUMO E1 and Ubc9 alone are able to sumoylate many substrates *in vitro*. However, the presence of an E3 ligase increases sumoylation efficiency and substrate specificity (Johnson, Blobel 1997, Zhao, Blobel 2005,(Johnson 2004).

To check whether sumoylation of cohesin requires a SUMO ligase, Scc1 was tagged with 18xmyc in wild-type and E3 ligase mutant backgrounds that also express HF-SUMO. Since *SIZ1* and *SIZ2* are not essential (Johnson 2004), we could create both single and double deletion mutants. Pull-down analysis show that although global sumoylation levels in the cell decrease when *SIZ1* is deleted, alone or in combination with *SIZ2*, Scc1 sumoylation levels do not seem to be affected (Figure 20A). Sumoylation levels of Scc1 in cells that have *SIZ2* deletion are also not affected. However, the sumoylation pattern of Scc1 in *siz1*,*siz2Δ* double mutant cells is slightly lower than in the wild-type, indicating that Siz1 and Siz2 might functionally contribute to Scc1 sumoylation.

The *NSE2* gene is essential, but its ligase domain, which is present in the C-terminal domain, is not and is only required during DNA damage (Duan, Sarangi et al. 2009). Cells that express *nse2ΔC*, which lacks the SUMO ligase domain, have increased global levels of sumoylation, which is indicative of accumulated DNA damage. On the other hand, sumoylation levels of Scc1 in *nse2ΔC* are lower, compared to those seen in the wild type or *siz1* and *siz2* single and double deletions (Figure 20A). This suggests that sumoylation of Scc1 mostly depends on Nse2, although all three SUMO ligases contribute to its sumoylation.

It might be possible that sumoylation of different subunits of the cohesin complex depend variably on E3 sumo ligases. Thus, we decided to check sumoylation of Smc1 and Smc3 in *nse2ΔC* cells. To this end, we tagged Smc1 and Smc3 with the 6xHA epitope in wild-type and *nse2ΔC* cells that also express HF-SUMO. Pull-down analysis show that sumoylation levels of Smc1 and Smc3 in *nse2ΔC* cells decrease significantly compared to those seen in wild-type cells (Figure 20B), suggesting that Smc1 and Smc3 require Nse2 SUMO E3 ligase for their efficient sumoylation.

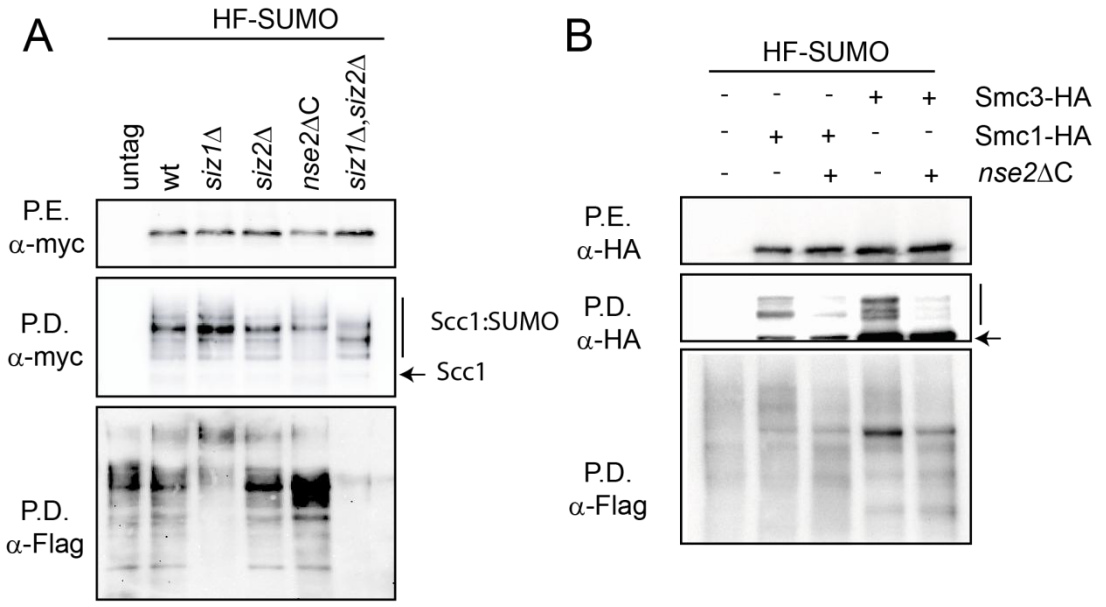

Figure 20. Sumoylation of different cohesin subunits depends variably on E3 ligases. (A) Scc1 sumoylation partially depends on Nse2. Pull-down analysis of exponentially growing wild-type and SUMO ligase mutant cells (Y557, YMB644, YMB642, YMB648, YMB650, YMB652), that express HF-SUMO and Scc1-18myc, show that *nse2ΔC* and double *siz1Δ siz2Δ* marginally affect the pattern and levels of sumoylated Scc1-18myc species. Note that most sumoylation in the cell is dependent on Siz1 and Siz2, while Nse2 mutation increases the levels of SUMO conjugates. **(B) Sumoylation of Smc1 and Smc3 depends on Nse2.** Pull-down analysis of exponentially growing wild-type and SUMO ligase mutant cells (Y557, YMB2214, YTR2373, YTR2374, YMB2164), that have an HF-SUMO and 6xHA tag on Smc1 and Smc3, shows that *nse2ΔC* drastically decreases sumoylation levels of Smc1 and Smc3. The arrow points at the unmodified form of the protein, while the straight line marks sumo modified forms of the protein.

V.1.3.2. **Nse2 binding to Smc5 is required for cohesin sumoylation**

Nse2 binds through its N-terminal to the coiled coil domain of Smc5. This binding is essential for viability, and can be disrupted by several mutations in Nse2 as described in (Duan, Sarangi et al. 2009). To check whether Nse2 binding to Smc5 is required for Nse2 dependent sumoylation of cohesin, we replaced the endogenous promoter of *NSE2* with the *GAL* promoter to be able to conditionally repress the endogenous copy of *NSE2*. Then, we tagged Smc1 with the 6xHA epitope, and SUMO with HF. Next, centromeric plasmids that express Nse2 wild-type or *nse2*^{5BD}, which has 2 mutations that abolish its binding to Smc5 based on (Duan, Yang et al. 2009), were transformed into this background.

Cells were grown with galactose overnight, and then, were transferred the next day to glucose to shut down the *GAL* promoter, and thus, avoid competition between the endogenous Nse2, and the ectopically-expressed copy. Next, cells were collected six hours after they were transferred to glucose, and were processed for SUMO pull-down analysis.

As seen in Figure 21 sumoylation of Smc1 decreases in glucose, when the *GAL* promoter is turned off, and the endogenous Nse2 is no longer present. However, when wild-type Nse2 is ectopically expressed, sumoylation of Smc1 is restored to wild-type levels, while ectopic expression of *nse2*^{5BD} shows decreased levels of sumoylation. Therefore, binding of Nse2 to Smc5 is required for efficient cohesin sumoylation.

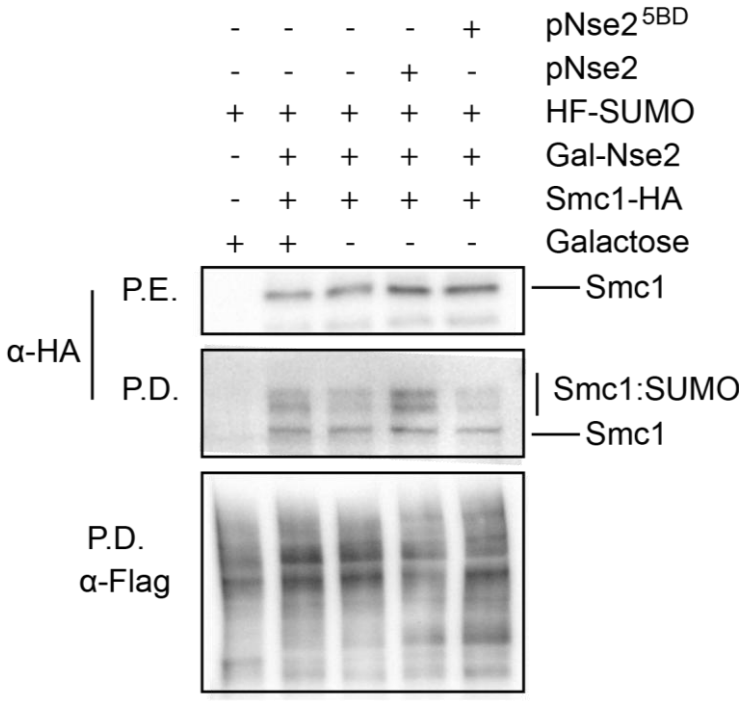

Figure 21. Nse2 binding to Smc5 is required for cohesin sumoylation. *NSE2* wild-type (pTR2395) or nse2 Smc5 binding deficient mutant allele (*nse2*^{5BD}) (pSM2401) were expressed ectopically in cells that also express *SMC1-6xHA* and *HF-SUMO*. To conditionally eliminate the endogenous Nse2 protein, its expression was engineered to be driven by the *GAL* promoter (YTR2403). Strains were grown overnight in minimum media supplemented with galactose. The next day, cells were washed and resuspended with YPD. After 6 hours, cells were collected and processed for pull-down analysis. Note that when the *GAL* promoter is turned off sumoylation of Smc1 decreases. However, when wild-type Nse2 is ectopically expressed sumoylation of Smc1 is restored to wild-type levels. On the contrary, ectopic expression of *nse2*^{5BD} as the only copy leads to decreased levels of Smc1 sumoylation.

V.1.3.3. **A functional Smc5/6 complex is required for cohesin sumoylation**

Nse3 is an essential subunit of the Smc5/6 complex, and the Nse2 ligase activity drops in thermosensitive *nse3-2* cells (unpublished data). To check whether inactivation of *nse3-2* also affects cohesin sumoylation, we tagged Scc1 with the 6xHA epitope and SUMO with HF in *nse3-2* and wild-type cells. For pull-down analysis, exponentially growing cultures (25°C) of *nse3-2* cells were split in two. One half was kept at 25°C, while the other half was shifted to 37°C for 2 hours, and then, both halves were collected. Wild-type cells were collected only after incubation at 37°C.

As seen in Figure 22 *nse3-2* cells show lower levels of Scc1 sumoylation, at both permissive and non-permissive temperatures, than those observed in wild-type cells. This result suggests that a functional Smc5/6 complex is required for cohesin sumoylation.

Smc6 is one of the core subunits of the Smc5/6 complex. *smc6-9* is a temperature sensitive allele that leads to inactivation of the Smc5/6 complex but, contrary to all other smc5/6 mutants tested, displays abnormally high levels of Nse2-dependent sumoylation (as assayed by testing Smc5 sumoylation; Marcelino Bermúdez and Jordi Torres-Rosell, unpublished data).

To check cohesin sumoylation, we tagged SUMO with the HF epitope, and *SCC1* with the 18xmyc epitope in wild-type, *nse2ΔC*, and *smc6-9* cells. Cells were grown exponentially at permissive temperatures (25°C), and then shifted to restrictive temperatures (37°C) to inactivate the temperature sensitive allele. Next, cells were collected and processed for pull-down analysis. As seen in Figure 22B, sumoylation of Scc1 decreases in *nse2ΔC* cells. On the other hand, Scc1 sumoylation in *smc6-9* decreases to a lesser extent, suggesting that inactivation of different subunits of the Smc5/6 complex affects cohesin sumoylation variably. It is possible that the less drastic effect observed in the *smc6-9* mutant, relative to the *nse2DC* mutant, is due to the fact that the Nse2 ligase activity in the former is not impaired.

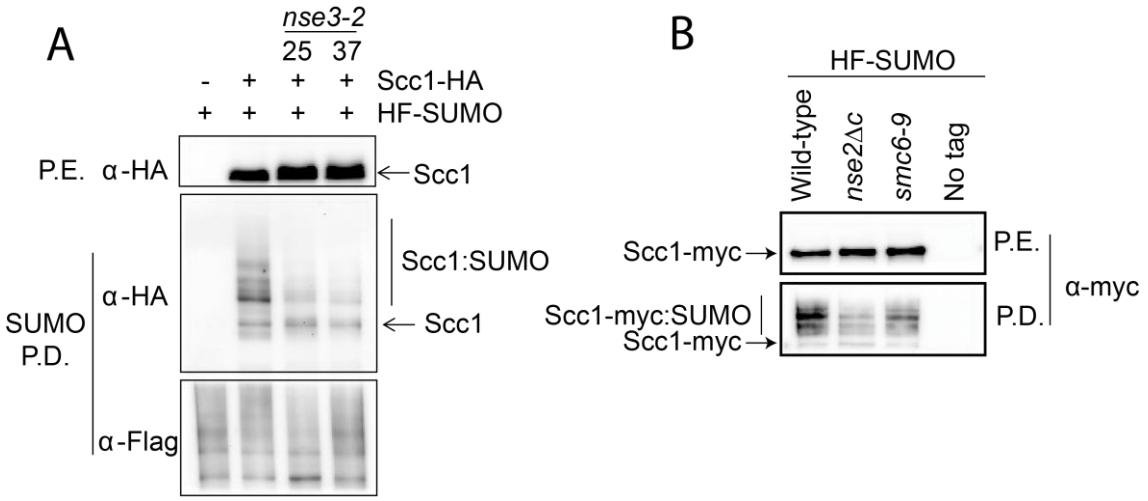

Figure 22. Scc1 sumoylation decreases in *nse3-2* and to a lesser degree in *smc6-9* mutants. (A) To check whether inactivation of *nse3-2* affects cohesin sumoylation, we tagged Scc1 with the 6xHA epitope and SUMO with HF in *nse3-2* and wild type cells (YTR907, YSM1227, YSM1689). For pull-down analysis, exponentially growing cultures (25°C) were split in two: one half was kept at 25°C, while the other half was placed at 37°C for 2 hours to inactivate the thermosensitive allele , and then, both halfs were collected. The wild-type strain was collected only after incubation at 37°C. Note that *nse3-2* cells show lower levels of Scc1 sumoylation, at both permissive and non-permissive temperatures, compared to wild-type cells. The pull-down was reblotted with α-Flag to check whether the differences seen in Scc1 sumoylation were due to differences in the total amount of SUMO conjugated proteins pulled down, which was not the case. **(B)** Wild-type, *nse2ΔC*, and *smc6-9* cells that express *HF-SUMO* and *SCC1-18xmyc* were grown exponentially at permissive temperatures (25°C), and then, temperature was shifted to 37°C to inactivated the thermosensitive allele. Next, cells were collected and processed for pull-down analysis. Note that sumoylation of Scc1 decreases in *nse2ΔC,* while sumoylation levels of Scc1 in *smc6-9* are decreased but to a lesser extent, when this allele is inactivated, suggesting that inactivation of different subunits of the Smc5/6 complex affects cohesin sumoylation variably (YMB648, YMB644, YTR746).

V.1.3.4. **Sumoylation of the cohesin complex takes place in a window between cohesin loading and chromatin entrapment**

Cohesin loading onto chromatin requires the Scc2/Scc4 loading complex and an ATP binding and hydrolysis cycle (Ciosk, Shirayama et al. 2000, Arumugam, Gruber et al. 2003). Cohesin sumoylation can occur before its loading, or afterwards once it is bound to chromatin. To check these two possibilities, we tagged Scc1 with the 6xHA epitope and SUMO with HF in wild-type cells, and in cells that express *scc2-4* temperature sensitive allele. In *scc2-4* cells, cohesin is not properly loaded onto chromatin at non-permissive temperatures (Ciosk, Shirayama et al. 2000). Cells were

exponentially grown at permissive temperatures (25°C), and then shifted to restrictive temperatures (37°C) for two hours to inactivate the *scc2-4* allele. Then, samples were collected and sumoylation levels were compared by pull-down analysis to similarly treated wild-type cells. As seen in Figure 23A, sumoylation levels of Scc1 in *scc2-4* cells are much lower than those seen wild type cells. Thus, cohesin loading onto chromatin is a prerequisite for its sumoylation.

Cohesin is loaded onto chromatin through an entry gate found at the hinge domain. Mutating the residue F584 to R within Smc1 hinge domain is lethal because it impairs heterodimerization with Smc3 hinge, and loading onto chromatin (Mishra, Hu et al. 2010). Wild-type *SMC1* and *SMC1 (F584R)* were tagged with the 9xmyc epitope and integrated in the *URA* locus, while keeping the endogenous *SMC1* copy. For pull-down analysis, SUMO was tagged with HF, and exponentially growing cells were collected and processed. As seen in Figure 23B, bands of slower mobility appeared in wild-type Smc1 but not in Smc1(F584R). These bands correspond to sumoylated forms of Smc1 since they are not present in cells that have no HF tag on SUMO. Smc1(F584R) shows no detectable levels of sumoylation compared to that seen in wild-type cells. This further confirms that cohesin loading onto chromatin is required for its sumoylation.

An ATP binding and hydrolysis cycle is required for initial loading and chromatin entrapment. Mutating the residue K39 to I within the Smc1 head domain is lethal because it abrogates ATP binding and interaction with Scc1 (Arumugam, Gruber et al. 2003). While mutating the residue E1158 to Q within the Smc1 head domain is lethal because it prevents ATP hydrolysis, and locks the NBDs in an engaged conformation, leading to unstable recruitment of the cohesin complex to chromatin (Hu, Itoh et al. 2011). *SMC1 (K39I)* or *SMC1 (E1158Q)* were tagged with the 9xmyc epitope and integrated in the *URA* locus, while keeping the endogenous *SMC1* copy. Sumoylation levels of Smc1 (K39I) or Smc1 (E1158Q) were compared to wild-type levels through pull-

down analysis of exponentially growing cultures. As seen in Figure 23B, Smc1 (K39I) shows no detectable levels of sumoylation, while Smc1 (E1158Q) shows detectable, albeit diminished, levels of sumoylation. Overall, these results suggests that cohesin sumoylation takes place in a window between initial loading and chromatin entrapment.

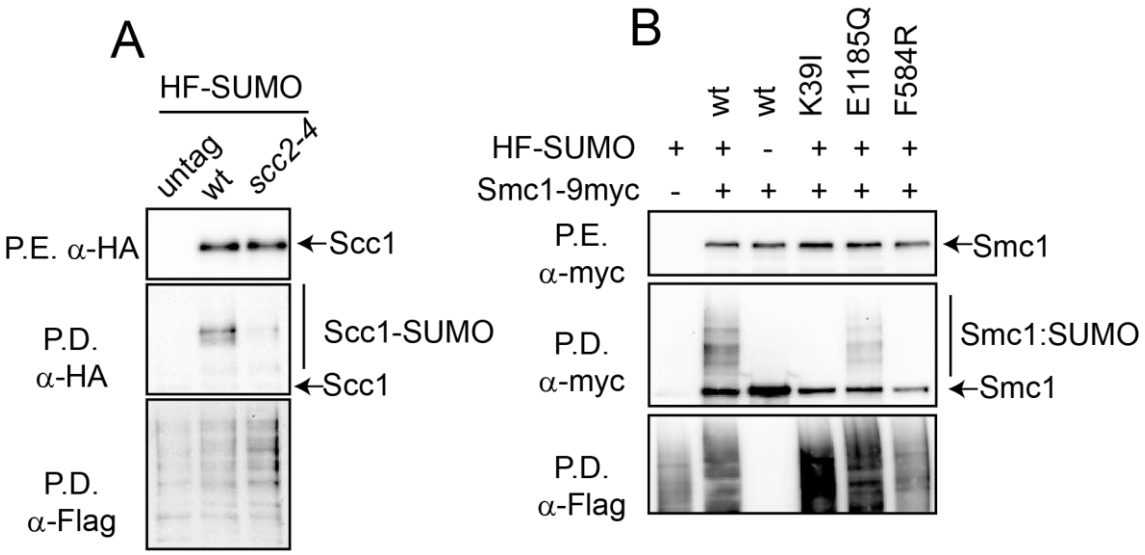

Figure 23. Sumoylation of the cohesin complex takes place in a window between cohesin loading and chromatin entrapment. (A) Cultures of wild-type and *scc2-4* mutant cells (YTR907, YTR1600, YMB1333), expressing *HF-SUMO* and *SCC1-6xHA*, were grown exponentially at 25°C, and then, placed at 37°C for two hours before collection to inactivate the thermosensitive allele. Note that sumoylation of Scc1 in *scc2-4* cells is lower than that seen in wild-type cells, indicating that a functional *SCC2* gene, and cohesin loading onto chromatin are required for its sumoylation. **(B)** Samples of wild-type cells expressing an ectopic copy of Smc1-9myc (wild-type or the indicated mutations) and HF-SUMO were analyzed by SUMO pull-down (YTR907,YSM1693, Y1636, YSM1695, YSM1697, YSM1691). Note that Smc1 sumoylation requires ATP binding (blocked in the K39I mutant) and association with chromatin (impaired in F584R mutant), but not ATP hydrolysis (blocked in the E1158Q mutant). Arrows point to position of unmodified form, while vertical lines indicate the position of sumoylated forms of cohesin.

V.1.4. *ULP1* Domain (*UD*)/ *UBC*9 fusion to *SCC1* as a model to down/up-regulate sumoylation of the cohesin complex

One approach to study the functional role of protein sumoylation is to mutate target lysines to arginines (Hoege, Pfander et al. 2002). Since we have seen that all subunits are sumoylated *in vivo*, we decided to design another approach that can down-

regulate cohesin sumoylation levels without the need to simultaneously mutate all the modifiable lysines in all cohesin subunits. Previously, it was shown that fusing *UBC9* to a target protein increases its sumoylation levels (Jakobs, Koehnke et al. 2007). We reasoned that fusing one cohesin subunit to a sumo peptidase should be able down-regulate its sumoylation. To down-regulate/up-regulate cohesin sumoylation, we fused the C terminus of Scc1 to the SUMO deconjugase domain of Ulp1 or the SUMO conjugase (Ubc9) respectively.

Ulp1 is a 72 KDa protein, but only the last 200 amino acids of the protein code for a fully functional Ulp domain (UD), which contains the catalytic residue C580 and other residues that are responsible for SUMO binding (F474) (Mossessova, Lima 2000). Thus, we fused the C-terminus of *SCC1* to the *UD* of *ULP1*, and we engineered the fusion to be attached by a 3xHA epitope, as a linker to allow the physical separation and proper folding of the two proteins (Figure 25A). As a control for this fusion, we used the same one but with the peptidase domain inactivated (C580S, F474A) (Mossessova, Lima 2000). On the other hand, the Ubc9 protein is around 18 KDa. Thus, the entire cDNA of *UBC9* was fused to C-terminal of *SCC1* using the 3xHA tag as a linker (Figure 24A). Both fusions were overexpressed from the *GAL* promoter in episomal, centromeric and integrative vectors (*URA* locus) because we did not know whether they would be toxic for the cell.

V.1.4.1. **Overexpression of *SCC1-UBC9* up-regulates sumoylation levels of the cohesin complex**

To check sumoylation levels of different cohesin subunits, when *SCC1-UBC9* is overexpressed, Smc1, Smc3, and Scc1 were tagged with 18xmyc and SUMO with HF. Then, centromeric vectors expressing *SCC1-UBC9* and *SCC1* under the *GAL* promoter were transformed into this background. Cells were grown exponentially in selective media supplemented with raffinose, and the next day, they were transferred to selective

media supplemented with galactose to induce the expression of the constructs. Two hours after adding galactose cells were collected for pull-down analysis.

As seen in Figure 24B Scc1-Ubc9 itself shows increased levels of sumoylation, while modification of overexpressed Scc1 and Scc1-UD was much lower and not detected in this western blot. Curiously, we observed that inactivation of the SUMO peptidase domain by mutation of the catalytic cysteine 580 leads to levels comparable to those of a Scc1-Ubc9 fusion. Overexpression of a *SCC1-UBC9* fusion up-regulates sumoylation of Smc1 and Smc3. The Scc1-Ubc9 fusion affects the sumoylation of Smc1 to a higher degree than Smc3, most probably because of the physical proximity of Smc1 to the fused Ubc9 enzyme. On the other hand, *SCC1-UBC9* overexpression leads to a decrease in endogenous sumoylation levels of Scc1, probably because it competes for SUMO conjugation (Figure 24C).

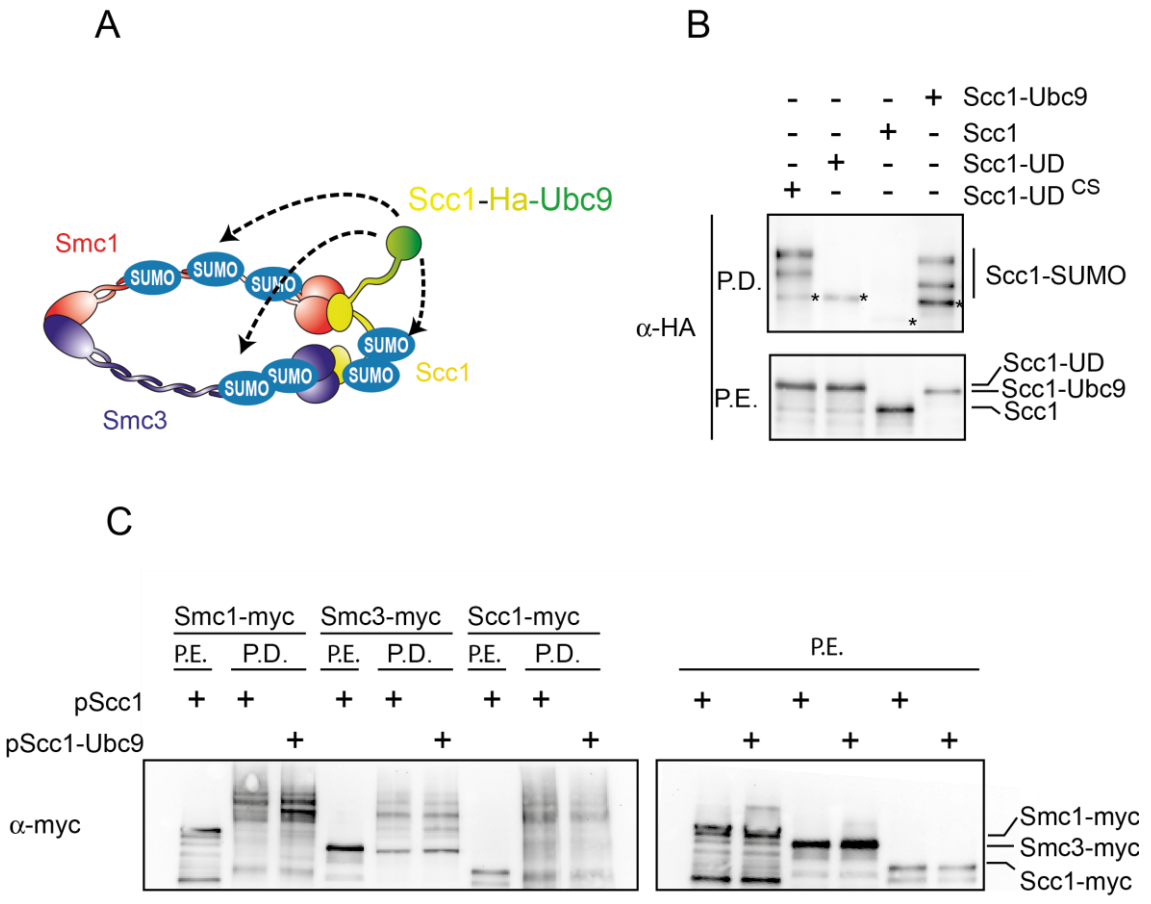

Figure 24. *UBC9* fusion to *SCC1* as a model to up-regulate sumoylation of the whole complex. (A) The C-terminus of Scc1 was fused to Ubc9 using the 3xHA epitope as a linker to allow the physical separation and proper folding of the two proteins. **(B,C) Overexpression of *SCC1-UBC9* up-regulates cohesin sumoylation.** To check sumoylation levels of different cohesin subunits when *SCC1-UBC9* was overexpressed, centromeric vectors overexpressing *SCC1-UBC9* (pTR918) and *SCC1* (pSM957) from the *GAL* promoter were transformed to cells that express *SMC1*, *SMC3*, and *SCC1* tagged with the 18xmyc epitope and HF-SUMO (YMB586, YSM1992, YMB748). Cells were grown exponentially in selective media supplemented with raffinose (raffinose: *GAL* promoter off), and then the next day, cells were transferred to selective media supplemented with galactose to induce the expression of the constructs. Two hours after adding galactose cells were collected for pull-down analysis. (B) Scc1-Ubc9 it self shows increased levels of sumoylation, while sumoylation of overexpressed Scc1 was not detected in this western. Scc1-UD shows no detectable levels of sumoylation, while inactivating the peptidase domain (Scc1-UD^{C580S}) restores sumoylation of Scc1. (C) Overexpression of *SCC1-UBC9* up-regulates sumoylation of Smc1 and Smc3. Sumoylation of Smc1 is more up-regulated with respect to Smc3 because of the proximity of this fusion to Smc1. Note that sumoyaltion of endogenous Scc1 is down-regulated when *SCC1-UBC9* is overexpressed, probably because it competes for SUMO conjugation.

V.1.4.2. **Scc1-UD down-regulates sumoylation levels of the cohesin complex**

To check sumoylation levels of different cohesin subunits when *SCC1-UD* is overexpressed, *SCC1-UD* and *SCC1-UD^{C580S}* were integrated in the *URA* locus in cells that express *HF-SUMO*, and *SMC1-9xmyc*, *PDS5-9xmyc*, or *SCC3-9xmyc*. Cells were grown exponentially in rich media supplemented with raffinose overnight, and then transferred to rich media supplemented with galactose to induce the expression of the constructs. Two hours after adding galactose, cells were collected and processed for pull-down analysis.

As seen in Figure 25B, overexpression of *SCC1-UD* lowers sumoylation of Smc1, Scc3 and Pds5. This decrease is dependent on the catalytic cysteine 580 in the Ulp domain, since its mutation to serine (Scc1-UD^{CS}) does not only allow recovery of wild-type cohesin sumoylation levels, but also up-regulates sumoylation of Smc1 and Pds5. Although sumoylation of Scc3 was detected when SCC1-UD^{cs} was overexpressed, the levels were slightly lower than in the wild-type. The up-regulation seen in Smc1 and Pds5 might be due to binding of the inactive domain to cohesin-SUMO conjugates, which would prevent the access of other SUMO peptidases. The reason why up-regulation of

sumoylation levels is stronger for some subunits than for others may be attributed to the position of this fusion with respect to these subunits.

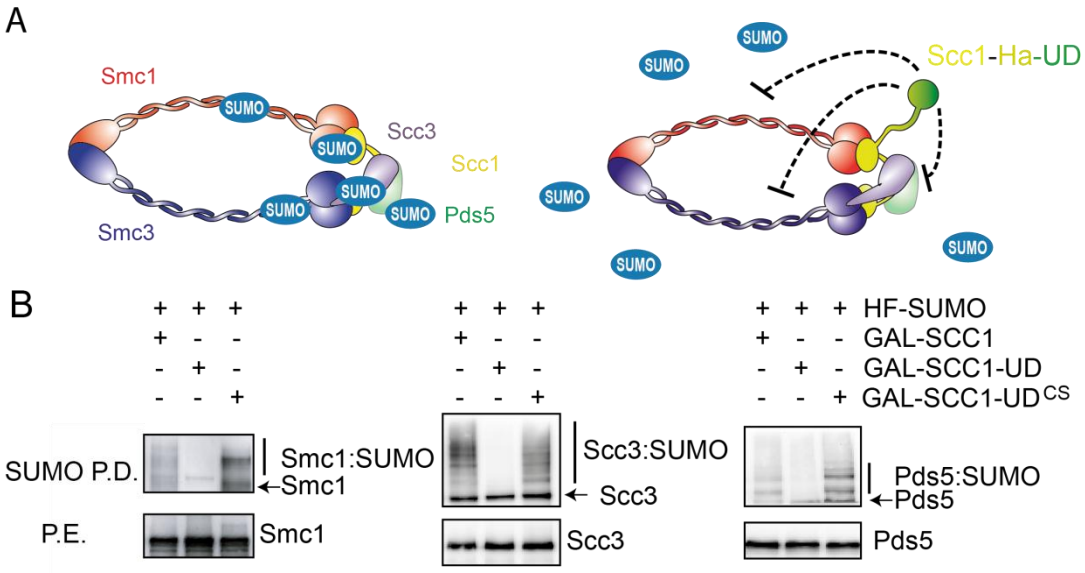

Figure 25. *ULP1* Domain (*UD*) fusion to *SCC1* as a model to down-regulate sumoylation of the cohesin complex. (A) The C-terminus of *SCC1* was fused to the *UD* of *ULP1* using the 3xHA epitope as a linker to allow the physical separation and proper folding of the two proteins. **(B) Overexpression of *SCC1-UD* decreases sumoylation levels of the cohesin complex.** To check sumoylation levels of different cohesin subunits, when *SCC1-UD* is overexpressed, *SMC1*, *PDS5*, and *SCC3* were tagged with the 9xmyc epitope, and SUMO was tagged with HF (YSM1486, YSM1488, YSM1490, YSM1744, YSM1746, YSM1748, YSM1750, YSM1752, YSM1754). Cells were grown exponentially in YP galactose, and then, collected for pull-down analysis. Note that overexpression of *SCC1-UD* lowers sumoylation of Smc1, Scc3 and Pds5. This decrease is dependent on the catalytic cysteine 580 in the Ulp domain, since its mutation to serine (Scc1-UD^{CS}) not only restores but actually up-regulates sumoylation of most cohesin subunits.

SUMO peptidases are very active, and their overexpression might reduce global protein sumoylation. We therefore replaced the strong *GAL* promoter with the *SCC1* promoter in the same integrative vector. Additionally, the endogenous *SCC1* gene was fused to an auxin inducible degron (Scc1-aid) to avoid competition with the fusions. As seen in Figure 26A, degradation of Scc1-aid by adding auxin to a final concentration of 1000 µM renders the cells inviable, which shows that the degron system is able to down-regulate the endogenous copy of Scc1. To check levels of sumoylation of different cohesin subunits in this background, *SMC1*, *SMC3*, *SCC3*, and *PDS5* were tagged with

the 9xmyc epitope and SUMO was tagged with HF. For pull-down analysis cells were grown exponentially in YPD, and then, auxin was added for two hours to degrade endogenous Scc1.

As shown in Figure 26B, the Scc1-UD fusion itself shows no detectable levels of sumoylation when expressed from its own promoter. Bands of slower mobility were detected above the unmodified form of Smc3-9xmyc in wild-type cells, but not in cells that express *SCC1-UD* as the only copy (Figure 26C). These bands correspond to SUMO modified forms of Smc3, since they are not detected when SUMO is not pulled down in a strain that lacks the HF tag on SUMO. As previously noted, inactivation of the catalytic site in the Ulp1 domain lead to abnormally high levels of sumoylation in Scc1-UD fusions. Similarly, sumoylation of Smc3 is up-regulated in the presence of Scc1-UD^{CS} (Figure 26C). We therefore created a new Scc1-UD fusion, called Scc1-UD^{FA,CS}, which contains an F474A mutation on the inactive UD^{CS} domain. This mutation is predicted to block binding of the Ulp domain to SUMO (Mossessova, Lima 2000). The Scc1-UD^{FA,CS} fusion restored wild-type levels of Scc1-UD and Smc3 sumoylation. Analogously to what we have seen when Scc1-UD is overexpressed from the *GAL* promoter, sumoylation of Smc1, Scc3, and Pds5 (Figure 26D) is down-regulated when *SCC1-UD* is expressed from the *SCC1* promoter as the only copy, an effect that is dependent on the catalytic and SUMO-binding activities of the UD.

Thus, fusing *SCC1* to the peptidase domain of Ulp1 (UD) down-regulates sumoylation of the whole complex whether expressed from the *SCC1* promoter as the only copy or overexpressed from the *GAL* promoter.

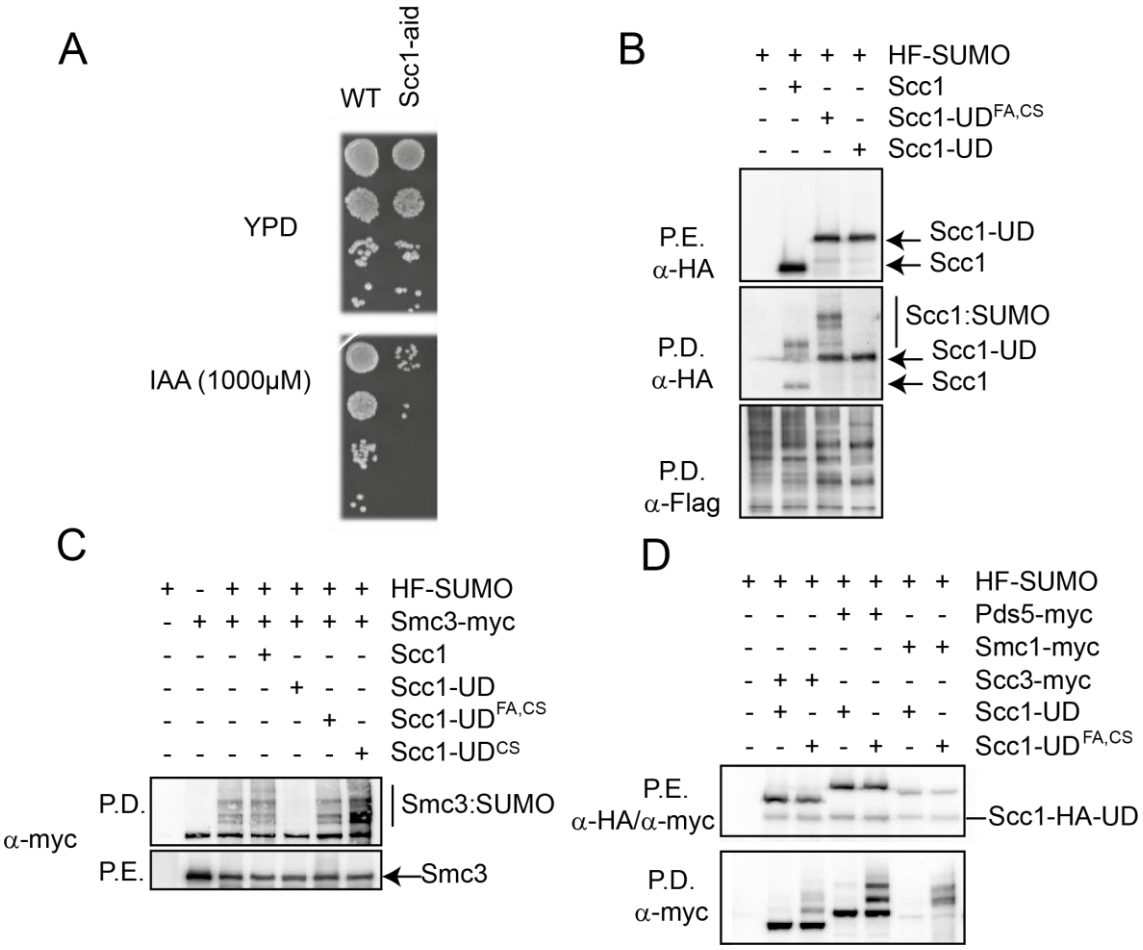

Figure 26. *SCC1-UD* expressed from the *SCC1* promoter decreases sumoylation levels of the cohesin complex. **(A)** Auxin down-regulates endogenous Scc1-aid. Note that cells that contain Scc1-aid are inviable in auxin (IAA) plates while wild- type cells are not affected (YMB1804, YSM1907). **(B)** The Scc1-UD fusion shows reduced levels of sumoylation when expressed at physiological levels. Sumoylation of Scc1 is restored to wild-type levels when the F474A mutation, known to prevent Ulp1 binding to SUMO was introduced in the inactive UD^{CS} domain ($Scc1\text{-}UD^{FA,CS}$) (YSM1907, YSM 2254, YSM 2256, YSM 2258). **(C)** Scc1 or the indicated Scc1-UD fusions were expressed under the control of the *SCC1* promoter from an ectopic location. The endogenous *SCC1* gene was fused to an auxin induced degron (Scc1-aid), and the protein was degraded before analyzing cohesin sumoylation. To check levels of sumoylation of cohesin subunits in this background, *SCC3*, *PDS5*, *SMC1*, and *SMC3* were tagged with the 9Xmyc epitope and SUMO with HF. Cells were grown exponentially in YPD, and then, auxin was added for two hours before pull down of SUMO conjugates. Sumoylation of Smc3 is also down-regulated when Scc1-UD is expressed from the *SCC1* promoter as the only copy. This decrease is dependent on the catalytic cysteine 580 in the UD, since its mutation to serine ($Scc1\text{-}UD^{CS}$) allows recovery of cohesin sumoylation. Note that this mutation not only restores but actually up-regulates sumoylation of Smc3, and that sumoylation of Smc3 is restored to wild-type levels when the F474A mutation is introduced in the inactive UD^{CS} domain ($Scc1\text{-}UD^{FA,CS}$) (YSM 1907, Y357, YSM 2297, YSM 2299, YSM 2301, YSM 2319). **(D)** sumoylation of Smc1, Scc3, and Pds5 is down-regulated when Scc1-UD is expressed from the *SCC1* promoter as the only copy. However, sumoylation levels are restored to wild-type levels when the $Scc1\text{-}UD^{FA,CS}$ is expressed (YTR907, YSM 2549, YSM 2550, YSM 2551, YSM 2552, YSM 2553, YSM 2554).

V.1.4.3. **Scc1-UD overexpression affects the growth rate of wild-type cells**

To check the phenotype of cohesin desumoylation we started by overexpressing *SCC1*, *SCC1-UD*, *SCC1-UD*^{CS} and *SCC1-UD*^{FA,CS} from the *GAL* promoter in wild-type background to avoid possible lethal effects. Serial dilution and replica plating of cells that express the different chimeras on glucose and galactose plates shows that overexpression of *SCC1-UD* is not toxic, but leads to subtle growth defects in wild-type cells. Cells that overexpress *SCC1-UD*^{CS} also seemed to interfere with growth of wild type cells (Figure 27A). To determine more accurately the effect on growth kinetics, we measured the generation time of cells that overexpress the different chimeras. Cells were grown overnight in YP raffinose, diluted to the same OD_{600} and split in two; in one half, the sugar raffinose was substituted with galactose to allow the expression of the fusions under the *GAL* promoter. As seen in Figure 27B wild-type cells that overexpress *SCC1-UD* have a slower growth rate, as indicated by the generation time (3,4 hours), compared to cells that overexpress *SCC1* or *SCC1-UD*^{FA,CS} (2 hours). This result indicates that overexpression of *SCC1-UD* might have a dominant negative effect on cohesin, and suggests that cohesin sumoylation might be required for proper cell growth.

A

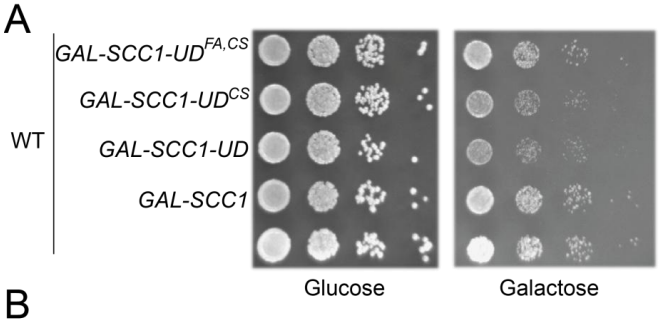

B

	Generation Time (hrs)	
	Raffinose	Galactose
Scc1	2,3	2,0
Scc1-UD	2,7	3,4
Scc1-UD^{FA,CS}	2,4	2,2

Figure 27. *SCC1-UD* overexpression shows growth defects in wild-type cells. (A) Overexpression of

SCC1-UD (YSM1494) in wild-type background (YSM1193) is toxic compared to that of *SCC1* (YSM 1492), *SCC1-UD*^{FA,CS} (YSM 1662) or *SCC1-UD*^{CS}(YSM 1496). **(B)** *SCC1-UD* overexpression affects growth rate of wild-type cells. Wild-type cells that overexpress *SCC1*, *SCC1-UD*, or *SCC1-UD*^{FA,CS} were grown overnight in YP plus raffinose. The next day cultures were diluted to the same OD_{600} and split in to two; in one of the two the sugar raffinose was substituted with galactose to allow the expression of the fusions under the *GAL* promoter. The OD_{600} was measured each hour for 8 hours. Note that wild-type cells that overexpress *SCC1-UD* have a slower growth rate, as indicated by the generation time (3,4 hours), compared to cells that overexpress *SCC1* or *SCC1-UD*^{FA,CS} (2 hours).

V.1.4.4. **Wild-type cells that overexpress *SCC1-UD* are sensitive to HU but not to MMS or UV**

Cohesin promotes SCR during DSB repair by bringing the two sister chromatids in close proximity (Heidinger-Pauli, Unal et al. 2008, Strom, Karlsson et al. 2007). In addition, cohesin is required for replication fork stability and for recovery of stalled replication forks (Tittel-Elmer, Lengronne et al. 2012). Cohesin mutants such as *scc1-73* are sensitive to replicative stress and to DNA damaging agents (Tittel-Elmer, Lengronne et al. 2012).

Thus, we decided to test whether cohesin sumoylation might also affect these functions. To this end we checked sensitivity of cells, that express/overexpress the different constructs, to MMS(0.01%), UV (25 mJ/cm^2), and HU (0.1M, 0.2M) by serial dilution and replica plating on glucose/ galactose plates. We used *nse2∆c* as a control because it is known to be sensitive to various types of DNA damage (Zhao, Blobel 2005, Andrews, Palecek et al. 2005).

As seen in Figure 28, *SCC1-UD* expressed under the *SCC1* promoter does not alter viability of cells in the presence of HU, MMS, or after exposure to UV light, compared to wild type cells. On the other hand, overexpression of *SCC1-UD* renders cells more sensitive to HU, but not to MMS or UV. This sensitivity depends on the SUMO peptidase activity of Ulp1, since inactivating this domain restores viability of these cells when exposed to HU. This suggests that cohesin sumoylation might be required during

replicative stress, but not in response to DNA the DNA lesions created by MMS or UV light.

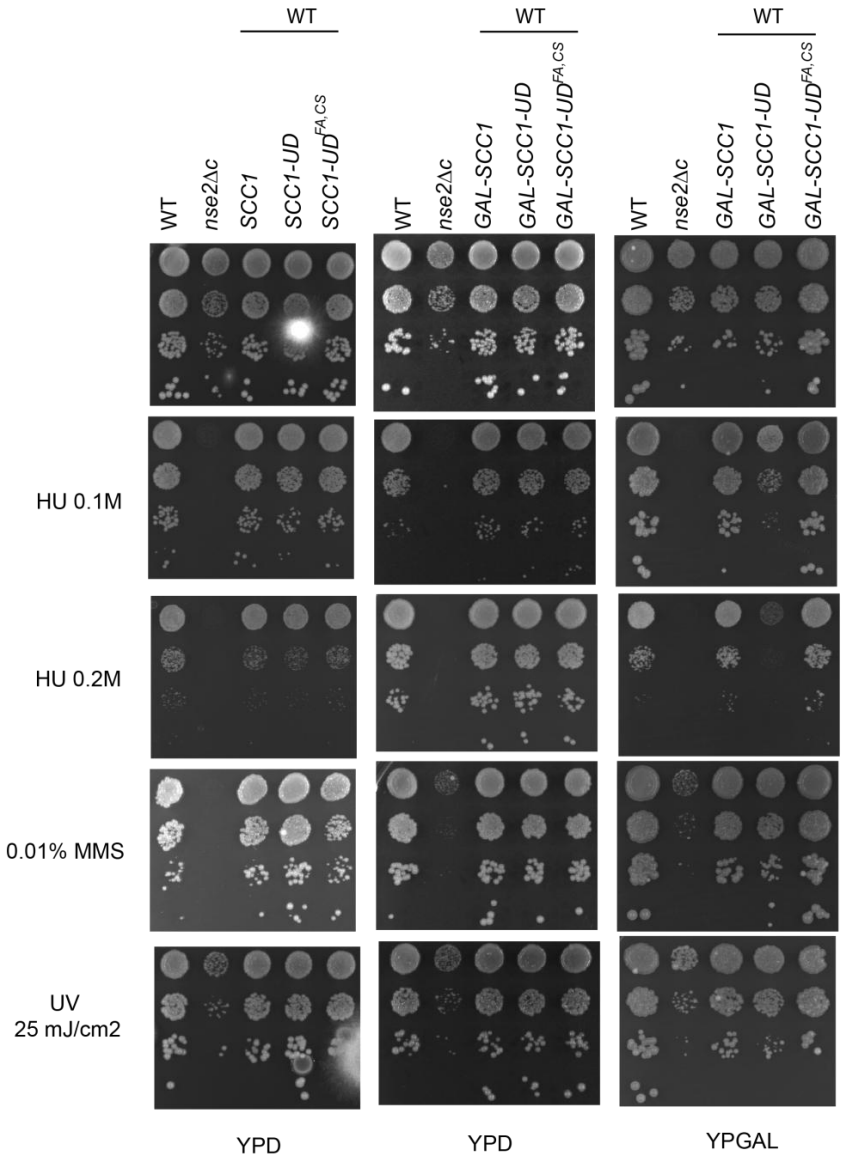

Figure 28. Wild-type cells that overexpress *SCC1-UD* are sensitive to HU but not to MMS or UV. Wild-type cells that express/overexpress *SCC1*, *SCC1-UD*, or *SCC1-UD*^{FA,CS} were plated by means of serial dilution and replica plating on their corresponding YPD and YP galactose plates and were exposed to UV light (25 μJ/cm^2). They were also plated on YPD and YP galactose plates that contained either MMS (0.01%) or HU (0.1M, 0.2M). Note that *SCC1-UD*, expressed from the *SCC1* promoter, does not alter viability of these cells in the presence of DNA damage (YSM1193, YSM 1864, YSM1758, YSM1961). On the other hand, overexpression of *SCC1-UD* renders cells more sensitive to HU, but not to MMS or UV (YSM1492, YSM1494, YSM 1662). This sensitivity depends on the SUMO peptidase activity of Ulp1 on cohesin, since inactivating this domain restores viability of these cells when exposed to HU. *nse2Δc* strain was used as a control due to its known sensitivity to DNA damage (YSM2406).

V.1.4.5. ***SCC1-UD*** **does not rescue growth defects of** ***scc1-73*** **at restrictive temperatures and is toxic at permissive temperatures when overexpressed**

To check the phenotype of cohesin desumoylation when *SCC1-UD* is expressed as the only copy in the cell, we transformed episomal vectors that overexpress from the *GAL* promoter *SCC1-UD*, *SCC1-UBC9*, *SCC1*, *ULP1* and *UBC9*, into *mcd1-1* thermosensitive allele. As seen in Figure 29A, overexpression of *SCC1* or *SCC1-UBC9* is able to recover the temperature sensitivity of *mcd1-1*, while overexpression of *ULP1*, *UBC9*, or *SCC1-UD* does not. This observation suggests that cohesin sumoylation is required for viability.

It has been shown that over-expression of a nuclear Ulp domain can be toxic (Mossessova, Lima 2000). Therefore, the phenotype observed in *mcd1-1* cells that overexpress the Scc1-UD fusion could be due to global desumoylation after accumulation of a SUMO peptidase in the nucleus.

To check this possibility we transformed episomal vectors that overexpress *SMC5-UD*, *SMC5-Ubc9*, *SMC5*, *ULP1* and *UBC9*, to an *smc5-11* thermosensitive allele. The *SMC5-UD* fusion is not toxic and is able to rescue growth of a thermosensitive *smc5-11* thermosensitive cells (Figure 29B), strongly suggesting that cohesin sumoylation is required for viability. We also noted that overexpression of *SMC5-UBC9* is toxic at permissive temperatures, suggesting that up-regulation of Smc5 sumoylation is lethal.

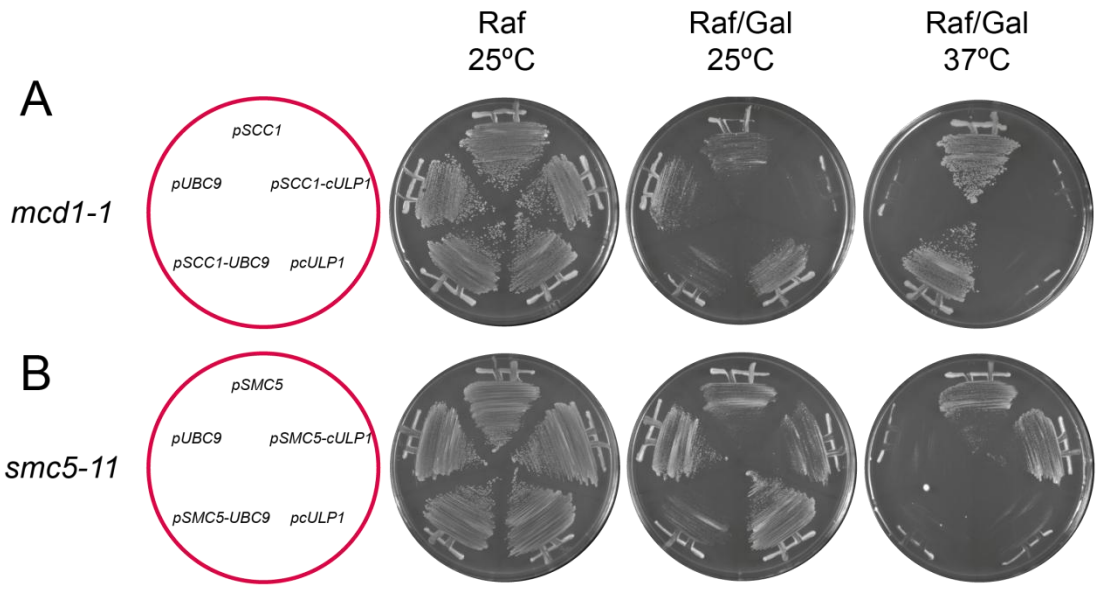

Figure 29. Overexpression of *SCC1-UD* from the *GAL* promoter is toxic in mcd1-1 thermosensitive background. (A) *mcd1-1 thermosensitive* cells (Y758), bearing multicopy vectors (pYES2) that express *SCC1* (pTR 879), *SCC1-UBC9* (pTR 871), *UBC9* (p827), *UD* (cUlp1 in the figure) (pTR 865) or *SCC1-UD* (pTR TR901) constructs from the *GAL* promoter, were plated on SC-raffinose (Raf; promoter off) or SC-galactose (Gal; promoter on) and allowed to grow at the permissive (25ºC) or restrictive (37ºC) temperature for *mcd1-1*. Note that *SCC1-UD* is toxic when overexpressed, and does not complement *mcd1-1* thermosensitivity. **(B)** *smc5-11* thermosensitive cells (YTR613), bearing multicopy vectors (pYES2) that express *SMC5* (pTR MB885), *SMC5-UBC9* (pTR 882), *UBC9* (pTR 827), *UD* or *SMC5-UD* (pTR 873) from the *GAL* promoter, were treated as in A. Note that both *SMC5* and *SMC5-UD* are able to complement the *smc5-11* thermosensitive phenotype, while overexpression of *SMC5-UBC9* does not, and is even toxic at permissive temperatures.

To check that these effects are dependent on the *SCC1* alleles used, we tested cell growth in *scc1-73* thermosensitive cells. Similar to what we have seen with the episomal vectors in *mcd1-1* thermosensitive cells, overexpression of *SCC1-UBC9* or *SCC1* is able to rescue temperature sensitivity of *scc1-73* cells, indicating that upregulation of cohesin sumoylation is not lethal (Figure 30A). On the other hand, overexpression of Scc1-UD does not suppress the temperature sensitivity of *scc1-73* cells at restrictive temperatures, and it is even toxic at permissive temperatures. This effect indicates a dominant gain of function of the Scc1-UD fusion over the endogenous hypomorphic *scc1-73* allele.

To avoid secondary effects of overexpression we substituted the *GAL* promoter with *SCC1* promoter and we integrated these constructs in the *URA* locus. The lethality is no longer observed when *SCC1-UD* is expressed at physiological levels from the *SCC1* promoter (Figure 30B); yet it does not complement the thermosensitive phenotype of *scc1-73* cells. Scc1-UD growth defects are suppressed by inactivation of the SUMO peptidase domain (Scc1-UD^{FA,CS}), suggesting that the phenotype seen is due to the specific SUMO peptidase activity on sumoylated cohesin.

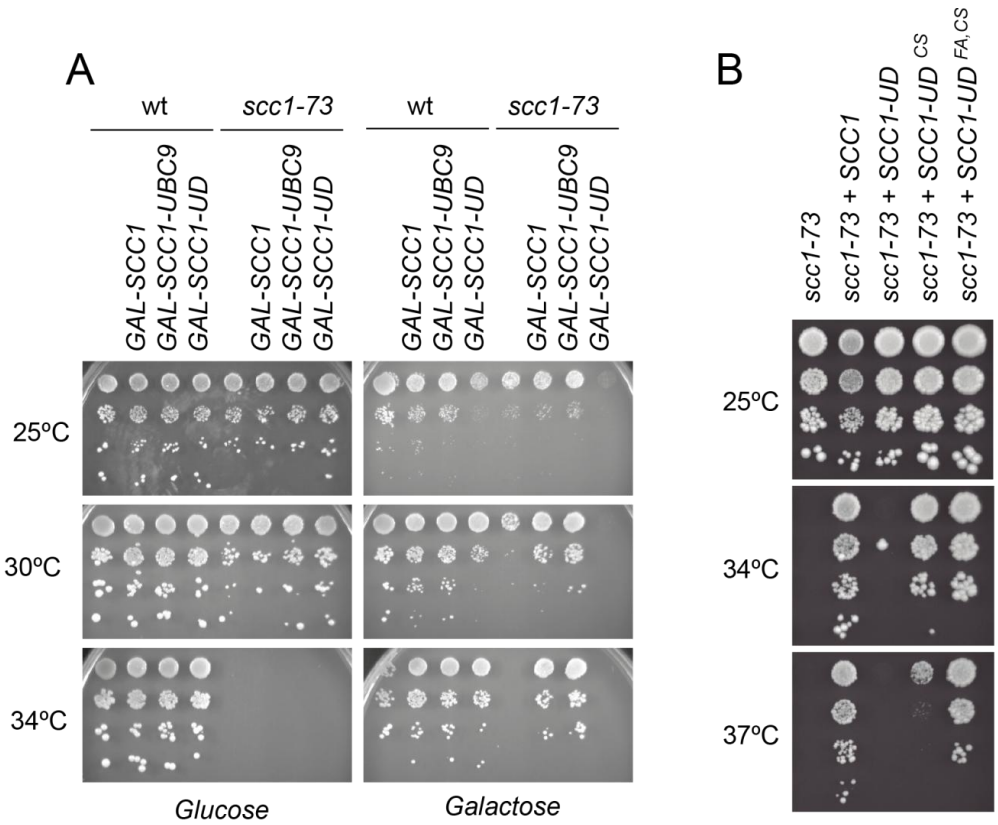

Figure 30. Cohesin sumoylation is required for viability. (A) Overexpression of *SCC1-UD* from the *GAL* promoter is toxic in *scc1-73* thermosensitive background. *scc1-73* thermosensitive cells (Y759) ectopically expressing *SCC1*, *SCC1-UD*, *SCC1-UBC9* (pSM957, pTR 918, pTR 921) from the *GAL* promoter in a centromeric vector (YCPlac111) were plated on glucose (promoter off) or galactose (promoter on) containing media, and allowed to grow at the indicated temperatures. Note that *SCC1-UD* is toxic when overexpressed in *scc1-73* cells, while an analogous fusion to the *UBC9* conjugase is not toxic and effectively complements the thermosensitive allele. **(B) *SCC1-UD* expressed from the *SCC1* promoter is not toxic at the permissive temperature, yet it does not complement the thermosensitive phenotype of *scc1-73* cells.** *scc1-73* thermosensitive cells ectopically expressing the indicated constructs from the *SCC1* promoter (YSM 1040, YSM1860, YSM1832, YSM1857, YSM 2155) were plated on YPD and allowed to grow at the

indicated temperatures. Note that expression of *SCC1-UD* does not complement *scc1-73* thermosensitivity, while expression of *SCC1-UD*^{FA,CS} completely rescues this phenotype.

Finally, we designed a different approach to down-regulate the endogenous copy of Scc1, using the degron system. The different DNA constructs were integrated at the *SCC1* locus by homologous recombination, leaving two copies of the *SCC1* gene driven by their corresponding *SCC1* promoters, one fused to the UD (SCC1-UD), and the other sensitive to auxin (*SCC1-aid*). As seen in Figure 31, cells are not viable when Scc1-aid is degraded by growth on auxin-containing plates, while expression of wild type *SCC1* restores viability. On the other hand, expression of *SCC1-UD* as the only copy in the cell renders cells inviable. This phenotype depends on the SUMO peptidase activity of Ulp1 because Scc1-UD growth defects can be suppressed by inactivation of the SUMO peptidase domain (Scc1-UD^{FA,CS}).

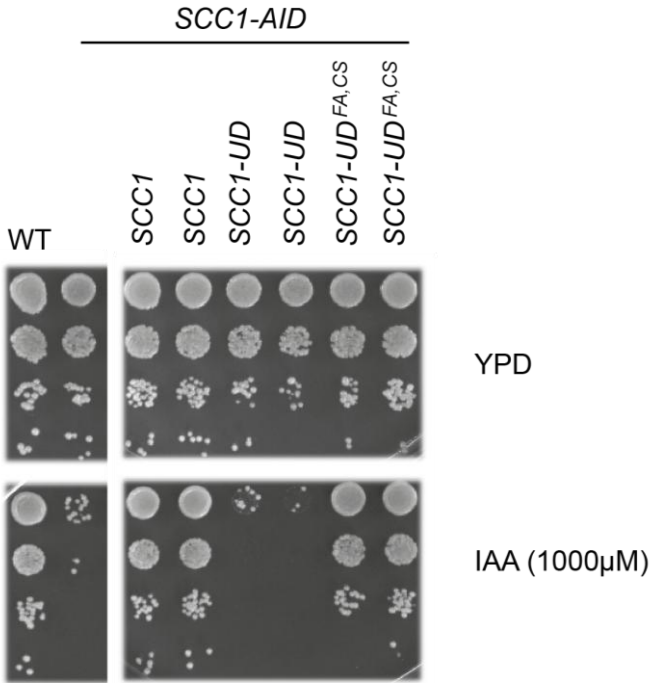

Figure 31. Expression of *SCC1-UD* as the only copy in the cell in Scc1 degron background is lethal. *SCC1*, *SCC1-UD*, and *SCC1-UD*^{FA,CS}, expressed from the *SCC1* promoter, were integrated in the *SCC1* locus (YSM2254/2255, YSM2256/2257, YSM2258/2259) in the Scc1-aid background (Y1907). Note that in the absence of Scc1 cells are not viable. Expression of *SCC1* restores viability, while expression of *SCC1-UD* as the only copy in the cell renders cells inviable. This phenotype depends on the SUMO peptidase

activity of Ulp1 because *SCC1-UD* growth defects can be suppressed by inactivation of the SUMO peptidase domain (*SCC1-UD*^{FA,CS}).

V.1.4.6. **Cells that express *SCC1-UD* as the only Scc1 copy accumulate in G2/M**

scc1-73 thermosensitive cells arrest in G2/M at the restrictive temperature. The arrest is dependent on activation of the spindle assembly checkpoint because of faulty cohesion and the inability to biorient chromosomes (Stern, Murray 2001). To understand the primary defect in cells expressing the Scc1-UD fusions, we studied cell cycle progression by FACS in synchronous cultures expressing *SCC1-UD* and the auxin-sensitive *SCC1-AID* allele. As seen in Figure 32, cells progress with normal kinetics through G1 and S phase, but arrest in G2/M when Scc1-aid is degraded. As expected, this effect is reversed by expression of wild-type *SCC1*. In contrast, the arrested cells do not progress beyond G2/M when *SCC1-UD* is expressed as the only copy. This failure depends on the SUMO peptidase activity of Ulp1, since cells that express *SCC1* fused to an inactive peptidase show normal cell cycle dynamics.

To monitor microscopically how cells that lack cohesin sumoylation progress throughout the cell cycle we arrested *scc1-73 thermosensitive* cells that have the tet operators(CenV)/tet repressor system and overexpress *SCC1, SCC1-UD, SCC1-UD*^{FA,CS} and *SCC1-UBC9* from the *GAL* promoter in G1 by α factor. Then, we released them at non permissive temperatures into a synchronous cell cycle and we added galactose to induce the *GAL* promoter. Next, we took samples every 15 minutes for analysis by FACS and fluorescence microscopy.

Similarly to what we have seen with the degron system, heat inactivation of *scc1* thermosensitive allele leads to cell cycle arrest in the G2/M transition (Figure 32B). In addition, overexpression of *SCC1*, *SCC1-UD*^{FACS}, or *SCC1-UBC9* allows cells to progress to the next cell cycle, while overexpression of *SCC1-UD* does not, further confirming our previous results with the degron system.

We analyzed the cells microscopically and scored them according to: budding, nuclear segregation, loss of SCC, and accumulation of mitotic cells with stretched nucleus in the neck (Figure 32 C,D). Cells that overexpress *SCC1* or *SCC1-UD* start to have small buds 30 minutes after release, and the number of budded cells reaches a maximum 105 minutes after release with similar kinetics. As expected, the number of budded cells in the wild-type culture starts to decrease as cells finish mitosis and start a new cell cycle. This decrease was not observed in cells that overexpress *SCC1-UD,* suggesting an accumulation of budded cells that are not able to finish cell division. The number of binucleated cells that overexpress wild-type *SCC1* peaks 135 minutes after release, while cells that overexpress *SCC1-UD* show a 60 minute delay in nuclear segregation; cells transiently arrest with two centromeric dots as mononucleated or with a stretched nucleus in the neck. It is worth noting that *SCC1-UD* overexpressing cells that eventually manage to finish mitosis have around 60% of missegregation (data not shown). Finally, we compared the kinetics of sister chromatid separation by counting budded cells with centromere V loss of cohesion (2 dots). Cells that express wild type *SCC1* start to lose SCC by 90 minutes, which corresponds to the time when cells start anaphase. In contrast, cells that express *SCC1-UD* start to show cohesion 60 minutes after G1 release, which corresponds to the time when cells start to replicate their DNA, as shown by the FACS profile. These results indicate that cells relying on Scc1-UD for cohesin function lose cohesion from the time of DNA replication, suggesting a defect in establishment of SCC.

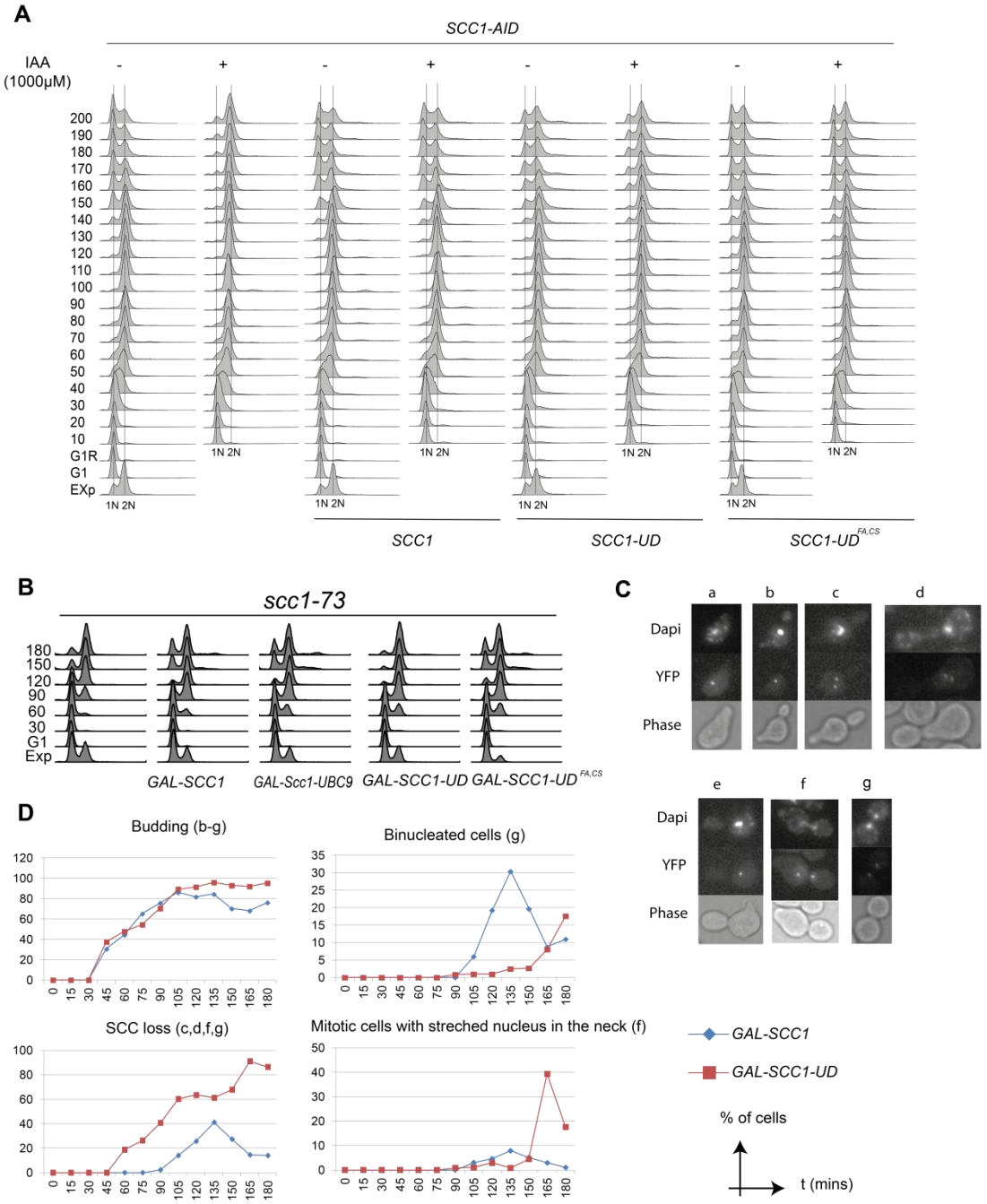

Figure 32. Cells that express *SCC1-UD* as the only copy accumulate in G2/M. (A) To study cell cycle progression of strains carrying *SCC1-UD* fusion in Scc1 degron background by FACS analysis, Auxin (1 mM) was added once cells were arrested in G1 with the alpha factor. Then, 30 minutes after auxin addition, cells were released by washing plus pronase addition, and samples were taken every 10 minutes for 200 minutes. Note that as Scc1-aid is degraded by auxin, cells accumulate in G2/M. When wild-type *SCC1* is expressed, cells manage to progress to the next cell cycle, while when *SCC1-UD* is expressed as the only copy, cells arrest again in G2/M. This arrest depends on the SUMO peptidase activity of Ulp1, as cells that express *SCC1*-UD^{FA,CS} do not arrest in G2/M (YSM1907, YSM 2254, YSM 2256, YSM 2258). **(B)** FACS analysis of *scc1-73 thermosensitive* cells (YSM1040) that have the tet operators(CenV)/tet repressor system and overexpress *SCC1* and *SCC1-UD SCC1-UD*^{FA,CS} *SCC1-UBC9* from the *GAL* promoter after arrest in G1 by α factor and release at 37°C in the presence of galactose. Note that overexpression of *SCC1* (YSM1860),

SCC1-UD^{FACS} (YSM1478), or *SCC1-Ubc9* (YSM1506) allows cells to progress to the next cell cycle, while overexpression of *SCC1-UD* does not. **(C)** Types of cells observed microscopically. a: G1 arrested cells with 1 nucleus and 1 dot, b: mononucleated cells that have a small bud and show one dot, c: mononucleated cells with separated dots and a small bud, d: mononucleated cells with separated dots and a large bud, e: mononucleated cells with one dot and a large bud, f: cells with a stretched nucleus in the neck and separated dots, g: binucleated cells with separated dots. **(D)** Budding was measured by counting all cells that have buds (b, c, d, e, f, g). SCC loss was measured by counting cells that show separated dots (c, d, f, g). The percentage of binucleated cells and mitotic cells with stretched nucleus in the neck was measured by counting one cell type (f and g respectively). Note that cells that overexpress *SCC1-UD* start to have cohesion defects at the onset of DNA replication and accumulate as mononucleated cells with large buds and separated dots or with stretched nucleus in the neck and fail to finish mitosis.

V.1.4.7. **Cohesin rings are properly assembled around an Scc1-UD fusion**

A possible explanation for the inviability of Scc1-UD fusions could be their inability to properly interact with the SMC (Smc1 and Smc3) and/or the non-SMC subunits (Scc3, Pds5). A different, but not contradictory possibility is that cohesin sumoylation might be required for cohesin ring formation. To check these possibilities we tagged *SMC3* with the 9xmyc epitope in cells that overexpress HA-tagged *SCC1*, *SCC1-UD*, and *SCC1-UBC9* from the *GAL* promoter. Cells were grown overnight in rich media supplemented with raffinose, and galactose was then added to induce expression of the different constructs. Cells were collected two hours after induction, and processed for anti-myc immunoprecipitation (IP). As seen in Figure 33A Scc1-UD coimmunoprecipitates (CoIP) with Smc3 to similar levels as Scc1-Ubc9 and Scc1.

Overexpression of cohesin subunits may trigger interaction between different cohesin complexes, something that is not normally seen under physiological conditions (Zhang, Kuznetsov et al. 2008). To make sure that the interaction that we see is not caused by overexpression conditions, we reanalyzed the co-immunoprecipitation in cells that expressed the different fusions from the *SCC1* promoter. Smc3-9xmyc is able to co-immunoprecipitate similar amounts of Scc1-UD, Scc1 or Scc1-UD^{CS} (Figure 33B). Scc1 binding to Smc1 is upstream to that with Smc3, which suggests that Scc1-UD is also able to properly interact with Smc1. These findings indicate that fusion of Scc1 to the

peptidase domain (UD) does not affect its interaction with the SMC subunits, and further indicates that sumoylation is not required for cohesin ring formation.

Next, we studied interaction with Scc3 and Pds5. CoIP experiments show that Scc1-UD interacts with Pds5 (Figure 33C) and Scc3 (Figure 33D) with similar efficiencies as wild-type Scc1 or Scc1-UD^{FA,CS}, suggesting that neither fusion of Scc1 to the SUMO peptidase nor decrease in sumoylation levels affect interaction between Scc1 and non-Smc subunits.

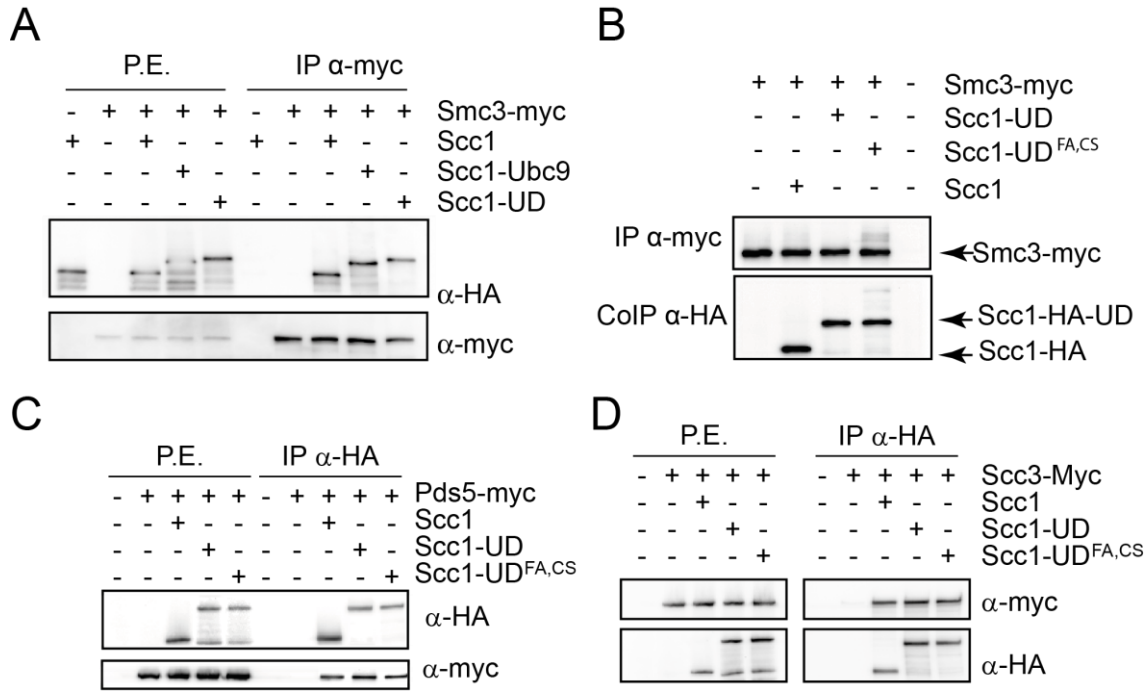

Figure 33. Cohesin rings are properly assembled around Scc1-UD. (A) Scc1**-UD overexpressed from the *GAL* promoter interacts with Smc3.** Smc3 was tagged with the 9xmyc epitope (Y1193) in cells that overexpress HA tagged *SCC1*, *SCC1-UD*, and *SCC1-UBC9* from the *GAL* promoter (pSM957, pTR921, pTR 918). A strain that has HA tag on *SCC1* but no myc tag on Smc3 was used as a control to check for nonspecific binding of Scc1 or HA epitope to the magnetic beads coupled to anti-myc antibody used in the immunoprecipitation experiment (IP). A strain that has no HA tag on *SCC1* was used to discard unspecific bands recognized by the primary anti-HA antibody. Cells were grown overnight in rich media supplemented with raffinose. The next day, raffinose was substituted with galactose to induce expression of the different constructs. Then, cells were collected two hours after induction, and processed for anti-myc IP. Eluted proteins were loaded in separate gels to check for both IP and coimmunoprecipitation (CoIP). Note that Scc1-UD coimmunoprecipitates with Smc3 similar to Scc1-Ubc9 and Scc1. **(B) Scc1-UD expressed from the *SCC1* promoter interacts with Smc3.** Scc1-UD expressed from the *SCC1* promoter

coimmunoprecipitates with Smc3-9xmyc under physiological conditions with similar efficiencies to Scc1 and Scc1-UD^{CS} (YSM1193, YSM1758, YSM1844, YSM1864) . **(C and D) Fusion of Scc1 to the SUMO peptidase domain (UD) does not interfere with its interactions with non-Smc subunits.** Pds5 and Scc3 were tagged with the 9xmyc epitope in cells that express *SCC1*, *SCC1-UD* , *SCC1-UD*^{FA,CS} from the *SCC1* promoter. Strains that have myc epitope tag on *SCC3*/ *PDS5*, but no HA epitope tag on *SCC1*, were used as a control to check for unspecific binding of Scc3/ Pds5 or the myc epitope to HA beads, used for the IP. Strains that have no epitope tag on any cohesin subunit were used to discard unspecific bands recognized by either the myc or HA primary antibodies. Exponentially growing cells were collected and processed for anti-HA IP. The eluted proteins were loaded in separate gels to check for both IP and CoIP. Note that Scc1-UD is able to interact with Pds5 (C) and Scc3 (D) with similar efficiencies as wild-type Scc1 or Scc1-UD^{FA,CS} (YSM2121, YSM 2123, YSM 2125, YSM 2126, YSM 2128, YSM 2130, YSM 1734, YSM 1735, YTR907).

V.1.4.8. **Cohesin rings assembled around an Scc1-UD fusion are efficiently recruited to chromatin**

Another possible explanation for the Scc1-UD inviability is that down-regulation of cohesin sumoylation might impair its binding to chromatin. To explore this possibility, exponentially growing cultures of wild-type strains that express *SCC1-UD* or *SCC1-UD*^{FA,CS} , were collected and processed by chromatin fractionation to separate Triton X-100 soluble supernatant and chromatin pellet fractions. Histone H3 was used as a chromatin marker, while hexokinase was used as a cytosolic marker. Additionally, Rpd3 was used as a marker for a nuclear protein that faintly binds to chromatin. As shown in Figure 34, we detected no difference in chromatin binding between Scc1-UD^{FA,CS} chimera and the unsumoylated Scc1-UD, suggesting that neither the fusion nor down-regulation of cohesin sumoylation can affect recruitment of cohesin to chromatin.

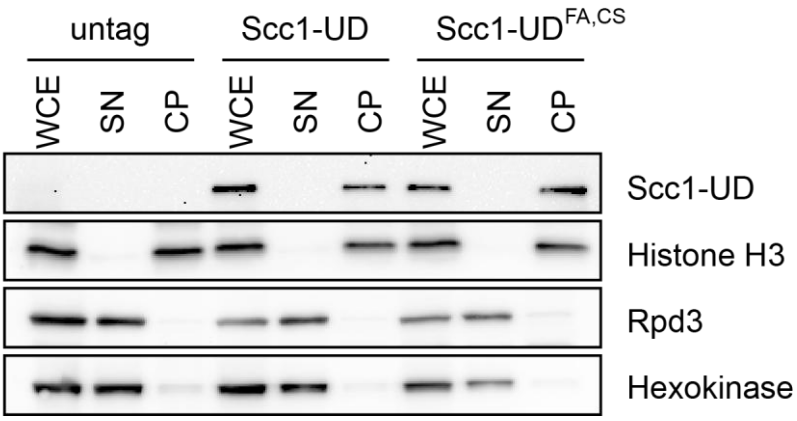

Figure 34. Cohesin rings assembled around Scc1-UD are efficiently recruited to chromatin. Cells expressing no HA-tagged protein (YSM1907), *SCC1-UD* (YSM2256), or *SCC1-UD*^{FA,CS} (YSM2258) were grown to exponential phase and samples were taken for chromatin fractionation. Blots were probed for the Scc1 fusions with anti-HA. Controls for a chromatin bound protein (histone H3), nuclear soluble (Rpd3), and cytoplasmic soluble (Hexokinase) proteins are also shown. Note that Scc1-UD and Scc1-UD^{FA,CS} are similarly bound to chromatin. WCE, whole-cell extract; SN, soluble supernatant; CP, chromatin pellet.

V.1.4.9. **Scc1-UD is found at known cohesin binding sites**

Although we have seen that unsumoylated cohesin is recruited to chromatin, it might not be recruited to the same sites as wild-type Scc1. To explore this possibility, exponentially growing cultures of wild-type strains that express wild-type *SCC1*, *SCC1-UD* or *SCC1-UD*^{FA,CS} , were cross linked with formaldehyde, collected and processed for anti-HA chromatin immunoprecipitation followed by CHIP hybridization (ChIP-on-CHIP). Analysis of obtained chromatin enrichment profiles showed that Scc1, Scc1-UD^{FA,CS} and the unsumoylated Scc1-UD bind to the same places on all chromosomes in *S. cerevisiae*. An example of the different profiles obtained for the three strains on chromosome I is seen in Figure 35.

As exemplified for the relatively small chromosome 1, cohesin loading is enriched at the centromere, convergent sites, and some origins of replication similarly in the wild-type Scc1, Scc1-UD^{FA,CS}, and the unsumoylated Scc1-UD. In addition, no enrichment is seen for any of the Scc1 chimeras in sites of divergent genes. We also determined average profiles for known binding sites including: early origins of replication, centromeres, and convergent ORFs. As shown in Figure 36, the profiles of the three strains coincide. Moreover, the average profiles also coincide for divergent ORFs, to which cohesin does not normally bind. These results support the notion that fusion of Scc1 to the SUMO peptidase domain (UD) does not affect its localization to known cohesin binding sites, and that cohesin sumoylation is not required to localize cohesin to these sites.

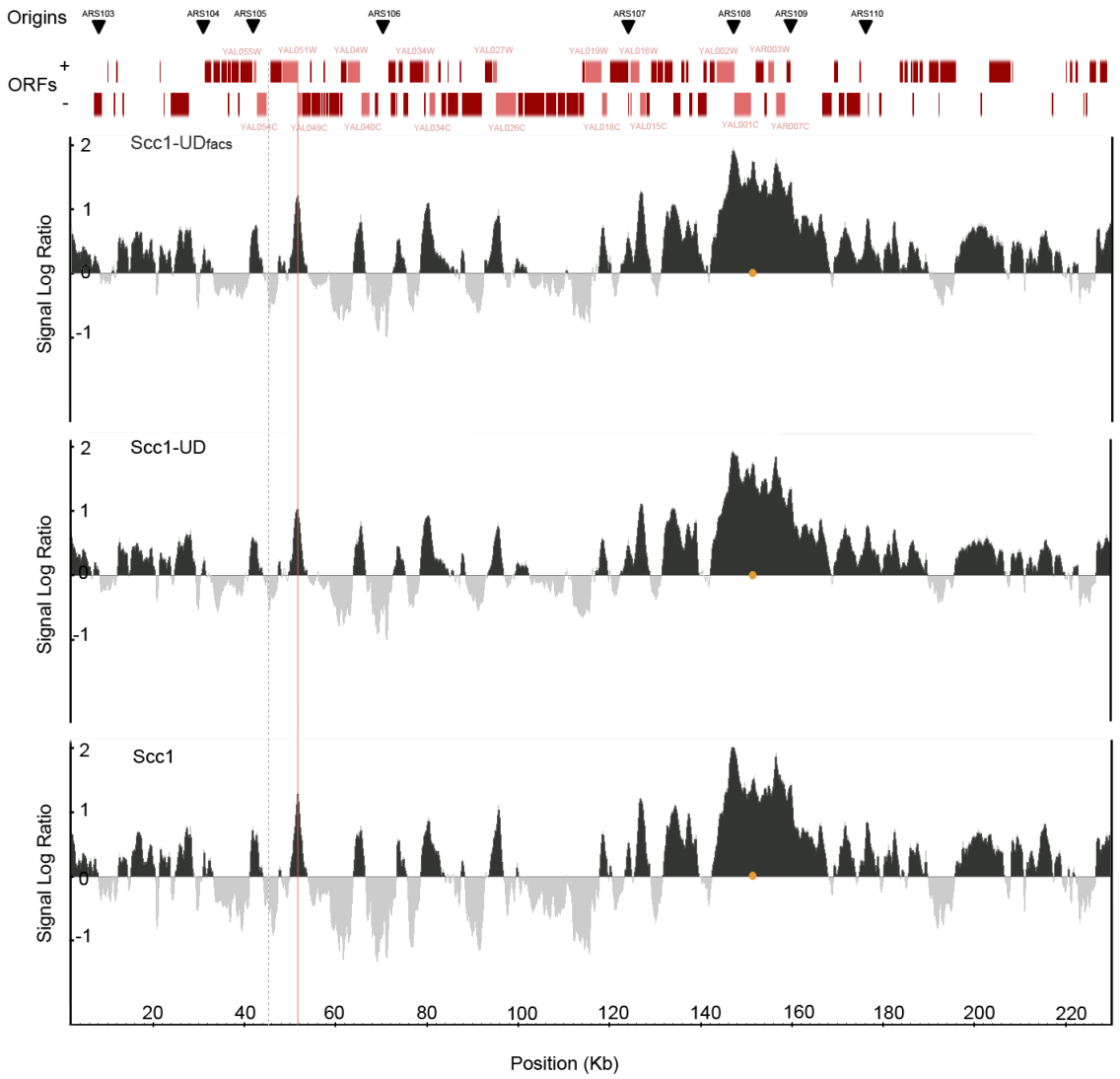

Figure 35. Cohesin ChIP-on-chip: Scc1-UD and Scc1-UD^{FA,CS} localize to the same regions as WT Scc1.. Exponentially growing cultures were cross-linked with formaldehyde (final concentration 1%). After cell breakage and sonication, chromatin Immunoprecipitation (Anti-HA) was performed. The precipitated DNA and the cell extract from each strain were reverse cross-linked, amplified, labeled, and hybridized to a separate GeneChip *S. cerevisiae* Tiling 1.0R Array. Cohesin Scc1 (YSM2254), Scc1-UD (YSM2256), and Scc1-UD^{FACS} (YSM2258) enrichment is shown for chromosome I. The signal log ratio (Log2), represented in the Y-axis, was generated from the two sample comparison analysis i.e. Scc1 enrichment in the Immunoprecipitated fraction relative to Input genomic DNA. The position is represented in (Kbs) in the X-axis. Red Bars represent genes transcribed from left to right and opposite. Pink bars within the red bars represent some convergent genes. The centromere is represented by a yellow circle. Origins of replication are depicted by black triangles. Note that cohesin loading is enriched at the centromere, convergent sites, and some origins of replication similarly in the three backgrounds. An example of 2 convergent genes is shown by a pink line. Cohesin doesn't bind to sites of divergent genes. An example of a divergent site is marked by a dashed black line.

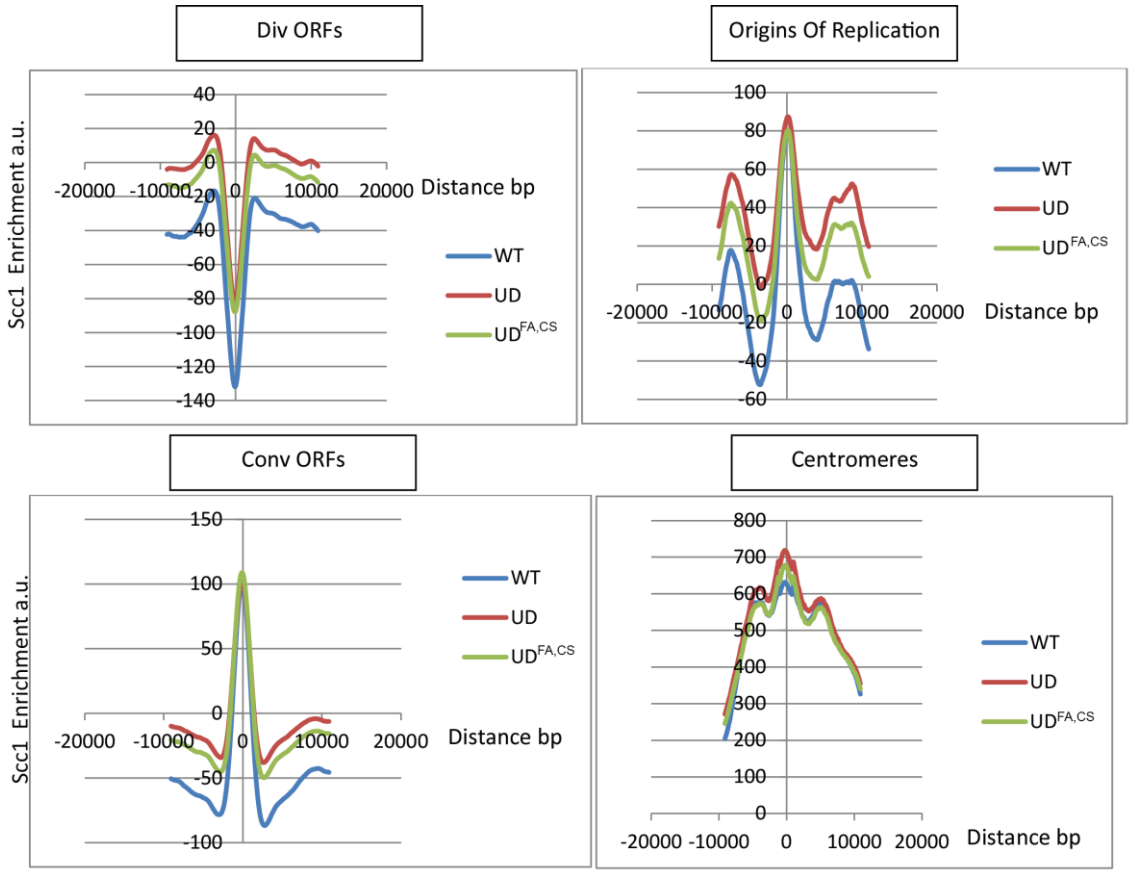

Figure 36. Average ChIP-On-CHIP profiles of the genome-wide localization of Scc1 (YSM2254), Scc1-UD (YSM2256), and Scc1-UD^{FA,CS} (YSM2258). Since cohesin is known to be enriched at origins of replication, centromeres, and between genes that are transcribed in converging directions (Conv), but not genes that are transcribed in diverging orientation (Div), the average profiles were compared in these four sites. Annotations from the *Saccharomyces* Genome Database (SGD) were used to determine median enrichment, which was calculated, in arbitrary units (a.u.), for 20 kb regions centered on these regions with a 2 kb window and a 100 bp step. The X-axis represents the distance in bp and the Y-axis represents Scc1 enrichment in a.u. Note that Scc1, Scc1-UD^{FA,CS}, and the unsumoylated Scc1-UD are enriched at known cohesin binding regions, and not between genes that are transcribed in diverging directions.

Cohesin is enriched in the vicinity of double strand breaks (DSB) in response to DNA damage, and is required to maintain sister chromatids in close proximity to promote SCR, and thus, damage repair. To see whether cohesin recruitment to DSB is affected by its sumoylation state, centromeric vectors, expressing Scc1 chimeras under the conditional *GAL* promoter, were introduced into wild-type cells that also express the HO endonuclease from the *GAL* promoter. Addition of galactose simultaneously triggered expression of the chimeras and induction of an HO-mediated single irreparable DSB. The efficiency of DSB formation were monitored microscopically by formation of Ddc2-

GFP DNA repair foci. As seen in Figure 37A, 6 hours after adding galactose almost all the cells had accumulated Ddc2-GFP DNA repair foci, reporting the formation of a DSB. Overexpression of *SCC1*, *SCC1-UBC9*, and *SCC1-UD* from the *GAL* promoter was monitored by western blot (Figure 37B). The presence of an irreparable double strand break lead to similar enrichment of Scc1, Scc1-UD, and Scc1-Ubc9 in the vicinity of DSBs (Figure 37D), as tested by quantitative Chromatin immunoprecipitation (ChIPq).

It is worth noting that the Scc1-UD fusion was quantitatively recruited with higher efficiency to the lesion. Although not quantitative, results from the Chip-on-chip experiments also suggest higher enrichment of unsumoylated cohesin (figure 36). We currently do not know the reason for this increase in binding of unsumoylated cohesin. An intriguing possibility is that cohesin sumoylation might be involved in separase-dependent removal of cohesin during resection. It has been described that cohesin needs to be removed by separase at the site of DSB so that resection proteins can access the damage site (McAleenan, Clemente-Blanco et al. 2013).

Nevertheless, our results show that unsumoylated cohesin is enriched in the vicinity of DSB and that sumoylation is not required for cohesin loading to DSBs.

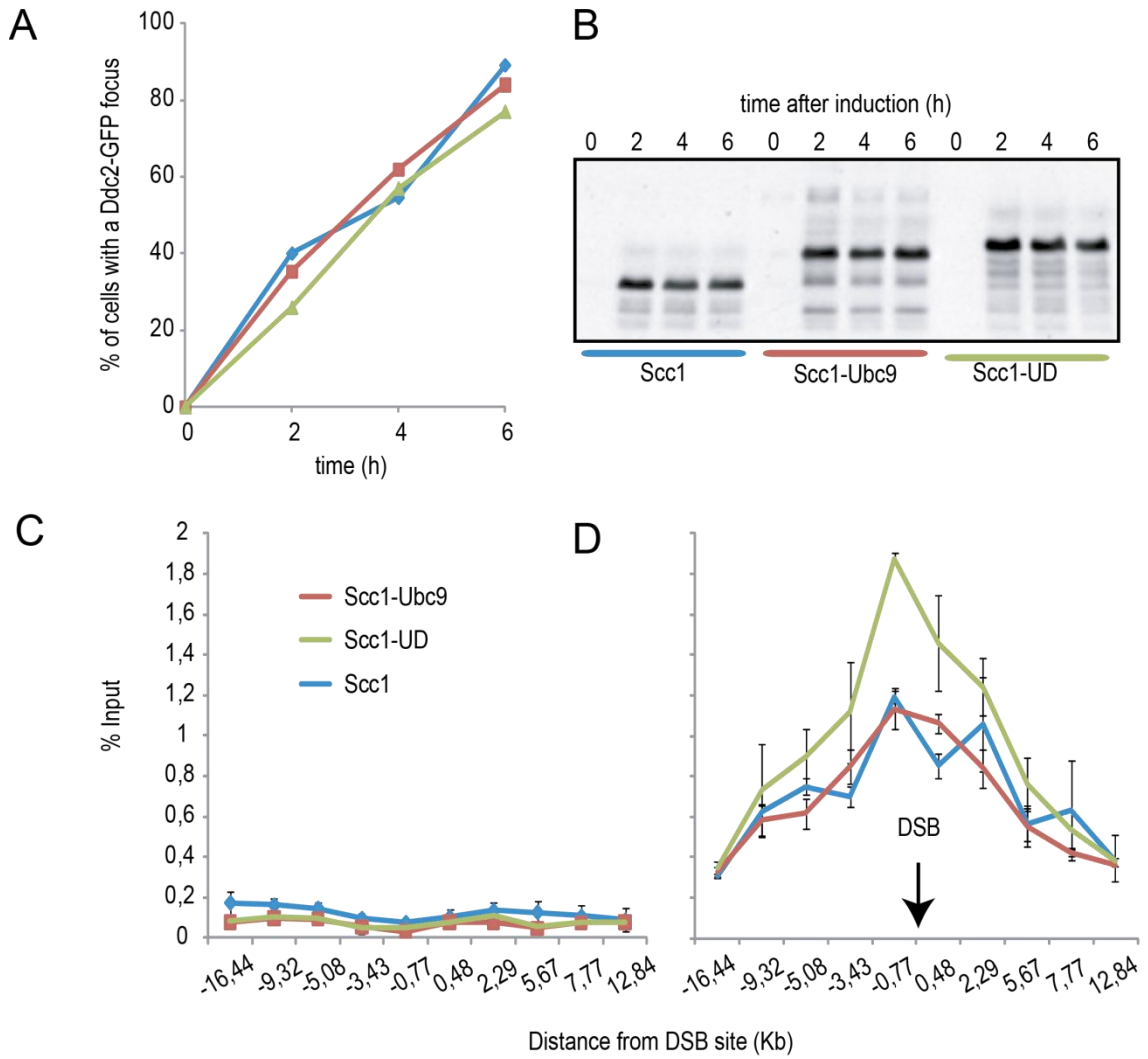

Figure 37. Scc1-Ubc9 and Scc1-UD are efficiently recruited to a DSB. Centromeric vectors, expressing *SCC1, SCC1-UD, SCC1-UBC9* from the conditional *GAL* promoter, were introduced in wild-type cells that also express the HO endonuclease from the *GAL* promoter. **(A)** HO induces a single irreparable double strand break (DSB), and the efficiency can be monitored microscopically by formation of Ddc2-GFP DNA repair foci. **(B)** Western blot analysis of protein fusion expression at different times after galactose addition. **(C and D)** Chromatin immunoprecipitation (ChIP) of Scc1 fusions. C: time0 before galactose addition. D: 6 hours after galactose addition. Note that both Scc1 and Scc1-Ubc9 are similarly enriched in the around DSBs, while Scc1-UD seems to be more enriched.

V.1.4.10. *SCC1-UD* overexpression does not affect global levels of sumoylation

One reason for the lethal phenotype of *SCC1-UD* expressing cells could be the desumoylation of other proteins in the cell. To check this possibility, we decided to check global sumoylation levels in both systems. Exponentially growing cultures of cells that express *SCC1-UD* from the *SCC1* promoter or from the *GAL* promoter, were compared

to cells that do not express any of the fusions by pull-down analysis. As seen in Figure 38, global sumoylation levels in cells that express *SCC1-UD* from the *GAL* promoter are very similar to those seen in cells that express *SCC1-UD* from the *SCC1* promoter or do not express any fusion. In addition, the levels of free SUMO, i.e. SUMO not conjugated to proteins, are also similar, indicating that the decrease in cohesin sumoylation upon expression/overexpression of *SCC1-UD* is specific and is not secondary to reduction in the global amount of sumoylated proteins in the cell.

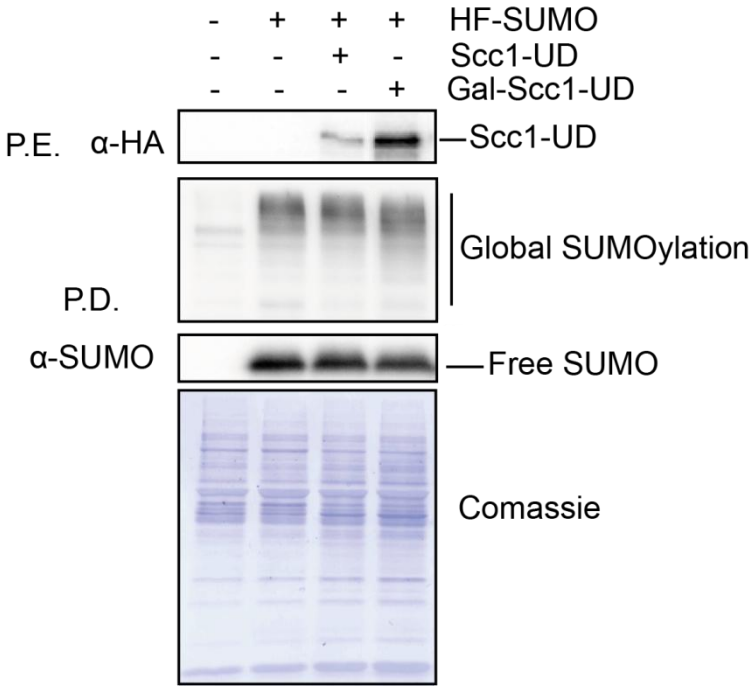

Figure 38. *SCC1-UD* overexpression does not affect global levels of sumoylation. Exponentially growing cultures of cells that express *SCC1-UD* from the *SCC1* promoter (YSM1758) or from the *GAL* promoter (YSM1660) were compared to cells that do not express any of the fusions (YSM1193) by pull-down analysis. Global sumoylation levels in cells that express *SCC1-UD* from the *GAL* promoter (fourth lane) are very similar to those seen in cells that express *SCC1-UD* from the *SCC1* promoter (third lane) or do not express any fusion (second lane). In addition, the levels of free SUMO, i.e. SUMO not conjugated to proteins, are also similar. Cells in the first lane (YTR248, control) have no tag on SUMO, and thus SUMO conjugates are not enriched. No difference is detected in the amount of protein loaded as seen by the comassie staining.

V.1.4.11. **Scc1-UD has minor effects in sumoylation of nearby proteins**

Next, we tried to check whether the presence of Scc1-UD within the cohesin ring can affect sumoylation of other nearby proteins. One of the first proteins that we checked was Ycs4, which belongs to the condensin complex, and has been reported to be sumoylated (D'Amours, Stegmeier et al. 2004). To this end, we tagged Ycs4 with the 9xmyc epitope in an Scc1 degron background; *SCC1-UD* or *SCC1-UD*^{FA,CS} were expressed from the *SCC1* promoter. As seen in Figure 39, there is no decrease in sumoylation levels of Ycs4 in *SCC1-UD* expressing cells as compared to *SCC1-UD*^{FA,CS}, indicating that the presence of Scc1-UD does not affect sumoylation of nearby condensin proteins.

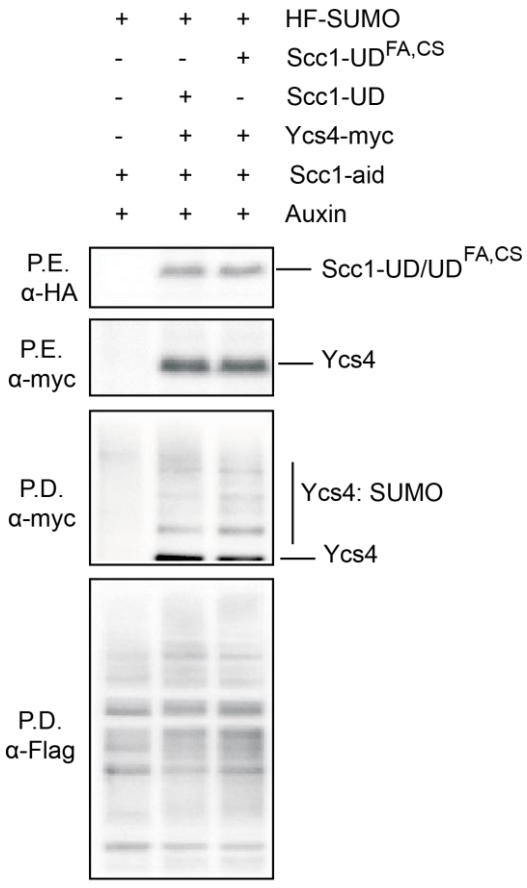

Figure 39. *SCC1-UD* expression as the only copy does not affect sumoylation of condensin. *YCS4* was tagged with the 9xmyc epitope in Scc1 degron background (YSM 1907), and *SCC1-UD* (YSM 2458) or *SCC1-UD*^{FA,CS} (YSM 2459) were expressed from the *SCC1* promoter. For pull-down analysis, auxin was

added to exponentially growing cultures for two hours to degrade the endogenous Scc1, and use Scc1-UD or Scc1-UD^{FA,CS} as the only copy in the cell. Note that there is no decrease in sumoylation levels of Ycs4 when Scc1-UD is expressed as the only copy (second lane) compared to that of Scc1-UD^{FA,CS} (third lane).

We also wondered whether sumoylation of proteins that are directly involved in DNA replication, such as PCNA, might be affected in the presence of Scc1-UD within the cohesin ring, and whether the change in sumoylation levels brought upon can affect their function during DNA replication. Sumoylation of PCNA at K164 is required during DNA replication to avoid unnecessary recombination intermediates in the presence of replicative stress. Siz1 is the SUMO E3 ligase required for PCNA sumoylation. PCNA monoubiquitylation at the same K164 by Rad18 E3 ligase is required for damage bypass. It has been described that *rad18*Δ cells are highly sensitive to MMS. However, abolishing PCNA sumoylation by *siz1*Δ can suppress this MMS sensitivity at low concentrations (0.001%) (Parker, Ulrich 2012).

We reasoned that if Scc1-UD has the same effect on PCNA as *siz1*Δ, sumoylation levels of PCNA when *SCC1-UD* is expressed would be as low as in *siz1*Δ. In addition, Scc1-UD expression might be able to suppress MMS sensitivity at 0.001%. As seen in Figure 40A, while *siz1*Δ abolishes sumoylation of PCNA, there is only a small decrease in sumoylation levels of PCNA when Scc1-UD is expressed compared to that of wild type Scc1 or Scc1-UD^{FA,CS} expression. In addition and as expected, we have seen that *rad18*Δ cells start to be sensitive to MMS at very low concentrations (0.0003%). Deletion of *SIZ1* in *rad18*Δ cells rescues their MMS sensitivity at 0.0005%, while expression of *SCC1-UD* does not (Figure 40B), suggesting that Scc1-UD might slightly affect PCNA sumoylation levels without affecting its function during replicative stress.

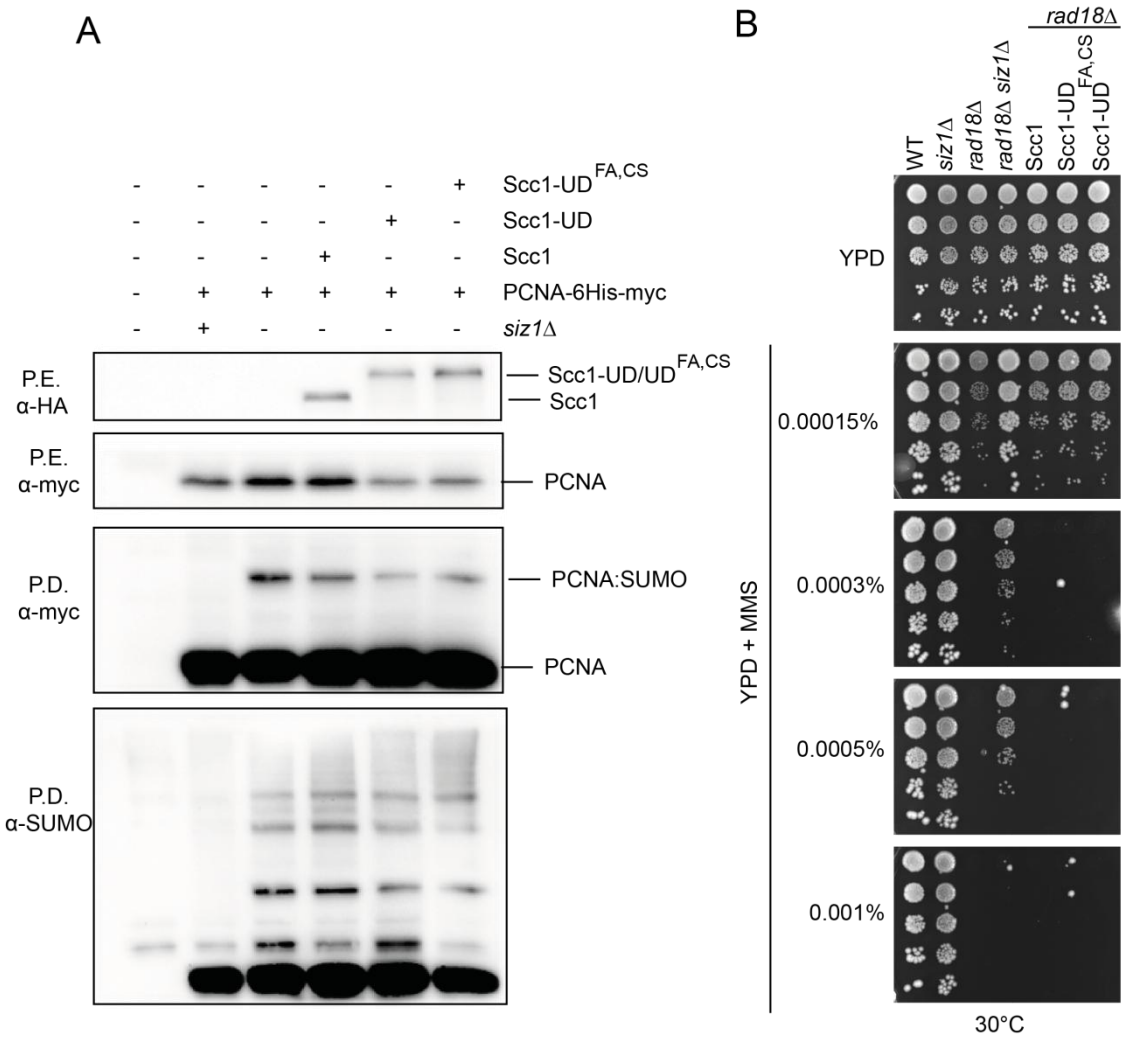

Figure 40. Scc1-UD might slightly affect sumoylation of PCNA without altering its function. (A) *siz1*Δ abolishes sumoylation of PCNA (Y756), while there is a small decrease in sumoylation levels of PCNA when *SCC1-UD* is expressed (YSM2420) compared to that of *SCC1-UD*^{FA,CS} (YSM2421), or wild type levels of sumoylation (Y735 and YSM2419 respectively). Yeast strain 312 was used as a negative control (first lane). **(B)** *rad18*Δ (Y402) starts to show MMS sensitivity at 0.00015%, and does not grow at all at 0.001%. Note that Expression of *SCC1* (YSM2533), *SCC1-UD* (YSM2535), or *SCC1-UD*^{FA,CS} (YSM2537) does not suppress MMS sensitivity of *rad18*Δ at 0.0005%, while deletion of *siz2* (YSM2655) rescues *rad18*Δ MMS sensitivity at this same concentration. Yeast strain 423 was used as a wild-type.

V.1.4.12. **Scc1-UD does not rescue the SCC defects of *scc1-73* cells.**

The lethal phenotype seen when Scc1-UD is expressed as the only cellular copy of *SCC1*, or overexpressed in *scc1-73* thermosensitive background could be due to defects in Sister Chromatid Cohesion. To check this possibility, centromere 5 and centromere 4 were tagged with tet operators in wild-type and *scc1-73* cells. Tet

repressors tagged with YFP bind to tet operators and allow visualization of centromeres as single dots under the fluorescence microscope. Scc1, Scc1-UD, Scc1-UD^{FA,CS}, Scc1-UD^{CS}, Scc1-Ubc9 overexpressed from the *GAL* promoter were integrated in the *URA* locus in *scc1-73* cells with centromere 5 tags.

To check metaphase cohesion cells were first arrested in G1 by alpha factor at the permissive temperature (25°C). Once arrested, the temperature was shifted to 37°C to inactivate *scc1-73* allele, and at the same time galactose was added to induce expression of the different constructs. 30 minutes after adding galactose, cells were released into a metaphase block by addition of nocodazole. Nocodazole-arrested cells were scored for metaphase cohesion by counting cells that have one dot, which represent cells that were able to establish and maintain SCC, and cells that have two dots, which represent cells with defects in SCC (Figure 41A). s*cc1-73* allele is not functional at restrictive temperatures and cells have defects in SCC. Overexpression of Scc1 or Scc1-Ubc9 restores these defects to wild-type levels (Figure 41B). On the other hand, overexpression of Scc1-UD does not restore defects in SCC (Figure 41C). This phenotype is dependent on UD binding to and deconjugating SUMO, since overexpression of Scc1-UD^{FA,CS} or Scc1-UD^{CS} could revert SCC defects.

The same phenotype was observed when the constructs were expressed from the *SCC1* promoter. As seen in Figure 42A expression of Scc1 or Scc1-UD^{CS} restores metaphase cohesion defects at centromere 5, while Scc1-UD does not. Similarly, expression of Scc1, Scc1-UD^{CS}, Scc1-UD^{FA,CS} from the *SCC* promoter restores defects in SCC at centromere 4, while Scc1-UD does not (Figure 42B). Thus, in the absence of cohesin sumoylation cells have defects in SCC, which suggests that cohesin sumoylation positively regulates SCC.

Binding sites for Scc1 were found near the silent loci, and coinciding with the boundary elements in the case of silenced mating-type loci *HMR*. To check SCC in the

HMR locus when cohesin sumoylation is absent, we transformed *SCC1*, *SCC1-UD* to *scc1-73* cells, where *HMR* was tagged with lac-GFP and flanked by binding sites for a *GAL*-inducible site-specific recombinase (Cre). Addition of galactose leads to excision of the locus in cells with sister chromatids producing two chromatin circles that remain associated with each other in wild-type cells but loose cohesion in *scc1-73* cells (Chang, Wu et al. 2005). Cells were arrested in G1, and then, galactose was added to express the *SCC1* constructs and the recombinases. The temperature was then shifted to 37ºC to inactivate the *scc1-73* allele. 30 min later, cells were released into a synchronous cell cycle at 37ºC, arrested in metaphase with nocodazole and observed microscopically for *HMR* cohesion. As seen in Figure 42C *scc1-73* cells have cohesion defects at the HMR locus. Overexpression of wild-type *SCC1* rescues the SCC defects in *scc1-73* cells, while overexpression of *SCC1* -UD does not, suggesting that cohesin sumoylation is also required at the *HMR* locus for SCC.

Intriguingly, we also found that *nse2ΔC* cells do not have gross defects in SCC, suggesting that the Nse2 SUMO ligase activity is not required for cohesion at the HMR locus (Figure 42D). As presented in Figure 42E, *smc6-9* cells also do not display major defects in SCC, suggesting that the Smc5/6 complex is also not required for cohesion at the HMR. Moreover, the minor SCC defects detected in *smc6-9* cells seem to be cohesin-dependent, as double *scc1-73 smc6-9* mutants display additive cohesion defects. These results indicate that the cohesin and Smc5/6 complex act cooperatively at the mating type locus for sister chromatid cohesion.

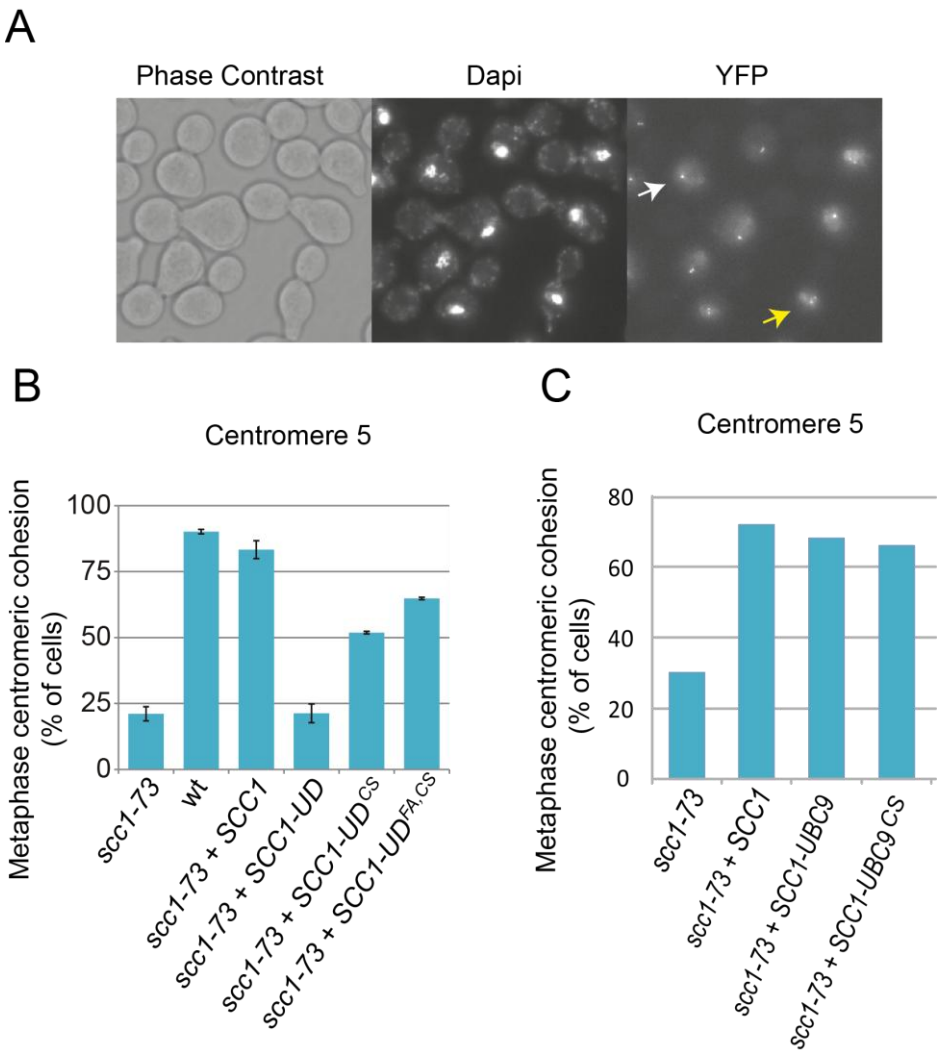

Figure 41. Overexpression of *SCC1-UD* does not rescue SCC defects of *scc1-73*. (A) Wild-type or *scc1-73* cells carrying a chromosome tag on centromere 5 were synchronized in G1 by alpha factor. Once arrested in G1, the *GAL* promoter was switched on to allow expression of *SCC1, SCC1-UD, SCC1UD^{CS}, SCC1-UD^{FA,CS}*, *SCC1-UBC9* or *SCC1-UBC9^{CS}* in *scc1-73* cells, and the temperature was shifted to 36°C to inactivate *scc1-73* thermosensitive allele. After 30 minutes, cells were released into a synchronous cell cycle at 36°C, arrested in metaphase with nocodazole and observed microscopically for centromere cohesion. Images of metaphase arrested cells taken with the fluorescence microscope are shown. Yellow arrow points at a cell with two separated dots, representing cells that failed to establish SCC. White arrow points at a cell with one dot, representing cells that have established SCC **(B)** Note that overexpression of *SCC1* restores SCC in a *scc1-73* cells, while overexpression of *SCC1-UD* does not. On the other hand, overexpression of *SCC1-UD^{FA,CS}* partially recovers centromeric cohesion (YSM1040, YSM1476, YSM1478, YSM1480, YSM1614, Y343). Bars indicate mean values for three independent experiments; lines on bars are standard deviation. **(C) Up-regulation of cohesin sumoylation restores SCC defects of *scc1-73*.** Overexpression of *SCC1-UBC9* or *SCC1-UBC9^{CS}* restore SCC defects of *scc1-73* (YSM1040, YSM1476,YSM1506, YSM1568).

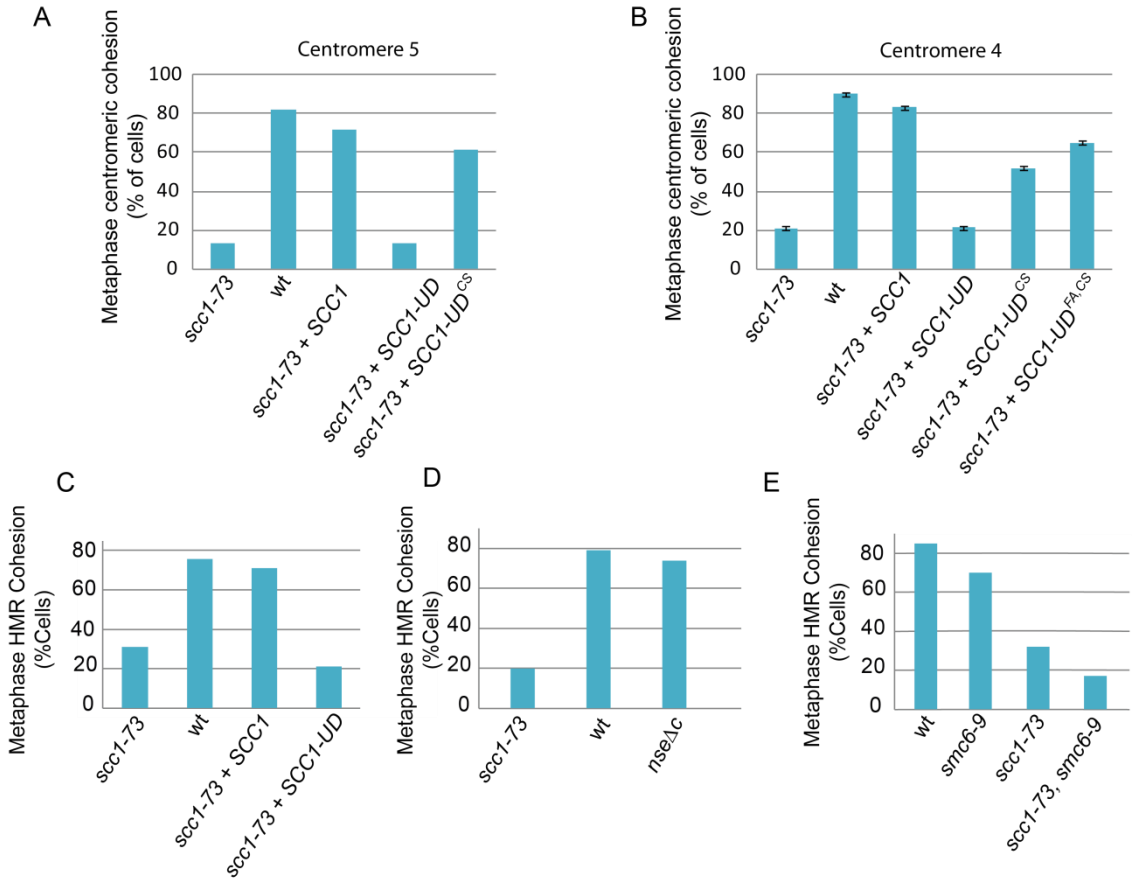

Figure 42. *SCC1-UD* expressed from the *SCC* promoter does not rescue SCC defects of *scc1-73* at centromere 4 and 5. Overexpression of *SCC1-UD* does not rescue SCC in *scc1-73* cells at the *HMR* locus, while *smc6-9* and *nse2*Δ*C* have no defects in SCC. (A) Wild type or *scc1-73* cells carrying a chromosome tag on centromere 5 and expressing *SCC1, SCC1-UD, SCC1UD*^{CS} from the *SCC1* promoter, were treated as in Figure 41 without galactose addition, and observed microscopically for centromere cohesion. Note that *SCC1* expression restores SCC in *scc1-73* cells, while *SCC1-UD* does not. Cells that express *SCC1-UD*^{CS} show partial recovery of centromeric cohesion (YSM1040, YSM1860, YSM1832, YSM2155, YSM1857, Y343). **(B)** Wild type or *scc1-73* cells carrying a chromosome tag on centromere 4 and expressing *SCC1, SCC1-UD, SCC1UD*^{CS} or *SCC1-UD*^{FA,CS} from the *SCC1* promoter, were treated as in (A), and observed microscopically for centromere cohesion. Note that *SCC1* expression restores SCC in *scc1-73* cells, while *SCC1-UD* does not. Cells that express *SCC1-UD*^{CS} show partial recovery of centromeric cohesion, while cells that express *SCC1-UD*^{FA,CS} show a higher percentage of centromeric cohesion (YSM1890, YSM1882, YSM1952, YSM1954, YSM1956, YSM1958). Bars indicate mean values for three independent experiments; lines on bars are standard deviation. **(C)** To check SCC in the *HMR* locus when cohesin sumoylation is absent, we transformed *SCC1*, *SCC1-UD* to *scc1-73* cells, where *HMR* was tagged with lac-GFP and flanked by binding sites for an inducible site-specific recombinase (HO). HO was placed under the *GAL* promoter. Addition of galactose leads to excision of the locus in cells with sister chromatids producing two chromatin circles that remain associated with one another in wild-type cells but loose cohesion in *scc1-73* cells. Cells were treated as in Figure 41 and observed microscopically for *HMR* cohesion. Note that *scc1-73* cells have defects in SCC. Overexpression of wild-type *SCC1* rescues SCC defects in *scc1-73* cells, while overexpression of *SCC1-UD* does not (Y504, Y503, YSM1514, YSM1516). **(D)** To check whether the same defects in SCC at the *HMR* locus are also seen in *nse2*Δ*c* cells, we transformed

this allele to cells that have lac-GFP tag on *HMR* and we scored for metaphase cohesion as in (C). Note that *nse2ΔC* cells do not have defects in SCC compared to those seen in *scc1-73* cells, suggesting that Nse2 SUMO ligase activity might not be required for SCC (Y504, Y503, YTR559). **(E)** To check whether the same defects in SCC at the *HMR* locus are also seen in *smc6-9* cells, we transformed this allele to cells that have lac-GFP tag on *HMR* and we scored for metaphase cohesion as in (C). Note that *smc6-9* cells do not have defects in SCC compared to those seen in *scc1-73* cells, suggesting that Smc5/6 complex might not be required for SCC. Also note that *scc1-73*, *smc6-9* double mutants have sever defects in SCC, suggesting that these mutations are additive (Y504, Y503, YTR519, YTR535).

V.1.5. **Sumoylation and acetylation are required independently during establishment of SCC**

During DNA replication, Eco1-dependent acetylation of Smc3 locks cohesin around newly replicated sister chromatids. We have seen that cohesin sumoylation is also required during establishment of SCC. One possibility is that cohesin sumoylation could be an upstream event to its acetylation. In order to understand the relationship between these two modifications, we started by checking Smc3 acetylation in the absence of SUMO conjugation in the cell. Wild-type and *ubc9-1* cells expressing *SMC3*-3xHA were grown exponentially at 25°C, and one half was shifted to 37°C for two hours. Both cultures were then collected and processed for anti-HA immunoprecipitation. As seen in Figure 43A, the acetylation levels of Smc3 are not affected by the absence of sumoylation in the cell, indicating that sumoylation is not required for Smc3 acetylation. The anti-acetyl lysine antibody is specific for the acetylated Smc3 since, as expected, *smc3*^{KKRR} shows no detectable acetylation (Figure 43B).

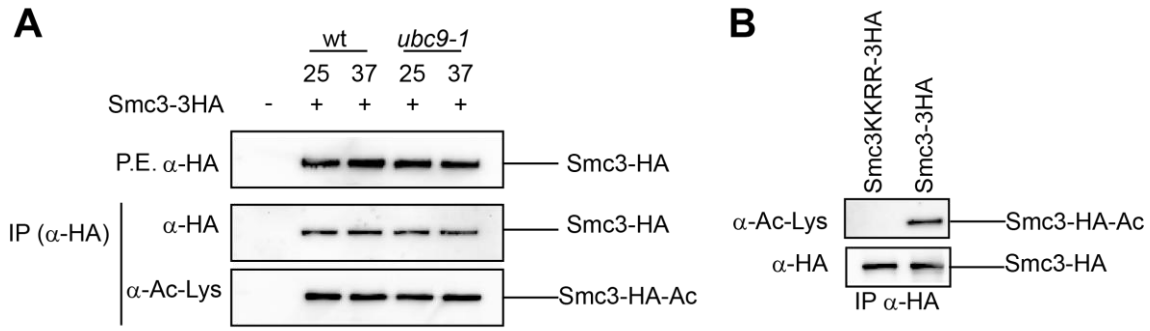

Figure 43. Smc3 acetylation does not depend on sumoylation. (A) Inactivation of the SUMO pathway in a *ubc9-1* thermosensitive mutant has no effect on Smc3 acetylation. *UBC9* wild-type (YSM1710) and *ubc9-1* mutant cells (YSM1756) that have a 3xHA tag on Smc3, were grown at 25ºC (25), and shifted to 37ºC for 2 hours to inactivate *ubc9-1* thermosensitive allele. Cells were collected and subjected to anti-HA IP. After elution the IP was divided in two PAG to probe with anti-HA to detect the total amount of Smc3-3HA or anti-acetyl lysine antibodies to test the levels of Smc3 acetylation. Note that Smc3 is efficiently acetylated in the absence of active SUMO conjugase.**(B) The anti-acetyl lysine antibody is specific for the acetylated Smc3.** Protein extracts (P.E.) from cells that express a 3HA tagged copy of wild-type Smc3 (YSM1650) or the nonacetylated mutant Smc3 protein (YSM1649, $Smc3^{KKRR}$), were subjected to anti-HA IP similar to (A). Note that the anti-acetyl lysine antibody does not recognize the unacetylated $Smc3^{KKRR}$, although it is immunoprecipitated.

Next, we specifically looked at the effect of cohesin desumoylation in scc1-aid cells expressing the *SCC1*, *SCC1-UD*, *SCC1-UD*^{FA,CS} constructs under the *SCC1* promoter. Degradation of the endogenous Scc1 copy is expected to prevent proper ring assembly and to lower Smc3 acetylation. Exponentially growing cells were treated with auxin and samples were taken at times 0, 30, 60, 90, and 120 after activation of the degron, and processed for anti-myc IP. Figure 44 shows that Smc3 acetylation levels drop, reaching a minimum 90 min after auxin addition. A similar effect is observed after inactivation of the *scc1-73* allele by shift to the restrictive temperature (Figure 45A). Scc1-aid cells that express the different chimeras were grown exponentially, and samples were taken at times 0 and 120 minutes after auxin addition. Cells expressing any of the fusions, *SCC1*, *SCC1-UD* or *SCC1-UD*^{FA,CS} did not show any change in acetylation levels 2 hours after triggering degradation of the endogenous copy, indicating once more that cohesin sumoylation is not required for its acetylation.

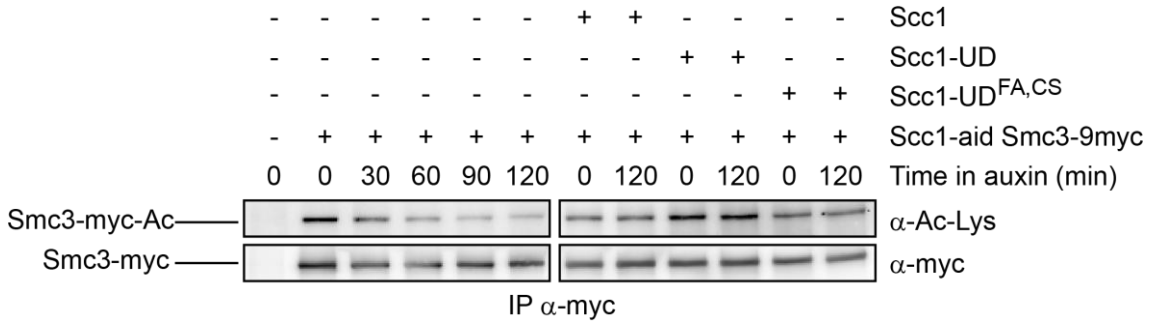

Figure 44. Smc3 acetylation does not depend on cohesin sumoylation. Scc1-aid, Smc3-9myc (YSM1965) cells expressing *SCC1*, *SCC1-UD*, *SCC1-UD*^{FA,CS} from the *SCC1* promoter (YSM2025, YSM2027, YSM2031) were grown to exponential phase, and protein extracts were subjected to anti-myc IP. Western blots were probed with anti-acetyl lysine antibody to detect levels of acetylation, and reprobed with anti-myc to detect the levels of immunoprecipitated Smc3. Note that Smc3 acetylation levels drop after addition of auxin, and this effect can be counteracted by expression of sumoylated (Scc1 and Scc1-UD^{FA,CS}) or unsumoylated (Scc1-UD) cohesin.

It is possible that unsumoylated cohesin rings (formed around Scc1-UD) fail to properly interact with acetylated Smc3 leading to loss of SCC. To test this possibility, *scc1-73* cells that express *SCC1*, *SCC1-UD*, and *SCC1-UD*^{FA,CS} were collected, and the ectopically-expressed Scc1 versions were immunopresipitated with anti-HA antibodies. As seen in Figure 45B, acetylated Smc3 co-immunoprecipitates with the 3xHA tagged Scc1-UD with similar efficiency to Scc1 or Scc1-UD^{FA,CS}, demosntrating that cohesin sumoylation is not required for its interaction with acetylated Smc3.

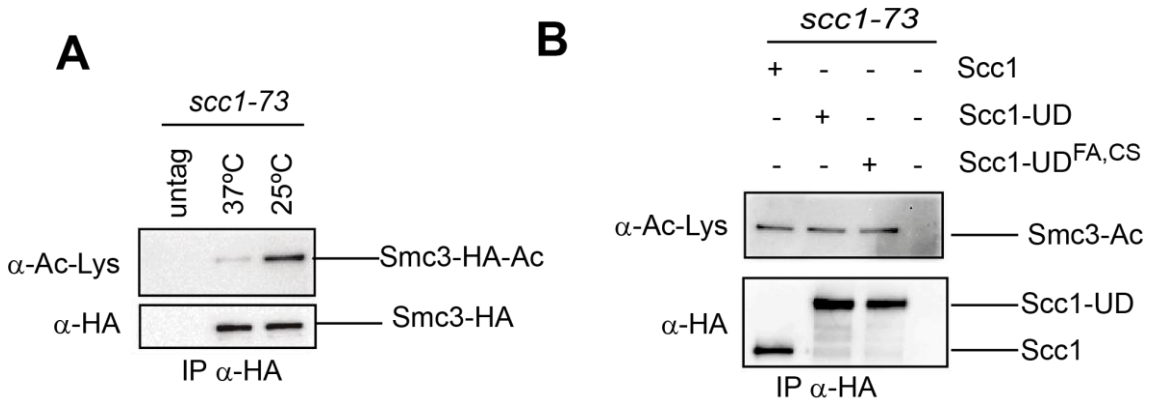

Figure 45. Unsumoylated cohesin subunits interact efficiently with acetylated Smc3. (A) *scc1-73* (Y759) cells that express *SMC3-6HA* (YSM2225) were grown at 25°C to exponential phase. Half of the culture was placed at 37°C for 2 hr to inactivate *scc1-73* thermosensitive allele. Cells were collected and

subjected to anti-HA IP as in Figure 43A. Note that inactivation of Scc1 leads to decrease in Smc3 acetylation levels. **(B)** *scc1-73* (YSM1040) cells expressing *SCC1*, *SCC1-UD*, *SCC1-UD*^{FA,CS} from the *SCC1* promoter (YSM1860, YSM1832, YSM2155) were grown to exponential phase and heat-shocked as in (A). Scc1-3HA and the Scc1-UD chimeras were immunoprecipitated and analyzed by western blot with anti-HA and anti-acetyl-lysine antibodies to detect the amount of co-immunoprecipitating acetylated Smc3. Note that the unsumoylated versions of cohesin coimmunoprecipitate efficiently with acetylated Smc3.

Acetylation of Smc3 counteracts the antiestablishment activity of Rad61/Wapl. It has been described that *rad61*Δ makes acetylation dispensable for maintenance of sister chromatid cohesion. To see whether sumoylation is similarly required to counteract the antiestablishment activity of Rad61, we deleted *RAD61* in *scc1-73* cells that express *SCC1* and *SCC1-UD* from the *SCC1* promoter, and we plated the cells by replica plating at permissive and non-permissive temperatures.

Figure 46 shows that, and as we have seen earlier, expression of wild-type *SCC1* in *scc1-73* rescues its temperature sensitivity, while expression of *SCC1-UD* is lethal in this background at restrictive temperatures. As previously reported (Rowland, Roig et al. 2009), *rad61*Δ cells are slightly thermosensitive, and thus, expression of *SCC1* from the *SCC1* promoter in *scc1-73*/*rad61*Δ double mutant does not completely suppress thermosensitivity of these cells. On the other hand, *rad61*Δ does not recover the growth defects of *scc1-73 SCC1-UD* expressing cells at restrictive temperatures. Thus, unlike acetylation, sumoylation is not required to counteract the antiestablishment activity of Rad61, although it is required for establishment of SCC.

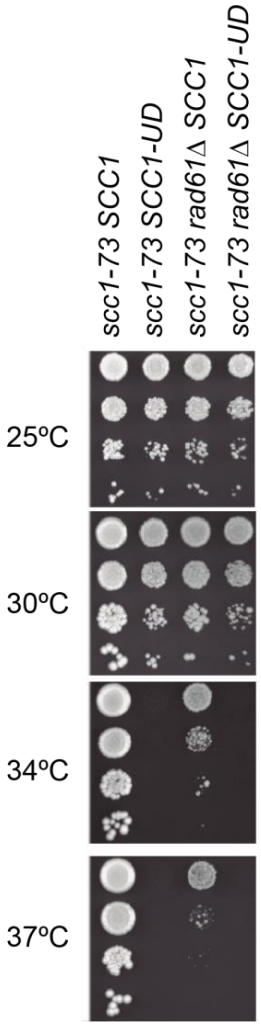

Figure 46. Inactivation of the anti-establishment activity does restore growth defects of cells with unsumoylated cohesin. Cohesin acetylation is no longer required when the antiestablishment activity is eliminated. This activity is dependent on three proteins bound to the α-kleisin, the Scc3 cohesin subunit Pds5 and Rad61. Analogously, we reasoned that SUMO could enable establishment through the same mechanisms as acetylation. In this case, mutation of anti-establishment factors should allow viability of cells relying on the Scc1-UD fusion as the only source of the α-kleisin in the cell. Rad61 is the only non-essential antiestablishment factor. Thus, to test this possibility, we deleted *RAD61* in a *scc1-73* thermosensitive background that also expresses the chimeras under the *SCC1* promoter. Serial dilutions of the indicated strains were plated on YPD and incubated at the indicated temperatures. The *scc1-73* mutant can be inactivated by incubation at 34ºC, and expression of wild type *SCC1* (YSM1860) rescues its temperature sensitivity, while expression of *SCC1* -UD (YSM1832) does not. Note that deletion of *RAD61* does not recover the growth defects of *scc1-73 SCC1* -UD (YSM2153) cells at 34ºC. Note also that *rad61*Δ (YSM2152) cells are slightly thermosensitive.

To see whether cohesin sumoylation depends on its acetylation, we crossed strains that express *HF-SUMO*, *SCC1-6xHA* and *SMC3-9xmyc* with *eco1-1*

thermosensitive cells, which have no detectable levels of Smc3 acetylation. After sporulation and tetrad dissection, wild-type *ECO1* or *eco1-1* thermosensitive allele plus *SCC1-6xHA* or *SMC3-9myc* were grown exponentially at 23°C (permissive temperature) and then shifted to 37°C for two hours to inactivate *eco1-1*. Samples were collected before and after shift to restrictive temperatures (37°C) and were processed for SUMO pull-down. As seen in Figure 47 sumoylation levels of Scc1 or Smc3 at either the permissive or restrictive temperature are similar in wild-type and *eco1-1* cells, indicating that cohesin acetylation is not required for its sumoylation.

All together, these results show that both acetylation and sumoylation are required independently during establishment of SCC.

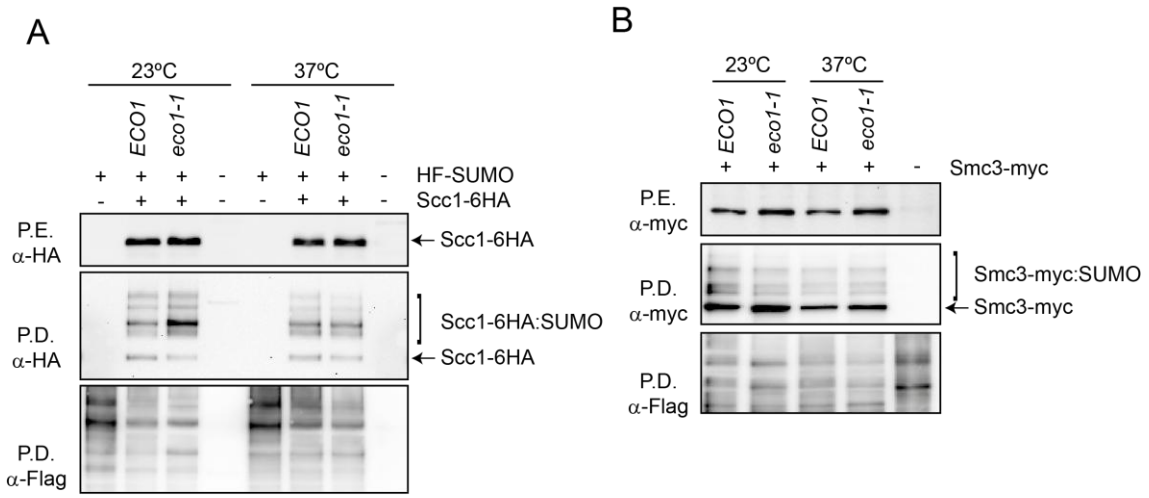

Figure 47. Cohesin sumoylation does not depend on its acetylation. *ECO1* and *eco1-1* cells, carrying HF-SUMO and Scc1-6HA (A)/Smc3-9myc (B) tags, were grown at 23°C (YTR907, YSM1227, YNC2184, YNC2186, YSM1193, Y1588). The cultures were split in two, and one half was incubated at 37°C to inactivate the *eco1-1* allele. Samples were taken two hours after transfer to the restrictive temperature. Note that both Scc1(A) and Smc3(B) are sumoylated in an *eco1-1* background.

V.1.6. **Sumoylation of Smc1 and Smc3 requires Scc1 dependent ring formation and Scc1 sumoylation**

Cohesin subunits might be sumoylated in a sequential manner, i.e. sumoylation of one subunit might be required for sumoylation of the next. To check this possibility we

decided to specifically block sumoylation of Scc1 using the two recently described *scc1* alleles (*scc1*^{11KR} and *scc1*^{3KR}). These two alleles bear lysine to arginine mutations in the primary (*scc1*^{3KR}) or primary plus secondary (*scc1*^{11KR}) SUMO acceptor sites, and have been shown to be deficient for DNA damage repair (McAleenan, Cordon-Preciado et al. 2012). First, we checked the functionality of these alleles under non-damage conditions. To this end, we expressed wild-type *SCC1*, *scc1*^{11KR}, and *scc1*^{3KR} ectopically in an Scc1-aid background and plated cells on YPD plates with or without auxin (IAA, 1mM) to degrade the endogenous Scc1. As seen in Figure 48A cells that express *scc1*^{11KR} as the only *SCC1* copy have growth defects even in the absence of DNA damage while those that express *scc1*^{3KR} or wild-type *SCC1* restore growth defects of Scc1-aid cells (Figure 48A). Equivalent results were obtained using thermosensitive *scc1-73* cells: the *scc13*^{KR} allele fully complements *SCC1* function, while the *scc1*^{11KR} allele displays growth defects at the restrictive temperature (Figure 48B).

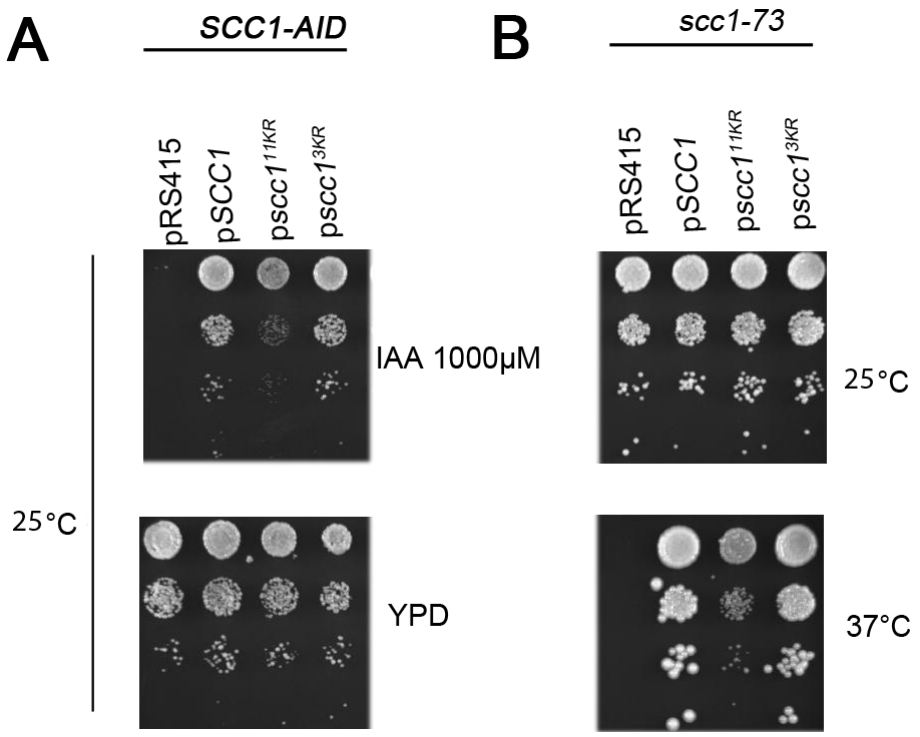

Figure 48. Strains that express *scc1*^{11KR} as the only copy of *SCC1* show growth defects. (A) Wild-type *SCC1* (p2015), *scc1*^{3KR} (p2006), or *scc1*^{11KR} (p2005) were ectopically expressed in Scc1 degron background

(YSM1907). Cells were plated on YPD plates, with or without Auxin (IAA, 1000µM), to degrade the endogenous *SCC1*. Note that cells that express *scc1*^{11KR} as the only *SCC1* copy have growth defects under physiological conditions, and in the absence of DNA damage when compared to those that express *scc1*^{3KR} or wild-type *SCC1*. **(B)** *scc1*^{11KR} mutant allele was expressed ectopically in *scc1-73* thermosensitive cells (YSM1040) and plated on YPD plates at permissive (25°C) and restrictive temperatures (37°C) to inactivate *scc1-73* thermosensitive allele. Note that *scc1*^{11KR} shows growth defects at 37°C, suggesting that this allele is thermosensitive.

Then, we decided to check sumoylation levels of Scc1^{11KR}, tagged with the 3HA epitope, under physiological conditions and in the absence of DNA damage, by ectopically expressing this allele in the Scc1-aid background. Samples were taken before and after addition of auxin (1 mM) for pull-down analysis. As seen in Figure 49A, sumoylation levels of Scc1^{11KR} are barely detectable in the presence of the endogenous copy of Scc1. Surprisingly, some sumoylation of Scc1^{11KR} is seen in the absence of the endogenous copy of Scc1, although sumoylation levels are lower than those seen in the ectopically expressed wild-type copy of Scc1. These results suggest that in the absence of DNA damage, there might be additional lysines targeted by SUMO in the Scc1 protein.

Next, we decided to test whether full sumoylation of Scc1 is required for the subsequent modification of Smc1. For this purpose, we tagged the *SMC1* gene with a 9xmyc epitope. Samples were taken for pull-down analysis before and after addition of auxin (1 mM). As seen in Figure 49B, in the absence of Scc1, Smc1 displays no detectable levels of sumoylation, showing that tripartite cohesin ring formation is a pre-requisite for its sumoylation. When wild-type Scc1 is ectopically expressed sumoylation of Smc1 is restored to wild-type level. In contrast, expression of *scc1*^{11KR} lowered Smc1 sumoylation, even in the presence of the endogenous Scc1. These results indicate that sumoylation of Scc1 is required for sumoylation of Smc1, and that cohesin might be sumoylated in a sequential manner.

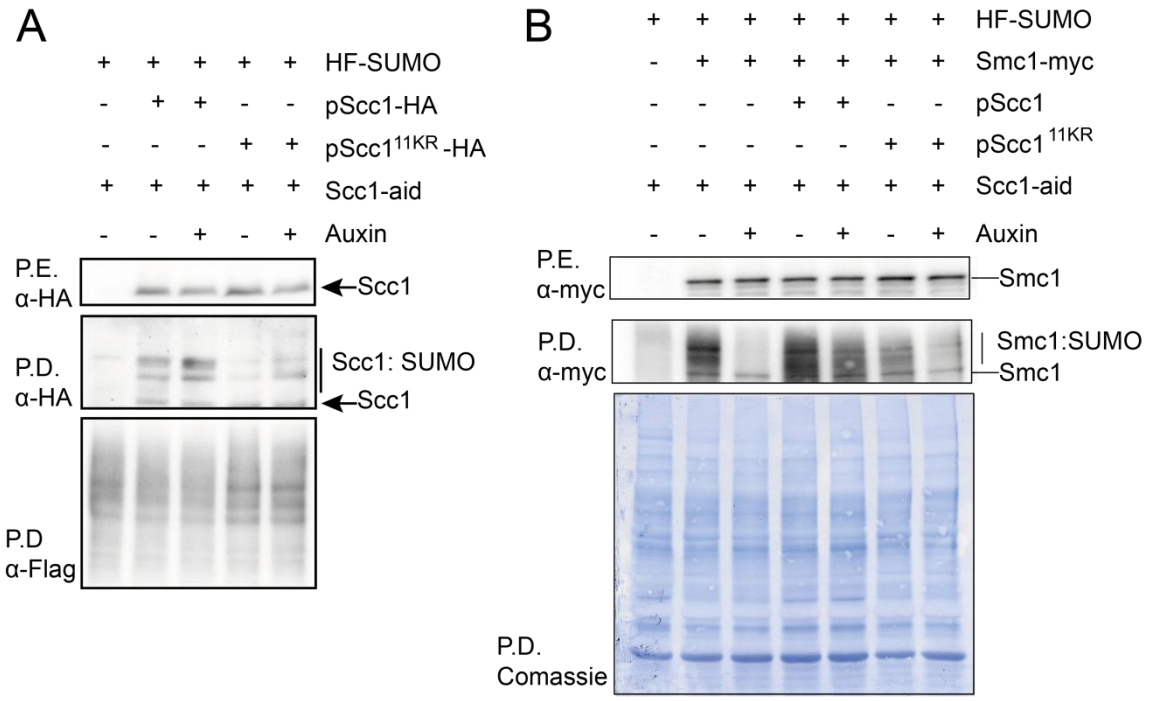

Figure 49. Sumoylation of Smc1 and Smc3 require Scc1 dependent ring formation and Scc1 sumoylation. (A) To check sumoylation levels of Scc1^{11KR}, tagged with the 3HA epitope, under physiological conditions and in the absence of DNA damage, *SCC1^{11KR}* was ectopically expressed in Scc1-aid background (YSM1907). For pull-down analysis, cells were grown exponentially at 25°C and then were split in two halves. To one half, Auxin was added to a final concentration of 1000 µM and incubated again for two hours. Both halves were collected, and processed for pull-down analysis. Note that sumoylation levels of Scc1^{11KR} are barely detectable in the presence of the endogenous copy of Scc1. However, some sumoylation of Scc1^{11KR} is seen in the absence of the endogenous copy of Scc1, although sumoylation levels are much lower than those seen in the ectopically expressed wild-type copy of Scc1. **(B)** Wild-type *SCC1* (p2015), or *scc1^{11KR} (*p2005) were ectopically expressed in Scc1-aid cells (YSM1963) that express Smc1-9xmyc and 6xHis-Flag-SUMO. Sumoylation of Smc1 was checked in the presence or absence of Auxin (IAA) which was used to degrade the endogenous Scc1 and use ectopically expressed wild-type *SCC1* or *scc1^{11KR}* as the only copy in the cell. Cells were grown and treated as in A and then were collected for pull-down analysis. Note that when wild-type *SCC1* is ectopically expressed sumoylation of Smc1 is restored to wild type levels. On the other hand, *scc1^{11KR}* shows decreased levels of sumoylation even in the presence of the endogenous Scc1 copy. These levels are drastically decreased when *scc1^{11KR}* is expressed as the only copy.

V.2. *UD* (*SENP1*) fusion to *RAD21* as model to down-regulate cohesin sumoylation in HEK293T human cell line

Sumoylation of human cohesin (Rad21) has been detected *in vitro*, suggesting that cohesin regulation by SUMO might be conserved in humans. To check this possibility, we decided to transfer our model to human cell lines and follow the same approach we used in budding yeast to characterize fusion of cohesin to Ulp domains.

First, we started by constructing the chimeras using mouse *RAD21* (m*RAD21*), which is the homolog of yeast Scc1, and the UD domain of human *SENP1*. We chose mouse Rad21 so that we can down-regulate specifically the endogenous copy of *RAD21* (h*RAD21*) by siRNA, while keeping m*RAD21* as the only copy in the cell. Similarly to what we have done in budding yeast, we used a 3x(4Gly-Ser)-4xHA-6x(Gly-Ala) tag as a linker between Rad21 and UD (SENP1) to allow separation and proper folding of the two proteins. In addition, the fusions were cloned in vectors that express GFP to allow *in vivo* monitoring by fluorescence microscopy. We also used the same fusion bearing an inactive peptidase domain (C603S) as a control.

V.2.1. Cohesin rings are properly assembled around mRad21-UD

To check whether these fusions are able to interact with the rest of the complex, we transfected vectors expressing m*RAD21*, m*RAD21-UD*, and m*RAD21-UD*^{CS} from the *CMV* promoter to HEK293T cells. Then, we performed an anti-HA IP on protein extracts from these cells. The IP product was loaded in two PAGE to check for IP using anti-Scc1 primary antibody, and CoIP of Smc1 and Smc3 using anti-Smc1 and anti-Smc3 primary antibodies (Supplementary Table 1). We used HEK293T cells that do not carry any vector as a control for the IP. As seen in Figure 50, Smc1 and Smc3 interact with mRad21-UD with the same efficiency as wild-type mRad21, and mRad21-UD^{CS}. This result shows that mRad21 is able to interact with human cohesin subunits, and that neither the SUMO peptidase domain attached to *mRAD21*, nor its activity, interfere with

cohesin ring formation. Intriguingly, we consistently observed a lower mobility form of Rad21- UD^{CS}. Expression of Scc1- UD^{CS} in budding yeast leads to the accumulation of a similarly running band of sumoylation, which is most probably due to binding of the inactive peptidase domain to sumoylated Scc1. We therefore suspect that the slow migration band in mRad21- UD^{CS} corresponds to the sumoylated form of this molecule.

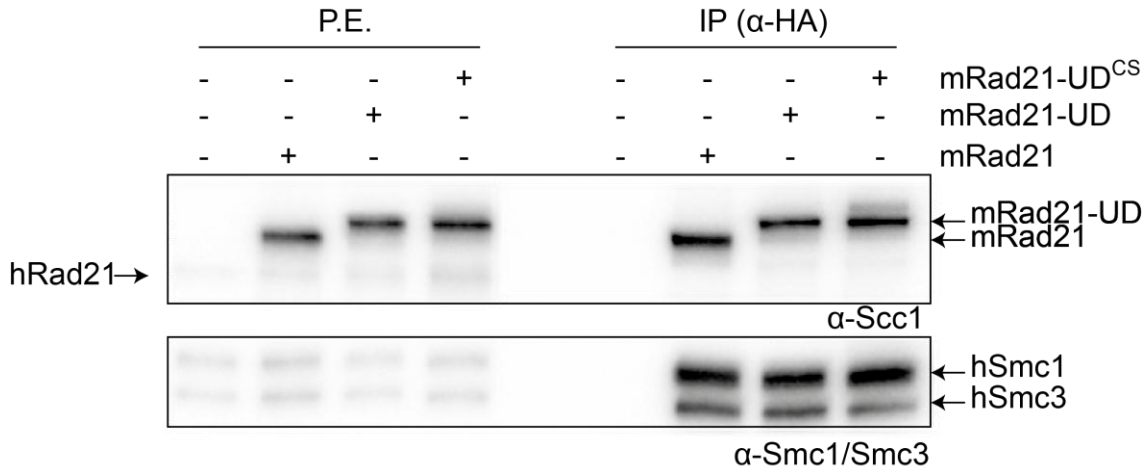

Figure 50. Cohesin rings are properly assembled around mRad21-UD fusion. 150x 10^4 HEK293Tcells were seeded and transfected using PEI with vectors that overexpress HA tagged m*RAD21* (pCB2389), m*RAD21-UD* (pCB2383), m*RAD21-UD^{CS}* (pCB2411). Cells were processed, as described in section IV.11.5, for anti-HA immunoprecipitation. Note that Smc1 and Smc3 CoIP with Rad21 chimeras with the same efficiency. Endogenous Rad21 was seen in the extract but not in the IP. A band of slower mobility is seen in cells that express *RAD21-UD$^{CS.}$* This band probably corresponds to SUMO conjugated Rad21, which is also up-regulated in budding yeast in cells expressing this fusion.

V.2.2. **mRad21-UD localizes to the nucleus**

Next, we checked by *in vivo* fluorescence and immunofluorescence whether the UD fusion localizes to the nucleus similarly to wild-type Rad21 in HEK293T cells. As seen in Figure 51 *in vivo* fluorescence signal of mRad21-UD localizes to the nucleus. Similarly, immunofluorescence using anti-GFP antibody shows localization of mRad21-UD to the nucleus (Figure 52). These observation indicate that the chimeras localize normally in HEK293T cells.

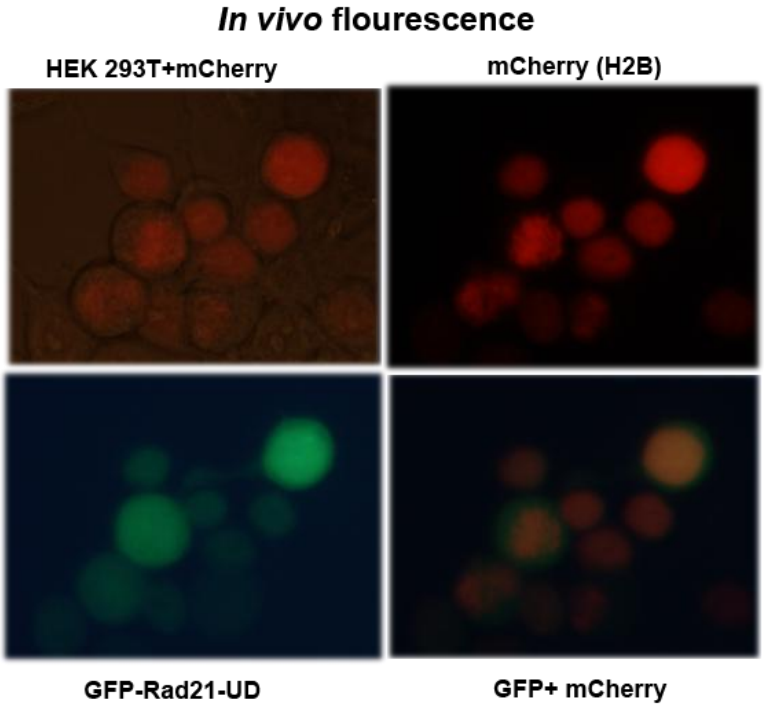

Figure 51. mRad21-UD localizes to the nucleus *in vivo*. 50x 10^3 of HEK 293T cells were seeded and transfected with the vectors expressing m*RAD21* (pCB2389), m*RAD21-UD* (pCB2383), m*RAD21-UD*^{CS} (pCB2411), and a vector containing mCherry tag on H2B to mark DNA using lipofectamine as described in IV.11.3.

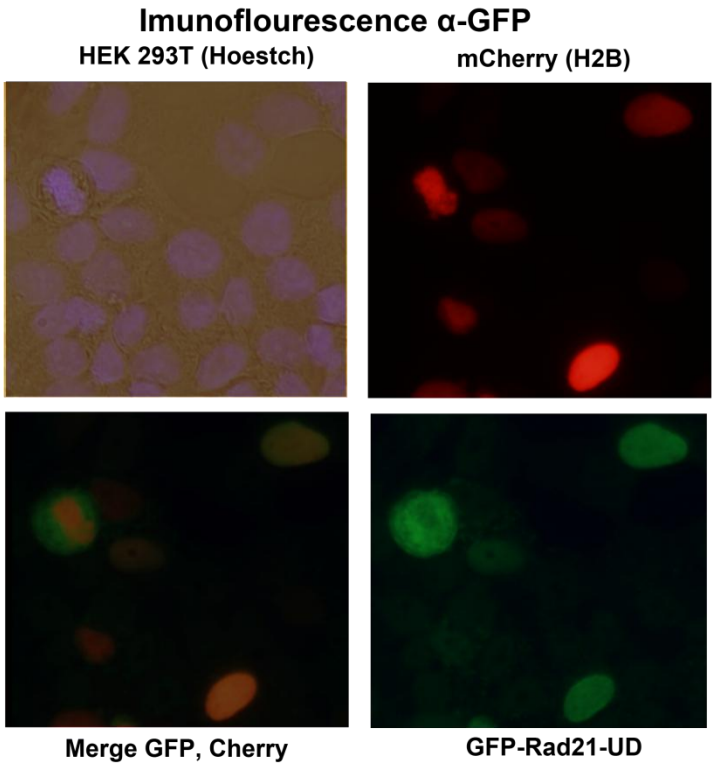

Figure 52. mRad21-UD fusion localizes to the nucleus (Immunofluorescence). 50x 10^3 of HEK 293T cells were seeded and transfected with the vectors expressing m*RAD21* (pCB2389), m*RAD21-UD* (pCB2383), m*RAD21-UD*^{CS} (pCB2411), and a vector containing mCherry tag on H2B to mark DNA using lipofectamine. Cells were washed fixed with 4% paraformaldehyde and processed for immunofluorescence, as described in section IV.11.4, using anti GFP antibody. Finally, cells were mounted with a solution containing Hoestch and slow fade.

V.2.3. **Cells that overexpress m*RAD21-UD* accumulate in G2/M**

In an attempt to see whether HEK293Tcells expressing mRad21-UD have cell cycle progression problems, as seen in budding yeast, we collected cells that were previously transfected with empty vector (GFP-NLS) or with vectors carrying wild-type Rad21 or Rad21-UD, and we fixed them with ethanol. Then, we processed the samples for FACS analysis.

As seen in Figure 53, FACS profiles of all fixed cells look similar irrespective to the presence of mRad21-UD or wild-type mRad21. We noticed that a small population of cells, presumably the ones expressing the highest levels of the fusions, retains the GFP fluorescence even after fixation and processing. Gating cells that have retained the GFP signal, shows that expression of mRad21-UD seem to accumulate in G2/M, as evident by an increase in the percentage of 4N cells (11.52%) compared to the percentage of 4N cells that express wild-type mRad21 (6.63%) or cells that express empty vector (6.58%). These findings suggests that, similar to what we have seen in budding yeast, human cells that lack cohesin sumoylation might have defects in SCC, what could potentially lead to activation of the spindle assembly checkpoint and G2/M arrest.

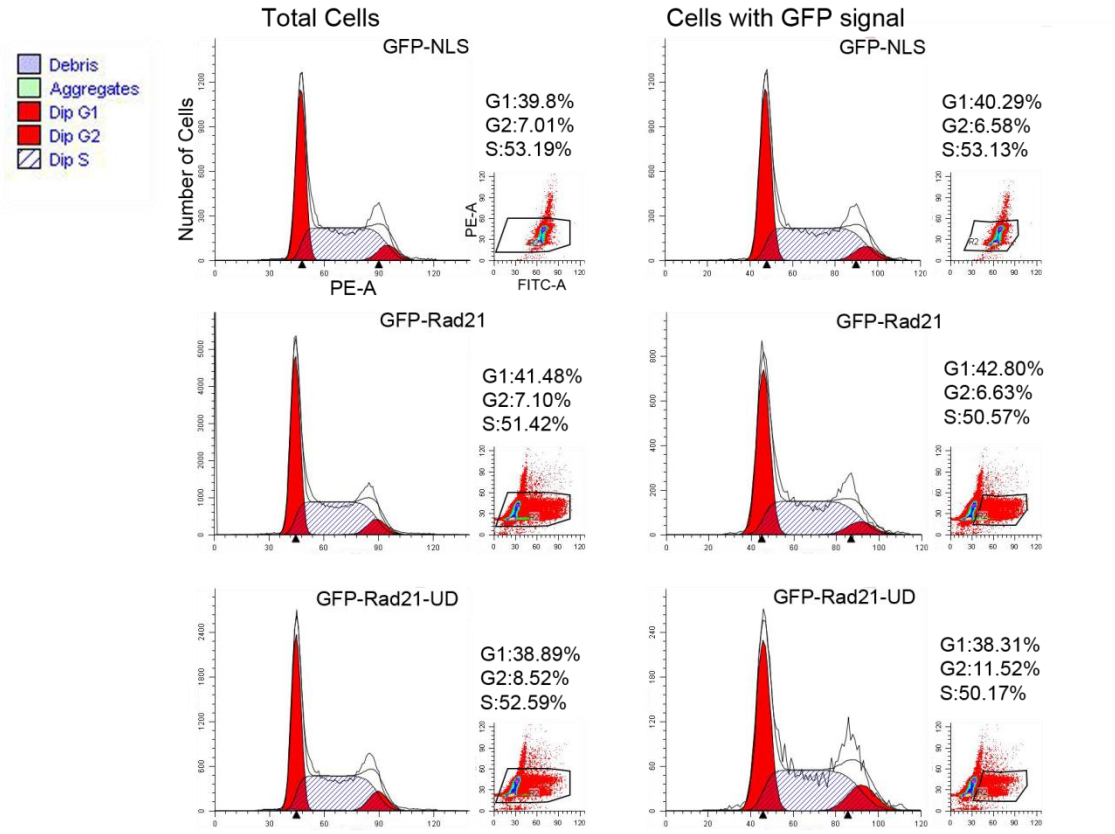

Figure 53. Cells that overexpress m*RAD21-UD* accumulate in G2/M. 50x 10^4 cells were seeded and transfected, using PEI, with the vectors expressing m*RAD21* (pCB2389), m*RAD21-UD* (pCB2383), or GFP-NLS. Next, cells were harvested by trypsinization, and processed for FACS as described in section IV.11.7. The efficiency of transformation was around 90%. However, GFP signal decreased drastically upon fixation with ethanol. Note that there is no difference in FACS profile between cells expressing the different vectors when all cells were included in the analysis. However, by gating cells that have retained the GFP signal we could see that, while cells that express empty vector (GFP-NLS) or wild-type *RAD21* have no problem in getting to the next cell cycle, cells that express *RAD21-UD* seem to accumulate in the G2/M transition, as evident by an increase in the percentage of cells in G2. Thus, indicating that these cells might have problems in progressing to the next cell cycle as seen in budding yeast.

"I was just guessing at numbers and figures….pulling the puzzles apart Questions of science, science and progress…don't speak as loud as my heart…"

The Scientist, Coldplay

Discussion

VI. Discussion

During DNA replication co-entrapment of sister chromatids by the cohesin complex is required for the biorientation of chromosomes in the mitotic spindle, which is essential for correct chromosome segregation. Defects in Sister Chromatid Cohesion (SCC) have serious consequences which can range from chromosomal translocations and cancer to cell death. This powerful multi-subunit molecule is now known to be required for other vital functions, such as holding sister chromatids during DNA damage repair, and regulating gene expression by stabilizing chromatin loops during gene expression. But how can one molecule do so many functions? Several proteins as well as post-translational modifications regulate the different functions of cohesin throughout the cell cycle. In this study, we describe sumoylation as another post-translational modification required for SCC.

VI.1. **Cohesin sumoylation is required for establishment of SCC**

In this work we have set up a novel approach to alter the sumoylation levels of the cohesin complex. This method is based on fusion of the C-terminal of Scc1 subunit of the cohesin complex to the SUMO conjugating enzyme or deconjugating domain. Ulp1 is a 72 KDa protein, but only the last 200 amino acids of the protein code for a fully functional Ulp domain (UD), which contains the catalytic residue C580 and other residues that are responsible for SUMO binding (F474) (Mossessova, Lima 2000). Thus, we fused the C-terminus of *SCC1* to the UD of *ULP1*, and we engineered the fusion to be connected by a 3xHA tag, as a linker to allow the physical separation and proper folding of the two proteins. We chose Ulp1 because it has been shown to have a greater activity than Ulp2 in vitro (Mukhopadhyay, Dasso 2007). To make sure that the phenotypes that we see are due to the peptidase activity and not because the fusion itself is affecting Scc1 folding or interaction with other cohesin subunits, we thought that a good control for this fusion would be to inactivate the peptidase domain

by point mutation of its catalytic site (C580S) (Mossessova, Lima 2000). Later on, we saw that by introducing another mutation in the UD^{CS}, which disables binding to SUMO (F474A) (Mossessova, Lima 2000), we even obtain a better control for this fusion. On the other hand, the Ubc9 protein is around 18 KDa. Thus, the entire cDNA of *UBC9* was fused to the C-terminus of *SCC1* using the 3xHA tag as a linker.

Since we did not know whether these fusions are lethal, we started by overexpressing them from the *GAL* promoter in wild-type cells. Overexpression of a Scc1-Ubc9 fusion shows no growth defects in a wild-type background, and complements the thermosensitive phenotype of *mcd1-1* and *scc1-73* mutant cells, what indicates that up-regulation of cohesin sumoylation does not affect viability (Figure 29A, Figure 30A). On the other hand, overexpression of an Scc1-UD fusion in wild-type cells leads to decreased growth rate, what suggests a possible toxic effect of depleting SUMO from cohesin rings (Figure 27). The toxicity is aggravated by overexpression in a *scc1-73* thermosensitive background, and cells become inviable even at permissive temperatures (Figure 30A). It has been shown that over-expression of a UD is toxic in budding yeast (Li, Hochstrasser 2003). However, the lethality of Scc1-UD over-expression cannot be simply due to increased nuclear levels of the Ulp1 domain because (i) a similarly expressed Smc5-UD fusion is not toxic, but able to rescue growth of a thermosensitive *SMC5* allele (Figure 29B); and (ii) Scc1-UD over-expression is not lethal in wild type cells. Moreover, expression of the Scc1-UD chimera from either the *GAL* or *SCC1* promoter does not change global sumoylation levels, indicating that the lethality is most probably due to a direct effect on cohesin sumoylation (Figure 38). However, we cannot currently discard that the desumoylation of other nearby protein/s is causing this lethality.

SUMO pull-down experiments in budding yeast showed that all subunits of the cohesin complex are sumoylated *in vivo* (Figure 17). The Scc1-UD fusion, whether expressed from the strong *GAL* promoter or from the *SCC1* promoter, lowers

sumoylation of all the cohesin subunits tested (Figure 25, Figure 26). This effect is remarkable, since it suggests that the chimeras can efficiently interact with the rest of the cohesin subunits. Moreover, our results indicate that our approach should be suitable to down-regulate sumoylation of other complexes/pathways. The decrease in cohesin sumoylation is due to the peptidase activity of Ulp1, since its inactivation restored wild-type levels of cohesin sumoylation (Scc1-UD^{FA,CS}) (Figure 26). Taken together these results suggest that the lethality seen in strains expressing Scc1-UD is due to decreased cohesin sumoylation, which means that cohesin sumoylation is required for viability.

Cells that can only assemble cohesin rings using Scc1-UD start to have cohesion defects during DNA replication and accumulate as mononucleated cells with large buds and separated dots or with stretched nucleus in the neck, transiently arresting in G2/M as seen by FACS analysis and fluorescence microscopy (Figure 32). These observations suggest that the presence of unsumoylated cohesin during S phase might eventually lead to activation of the spindle checkpoint and G2/M arrest, similarly to cells that lack proper cohesin function (Stern, Murray 2001). A functional cohesin complex is required to resist pulling by microtubules, what leads to biorientation of sister chromatids in the metaphase plate. To check metaphase cohesion, *scc1-73* cells were pre-arrested in G1 and released into a metaphase block after induction of the Scc1-UD chimeras (Figure 41A, Figure 14), and SCC was measured by evaluating the levels of separated fluorescent chromosome tags inserted next to centromere 5, centromere 4 or the *HMR* locus (Figure 41, Figure 42). Expression of the *SCC1-UD* does not rescue the SCC defects of *scc1-73* mutant cells. This phenotype is dependent on UD binding to and deconjugating SUMO, since its inactivation (Scc1-UD^{FA,CS}) restored wild-type levels of SCC. The fact that Scc1-UD fusions have a specific defect in SCC strongly suggests that its effect on viability is direct through inactivation of the cohesin complex itself. Although this is the most likely

explanation, we cannot formally exclude the possibility that desumoylation of other nearby factors, together with cohesin itself, is the cause of the inviability. The metaphase SCC failures could arise from defects during establishment or afterwards, mainly due to the inability to maintain SCC after co-entrapment of sister DNAs. A main handicap with our UD-fusion approach is that we cannot distinguish between cohesion establishment and maintenance, because we cannot deplete SUMO from cohesin rings at a later time point, after establishment. However, we have observed that cohesin sumoylation takes place during S phase (Figure 19), after its loading onto chromatin and in a process that requires binding of ATP to the SMC heads, and to a lesser extent, its hydrolysis (Figure 23). These molecular requirements resemble those of acetylation, suggesting that sumoylation is required at the time of SCC establishment.

The fundamental regulatory mechanisms of cohesin loading and establishment of SCC are conserved from yeast to humans (Nasmyth, Haering 2009). Therefore, it is probable that the SUMO-mediated step for SCC is conserved in humans too. Crucially, our preliminary results with human cell lines point in this direction. Following the same approach used in budding yeast, we fused the human SUMO peptidase domain of SENP1 to the C-terminus of murine *SCC1* using the 4HA epitope as a linker. We chose SENP1 because it has no specific substrate preference for the different SUMO proteins (SUMO1-4) (Shen, Tatham et al. 2006). In addition, mRad21 was chosen because its sequence is very similar to human Rad21, but different enough to be resistant to human-specific siRNA (Guillou, Ibarra et al. 2010). Cells that express the highest levels of GFP-mRad21-UD partially accumulate in G2/M, suggesting that fusion of cohesin to a SUMO-peptidase domain might negatively affect cohesin function, as also occurs in yeast (Figure 53). In this experiment, cells were fixed with ethanol, and only those that still displayed GFP signal after processing (presumably the ones with the highest degree of Rad21 over-expression) showed a partial cell cycle arrest phenotype. It is worth keeping in mind that the endogenous Rad21 was also present in these cells,

what might explain why the G2/M arrest is not as obvious as that observed in yeast. This experiment should be repeated including the SENP1^{CS,BD} fusion and using *in vivo* FACS analysis instead of ethanol-fixed cells, a process that decreases the GFP signal. In addition, the competition with the endogenous Rad21 should be removed by depletion with specific siRNAs. Finally, metaphase spreads can be used to evaluate the functionality of unsumoylated cohesin during replicative cohesion establishment.

Co-immunoprecipitation experiments indicate that Scc1-UD fusion protein is able to interact with Smc3 (Figure 33B). Scc1 first binds to Smc1, before interacting with Smc3, what suggests that the fusions also interact with Smc1 and thus, they do not interfere with cohesin ring formation. In addition, interaction of Scc3 and Pds5 with Scc1 is not affected either (Figure 33C,D). This also suggests that sumoylation is not required for cohesin ring formation or interaction with non-SMC subunits. However, the opposite is not true, i.e. cohesin ring formation is required for its sumoylation, as Smc1 is not sumoylated when Scc1 is absent (Figure 49), probably because these complexes are not integer and are never loaded onto chromatin, a prerequisite for cohesin sumoylation. Analogously, *RAD21-UD* fusions overexpressed from the *CMV* promoter in HEK293T cells interact with the same efficiency as wild-type Rad21 with SMC subunits of the cohesin complex in human cell lines (Figure 50), what suggests that cohesin sumoylation is not required for ring formation in humans. We have been unable to detect sumoylation of human cohesin subunits, as has also been described in (Wu, Kong et al. 2012). In fact, Scc1 sumoylation has only been detected after overexpression of SUMO and the Mms21 E3 ligase (Wu, Kong et al. 2012), and we still do not know whether other cohesin subunits are also sumoylated, as occurs in yeast. To our surprise, a band of slower mobility was detected above mRad21-UD^{CS} (Figure 50). We suspect that this band corresponds to SUMO-conjugated Rad21 since inactivation of the peptidase domain in the budding yeast Scc1-UD fusion did not only restore wild-type levels of cohesin sumoylation, but also led to its hypersumoylation;

this effect is probably due to hindering the access of other SUMO peptidases, thus effectively up-regulating sumoylation levels. To confirm this hypothesis in the future, we should prevent binding of SENP1 to SUMO by combining the SUMO binding-deficient (BD) and inactive peptidase (CS) mutations. Future pull-down experiments should also confirm whether other human cohesin subunits are sumoylated and if mRad21-UD fusion can deplete sumoylation from cohesin rings.

One possible explanation for the Scc1-UD phenotype is that down-regulation of cohesin sumoylation might impair its binding to chromatin, or relocation at known cohesin binding sites. In order to explore this possibility, we used chromatin fractionation in budding yeast to separate Triton X-100 soluble supernatant and chromatin pellet fractions. Our results indicated that there is no difference in chromatin binding between the functional Scc1-UD^{FA,CS} chimera and the unsumoylated Scc1-UD fusion protein (Figure 34). Cohesin ChIP-on-CHIP experiments confirmed this result, and further showed that unsumoylated cohesin binds to centromeric and pericentromeric regions, origins of replication, and regions of converging transcription, which have already been described as main cohesin binding sites (Lengronne, Katou et al. 2004). In addition, UD-fused Scc1 is depleted from sites of divergent transcription, similar to what has been described for wild-type cohesin (Figure 35) (Lengronne, Katou et al. 2004). These findings suggest that, although they are not functional for SCC, unsumoylated cohesin rings can be pushed by the transcription machinery, and should therefore interact normally with chromatin. In human cells, the GFP-mRad21-UD chimera localizes properly to the nucleus (Figure 51, Figure 52). However, we could not detect its mitotic chromosome localization neither for the wild-type nor the mRad21-UD chimeras. In fact, metaphase chromosomes showed exclusion of cohesin staining. It is possible that very little cohesin remains bound to centromeres at metaphase, making it extremely difficult to detect. Further experiments

will be required to test its binding to metaphase chromosomes and to determine any alterations in its binding sites.

As stated above, we have contemplated the possibility that the Scc1-UD fusion might affect sumoylation of other nearby proteins with potential roles in SCC. As controls, we have studied condensin and PCNA (Moldovan, Pfander et al. 2006, Hoege, Pfander et al. 2002). The Ycs4 subunit of the condensin complex is sumoylated, and it has been proposed that this modification is required for proper localization to and segregation of the rDNA locus (D'Amours, Stegmeier et al. 2004). We have observed that sumoylation of condensin is not affected in the presence of either Scc1-UD or Scc1-UD^{FA,CS} (Figure 39). In contrast, our results also show that the levels of PCNA sumoylation are slightly decreased in Scc1-UD expressing cells (Figure 40). These results suggest that in some cases, the Scc1-UD chimeras might affect sumoylation of other proteins/complexes, potentially interfering with other cellular functions. Siz1-dependent sumoylation of PCNA triggers its monoubiquitylation by the Rad18 ubiquitin ligase to promote damage bypass. *rad18*Δ cells are highly sensitive to MMS due to accumulation of recombination structures and fork collapse (Parker, Ulrich 2012), and this sensitivity can be alleviated by preventing PCNA sumoylation in a *siz1*Δ mutant. In contrast, expression of Scc1-UD has no effect on the MMS sensitivity of *rad18*Δ cells (Figure 46), indicating that Scc1-UD might slightly affect sumoylation of PCNA without affecting its SUMO-dependent functions.

VI.2. **Sumoylation target/s for Sister Chromatid Cohesion**

Our results indicate that all the cohesin subunits tested in this study are sumoylated. Which is then the relevant target for SCC? Or is sumoylation of different cohesin subunits redundant for its function in SCC?

Two different reports that analyze the role of cohesin sumoylation have been recently published. These studies are based on the identification and mutation of

sumoylatable lysine residues in the Scc1 protein. The conclusion from both papers is that sumoylation of Scc1 is required for DNA damage-induced cohesion in budding yeast and human cells (Wu, Kong et al. 2012, McAleenan, Cordon-Preciado et al. 2012), what looks strikingly similar to our results using the UD-fusion approach. Therefore, Scc1 appears to be the most relevant SUMO-target in the cohesin complex for cohesion-mediated DNA repair, and this role has been probably conserved during evolution. Scc1 is also the main acetylation target during DNA repair, at least in budding yeast (Heidinger-Pauli, Unal et al. 2009). It is therefore possible that Scc1 functions as a central element in response to DNA damage, integrating different signals through various post-translational modifications. However, Scc1 might not be the main SUMO target for SCC during an unperturbed cell cycle. Interestingly, expression of the SUMO-impaired *scc1*^{11KR} allele from its own promoter partially complements the thermosensitivity of *scc1-73* cells (McAleenan, Cordon-Preciado et al. 2012). In accordance with these reports, we have seen that expression of the *scc1*^{11KR} partially rescues the inviability of auxin-sensitive Scc1-aid cells (Figure 48). Moreover, cells that ectopically overexpress *scc1*^{11KR} show no defects in SCC in the absence of DNA damage, while some defects in SCC are detected when expressed from the *SCC1* promoter (McAleenan, Cordon-Preciado et al. 2012). In addition, we have seen that sumoylation of Scc1^{11KR} is low in the presence of the endogenous copy of Scc1, yet some sumoylation was detected when the endogenous copy was depleted using the degron system (Figure 49A). This observation suggests that the 11KR allele might be recessive and might not be able to compete with wild-type Scc1 for tripartite ring formation. The low levels of sumoylation might explain why Scc1^{11KR} can partially rescue the inviability of auxin sensitive Scc1-aid cells. It would be interesting to know if the same lysine residues are used during a normal S phase and in response to DNA damage, in order to finally rule out an essential role for Scc1 sumoylation during S phase. Cells relying only on the *scc1*^{11KR} allele display growth defects (Figure 48). Currently, it is difficult to ascertain whether the growth defects are due to lower

sumoylation or to alteration of the structural properties of the Scc1 protein by mutation of 11 lysine residues.

We have also observed that down-regulation of Scc1 sumoylation in cycling cells, by expression of the *scc1*^{11KR} allele, decreases sumoylation of other cohesin subunits (Figure 49B), what suggests that the cohesin complex might be sumoylated in a sequential manner with Scc1 sumoylation leading to sumoylation of the rest of the complex. It is also possible that sumoylation of any other subunit might also potentiate sumoylation of the rest of the complex by attracting more SUMO proteins through SUMO-interacting motifs (SIMs) present in covalently bound SUMO. However, we cannot exclude the possibility that the decrease in Smc1 sumoylation levels in *scc1*^{11KR} are secondary to alterations in Scc1 that do not involve sumoylation, like other post-translational modifications, protein folding and interactions with other proteins.

Previous reports have described an opposite role for sumoylation during mitosis for SCC maintenance and cohesin release. *ULP2* (*SMT4*) SUMO peptidase is required for maintenance of SCC when cells are arrested for prolonged periods in metaphase (Bylebyl, Belichenko et al. 2003). Two mitotic targets that are involved in SCC have been described for Ulp2, Pds5 and Top2 (Bachant, Alcasabas et al. 2002, Stead, Aguilar et al. 2003). Sumoylation enhances Top2 function in centromeric resolution, a function that could enhance cohesion loss at these loci (Bachant, Alcasabas et al. 2002). SUMO has also been proposed to negatively regulate the Pds5 subunit of the cohesin complex (Stead, Aguilar et al. 2003). Sumoylation of Pds5 starts during DNA replication and seems to maintained high until the anaphase onset. Based on genetic evidence, it has been proposed that Pds5 sumoylation would be detrimental for SCC: *pds5* thermosensitive mutants suffer from precocious loss of SCC and arrest in G2/M, although they are able to establish SCC during DNA replication; and overexpression of *SMT4* (*ULP2*) suppresses this phenotype. Pds5 sumoylation has been therefore proposed to disrupt the interaction between Pds5 and cohesin, leading to cohesin

destabilization and release (Stead, Aguilar et al. 2003). However, one should take into account that Pds5 is a subunit that has apparent antagonistic roles in cohesin function. On one hand, it forms part of the antiestablishment complex that inhibits co-entrapment of sister chromatids during DNA replication (Rowland, Roig et al. 2009). On the other hand, it is required for maintenance of SCC after DNA replication (Panizza, Tanaka et al. 2000). This duality might be easily explained by a putative role of Pds5 in preventing ring opening, a function that should be inhibited during establishment and co-entrapment of sister chromatids, and shortly afterwards reactivated to prevent DNA release. Similarly, sumoylation might promote cohesion through mechanisms that involve transient opening of the ring during the process of cohesion establishment at the replication fork. In this scenario, Pds5 sumoylation could aid in opening the ring at the time of cohesion establishment.

In support for this hypothesis, it is interesting to note that both Pds5 and SUMO are not essential in the fission yeast *Schizoaccharomyces pombe.* Although speculative, these observations suggest that the function of Pds5 and SUMO are intimately linked (Wang, Read et al. 2002, Tanaka, Nishide et al. 1999). This also suggests that Pds5 might be the main SUMO target during an unperturbed cell cycle. In fact, in our hands, Pds5 sumoylation seems to be the highest among the rest of the subunits of cohesin (Figure 17). However, how this regulation is important for establishment of sister chromatid cohesion, and how it is coordinated with acetylation dependent closure of the ring are two interesting issues to be addressed in the future. One point that should be taken into consideration is that although Pds5 is normally bound close to the ATPase domains of Smc1 and Smc3, FRET studies have shown that Pds5 might also interact with their hinge domain (Mc Intyre, Muller et al. 2007). One can imagine that this interaction could be promoted by sumoylation and might stabilize foldback structures potentially involved during sister chromatid co-entrapment (Gruber, Arumugam et al. 2006).

Our results also suggest that a proper sumoylation-desumoylation cycle of cohesin might be important for its function. Fusion of Scc1 to an inactive peptidase domain (UD^{C580S}) up-regulates cohesin sumoylation (Figure 25). This up-regulation most likely reflects the binding of the inactive domain to cohesin-SUMO conjugates, and the consequent block in deconjugation by the endogenous Ulp peptidases. The latter is supported by the finding that sumoylation of cohesin (Figure 26), viability (Figure 30B) and SCC defects (Figure 41, Figure 42), are all restored to wild-type levels when the F474A mutation is introduced in the inactive UD^{CS} domain (Scc1-$UD^{FA,CS}$). Since a substantial loss of SCC occurs when the Scc1-UD^{CS} fusion is expressed in *scc1-73* cells (Figure 41B), we estimate that the failure to desumoylate cohesin is detrimental for SCC. In accordance, *ulp2* mutants also show SCC defects (Mossessova, Lima 2000), (Bylebyl, Belichenko et al. 2003). Altogether, these observations suggest that desumoylation might be required to fine-tune the function of cohesin, a scenario that would nicely fit with cohesin sumoylation promoting the opening of the cohesin ring. It is worth noting that the levels of sumoylation are quantitatively similar in Scc1-UD^{CS} and Scc1-Ubc9 expressing cells. However, and assuming a higher rate of deconjugation than sumoylation, a fundamental difference arises between the two fusions: while the half-life of SUMO conjugates is probably very short in the Ubc9 fusion, it might substantially increase when fused to the inactive peptidase.

VI.3. **Molecular determinants of cohesin sumoylation**

Nse2 dependent sumoylation of Smc1 and Smc3 has been previously detected in nocodazole arrested *S. cerevisiae* cells but not in cycling cells (Takahashi, Dulev et al. 2008). In addition, sumoylation of human Scc1 has been shown to be dependent on Nse2 SUMO ligase *in vitro* (Potts, Yu 2005). We have seen that sumoylation of Scc1 partially depends on Nse2 in cycling cells. On the other hand, sumoylation of both Smc1 and Smc3 depends largely on Nse2 (Figure 20). Recently, two concurrent

studies identified key lysine residues that contribute to most of Scc1 sumoylation in budding yeast and in humans during DNA damage also in an Nse2 dependent manner (Wu, Kong et al. 2012, McAleenan, Cordon-Preciado et al. 2012), what suggests that Nse2 might have different targets during DNA damage and under unperturbed cell cycle conditions. Interestingly, we have seen that Nse2-dependent sumoylation of cohesin is much lower when Nse2 is not able to bind to Smc5, which suggests that Nse2 might use Smc5/6 to reach its targets (Figure 21). If this is the case, when Smc5/6 complex function is compromised, sumoylation of cohesin should also be lowered. Indeed, we have seen that in *nse3-2* thermosensitive cells sumoylation of Scc1 is decreased, which confirms our hypothesis (Figure 22). Down-regulation of Nse2 function disrupts DNA damage-induced cohesion in both budding yeast and human cells (Andrews, Palecek et al. 2005, Zhao, Blobel 2005). However, we have not observed SCC defects at the *HMR* locus in *smc5/6* or *nse2*Δ*c* mutants under unperturbed conditions. More strikingly, the little cohesion defects we have detected in *smc6-9* cells seems to be cohesin-independent, a phenomenon for which we currently do not have any explanation (Figure 42C,D,E). It is possible that DNA damage induced cohesion is more sensitive to cohesin sumoylation levels than normal SCC. In support for this hypothesis, it has been proposed that the amount of cohesin required for DNA repair is much larger than the amount required for normal SCC (Heidinger-Pauli, Mert et al. 2010).

Cohesin loading onto chromatin is required for its sumoylation (Figure 23). Sumoylation of other proteins such as PCNA also requires their residence on chromatin (Parker, Ulrich 2012). F584R mutation within the Smc1 hinge domain is lethal because it impairs heterodimerization with Smc3 hinge and loading onto chromatin (Mishra, Hu et al. 2010). Smc1 in this case is not sumoylated, suggesting that not only loading but also heterodimerization of Smc proteins is required for cohesin sumoylation. Cohesin sumoylation seems to occur in a time space between ATP

binding and hydrolysis. Smc1 mutants that lack ATP binding and interaction with Scc1 (*smc1K39I*) are not sumoylated. ATP binding and hydrolysis are required for cohesin loading to chromatin and relocation away from initial loading sites (Arumugam, Gruber et al. 2003). This indicates that Scc1-Smc1 interaction and ATP binding are both required for cohesin sumoylation. ATPase head domains of cohesin rings that are formed around *smc1E1158Q*, are locked in an engaged conformation because they cannot hydrolyze ATP and are not able to move away from initial loading sites. This mutation also causes unstable recruitment of the cohesin complex to chromatin (Hu, Itoh et al. 2011) and is inviable. Interestingly, Smc1E1158Q is sumoylated although sumoylation levels are decreased with respect to wild-type Smc1. This suggests that cohesin sumoylation somehow depends on its relocalization away from initial Scc2/4 loading sites and on its stable recruitment to chromatin.

During DNA replication, establishment of SCC requires Eco1/Ctf7 dependent acetylation of two lysine residues (K112 and K113) within Smc3 head domain (Rolef Ben-Shahar, Heeger et al. 2008). Certain mutations in Scc3, Pds5, and Rad61 reverse the lethality of *eco1*Δ and have lead to the proposal of the antiestablishment complex, which is composed by these three proteins. Upon Eco1 dependent acetylation of Smc3 cohesin rings become cohesive (tightly shut), which counteracts the antiestablishment activity (Rowland, Roig et al. 2009). Scc1 sumoylation levels are not affected by the presence of the *eco1-1* mutation, neither at the permissive (23°C) nor after shift to the restrictive (37°C) temperatures. Sumoylation of the Smc3 subunit is also not affected by inactivation of Eco1, indicating that sumoylation is required before, or in parallel to, acetylation, for the establishment of SCC (Figure 47). To test the acetylation state of Smc3 in cells that are impaired in cohesin sumoylation, we used anti-acetyl lysine antibodies. Smc3 is efficiently acetylated in a *ubc9-1* thermosensitive background, both at the permissive and restrictive temperatures (Figure 43A). Furthermore, cells that express the Scc1 or Scc1-UD as the only copy of Scc1 in the cell do not show

differences in Smc3 acetylation levels nor in Scc1-Smc3 interaction, what indicates that sumoylation is not required for cohesin acetylation. Cohesin acetylation is no longer required when the antiestablishment activity is eliminated (Rowland, Roig et al. 2009). However, deletion of *RAD61* did not recover the growth defects of the *SCC1-UD* fusion, indicating that both modifications, acetylation and sumoylation, must be required in parallel for the establishment of SCC. While acetylation promotes establishment of SCC by counteracting the antiestablishment activity, sumoylation must promote SCC through a mechanism different from the latter (Figure 46). To our knowledge, this is the first case reported in which Smc3 is acetylated but has not yet established SCC. It is possible that while acetylation locks the ring in a closed conformation around sister chromatids at the exit gate after co-entrapment, sumoylation might stabilize the open hinge conformation to allow co-entrapment of both sisters (Figure 54).

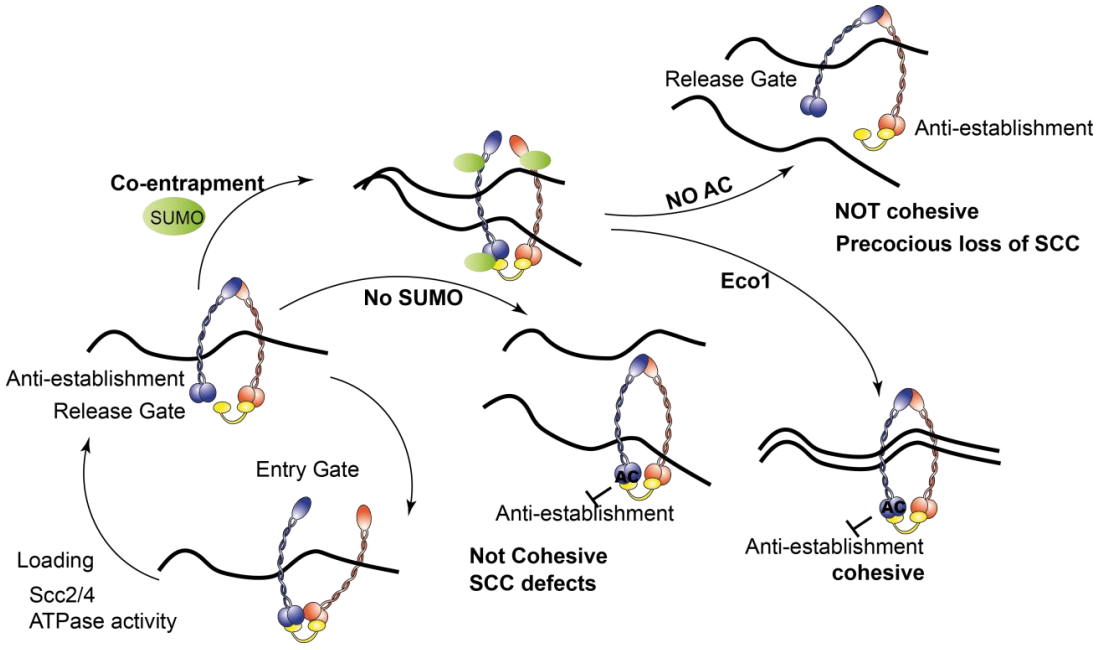

Figure 54. Model: Cohesin sumoylation might be required during coentrapment of sister chromatids. Cohesin is loaded during G1 phase of the cycle through the entry gate located at the hinge domain (Gruber, Arumugam et al. 2006). Cohesin loaded at this stage has a short residence time on chromatin and can be released by the action of the antiestablishment complex through the exit gate located at the Smc3 Scc1 interface (Nasmyth 2011). During DNA replication cohesin is sumoylated which promotes coentrapment of sister chromatids by stabilizing the open hinge conformation. Eco1 dependent Acetylation of Smc3 locks the ring in a cohesive state around sister chromatids which counteracts the

antiestablishment activity and allows establishment of sister chromatid cohesion. In the absence of acetylation the antiestablishment activity releases cohesin from sister chromatids leading to precocious loss of SCC. On the other hand, in the absence of sumoylation cohesin rings are efficiently acetylated but they are not able to establish SCC. This is probably because they are locked in a closed conformation around one sister chromatid and they are not able to embrace both sisters.

VI.4. **Cohesin sumoylation is required for DI cohesion in yeast and in humans**

DSBs are one of the most dangerous forms of DNA damage because they might lead to chromosome translocations and cancer. Cells repair DSBs by HR when CDK activity is high, and when an undamaged DNA template is available, which can be either the sister chromatid or the homologous chromosome. However, DSB repair with HR between sister chromatids (SCR) is preferable during the mitotic cell cycle because HR between homologues can lead to loss of heterozygosity (LOH) (Branzei, Foiani 2008). Cohesin promotes SCR during DSB repair by bringing the two sister chromatids in close proximity (Heidinger-Pauli, Unal et al. 2008, Strom, Karlsson et al. 2007). Different cohesin subunits are further sumoylated by various DNA damaging agents in budding yeast (Figure 18) (McAleenan, Cordon-Preciado et al. 2012). In contrast, it does not seem to be up-regulated by DNA damage in human cells (Wu, Kong et al. 2012).

Although we have seen that cohesin sumoylation promotes SCC through a mechanism different from counteracting the antiestablishment activity in yeast, we still do not know whether this is also the case in response to DNA damage. In accordance with our results, the absence of Scc1 phosphorylation by the Chk1 checkpoint kinase, which promotes acetylation, does not affect cohesin sumoylation. In fact, these results suggest that acetylation might be a downstream event (McAleenan, Cordon-Preciado et al. 2012). In striking contrast, sumoylation of human Scc1 has been proposed to counteract the antiestablishment activity of Wapl (Rad61 homolog) in response to DSBs, thereby enabling SCC and sister chromatid exchange (Wu, Kong et al. 2012). In

spite of the apparent differences, the mechanism of SUMO-mediated cohesion might not be so different, as it also does not seem to depend on cohesin acetylation in human cells.

Cohesin sumoylation does not seem to be required for loading of cohesin to DSBs; rather it is necessary for transforming unstably bound cohesin complexes to cohesive ones to promote sister chromatid recombination (Wu, Kong et al. 2012, McAleenan, Cordon-Preciado et al. 2012). In accordance with these observations, we have seen by ChIP-qPCR that Scc1-UD is efficiently loaded in the vicinity of DSBs in budding yeast (Figure 37). However, it seems to be more enriched than Scc1 wild type or Scc1-Ubc9. These results suggest that unsumoylated cohesin is recruited more efficiently to damaged sites or is more resistant to removal from chromatin. If the latter case was correct, it could be speculated that sumoylation might be required for opening of pre-loaded cohesin rings, maybe to allow the capture and co-entrapment of the sister chromatid.

Cohesin is not only required for homologous-recombination DSB-repair, but also for replication fork stability and the recovery of stalled replication forks (Tittel-Elmer, Lengronne et al. 2012). Replication forks can stall due to natural replication fork barriers or slow replication zones (replicative stress) (Branzei, Foiani 2005). Replicative stress can be also provoked externally by adding hydroxyurea (HU) (Slater 1973). Interestingly, we have seen that wild-type cells that overexpress Scc1-UD are sensitive to hydroxyurea (Figure 28), which suggests that cohesin sumoylation might also be required during replicative stress. In the future, it would be interesting to test replication fork progression in the absence of cohesin sumoylation by DNA combing.

VI.5. How might sumoylation promote co-entrapment of sister chromatids

Since all subunits are conjugated to SUMO, sumoylation of different subunits of the cohesin complex might be redundant during unperturbed cell cycle, and might be required as a sum to stabilize certain interactions between the same complex, with other cohesin complexes, or with other proteins involved in SCC. In accordance with this hypothesis, it has been recently shown that sumoylation of many proteins involved in the DNA damage repair is up-regulated in response to DNA damage. Individual sumoylation seems to stabilize physical interactions between these proteins adding up for efficient repair (Psakhye, Jentsch 2012). Our results show that, in the case of cohesin, sumoylation is not required for interactions between cohesin subunits within the same complex, since we were able to detect such interactions in the absence of sumoylation (Figure 33).

Thus, sumoylation might potentiate interaction between different cohesin complexes in places where cohesin is extensively required, like in centromeres, and thus, cohesin sumoylation might promote cohesion through ring stacking which could facilitate re-capture of escaping chromatin fibers inside an adjacent ring (Figure 55). However, interactions between different cohesin complexes have never been detected under physiological conditions. If sumoylation is required for these interactions, then these interactions might have been missed due to the short lived nature of sumoylation.

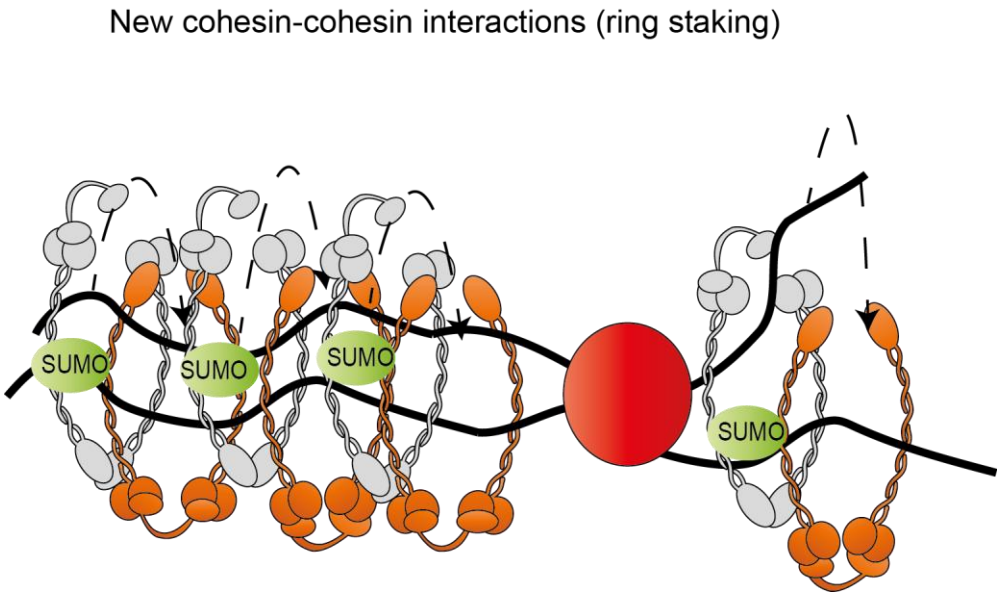

Figure 55. Sumoylation can promote co-entrapment of sister chromatids through ring stacking. Sumoylation might potentiate interaction between different cohesin complexes in places where cohesin is extensively required like in centromeres, and thus, cohesin sumoylation might promote cohesion through ring stacking which could facilitate re-capture of escaping chromatin fibers inside an adjacent ring

Moreover, cohesin sumoylation might act as a platform to recruit new cohesion factors (Figure 56), like in the case of PCNA were sumoylation recruits Srs2 (Pfander, Moldovan et al. 2005). Alternatively, cohesin sumoylation might mask sites important for cohesin interaction with other proteins that would otherwise regulate SCC negatively (Figure 56), like in the case of transcription repressors (Zheng, Yang 2004). In the future it would be important to identify suppressors of the growth defects of SUMO-impaired cohesin mutants to confirm such hypothesis.

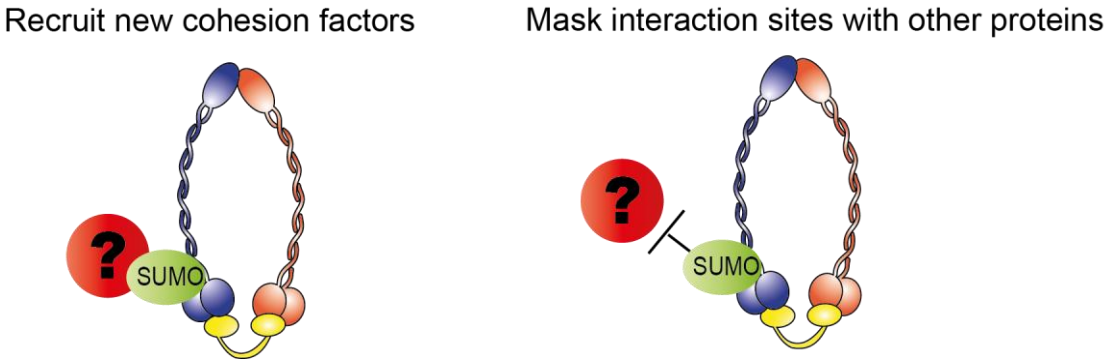

Figure 56. **Sumoylation can promote co-entrapment of sister chromatids by promoting/ inhibiting interaction with other proteins.** Cohesin sumoylation might act as a platform to recruit new cohesion

factors. Alternatively, cohesin sumoylation might mask sites important for cohesin interaction with other proteins that would otherwise regulate SCC negatively.

It is becoming more obvious nowadays that the structure of cohesin is far more flexible than the typical ring structure that we have drawn in our heads. This flexibility is highly attributed to the presence of breaks in the coiled coil probability, which allow cohesin to adapt different conformations including the recently proposed foldback structures (Gruber, Arumugam et al. 2006, Hu, Itoh et al. 2011). It has been proposed that folding of cohesin rings could be required during chromatin entrapment to allow ATPase mediated opening of the entry gate (Kurze, Michie et al. 2011). Cohesin sumoylation might cause a conformational change in the cohesin ring structure similar to what has been described for TDG (Hardeland, Steinacher et al. 2002)(Figure 57).

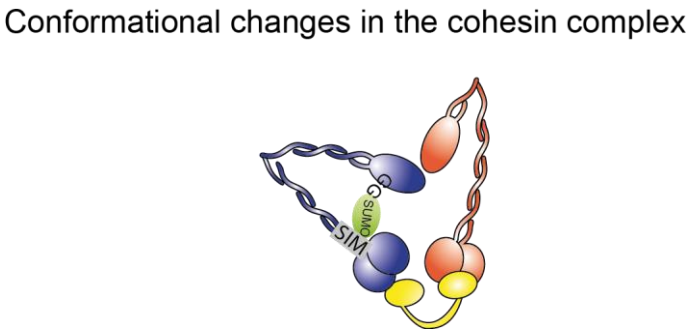

Figure 57. Sumoylation can promote co-entrapment of sister chromatids through promoting a conformational change. Cohesin sumoylation might cause a conformational change in the cohesin ring structure which can be stabilized by SUMO-SIM intra-complex interactions.

VI.6. **Implications**

Defects in cohesin establishment due to a homozygous mutation in Esco2 allele lead to a developmental disease in humans called Roberts Syndrome (RBS) (Horsfield, Print et al. 2012). If cohesin sumoylation is also required for establishment of SCC, one cannot help but wonder whether defects in cohesin sumoylation might lead to similar phenotypes in humans.

In humans, cohesin is additionally required for other vital functions that also involve chromatin coentrapment, such as holding sister chromatids during DNA damage repair (Heidinger-Pauli, Unal et al. 2008), and stabilizing chromatin loops during gene expression (Guillou, Ibarra et al. 2010). It would be tempting to think that the mechanism of coentrapment is universal for all these functions. If cohesin sumoylation has a role in co-entrapment, it might be similarly required during cohesin dependent regulation of gene expression or during DI cohesion establishment.

Cornelia de Lange syndrome (CDLS) is a developmental disease with 60% of the cases resulting from haploinsufficient mutations within the loading factor Nipbl, and 5-10% due to other mutations in Smc1, Smc3, Scc1, and HDAC8. Around 30% of the cases reported are of unknown reason. Importantly, unlike cells from RBS, cells from patients with CDLS have no apparent defects in SCC, which suggests that the developmental defects seen in these patients are due to defects in cohesin function in regulating gene expression (Horsfield, Print et al. 2012). If sumoylation is required for cohesin dependent chromatin loops formation during gene expression, it is possible that mutations in the SUMO pathway or in the mechanism of sumo-dependent coentrapment might be one of the reasons leading to the pathology of this disease.

Defects in cohesin itself or its regulators can lead to chromosomal translocations and cancer (Xu, Tomaszewski et al. 2011). Whether defects in sumoylation dependent regulation of cohesin lead to pathologies such cancer is an interesting issue that should be addressed in the future.

"Through chaos as it swirls, It's us against the world"

Us against the world, Colplay

Conclusions

VII. Conclusions

- All subunits of the cohesin complex are sumoylated *in vivo* under physiological conditions in *S. cerevisiae*.
- Cohesin sumoylation occurs during S phase and is up-regulated by DNA damage.
- Cohesin sumoylation is mostly dependent on Nse2 E3 SUMO ligase and the Smc5/6 complex.
- Cohesin sumoylation occurs at the time of cohesion establishment, after cohesin loading and ATP binding, and independently from Eco1-mediated cohesin acetylation.
- Fusion of the Scc1 subunit to a SUMO peptidase Ulp domain (UD) is a novel and efficient approach to specifically down-regulate sumoylation of all cohesin subunits.
- SUMO-depleted cohesin rings are properly formed and efficiently recruited to known cohesin binding sites on chromatin.
- Cells that lack cohesin sumoylation arrest in G2/M.
- Cohesin sumoylation is essential for Sister Chromatid Cohesion and cell viability.
- Sumoylation does not enable SCC by counteracting Rad61-dependent antiestablishment activity.
- Human cell lines that overexpress mRad21-UD accumulate in G2/M.

"...People moving all the time , inside a perfectly straight line Don't you wanna curve away? When it's such... It's such a perfect day..."

Strawbery swing, Coldplay

Supplementary Tables

VIII. Supplementary Tables

Supplementary Table 1. List of Antibodies used in Western blot analysis and immunofluorescence.

Primary Antibody	Source	Conditions	Secondary Antibody	Source	Conditions
3F10 Rat Monoclonal (α-HA)	Roche	2hours at room temperature, or overnight at 4°C 1:5000, 5% TBST Milk	AP136P Goat α-Rat IgG horse reddish peroxidase linked	Chemicon International	1 hour at room temperature, 1:10,000, TBST
9E10 Mouse Monoclonal (α-MYC)	Roche	2hours at room temperature, or overnight at 4°C 1:5000, 5% TBST Milk	NXA931 Sheep α-Mouse IgG horse reddish peroxidase linked	ECL	1 hour at room temperature, 1:10,000, TBST
F3165 M2 Mouse Monoclonal (α-FLAG)	SIGMA	2hours at room temperature, or overnight at 4°C 1:5000, 5% TBST Milk	NXA931 α-Mouse	ECL	1 hour at room temperature, 1:10,000, TBST
ST1027 Rabbit Monoclonal (α-acetylated lysine)	Millipore	2hours at room temperature, or overnight at 4°C 1:5000, 0.025% TBST Milk	NA934V Donkey α-Rabbit IgG horse reddish peroxidase linked	ECL	1 hour at room temperature, 1:10,000, TBST
AT14405 Rabbit Polyclonal (α-SUMO)	abcam	2hours at room temperature, or overnight at 4°C 1:5000, 5% TBST Milk	NA934V α-Rabbit	ECL	1 hour at room temperature, 1:10,000, TBST

A21311 Rabbit IgG Alexa Flour 488 conjugate (α-GFP) (IF)	Molecular Probes	2hours at room temperature, 1:200, PBS	A11008 Alexa Flour 488 goat α-rabbit IgG	Molecular Probes	1 hour at room temperature, 1:500, BS
Ab1791 Rabbit Polyclonal (α-Histone H3)	abcam	2hours at room temperature, or overnight at 4°C 1:1000, 5% TBST	NA934V α-Rabbit	ECL	1 hour at room temperature, 1:10,000, TBST
H2035-01 Rabbit Monoclonal (α-Hexokinase)	US Biological	2hours at room temperature, or overnight at 4°C 1:5000, 5% TBST Milk	NA934V α-Rabbit	ECL	1 hour at room temperature, 1:10,000, TBST
Ab18085 Rabbit polyclonal (α-rpd3)	abcam	2hours at room temperature, or overnight at 4°C 1:1000, 5% TBST	NA934V α-Rabbit	ECL	1 hour at room temperature, 1:10,000, TBST
AfRS115-4 (α-Smc1A)	Ana Losada	2hours at room temperature, or overnight at 4°C 1:100, 5% TBST Milk	NA934V α-Rabbit	ECL	1 hour at room temperature, 1:10,000, TBST
AfR24-3 (α-Smc3A)	Ana Losada	2hours at room temperature, or overnight at 4°C 1:300, 5% TBST Milk	NA934V α-Rabbit	ECL	1 hour at room temperature, 1:10,000, TBST
AfRS55-3 (α-Rad21)	Ana Losada	2hours at room temperature, or overnight at 4°C 1:100, 5% TBST Milk	NA934V α-Rabbit	ECL	1 hour at room temperature, 1:10,000, TBST

Supplementary Table 2. List of yeast strains used in this work.

Strain	Genotype	Procedure
Y759	**MATa scc1-73 ade2-1 TRP+ can1-100 leu2-3,112 his3-11,15 GAL, psi**	The strain 759 (W303 MATa *scc1-73*) and strain 758 (BY4741 MATα mcd1-1) were obtained from Luis Aragon's laboratory. Scc1 constructs that were cloned into YIPlac211 plasmid and expressed from the *GAL* promoter were cut with StuI for integration in the URA locus in 759 background.
YSM1498	759+ ura3:Gal-Scc1-3HA	
YSM1500	759+ ura3:Gal-Scc1-3HA-UD	
YSM1502	759+ ura3:Gal-Scc1-3HA-UD(C580S)	
Y758	MATalpha ade2 ade3 his7 leu2 trp1-1 ura3 mcd1-1	
YSM2225	759+ Smc36HA (hph)	759 was transformed with a PCR to tag Smc3 with 6HA using S2 S3 primers and pYM 16 (Janke, Magiera et al. 2004).
YSM1040	759+ TetR-YFP:ADE2 CEN5::tetO2x112::HIS3	Centromere V in 759 was tagged with 112 tet operators (1.4Kbs away), and tet repressor fused to YFP was integrated in the *ADE2* locus to generate strain 1040. This back ground was transformed with Scc1 constructs expressed from the *GAL* promoter and the *SCC1* promoter to study SCC.
YSM1476	1040+ ura3:Gal-Scc1-3HA	
YSM1478	1040+ ura3:Gal-*SCC1* -3HA-UD	
YSM1480	1040+ ura3:Gal-Scc1-3HA-UD(C580S)	
YSM1506	1040+ ura3:Gal-Scc1-3HA-Ubc9	
YSM1614	1040+ ura3:Gal-Scc1-3HA-UD(C580S, F474A)	
YSM1832	1040+ ura3:*SCC1* p-Scc1-3HA-UD	
YSM1857	1040+ ura3:*SCC1* p-Scc1-3HA-UD(C580S)	
YSM1860	1040+ ura3:*SCC1* p-Scc1-3HA	
YSM2155	1040+ ura3:*SCC1* p-Scc1-3HA-UD(C580S, F474A)	

Y343	MATa leu2::LEU2-tetR-GFP 1.4kb left of CEN5::tetO2x112::HIS3	The strain 343 (W303) that has tet operators on centromere V and tet repressor integrated in the *LEU2* locus was obtained from Tomoyuki Tanaka's lab.
Y1882	**Mata scc1-73 ade2-1 TRP1+ can1-100 leu2-3, 112 his3-11,15 ura3 GAL psi+ 3x backcrossed tetR-YFP tetO 620K ChrIV HIS**	WT strain Y1890 (original name CCG8946) and *scc1-73* strain Y1882 (original name CCG 9151) were both received from Luis Aragon's lab. These strains contain tet operators (HIS) that are 620 bp away from centromere IV and tet repressor fused to GFP (*ADE2* locus). 1882 was transformed with Scc1 constructs expressed from the *SCC1* promoter to study sister chromatid cohesion.
Y1890	**MATa ade2::ADE2 tetR-GFP, leu2 ura3 trp1 his3 his::HIS TetO ChrIV:620**	
YSM1952	1882+ ura3: *SCC1* p-Scc1-3HA-UD	
YSM1954	1882+ ura3: *SCC1* p-Scc1-3HA-UD(C580S)	
YSM1956	1882+ ura3: *SCC1* p-Scc1-3HA-UD(C580S, F474A)	
YSM1958	1882+ ura3: *SCC1* p-Scc1-3HA	
Y503	**MATa Dbar1::hisG can1-100 his3-11,15 trp1-1 ura3-1 Δlys2 Δhml::loxP-(kanMX-loxP) 2 (LEU2::GAL1-R)2::leu2-3,112 RS::HMR-tRNA-GIT1-TRP1-256lacop::RS ADE2::HIS3P-lacGFP::ade2-1**	Strains 503 (WT) and 504 (*scc1-73*) (W303 MATa bar1Δ) were obtained from Marc Gartenberg's lab. These strains have 256 lac operators integrated close to the *HMR* locus and the lac repressor fused to GFP. This background was transformed with Scc1 constructs expressed from the *GAL* promoter to study SCC.
Y504	**MATa Dbar1::hisG can1-100 his3-11,15 trp1-1 ura3-1 Δlys2 scc1-73 Δhml::loxP-(kanMX-loxP) 2 (LEU2::GAL1-R)2::leu2-3,112 RS::HMR-tRNA-GIT1-TRP1-256lacop::RS ADE2::HIS3P-lacGFP::ade2-1**	
YSM1514	504+ ura3:Gal-Scc1-3HA	
YSM1516	504+ ura3:Gal-Scc1-3HA-UD	
YTR559	504+ *nse2ΔC* (hph)	
YTR519	503+ *smc6-9* (NAT)	
YTR535	504+ *smc6-9* (NAT)	

YTR907	**MATa ade2-1 trp1D2 can1-100 leu2-3,112 his3-11,15 ura3-52 6his-Flag-SMT3:KanMX4**	**WT W303 strain**
YSM1486	1191+ ura3:Gal-Scc1-3HA	The strain 1191 was obtained from transforming **907** with Smc1-18myc PCR. This strain was transformed later on with Scc1 constructs expressed from the *GAL* promoter and integrated in the URA locus.
YSM1488	1191+ ura3:Gal-Scc1-3HA-UD	
YSM1490	1191+ ura3:Gal-Scc1-3HA-UD(C580S)	
YSM1492	1193+ ura3:Gal-Scc1-3HA	The strain 1193 was obtained from transforming **907** with Smc3-18MYC PCR. This strain was transformed later on with Scc1 constructs expressed from the *GAL* promoter /*SCC1* promoter and integrated in the URA locus.
YSM1494	1193+ ura3:Gal-Scc1-3HA-UD	
YSM1496	1193+ ura3:Gal-Scc1-3HA-UD(C580S)	
YSM1660	1193+ ura3:Gal-Scc1-3HA-UD(F474A)	
YSM1662	1193+ ura3:Gal-Scc1-3HA-UD(C580S, F474A)	
YSM1864	1193+ ura3:*SCC1* p-Scc1-3HA	
YSM1758	1193+ ura3:*SCC1* p-Scc1-3HA-UD	
YSM1844	1193+ ura3:*SCC1* p-Scc1-3HA-UD(C580S)	
YSM1961	1193+ ura3:*SCC1* p-Scc1-3HA-UD(C580S, F474A)	
YSM1907	**MATa ade2-1 trp1D2 can1-100 leu2-3,112 his3-11,15 ura3-52 6his-Flag-SMT3:KanMX4 + Tir1-9myc (His)+ Scc1-AID (hph)**	The strain 1907 was obtained by integrating Tir1-9MYC in the HIS locus (BsiwI4) in **907** which was then transformed with Scc1-AID (hph) PCR using Scc1 S2/S3 primers on p1596. This strain was transformed with Smc1/Smc3-18MYC PCR and then with Scc1 chimeras under the *SCC1* promoter integrated in the URA3 locus (StuI restriction).
YSM1963	1907+ Smc1-myc18::TRP	
YSM1965	1907+ Smc3-myc9::TRP	
YSM2017	1963+ ura3:*SCC1* p-*SCC1* -3HA	
YSM2019	1963+ ura3:*SCC1* p-*SCC1* -3HA-UD	
YSM2021	1963+ ura3:*SCC1* p-*SCC1* -3HA-UD(C580S)	
YSM2023	1963+ ura3:*SCC1* p-*SCC1* -3HA-UD(C580S, F474A)	
YSM2025	1965+ ura3:*SCC1* p-*SCC1* -3HA	
YSM2027	1965+ ura3:*SCC1* p-*SCC1* -3HA-UD	
YSM2029	1965+ ura3:*SCC1* p-*SCC1* -3HA-UD(C580S)	

YSM2031	1965+ ura3:*SCC1* p-*SCC1* -3HA-UD(C580S, F474A)	
YSM2254	1907+ Scc1-3HA-CYCt:URA3:*SCC1* p-Scc1-AID (hph)	The strain **1907** was also transformed with Scc1 constructs expressed from the *SCC1* promoter, but this time integrated in the Scc1 locus (by restriction digestion of the same vectors with *BsptI*). Then, Smc1, Smc3, Ycs4, Scc3, or Pds5 PCRs all tagged with the 9xmyc epitope were transformed to these backgrounds.
YSM2256	1907+ Scc1-3HA-UD-CYCt:URA3:*SCC1* p-Scc1-AID (hph)	
YSM2258	1907+ Scc1-3HA-UD(C580S-F474A)-CYCt:URA3:*SCC1* p-Scc1-AID (hph)	
YSM2297	2254+ Smc3-9myc (TRP)	
YSM2299	2256+ Smc3-9myc (TRP)	
YSM2301	2258+ Smc3-9myc (TRP)	
YSM2319	1965+ + Scc1-3HA-UD(C580S)-CYCt:URA3:*SCC1* p-Scc1-AID (hph)	
YSM2456	2254+ Ycs4-9myc (NAT)	
YSM2458	2256+ Ycs4-9myc (NAT)	
YSM2459	2258+ Ycs4-9myc (NAT)	
YSM2468	1907+ Ycs4-9myc (NAT)	
YSM2549	2256+ Pds5-9myc	
YSM2550	2258+ Pds5-9myc	
YSM2551	2256+ Scc3-9myc	
YSM2552	2258+ Scc3-9myc	
YSM2553	2256+ Smc1-9myc	
YSM2554	2258+ Smc1-9myc	
Y355	MATa ade2-1 trp1-1 can1-100 leu2-3,112 his3-11,15 ura3 *GAL* psi+ pep4::URA3 bar1::hisG Scc1-myc18 HIS	Original name K10611. Obtained from Frank Uhlmann's lab.
Y356	MATa ade2-1 trp1-1 can1-100 leu2-3,112 his3-11,15 ura3 *GAL* psi+ pep4::URA3 bar1::hisG Smc1-myc18::TRP	Original name K1300. Obtained from Frank Uhlmann's lab.
Y357	MATalpha ade2-1 trp1-1 can1-100 leu2-3,112 his3-11,15 ura3 *GAL* psi+ pep4::URA3 bar1::hisG Smc3-9myc (Trp)	Original name K911. Obtained from Frank Uhlmann's lab.
Y586	355+ 6xHIS-FLAG-SMT3	

Y784	357+ 6xHIS-FLAG-SMT3	
Y644	MATa his3D1 leu2D0 met15D0 ura3D0 6HisFLAG-smt3::kanMX6 Scc1-myc18 HIS	
Y746	MATa his3D1 leu2D0 met15D0 ura3D0 6HisFLAG-smt3::kanMX6 Scc1-myc18 HIS smc6-9 (NAT)	
Y1992	356+ 6xHIS-FLAG-SMT3	
YSM1227	907+ Scc1-6HA:hphNT1	
YSM1994	MATa ade2-1 trp1D2 can1-100 leu2-3,112 his3-11,15 ura3-52 6his-Flag-SMT3:KanMX4 smc1-9myc(hph)	
YSM1996	MATa ade2-1 trp1D2 can1-100 leu2-3,112 his3-11,15 ura3-52 6his-Flag-SMT3:KanMX4 scc1-9myc(hph)	
YSM1418	907+ ura3:Gal-Scc1-3HA	The strain **907** was transformed with Scc1 chimeras, which were expressed from the *GAL* promoter and integrated in the URA locus.
YSM1472	907+ ura3:Gal-Scc1-3HA-UD	
YSM1474	907+ ura3::Gal-Scc1-3HA-UD(C580S)	
YSM1520	907+ ura3:Gal-Scc1-3HA-Ubc9	
YSM1522	907+ ura3:Gal-Scc1-3HA-ubc9(c93s)	
YSM2033	1907+ p*SCC1* :*SCC1* (K165,290,252,345,391,392,394,460,500,509,521R) -3HA	**1907** was transformed with the centromeric plasmids pRS415 expressing the different Scc1(KR) alleles under the *SCC1* promoter.
YSM2034	1907+ p*SCC1* :*SCC1* -3HA	
YSM2035	1907+p*SCC1* :*SCC1* -3HA K165_290_460R (K165,290,460R)	
YSM2036	1907+pRS415	
YSM1734	907+ Pds5-9myc (hyg)	**907** was transformed with Pds5/Scc3-9MYC to obtain strains 1734 and 1736 respectively. These strains were then transformed with the Scc1 contructs expressed from the e
YSM1736	907+ Scc3-9myc(hyg)	
YSM1744	1734+ ura3:Gal-Scc1-3HA	
YSM1746	1734+ ura3::Gal-Scc1-3HA-UD	
YSM1748	1734+ ura3:Gal-Scc1-3HA-UD(C580S)	

YSM2121	1734+ ura3:*SCC1* p-*SCC1* -3HA	*GAL*/*SCC1* promoter (integrated in the URA locus). Scc1 chimeras under the *SCC1* promoter were also integrated in the Scc1 locus.
YSM2123	1734+ ura3:*SCC1* p-*SCC1* -3HA-UD	
YSM2125	1734+ ura3:*SCC1* p-*SCC1* -3HA-UD(C580S, F474A)	
YSM1750	1736+ ura3:Gal-Scc1-3HA	
YSM1752	1736+ ura3::Gal-Scc1-3HA-UD	
YSM1754	1736+ ura3:Gal-Scc1-3HA-UD(C580S)	
YSM2126	1736+ ura3:*SCC1* p-*SCC1* -3HA	
YSM2128	1736+ ura3:*SCC1* p-*SCC1* -3HA-UD	
YSM2130	1736+ ura3:*SCC1* p-*SCC1* -3HA-UD(C580S, F474A)	
YSM2329	1736+ Scc1: Scc1p-Scc1-3HA-UD:URA3	
YSM2331	1736+ Scc1:Scc1p-Scc1-3HA-UD(C580S, F474A):URA3	
YSM2333	1734+ Scc1: Scc1p-Scc1-3HA-UD:URA3	
YSM2335	1734+ Scc1: Scc1p-Scc1-3HA-UD(C580S, F474A):URA3	
YSM2337	1994+ Scc1: Scc1p-Scc1-3HA-UD:URA3	
YSM2339	1994+ Scc1: Scc1p-Scc1-3HA-UD(C580S, F474A):URA3	
1589	**MATalpha ade2-1 trp1D2 can1-100 leu2-3,112 his3-11,15 ura3-52 eco1-1 ura3::3XURA3 tetO112 his3::HIS3tetR-GFP**	The strain 1589 was obtained from Armelle Lengronne's lab (original name FU78). This strain is W303 MATalpha and *eco1-1*. We crossed 1589 with 1227and 1193 strains and then sporulated to obtain the following strains.
YNC2236	MAT a Smc1-myc18::TRP *eco1-1*6His-FLAG-Smt3 (GEN)	
YNC2208	MATa 6his-Flag-SMT3:KanMX4,Smc3-myc18::TRP	
YNC2184	MAT a 6his-Flag-SMT3:KanMX4, *eco1-1*Scc1-6HA:hphNT1	
Y898	**MATa ade2-1 trp1-1 can1-100 leu2-3,112 his3-11,15 GAL psi+ scc2-4**	The strain 898 was obtained from Ethel Queralt's lab. This

YMB1600	898+ 6HisFlag-SMT3:KanMX4, Scc1-6HA:hphNT	strain is W303 and *scc2-4*. 898 was transformed with Smt3-6HIS-FLAG and Scc1-6HA to obtain strain 1600
Y680	MATa trp1-1 his3-11,15 leu2-3,112-ubc9-1-LEU2 ura3-1 ade2-1 can1-100 ubc9::TRP1 pJBN214 (pCEN ARS URA3 TOP2-HA3x-KanMX)	The strain 680 was obtained from Stephen J. Elledge's lab. This strain is W303 and *ubc9-1*. 680 was transformed with Scc1-18xmyc (HIS) PCR to obtain strain 692. 680 was also transformed with Smt3-6HIS-FLAG to obtain strain 1249, which was then transformed with Smc3-3HA PCR.
YTR692	680+ Scc1-18myc (HIS)	
YSM1756	MATa trp1-1 his3-11,15 leu2-3,112-ubc9-1-LEU2 ura3-1 ade2-1 can1-100 ubc9::TRP1 6his-Flag-SMT3:KanMX4+ SMC3-3HA(his)	
YSM1249	MATa trp1-1 his3-11,15 leu2-3,112-ubc9-1-LEU2 ura3-1 ade2-1 can1-100 ubc9::TRP1 6his-Flag-SMT3:KanMX4	
YSM1308	MATa ade2-1 trp1D2 can1-100 leu2-3,112 his3-11,15 ura3-52 6his-Flag-SMT3:KanMX4 NSE2-TEV-3HA:HIS 10x(*GAL* p-NLS-myc9-TEVprotease-NLS2)::TRP1+ Scc1-6HA(hphNT1)	
YSM1689	Mata bar1D leu2-3,112 ura3-52 his3-D200 trp1-D63 ade2-1 lys2-801 pep4;nse3-ts2-9myc (TRP) + 6HisFlag SMT3 (GEN) Scc1-6HA	
YSM2152	1860+ rad61::kanMx4	DR014W (4,1941)::KanMX4 PCR was transformed to 1860 and 1832 strains.
YSM2153	1832+ rad61::kanMx4	
Y1649	Smc3:URA3:Smc3-3HA-HIS3MX leu2-3, 112 his3-11, 15 lys2-801 trp1-1 bar1 *GAL* +	The following strains were obtained from Elcin Unal's lab. They were then transformed with Smt3-6HIS-FLAG.
Y1650	Smc3:URA3:Smc3(K112RK113R)-3HA-HIS3MX leu2-3, 112 his3-11, 15 lys2-801 trp1-1 bar1 *GAL* +	
YSM1701	1650+ Smt3-6his-Flag (GEN)	
YSM1714	1649+ Smt3-6his-Flag (GEN)	
Y1636	ura3:Smc1.myc9	The following strains were obtained from Douglas
Y1637	ura3:Smc1(K39I)-myc9	

Y1638	ura3:Smc1(E1158Q)-myc9	Koshland's lab. They were then transformed with Smt3-6HIS-FLAG.
Y1639	ura3:Smc1(F584R)-myc9 leu2:Smc3-HA3	
Y1640	Scc1-PK9:KanMX4 smc1::kanMX4 ura3:Smc1(K554D, K661D)-myc9	
Y1641	Smc3(R665A, R668A, K669A) ura3:Smc1(K554D, K661D)-myc9	
YSM1691	1636+ Smt3-6his-Flag (GEN)	
YSM1693	1637+ Smt3-6his-Flag (GEN)	
YSM1695	1638+ Smt3-6his-Flag (GEN)	
YSM1697	1639+ Smt3-6his-Flag (GEN)	
YSM1699	1640+ Smt3-6his-Flag (HYG)	
YSM1710	1641 + Smt3-6his-Flag (GEN)	
Y312	**MATa his3-D200 leu2-3, 112 lys2-801 trp1-1 (am) ura3-52**	The strain 312 was obtained from Marco Foiani (original name CCG3144, DF5a background). We transformed this strain with Pol30-myc-7his:KanMX4 PCR done with Pol30 S2/S3 primers on pYM46 to obtain the strain 735. 735 was transformed with siz1 deletion PCRs to obtain strain 756. 735 was also transformed with Scc1 chimeras expressed from the *SCC1* promoter.
Y735	MATa his3-D200 leu2-3, 112 lys2-801 trp1-1 (am) ura3-52 Pol30-myc-7his:KanMX4	
Y756	735+ siz1::hphMX4	
YSM2419	735+ Scc1-3HA-CYCt:URA3:*SCC1* p	
YSM2420	735+ Scc1-3HA-UD-CYCt:URA3:*SCC1* p	
YSM2421	735+ Scc1-3HA-UD(fa,cs)-CYCt:URA3:*SCC1* p	
Y402	**Mat a his3Δ1 leu2Δ0 met15Δ0 ura3Δ0 rad18::kanMX4**	The strain 423, 402 were obtained from EUROSCARF and have BY4741 background. These strains were transformed with Scc1 chimeras expressed from the *SCC1* promoter and integrated in the *SCC1* locus.
Y423	**MATa his3Δ1 leu2Δ0 met15Δ0 ura3Δ0**	
YSM2533	402+ Scc1-3HA-CYCt:URA3:*SCC1* p	
YSM2535	402+ Scc1-3HA-UD-CYCt:URA3:*SCC1* p	
YSM2537	402+ Scc1-3HA-UD(fa,cs)-CYCt:URA3:*SCC1* p	
YSM2655	402+ *siz2Δ::HYG*	

Y557	**MATa his3Δ1 leu2Δ0 met15Δ0 ura3Δ0 6HisFLAG-smt3::kanMX6**	The strain 557 was obtained from Xiolan Zhao's lab (original name HZY1017, BY4741). 557 was transformed with nse2dc PCR to obtain strain 570. 557 and 570 were transformed with Scc1-18MYC and Smc1/Smc3-6HA PCRs.
Y570	557+ nse2Dc::hphMX4	
YMB648	570+Scc1-18myc	
YMB644	557+ Scc1-18myc	
YSM1959	644+ ura3: *SCC1* p-Scc1-3HA-UD	
Y569	**MATa his3Δ1 leu2Δ0 met15Δ0 ura3Δ0 6HisFLAG-smt3::kanMX6 siz1::hphMX4**	569 (siz1::hphMX4), 571 (siz2::hphMX4), 572 (siz1::natMX4 siz2::hphMX4) are derivatives of HZY1017 and were obtained from Luis Aragon's lab. These strains were transformed with Scc1-18xmyc.
Y571	**MATa his3Δ1 leu2Δ0 met15Δ0 ura3Δ0 6HisFLAG-smt3::kanMX6 siz2::natMX4**	
Y572	**MATa his3Δ1 leu2Δ0 met15Δ0 ura3Δ0 6HisFLAG-smt3::kanMX6 siz1::natMX4**	
YMB650	569+ Scc1-18myc HIS	
YMB642	571+ Scc1-18myc HIS	
YMB652	572+ Scc1-18myc HIS	
YMB2373	570+Smc1-6HA	
YMB2214	557+Smc1-6HA	
YMB2374	570+Smc3-6HA	
YMB2164	557+Smc3-6HA	
YTR2403	557+ *GAL* S-3HA-NSE2:natNT2	The strain 2403 was obtained by replacing the endogenous promoter of Nse2 in 557 with the *GAL* promoter which was done by transforming Nse2 S1/S4 PCR on pYM-N32. 2403 was transformed with Smc1/Smc3-6HA S2/S3 PCR from pYM15.
YSM2465	2403+ Smc1-6HA(HIS)	
YSM2467	2403+ Smc3-6HA(HIS)	

Supplementary Table 3. List of plasmids used in this work

Plasmid	Genotype	Procedure
pSM957	YCplac111-[LEU2]-[(SalI)-Gal-(KpnI-XhoI)-*SCC1* -(SphI)-3HA-CYCt]	*SCC1* constructs were first made in pYES2 vector then they were transformed to YCplac111 and finally they were transferred to YIplac211. First the 3HA tag was cloned to pYES2 by PCR using 1274/5 primers from pYMN24 and then ligation with pYES2. Then the cDNA of UBC9 was cloned after the 3HA tag by PCR using 1282/3 primers (pTR827). Next, *SCC1* was cloned before the HA tag in p827 using primers1288/9 from genomic DNA (pTR871). UD (c-terminal Ulp1 domain) PCR using primers 1206/7 was cloned after the 3HA in pYES2 (p865). Then *SCC1* was cloned before the HA tag in p865 to get p881. SMC5 was also cloned before the 3HA tag using primers 1290/1 (p873). To get pYES2 *SCC1* -3HA without Ubc9 fusion, Ubc9 was removed by restriction with XbaI in p871 and then relegation (p901). To transform *SCC1* constructs in to YCplac111 was transformed with *GAL* -3HA PCR using primers 1325/6, and then *SCC1* , *SCC1* -UD, and *SCC1* -Ubc9 were amplified from p871, p881, p901 respectively and cloned into this vector. Mutations on the UD and Ubc9 were done by SDM. Recombinations were done in MC1061 E.coli strain then transferred in to Dh5α. The gal promoter was replaced by the *SCC1* promoter in 1624 by PCR from 1624 (primers1288/1790) and recombination with PCR *SCC1* promoter (primers1782/1783). *SCC1* -3HA alone was obtained by Sph1 restriction to
pTR918	YCplac111-[LEU2]-[(SalI)-Gal-(KpnI-XhoI)-*SCC1* -(SphI)-3HA-(XbaI)-UBC9-CYCt]	
pTR920	YCplac33-[URA3]-[(SalI)-Gal-(KpnI-XhoI)-SMC5-(SphI)-3HA-(XbaI)-UD-CYCt]	
pTR1124	YCplac111-[LEU2]-[(SalI)-Gal-(KpnI-XhoI)-*SCC1* -(SphI)-3HA-(XbaI)-UD(C580S)-CYCt]	
pTR873	pYES2-[URA3]-(KpnI-XhoI)-SMC5-(SphI)-3HA-(XbaI)-UD	
pTR882	pYES2-[URA3]-(KpnI-XhoI)-SMC5-(SphI)-3HA-(XbaI)-UBC9	
pSM1718	YIplac211-[URA3]-(SalI, EcorI)-Gal-(KpnI-XhoI)-*SCC1* -(SphI)-3HA-CYCt	
pSM1526	YIplac211-[URA3]-Gal-(KpnI-XhoI)-*SCC1* -(SphI)-3HA-(XbaI)-UBC9-CYCt	
pSM1527	YIplac211-[URA3]-Gal-(KpnI-XhoI)-*SCC1* -(SphI)-3HA-(XbaI)-UBC9(c93s)i-CYCt	
pSM1624	YIplac211-[URA3]-Gal-(KpnI-XhoI)-*SCC1* -(SphI)-3HA-(XbaI)-UD-CYCt	
pSM1720	YIplac211-[URA3]-Gal-(KpnI-XhoI)-*SCC1* -(SphI)-3HA-(XbaI)-UD(C580S)-CYCt	
pSM1570	YIplac211-[URA3]-Gal-(KpnI-XhoI)-*SCC1* -(SphI)-3HA-(XbaI)-UD(D451N)-CYCt	
pSM1572	YIplac211-[URA3]-Gal-(KpnI-XhoI)-*SCC1* -(SphI)-3HA-(XbaI)-UD(F474A)-CYCt	
pSM1612	YIplac211-[URA3]-Gal-(KpnI-XhoI)-*SCC1* -(SphI)-3HA-(XbaI)-UD(F474A)(C580S)-CYCt	

pSM1653	YIplac211-[URA3]-*SCC1* p-*SCC1* -(SphI)-3HA-(XbaI)-UD-CYCt	remove the UD and religation.
PSM1842	YIplac211-[URA3]-*SCC1* p-*SCC1* -(SphI)-3HA-(XbaI)-UD(C580S)-CYCt	
pSM1846	YIplac211-[URA3]-(SalI, EcorI)-*SCC1* promoter-*SCC1* -(SphI)-3HA-CYCt	
pSM1909	YIplac211-[URA3]-*SCC1* p-*SCC1* -(SphI)-3HA-(XbaI)-UD(C580S, F474A)-CYCt	
pTR2395	pRS315-NSE2promoter-NSE2-3HA (Leu2, Amp)	NSE2-3HA was amplified with 5'-HindIII-Nse2promoter and 3'-SacI -3HA, and cloned in to HindIII-SacI sites in pRS315. M1 and M2 single and double mutations on Nse2 were done by site-directed mutagenesis.
pTR2397	pRS315-NSE2promoter-nse2-3HA M2 (Leu2, Amp)	
pSM2399	pRS315-NSE2promoter-nse2-3HA M1 (Leu2, Amp)	
pSM2400	pRS315-NSE2promoter-nse2-3HA M1 (Leu2, Amp)	
pSM2401	pRS315-NSE2promoter-nse2-3HA M2+M1 (Leu2, Amp)	
pSM2402	pRS315-NSE2promoter-nse2-3HA M2+M1 (Leu2, Amp)	
p2006	p*SCC1* :*SCC1* -3HA K2ndR+K460R (K165,290,252,345,391,392,394,460,500,509,521R)	The following plasmids were provided by Luis Aragon's lab.
p2007	p*SCC1* :*SCC1* -3HA K165_290_460R (K165,290,460R)	
p2015	p*SCC1* :*SCC1* -3HA	
p2016	pRS415	

pCJ097	*tetR-YFP* (Ade) in pRS402	Received from Elmar Schiebel lab. Cut with *StuI* and integrated in the *ADE* locus
pTR 600	pRS303 (YIpHIS3) (BamHI/BglII) tetO2x112 [5,6kb] (BamHI/BamHI)900bpDNA"TO2"[1,4-0,5kb left of CEN5; AACGTAACGTCTTG---CAACAAAAAC](XbaI/XbaI)	Original name pT271. Received from T. Tanaka. Cut with *SpeI* to integrate 1.4 Kb away from CenV.
p1596	plinker-IAA17:hphNT (PCR template for C-aid tagging, IAA17 from Arabidopsis thaliana)	The following plasmids were obtained from Yeast Genetic Resource Center
p1598	plinker-IAA17:natNT (PCR template for C-aid tagging, IAA17 from Arabidopsis thaliana)	
p1361	pADH11 promoter-OsTIR1-9myc (Digest with StuI for integration at the URA3 locus.	
pNC1854	pADH11 promoter-OsTIR1-9myc (Digest with BsiwI 4 for integration at the HIS locus.	
pCB2408	CMVp-FLAG-GFP-RAD21-4HA-UD C603S	Human full length 4HA-SENP1 was cloned in the c-terminus of human Scc1 found in the commercial vector CMV FLAG-GFP-*SCC1* . On the newly made vector, human Scc1 was substituted by mouse Scc1 using the restriction sites BsrGI and NotI (pCB2383). To obtain mouse Scc1 vector without SENP1, SENP1 was removed by digesting the vector with SpeI (pCB2389). SENP1 active site C603 was mutated to Serine by site directed mutagenesis (pCB2411).
pCB2411	CMVp-FLAG-GFP-MmRAD21-4HA-UD C603S	
pCB2389	CMVp-FLAG-GFP-MmRAD21-4HA	
pCB2383	CMVp-FLAG-GFP-MmRAD21-4HA-UD	
pTR2328	pUC57-4HA-SENP1	
p2320	pET28-SENP1-Kan David Reverter UAB	

p2321	pm*SCC1* -AMP Ana Losada CNIO	
p2322	pEGFP-h*SCC1* (KAN) EUROSCARF	
p2323	pH2B-mCherry (KAN) EUROSCARF	
p2326	pYM1 3HA-KAN	
pSR2377	pTR2328-p2322 (kan)	
pSR2376	pTR2328-p2322 (Kan)	
p2327	pYM4 3myc-Kan	

Supplementary Table 4. List of primers used in this work

Primer	Description	SEQUENCE	Procedure
CYO1554	Nse2 (134)	AAACAAATTGATGAGACCAT	Primers used to clone Nse2, or check deletion of c terminal of Nse
CYO1920	5'-HindIII-NSE2p (to clone Nse2 promoter plus NSE2 ORF	AATAAAGCTTCTATGCGTTCCTTTGATTCTGGTTACTC	
CYO1921	3' SacI-pYM (to clone Nse2-3HA)	AGGAATGAGCTCCTAGCACTGAGCAGCGTAATCTGG	
CYO1936	Reverse primer to create M1 mutations on 5BD domain of NSE2 by ExSite method (up to ATG). ApaLI site for diagnosis	P-CACTCTTAGCGATCGGATTATCGTTCAAGGCCAT	
CYO1699	Forward primer to create M1 mutations on 5BD domain of NSE2 by ExSite method. ApaLI site for diagnosis	P-CACCTGCAGCTCCAAAATCAGGTAAGTACTTCC	
CYO1701	Forward primer to create M2 mutations on 5BD domain of NSE2 by ExSite method. XhoI site for diagnosis	P-GAGACGCTAGCAATATATATCAACAATGCTAC	
CYO1702	Reverse primer to create M2 mutations on 5BD domain of NSE2 by ExSite method. XhoI site for diagnosis	P-GAGCATGAGCATTATGGAAGTACTTACCTG	
CYO1179	KanB	CTGCAGCGAGGAGCCGTAAT	Kan B was used to check gene deletions marked by antibiotics resistance genes
CYO1274	5'-SphI-3HA	GAGTGCATGCATGGGTTACCCATACGAT	Primers used to create Scc1

CYO1275	3'-SphI-3HA	GAGCGCATGCAGGGAGACCGGCAGATCC	constructs
CYO1277	5'-*SCC1* (834)	TGAATCAATCATGTCTGAGGAG	
CYO1282	5'-XbaI-Ubc9(+intron)	GTAAGTCTAGAATGAGTAGTTTGTGTCTACAGC	
CYO1283	3-XbaI-STOP-Ubc9	AGGAATTCTAGACTATTTAGAGTACTGTTTAGCT	
CYO1288	5'-KpnI-Scc1	GTAAGGGTACCATGGTTACAGAAAATCCTCAACG	
CYO1289	3'-XhoI-Scc1	AGAAGCTCGAGCAGCATTGATAAACCTTTCAAATA	
CYO1306	3'-XbaI-ULP1	AGGAATTCTAGATTTTAAAGCGTCGGTTAAAATC	
CYO1307	5'-XbaI-ULP1C	GTAAGTCTAGAATGGCTTTGGCAAGTAGAGAAAATACTCAGTTAATG	
CYO1325	5'-*GAL* (pYES2)-SalI	GTAAGGTCGACCGGATTAGAAGCCGCCGAGCGGG	
CYO1326	3'-CYCt(pYES2)-SalI	AGAAGGTCGACAAAGCCTTCGAGCGTCCCAAAA	
CYO1516	5'-ulp1SDMC580S	GCAACCAAATGGCTACGACTCCGGAATATATGTTTGTATGAATAC	
CYO1517	3'-ulp1SDMC580S	GTATTCATACAAACATATATTCCGGAGTCGTAGCCATTTGGTTGC	
CYO1541	Gal 3'. To create gap in pTR899 or pTR900	CATGTAATTAGTTATGTCACGC	
CYO1542	CYCt 5'. To create gap in pTR899 or pTR900	TTTTTTCTCCTTGACGTTAAAG	
CYO1766	SDM oligo for F474A on Ulp1	CAGTGGCGTTTAATTCAGCTTTCTATACCAATTTATC	
CYO1767	SDM oligo for F474A on Ulp1	GATAAATTGGTATAGAAAGCTGAATTAAACGCCACTG	

CYO1782	5'-*SCC1* promoter to recombine in YIP (PstI digested) vectors	ATGATTACGCCAAGCTTGCATGCA GAGAAACCGTTTATTAGCGT	
CYO1783	3'-*SCC1* (125)	TGTGTTTGGATAACCGATCCTC	
CYO1790	3'-*SCC1* promoter to recombine in YIP. Anneals on Yips	ACGCTAATAAACGGTTTCTCTGCA TGCAAGCTTGGCGTAATCAT	
CYO1816	5'-Ubc9/cUlp1-Marker fusion. Use for amplification from pYM plasmids	CATGTAATTAGTTATGTCACGTAAA AAGTGGAACGATCATTCAAG	
CYO1817	3'-Ubc9/cUlp1-Marker fusion. Use for amplification from pTR1138 or pTR1140	CTTGAATGATCGTTCCACTTTTTAC GTGACATAACTAATTACATG	
CYO1837	5' Ubc9/cUlp1 deletion HpaI	AACGCATGCAGGGAGACCGGCAG	
CYO1838	3' Ubc9/cUlp1 deletion HpaI	AACCATCATGTAATTAGTTATGTCA CG	
CYO1885	3'-SacI-6HA. To clone any gene tagged with pYM in YC/Iplac series.	AGGAATGAGCTCAAGACTGTCAAG GAGGGTATTCTGG	
CYO1871	3' *SCC1* -457 (promoter region)	CACATCCAGTCTACAGGGATC	
CYO1872	3' *SCC1* (340)	CTGTAGAAGTCATCTTCTGGCTTG	
CYO1859	5' 6HA-cUlp1 fusion	GTTCCAGATTACGCTTCTAGCATG GCTTTGGCAAGTAGAGAA	
CYO1860	3' 6HA-cUlp1 fusion	TTCTCTACTTGCCAAAGCCATGCT AGAAGCGTAATCTGGAAC	
CYO1861	S2-Scc1 (only works for recombination in the integrative Scc1 vectors)	GTAAGCGTGACATAACTAATTACA TGATGCGGCCCTCTAGAATCGATG AATTCGAGCTCG	
CYO1060	*SCC1* (1463)	GGCGAAGATTTTAAGGAAGGAA	Primers to amplify cohesin subunits or check there integration in the
CYO1061	*SCC1* +288	TGAGAAAATTTCGGCTTCACC	
CYO1207	SMC3(3394)	CTGTATGTGCCATTGCTTTGATTC	

CYO1208	SMC3+329	CAGTAGAATACACGTCACAGAAAGCT	genome
CYO1209	SMC1(3367)	TCAAAGACATGGAATATCTTTCTGG	
CYO1210	SMC1+316	GTTTATGTATGCAAATACAGCTACAA	
CYO1800	pds5 5'	ACATACCAGAGAGCTTGACTG	
CYO1801	pds5 3'	TAACGTAGTCGTGCCGAACG	
CYO1802	scc3 5'	CCCGCTGTTCAAAAAAATCGTAG	
CYO1803	scc3 3'	TGCTACAATTAACATGCATAACAAC	
CYO1854	5' RAD61 -293	GATTCAACAAGGTTATTTGCAGAAG	
CYO1855	3' RAD61 +302	CCACCAAACTTATGTCGTGAAAAA	
CYO1856	5' RAD61 -391	ATGTTAGAGTGCTCAAAGATGCTGG	
CYO 1073	SMT3+154	GGAAAGAGGCGTGGACAAAACTAT	Primers to amplify Smt3 or check its integration in the genome
CYO 1074	SMT3-222	TATGAATATGTTGGGTTACCCAGC	
CYO1914	5'SDM on pCMV-GFP-h*SCC1* to remove STOP and BglII site	CGGCGGAGGAGGGTCCGGAGGC	Primers used to clone mouse and human Rad21-SENP1 in to the vector CMV and SDM on SENP1
CYO1915	3'SDM on pCMV-GFP-h*SCC1* to remove STOP and BglII site	CGGCCGCTTATAATATGGAACCTTGGTCCAGGTG	
CYO1916	5' BsrGI Mouse RAD21 for cloning in pCMV-Flag-GFP-RAD21-4HA-UD	CGCGTGTACAAGGGGGGAGGAGGGGGATCCGGATTCTACTTCTACGCACATTTTGTCC	
CYO1917	3' NotI Mouse RAD21 for cloning in pCMV-Flag-GFP-RAD21-4HA-UD	CGCGGCGGCCGCTGATAATATGGAACCGTGGTC	

CYO1931	Forward primer for sequencing inserts downstream EGFP (original vector from Euroscarf)	TGGTCCTGCTGGAGTTCGTG	
CYO1932	Reverse primer for sequencing Hs or Mm Scc1	CTCCTGTCTCTTTCCACATC	
CYO1933	duplex siRNA to inhibit only Hs Scc1 (Ana Losada Rad21-2)	GGUGAAAAUGGCAUUACGGDTDT CYO1933B CCGUAAUGCCAUUUUCACCDTDT	
CYO1934	Forward primer for C602S exsite on HsSENP1	5'P-GGAATGTTTGCCTGCAAATATGC	
CYO1935	Reverse primer for C602S exsite on HsSENP1	5'P-GGAGTCACTTCCATTCATCTGC	
CYO1936	Reverse primer to create M1 mutations on 5BD domain of NSE2 by ExSite method (up to ATG). ApaLI site for diagnosis	P-CACTCTTAGCGATCGGATTATCGT TCAAGGCCAT	
CYO1949	Forward primer to sequence Hs or Mm Scc1	GCCAAGAGGAAGAGGAAG	
CYO1950	Reverse primer to sequence SENP1 on pGFP-RAD21-UD constructs	ATTCGAAGCTTGAGCTCG	
CYO1261	S3-SMT3	CCCAGTTCAGTTCTAGTTTTACAAA TAAATACACGAGCGATGCGTACGC TGCAGGTCGAC	S2/S3 primers
CYO1918	S1-NSE2 (5' for GalNSE2)	CCAAGGCAAGACTATATAAAAAAA GAATAACTTTAAAAATGCGTACGC TGCAGGTCGAC	
CYO1919	S4-NSE2 (3' for GalNSE2)	GTAGAGGAACTGACTTGGGTATAG GATTATCGTTCAAGGCCATCGATG AATTCTCTGTCG	

CYO1862	S3-Nse2	CAGGAACAGGATAAAAGAAGTAGT CAAGCCATCGATGTTTTACGTACG CTGCAGGTCGAC	
CYO1863	S2-Nse2	CGGGCCGAAGGGCTCGGATAAGA GAAACAATAATTTTGTTTATCGATG AATTCGAGCTCG	
CYO1430	S3-nse2dc	ACGAAGACGATCTACAAATAGAAG GTGGTAAAATTGAATTGACTCGTA CGCTGCAGGTCGAC	
CYO1818	S2-SMC3	CAAAACTGATATTTTTATATACAAA TCGTTTCAAATATCTCATCGATGAA TTCGAGCTCG	
CYO1819	S3-SMC3	GCAATCGGATTCATTAGAGGTAGC AATAAATTCGCTGAAGTCCGTACG CTGCAGGTCGAC	
CYO1834	S2-Smc1	TTAGTTATTTGACGGGTTATAGCA GAGGTTGGTTTCATAGAATCGATG AATTCGAGCTCG	
CYO1835	S3-Smc1	TCGTCGAAGATCATAACTTTGGAC TTGAGCAATTACGCAGAACGTACG CTGCAGGTCGAC	
CYO1639	S3-*SCC1*	AAAATAGACGCCAAACCTGCACTA TTTGAAAGGTTTATCAATGCTCGTA CGCTGCAGGTCGAC	
	-46kb	F: GTATCACGAGCCCATCTCCAAT AG R: CATCCCTCACCAAGGAAGAAA GAG	Primer used for real time PCR: *HMR* DSB
	-30Kb	F: TCGTCGTCGCCATCATTTTC R: GCCCAAGTTTGAGAGAGGTTG C	

	-9.3kb	F: TCAGGGTCTGGTGGAAGGAATG R: CAAAGGTGGCAGTTGTTGAACC	
	-5kb	F: ATTGCGACAAGGCTTCACCC R: CACATCACAGGTTTATTGGTTCCC	
	-3.4kb	F: ATTCTGCCATTCAGGGACAGCG R: CGTGGGAAAAGTAATCCGATGC	
	-0.7kb	F: CCACATTAAATACCAACCCATCCG R: TAGTGATGAGGAGAAGAAGTTGTTGC	
	+0.5kb	F: CATGCGGTTCACATGACTTTTGAC R: GGAAGTAACCTCTACTGTGGAGGCAC	
	+2.2kb	F: AACGCTCGTCGATCGCCGTTCTAA R: AATGGATTTGCCAAATGCACAT	

	+5.6kb	F: CAGGTTTATATCCACCTTCATCGG R: TTTGGGGCAACAGTAGGCAGTG	
	+7.7kb	F: GCAATCGTGTCAATGTGGTCATC R: GTTTCAGGAGCCCCATAATCAAC	
	+12.8kb	F: CGTTGTCTTTTCGTTTGGTGTCTG R: GCTCTTTGCCCCTGTCTTTGAC	
	+30kb	F: TCCAGGCGGGTGTGAAAAAC R: ATGGGGAATACGGAAGTGGGTC	

"...Honey you are a rock, upon which I stand... I came here with a load, and it feels so much lighter now I met you, and honey you should know, that I could never go on without you..."

Green eyes, Coldplay

References

IX. References

ALEXANDRU, G., UHLMANN, F., MECHTLER, K., POUPART, M.A. and NASMYTH, K., 2001. Phosphorylation of the cohesin subunit Scc1 by Polo/Cdc5 kinase regulates sister chromatid separation in yeast. *Cell,* **105**(4), pp. 459-472.

ANDERSON, D.E., LOSADA, A., ERICKSON, H.P. and HIRANO, T., 2002. Condensin and cohesin display different arm conformations with characteristic hinge angles. *The Journal of cell biology,* **156**(3), pp. 419-424.

ANDREWS, E.A., PALECEK, J., SERGEANT, J., TAYLOR, E., LEHMANN, A.R. and WATTS, F.Z., 2005. Nse2, a component of the Smc5-6 complex, is a SUMO ligase required for the response to DNA damage. *Molecular and cellular biology,* **25**(1), pp. 185-196.

ARUMUGAM, P., GRUBER, S., TANAKA, K., HAERING, C.H., MECHTLER, K. and NASMYTH, K., 2003. ATP hydrolysis is required for cohesin's association with chromosomes. *Current biology : CB,* **13**(22), pp. 1941-1953.

ARUMUGAM, P., NISHINO, T., HAERING, C.H., GRUBER, S. and NASMYTH, K., 2006. Cohesin's ATPase activity is stimulated by the C-terminal Winged-Helix domain of its kleisin subunit. *Current biology : CB,* **16**(20), pp. 1998-2008.

BACHANT, J., ALCASABAS, A., BLAT, Y., KLECKNER, N. and ELLEDGE, S.J., 2002. The SUMO-1 isopeptidase Smt4 is linked to centromeric cohesion through SUMO-1 modification of DNA topoisomerase II. *Molecular cell,* **9**(6), pp. 1169-1182.

BAK, A.L., ZEUTHEN, J. and CRICK, F.H., 1977. Higher-order structure of human mitotic chromosomes. *Proceedings of the National Academy of Sciences of the United States of America,* **74**(4), pp. 1595-1599.

BANNISTER, L.A., REINHOLDT, L.G., MUNROE, R.J. and SCHIMENTI, J.C., 2004. Positional cloning and characterization of mouse mei8, a disrupted allelle of the meiotic cohesin Rec8. *Genesis (New York, N.Y.: 2000),* **40**(3), pp. 184-194.

BAXTER, J., SEN, N., MARTINEZ, V.L., DE CARANDINI, M.E., SCHVARTZMAN, J.B., DIFFLEY, J.F. and ARAGON, L., 2011. Positive supercoiling of mitotic DNA drives decatenation by topoisomerase II in eukaryotes. *Science (New York, N.Y.),* **331**(6022), pp. 1328-1332.

BAYER, P., ARNDT, A., METZGER, S., MAHAJAN, R., MELCHIOR, F., JAENICKE, R. and BECKER, J., 1998. Structure determination of the small ubiquitin-related modifier SUMO-1. *Journal of Molecular Biology,* **280**(2), pp. 275-286.

BECKOUET, F., HU, B., ROIG, M.B., SUTANI, T., KOMATA, M., ULUOCAK, P., KATIS, V.L., SHIRAHIGE, K. and NASMYTH, K., 2010. An Smc3 acetylation cycle is essential for establishment of sister chromatid cohesion. *Molecular cell,* **39**(5), pp. 689-699.

BERMUDEZ-LOPEZ, M., CESCHIA, A., DE PICCOLI, G., COLOMINA, N., PASERO, P., ARAGON, L. and TORRES-ROSELL, J., 2010. The Smc5/6 complex is required for dissolution of DNA-mediated sister chromatid linkages. *Nucleic acids research,* **38**(19), pp. 6502-6512.

BERNIER-VILLAMOR, V., SAMPSON, D.A., MATUNIS, M.J. and LIMA, C.D., 2002. Structural basis for E2-mediated SUMO conjugation revealed by a complex

between ubiquitin-conjugating enzyme Ubc9 and RanGAP1. *Cell,* **108**(3), pp. 345-356.

BORGES, V., SMITH, D.J., WHITEHOUSE, I. and UHLMANN, F., 2013. An Eco1-independent sister chromatid cohesion establishment pathway in S. cerevisiae. *Chromosoma,* **122** (1-2), pp. 121-34.

BRANZEI, D. and FOIANI, M., 2008. Regulation of DNA repair throughout the cell cycle. *Nature reviews.Molecular cell biology,* **9**(4), pp. 297-308.

BRANZEI, D. and FOIANI, M., 2005. The DNA damage response during DNA replication. *Current opinion in cell biology,* **17**(6), pp. 568-575.

BRANZEI, D., SOLLIER, J., LIBERI, G., ZHAO, X., MAEDA, D., SEKI, M., ENOMOTO, T., OHTA, K. and FOIANI, M., 2006. Ubc9- and mms21-mediated sumoylation counteracts recombinogenic events at damaged replication forks. *Cell,* **127**(3), pp. 509-522.

BUHEITEL, J. and STEMMANN, O., 2013. Prophase pathway-dependent removal of cohesin from human chromosomes requires opening of the Smc3-Scc1 gate. *The EMBO journal,* **32**(5); pp. 666-76.

BYLEBYL, G.R., BELICHENKO, I. and JOHNSON, E.S., 2003. The SUMO isopeptidase Ulp2 prevents accumulation of SUMO chains in yeast. *The Journal of biological chemistry,* **278**(45), pp. 44113-44120.

CANUDAS, S. and SMITH, S., 2009. Differential regulation of telomere and centromere cohesion by the Scc3 homologues SA1 and SA2, respectively, in human cells. *The Journal of cell biology,* **187**(2), pp. 165-173.

CARTER, S.D. and SJOGREN, C., 2012. The SMC complexes, DNA and chromosome topology: right or knot? *Critical reviews in biochemistry and molecular biology,* **47**(1), pp. 1-16.

CHAN, K.L., ROIG, M.B., HU, B., BECKOUET, F., METSON, J. and NASMYTH, K., 2012. Cohesin's DNA exit gate is distinct from its entrance gate and is regulated by acetylation. *Cell,* **150**(5), pp. 961-974.

CHANG, C.R., WU, C.S., HOM, Y. and GARTENBERG, M.R., 2005. Targeting of cohesin by transcriptionally silent chromatin. *Genes & development,* **19**(24), pp. 3031-3042.

CHATTERJEE, A., ZAKIAN, S., HU, X.W. and SINGLETON, M.R., 2013. Structural insights into the regulation of cohesion establishment by Wpl1. *The EMBO journal,* **6**; 32(5), pp. 677-87.

CHAVEZ, A., GEORGE, V., AGRAWAL, V. and JOHNSON, F.B., 2010. Sumoylation and the structural maintenance of chromosomes (Smc) 5/6 complex slow senescence through recombination intermediate resolution. *The Journal of biological chemistry,* **285**(16), pp. 11922-11930.

CHENG, C.H., LO, Y.H., LIANG, S.S., TI, S.C., LIN, F.M., YEH, C.H., HUANG, H.Y. and WANG, T.F., 2006. SUMO modifications control assembly of synaptonemal complex and polycomplex in meiosis of Saccharomyces cerevisiae. *Genes & development,* **20**(15), pp. 2067-2081.

CIOSK, R., SHIRAYAMA, M., SHEVCHENKO, A., TANAKA, T., TOTH, A., SHEVCHENKO, A. and NASMYTH, K., 2000. Cohesin's binding to chromosomes depends on a separate complex consisting of Scc2 and Scc4 proteins. *Molecular cell,* **5**(2), pp. 243-254.

CIOSK, R., ZACHARIAE, W., MICHAELIS, C., SHEVCHENKO, A., MANN, M. and NASMYTH, K., 1998. An ESP1/PDS1 complex regulates loss of sister chromatid cohesion at the metaphase to anaphase transition in yeast. *Cell,* **93**(6), pp. 1067-1076.

COBBE, N. and HECK, M.M., 2004. The evolution of SMC proteins: phylogenetic analysis and structural implications. *Molecular biology and evolution,* **21**(2), pp. 332-347.

CREMONA, C.A., SARANGI, P., YANG, Y., HANG, L.E., RAHMAN, S. and ZHAO, X., 2012. Extensive DNA Damage-Induced Sumoylation Contributes to Replication and Repair and Acts in Addition to the Mec1 Checkpoint. *Molecular cell,* **45**(3); pp. 422-32.

D'AMOURS, D., STEGMEIER, F. and AMON, A., 2004. Cdc14 and condensin control the dissolution of cohesin-independent chromosome linkages at repeated DNA. *Cell,* **117**(4), pp. 455-469.

DEARDORFF, M.A., BANDO, M., NAKATO, R., WATRIN, E., ITOH, T., MINAMINO, M., SAITOH, K., KOMATA, M., KATOU, Y., CLARK, D., COLE, K.E., DE BAERE, E., DECROOS, C., DI DONATO, N., ERNST, S., FRANCEY, L.J., GYFTODIMOU, Y., HIRASHIMA, K., HULLINGS, M., ISHIKAWA, Y., JAULIN, C., KAUR, M., KIYONO, T., LOMBARDI, P.M., MAGNAGHI-JAULIN, L., MORTIER, G.R., NOZAKI, N., PETERSEN, M.B., SEIMIYA, H., SIU, V.M., SUZUKI, Y., TAKAGAKI, K., WILDE, J.J., WILLEMS, P.J., PRIGENT, C., GILLESSEN-KAESBACH, G., CHRISTIANSON, D.W., KAISER, F.J., JACKSON, L.G., HIROTA, T., KRANTZ, I.D. and SHIRAHIGE, K., 2012. HDAC8 mutations in Cornelia de Lange syndrome affect the cohesin acetylation cycle. *Nature,* **489**(7415), pp. 313-317.

DEGNER, S.C., WONG, T.P., JANKEVICIUS, G. and FEENEY, A.J., 2009. Cutting edge: developmental stage-specific recruitment of cohesin to CTCF sites throughout immunoglobulin loci during B lymphocyte development. *Journal of immunology (Baltimore, Md.: 1950),* **182**(1), pp. 44-48.

DENISON, C., RUDNER, A.D., GERBER, S.A., BAKALARSKI, C.E., MOAZED, D. and GYGI, S.P., 2005. A proteomic strategy for gaining insights into protein sumoylation in yeast. *Molecular & cellular proteomics : MCP,* **4**(3), pp. 246-254.

DIECKHOFF, P., BOLTE, M., SANCAK, Y., BRAUS, G.H. and IRNIGER, S., 2004. Smt3/SUMO and Ubc9 are required for efficient APC/C-mediated proteolysis in budding yeast. *Molecular microbiology,* **51**(5), pp. 1375-1387.

DONZE, D., ADAMS, C.R., RINE, J. and KAMAKAKA, R.T., 1999. The boundaries of the silenced HMR domain in Saccharomyces cerevisiae. *Genes & development,* **13**(6), pp. 698-708.

DOU, H., HUANG, C., VAN NGUYEN, T., LU, L.S. and YEH, E.T., 2011. SUMOylation and de-SUMOylation in response to DNA damage. *FEBS letters,* **585**(18), pp. 2891-2896.

DOYLE, J.M., GAO, J., WANG, J., YANG, M. and POTTS, P.R., 2010. MAGE-RING protein complexes comprise a family of E3 ubiquitin ligases. *Molecular cell,* **39**(6), pp. 963-974.

DUAN, X., SARANGI, P., LIU, X., RANGI, G.K., ZHAO, X. and YE, H., 2009. Structural and functional insights into the roles of the Mms21 subunit of the Smc5/6 complex. *Molecular cell,* **35**(5), pp. 657-668.

DUAN, X., YANG, Y., CHEN, Y.H., ARENZ, J., RANGI, G.K., ZHAO, X. and YE, H., 2009. Architecture of the Smc5/6 Complex of Saccharomyces cerevisiae

Reveals a Unique Interaction between the Nse5-6 Subcomplex and the Hinge Regions of Smc5 and Smc6. *The Journal of biological chemistry,* **284**(13), pp. 8507-8515.

DUMONT, J.N., 1972. Oogenesis in Xenopus laevis (Daudin). I. Stages of oocyte development in laboratory maintained animals. *Journal of Morphology,* **136**(2), pp. 153-179.

FREEMAN, L., ARAGON-ALCAIDE, L. and STRUNNIKOV, A., 2000. The condensin complex governs chromosome condensation and mitotic transmission of rDNA. *The Journal of cell biology,* **149**(4), pp. 811-824.

GOLDSTEIN, A.L. and MCCUSKER, J.H., 1999. Three new dominant drug resistance cassettes for gene disruption in Saccharomyces cerevisiae. *Yeast (Chichester, England),* **15**(14), pp. 1541-1553.

GOLDSTEIN, L.S., 1981. Kinetochore structure and its role in chromosome orientation during the first meiotic division in male D. melanogaster. *Cell,* **25**(3), pp. 591-602.

GRUBER, S., ARUMUGAM, P., KATOU, Y., KUGLITSCH, D., HELMHART, W., SHIRAHIGE, K. and NASMYTH, K., 2006. Evidence that loading of cohesin onto chromosomes involves opening of its SMC hinge. *Cell,* **127**(3), pp. 523-537.

GUACCI, V. and KOSHLAND, D., 2011. Cohesin-independent segregation of sister chromatids in budding yeast. *Molecular biology of the cell,* **23**(4); pp.729-39.

GUACCI, V., KOSHLAND, D. and STRUNNIKOV, A., 1997. A direct link between sister chromatid cohesion and chromosome condensation revealed through the analysis of MCD1 in S. cerevisiae. *Cell,* **91**(1), pp. 47-57.

GUILLOU, E., IBARRA, A., COULON, V., CASADO-VELA, J., RICO, D., CASAL, I., SCHWOB, E., LOSADA, A. and MENDEZ, J., 2010. Cohesin organizes chromatin loops at DNA replication factories. *Genes & development,* **24**(24), pp. 2812-2822.

GULLEROVA, M. and PROUDFOOT, N.J., 2008. Cohesin complex promotes transcriptional termination between convergent genes in S. pombe. *Cell,* **132**(6), pp. 983-995.

GUO, D., LI, M., ZHANG, Y., YANG, P., ECKENRODE, S., HOPKINS, D., ZHENG, W., PUROHIT, S., PODOLSKY, R.H., MUIR, A., WANG, J., DONG, Z., BRUSKO, T., ATKINSON, M., POZZILLI, P., ZEIDLER, A., RAFFEL, L.J., JACOB, C.O., PARK, Y., SERRANO-RIOS, M., LARRAD, M.T., ZHANG, Z., GARCHON, H.J., BACH, J.F., ROTTER, J.I., SHE, J.X. and WANG, C.Y., 2004. A functional variant of SUMO4, a new I kappa B alpha modifier, is associated with type 1 diabetes. *Nature genetics,* **36**(8), pp. 837-841.

HADJUR, S., WILLIAMS, L.M., RYAN, N.K., COBB, B.S., SEXTON, T., FRASER, P., FISHER, A.G. and MERKENSCHLAGER, M., 2009. Cohesins form chromosomal cis-interactions at the developmentally regulated IFNG locus. *Nature,* **460**(7253), pp. 410-413.

HAERING, C.H., FARCAS, A.M., ARUMUGAM, P., METSON, J. and NASMYTH, K., 2008. The cohesin ring concatenates sister DNA molecules. *Nature,* **454**(7202), pp. 297-301.

HAERING, C.H., LOWE, J., HOCHWAGEN, A. and NASMYTH, K., 2002. Molecular architecture of SMC proteins and the yeast cohesin complex. *Molecular cell,* **9**(4), pp. 773-788.

HAERING, C.H., SCHOFFNEGGER, D., NISHINO, T., HELMHART, W., NASMYTH, K. and LOWE, J., 2004. Structure and stability of cohesin's Smc1-kleisin interaction. *Molecular cell,* **15**(6), pp. 951-964.

HARDELAND, U., STEINACHER, R., JIRICNY, J. and SCHAR, P., 2002. Modification of the human thymine-DNA glycosylase by ubiquitin-like proteins facilitates enzymatic turnover. *The EMBO journal,* **21**(6), pp. 1456-1464.

HARTMAN, T., STEAD, K., KOSHLAND, D. and GUACCI, V., 2000. Pds5p is an essential chromosomal protein required for both sister chromatid cohesion and condensation in Saccharomyces cerevisiae. *The Journal of cell biology,* **151**(3), pp. 613-626.

HEIDINGER-PAULI, J.M., MERT, O., DAVENPORT, C., GUACCI, V. and KOSHLAND, D., 2010. Systematic reduction of cohesin differentially affects chromosome segregation, condensation, and DNA repair. *Current biology : CB,* **20**(10), pp. 957-963.

HEIDINGER-PAULI, J.M., UNAL, E., GUACCI, V. and KOSHLAND, D., 2008. The kleisin subunit of cohesin dictates damage-induced cohesion. *Molecular cell,* **31**(1), pp. 47-56.

HEIDINGER-PAULI, J.M., UNAL, E. and KOSHLAND, D., 2009. Distinct targets of the Eco1 acetyltransferase modulate cohesion in S phase and in response to DNA damage. *Molecular cell,* **34**(3), pp. 311-321.

HIETAKANGAS, V., ANCKAR, J., BLOMSTER, H.A., FUJIMOTO, M., PALVIMO, J.J., NAKAI, A. and SISTONEN, L., 2006. PDSM, a motif for phosphorylation-dependent SUMO modification. *Proceedings of the National Academy of Sciences of the United States of America,* **103**(1), pp. 45-50.

HIRANO, M. and HIRANO, T., 2004. Positive and negative regulation of SMC-DNA interactions by ATP and accessory proteins. *The EMBO journal,* **23**(13), pp. 2664-2673.

HIRANO, T., KOBAYASHI, R. and HIRANO, M., 1997. Condensins, chromosome condensation protein complexes containing XCAP-C, XCAP-E and a Xenopus homolog of the Drosophila Barren protein. *Cell,* **89**(4), pp. 511-521.

HOCHSTRASSER, M., 2001. SP-RING for SUMO: new functions bloom for a ubiquitin-like protein. *Cell,* **107**(1), pp. 5-8.

HOEGE, C., PFANDER, B., MOLDOVAN, G.L., PYROWOLAKIS, G. and JENTSCH, S., 2002. RAD6-dependent DNA repair is linked to modification of PCNA by ubiquitin and SUMO. *Nature,* **419**(6903), pp. 135-141.

HORSFIELD, J.A., PRINT, C.G. and MONNICH, M., 2012. Diverse developmental disorders from the one ring: distinct molecular pathways underlie the cohesinopathies. *Frontiers in genetics,* **3**, pp. 171.

HU, B., ITOH, T., MISHRA, A., KATOH, Y., CHAN, K.L., UPCHER, W., GODLEE, C., ROIG, M.B., SHIRAHIGE, K. and NASMYTH, K., 2011. ATP hydrolysis is required for relocating cohesin from sites occupied by its Scc2/4 loading complex. *Current biology : CB,* **21**(1), pp. 12-24.

HUANG, X., HATCHER, R., YORK, J.P. and ZHANG, P., 2005. Securin and separase phosphorylation act redundantly to maintain sister chromatid cohesion in mammalian cells. *Molecular biology of the cell,* **16**(10), pp. 4725-4732.

IRA, G., PELLICIOLI, A., BALIJJA, A., WANG, X., FIORANI, S., CAROTENUTO, W., LIBERI, G., BRESSAN, D., WAN, L., HOLLINGSWORTH, N.M., HABER, J.E. and FOIANI, M., 2004. DNA end resection, homologous recombination and DNA damage checkpoint activation require CDK1. *Nature,* **431**(7011), pp. 1011-1017.

IVANOV, D. and NASMYTH, K., 2005. A topological interaction between cohesin rings and a circular minichromosome. *Cell,* **122**(6), pp. 849-860.

IVANOV, D., SCHLEIFFER, A., EISENHABER, F., MECHTLER, K., HAERING, C.H. and NASMYTH, K., 2002. Eco1 is a novel acetyltransferase that can acetylate proteins involved in cohesion. *Current biology : CB,* **12**(4), pp. 323-328.

JANKE, C., MAGIERA, M.M., RATHFELDER, N., TAXIS, C., REBER, S., MAEKAWA, H., MORENO-BORCHART, A., DOENGES, G., SCHWOB, E., SCHIEBEL, E. and KNOP, M., 2004. A versatile toolbox for PCR-based tagging of yeast genes: new fluorescent proteins, more markers and promoter substitution cassettes. *Yeast (Chichester, England),* **21**(11), pp. 947-962.

JANKE, C., ORTIZ, J., TANAKA, T.U., LECHNER, J. and SCHIEBEL, E., 2002. Four new subunits of the Dam1-Duo1 complex reveal novel functions in sister kinetochore biorientation. *The EMBO journal,* **21**(1-2), pp. 181-193.

JAZAYERI, A., FALCK, J., LUKAS, C., BARTEK, J., SMITH, G.C., LUKAS, J. and JACKSON, S.P., 2006. ATM- and cell cycle-dependent regulation of ATR in response to DNA double-strand breaks. *Nature cell biology,* **8**(1), pp. 37-45.

JOHNSON, E.S., 2004. Protein modification by SUMO. *Annual Review of Biochemistry,* **73**, pp. 355-382.

JOHNSON, E.S. and BLOBEL, G., 1997. Ubc9p is the conjugating enzyme for the ubiquitin-like protein Smt3p. *The Journal of biological chemistry,* **272**(43), pp. 26799-26802.

JOHNSON, E.S. and GUPTA, A.A., 2001. An E3-like factor that promotes SUMO conjugation to the yeast septins. *Cell,* **106**(6), pp. 735-744.

JOHNSON, E.S., SCHWIENHORST, I., DOHMEN, R.J. and BLOBEL, G., 1997. The ubiquitin-like protein Smt3p is activated for conjugation to other proteins by an Aos1p/Uba2p heterodimer. *The EMBO journal,* **16**(18), pp. 5509-5519.

KAMITANI, T., NGUYEN, H.P. and YEH, E.T., 1997. Preferential modification of nuclear proteins by a novel ubiquitin-like molecule. *The Journal of biological chemistry,* **272**(22), pp. 14001-14004.

KEGEL, A., BETTS-LINDROOS, H., KANNO, T., JEPPSSON, K., STROM, L., KATOU, Y., ITOH, T., SHIRAHIGE, K. and SJOGREN, C., 2011. Chromosome length influences replication-induced topological stress. *Nature,* **471**(7338), pp. 392-396.

KRANTZ, I.D., MCCALLUM, J., DESCIPIO, C., KAUR, M., GILLIS, L.A., YAEGER, D., JUKOFSKY, L., WASSERMAN, N., BOTTANI, A., MORRIS, C.A., NOWACZYK, M.J., TORIELLO, H., BAMSHAD, M.J., CAREY, J.C., RAPPAPORT, E., KAWAUCHI, S., LANDER, A.D., CALOF, A.L., LI, H.H., DEVOTO, M. and JACKSON, L.G., 2004. Cornelia de Lange syndrome is caused by mutations in NIPBL, the human homolog of Drosophila melanogaster Nipped-B. *Nature genetics,* **36**(6), pp. 631-635.

KUENG, S., HEGEMANN, B., PETERS, B.H., LIPP, J.J., SCHLEIFFER, A., MECHTLER, K. and PETERS, J.M., 2006. Wapl controls the dynamic association of cohesin with chromatin. *Cell,* **127**(5), pp. 955-967.

KULEMZINA, I., SCHUMACHER, M.R., VERMA, V., REITER, J., METZLER, J., FAILLA, A.V., LANZ, C., SREEDHARAN, V.T., RATSCH, G. and IVANOV, D., 2012. Cohesin rings devoid of Scc3 and Pds5 maintain their stable association with the DNA. *PLoS genetics,* **8**(8), pp. e1002856.

KURZE, A., MICHIE, K.A., DIXON, S.E., MISHRA, A., ITOH, T., KHALID, S., STRMECKI, L., SHIRAHIGE, K., HAERING, C.H., LOWE, J. and NASMYTH, K., 2011. A positively charged channel within the Smc1/Smc3 hinge required for sister chromatid cohesion. *The EMBO journal,* **30**(2), pp. 364-378.

LEHMANN, A.R., 2005. The role of SMC proteins in the responses to DNA damage. *DNA repair,* **4**(3), pp. 309-314.

LEHOCZKY, P., MCHUGH, P.J. and CHOVANEC, M., 2007. DNA interstrand cross-link repair in Saccharomyces cerevisiae. *FEMS microbiology reviews,* **31**(2), pp. 109-133.

LENGRONNE, A., KATOU, Y., MORI, S., YOKOBAYASHI, S., KELLY, G.P., ITOH, T., WATANABE, Y., SHIRAHIGE, K. and UHLMANN, F., 2004. Cohesin relocation from sites of chromosomal loading to places of convergent transcription. *Nature,* **430**(6999), pp. 573-578.

LENGRONNE, A., MCINTYRE, J., KATOU, Y., KANOH, Y., HOPFNER, K.P., SHIRAHIGE, K. and UHLMANN, F., 2006. Establishment of sister chromatid cohesion at the S. cerevisiae replication fork. *Molecular cell,* **23**(6), pp. 787-799.

LI, S.J. and HOCHSTRASSER, M., 2003. The Ulp1 SUMO isopeptidase: distinct domains required for viability, nuclear envelope localization, and substrate specificity. *The Journal of cell biology,* **160**(7), pp. 1069-1081.

LI, S.J. and HOCHSTRASSER, M., 1999. A new protease required for cell-cycle progression in yeast. *Nature,* **398**(6724), pp. 246-251.

LIMA, C.D. and REVERTER, D., 2008. Structure of the human SENP7 catalytic domain and poly-SUMO deconjugation activities for SENP6 and SENP7. *The Journal of biological chemistry,* **283**(46), pp. 32045-32055.

LINDROOS, H.B., STROM, L., ITOH, T., KATOU, Y., SHIRAHIGE, K. and SJOGREN, C., 2006. Chromosomal association of the Smc5/6 complex reveals that it functions in differently regulated pathways. *Molecular cell,* **22**(6), pp. 755-767.

LIU, H., RANKIN, S. and YU, H., 2012. Phosphorylation-enabled binding of SGO1-PP2A to cohesin protects sororin and centromeric cohesion during mitosis. *Nature cell biology,* **15**(1), pp. 40-49.

LOPEZ-SERRA, L., LENGRONNE, A., BORGES, V., KELLY, G. and UHLMANN, F., 2013. Budding yeast wapl controls sister chromatid cohesion maintenance and chromosome condensation. *Current biology : CB,* **23**(1), pp. 64-69.

LOSADA, A., YOKOCHI, T. and HIRANO, T., 2005. Functional contribution of Pds5 to cohesin-mediated cohesion in human cells and Xenopus egg extracts. *Journal of Cell Science,* **15**(118(Pt 10)), pp. 2133-41.

LOSADA, A., YOKOCHI, T., KOBAYASHI, R. and HIRANO, T., 2000. Identification and characterization of SA/Scc3p subunits in the Xenopus and human cohesin complexes. *The Journal of cell biology,* **150**(3), pp. 405-416.

MAHAJAN, R., DELPHIN, C., GUAN, T., GERACE, L. and MELCHIOR, F., 1997. A small ubiquitin-related polypeptide involved in targeting RanGAP1 to nuclear pore complex protein RanBP2. *Cell,* **88**(1), pp. 97-107.

MANN, N.P., FITZSIMMONS, J., FITZSIMMONS, E. and COOKE, P., 1982. Roberts syndrome: clinical and cytogenetic aspects. *Journal of medical genetics,* **19**(2), pp. 116-119.

MATUNIS, M.J., COUTAVAS, E. and BLOBEL, G., 1996. A novel ubiquitin-like modification modulates the partitioning of the Ran-GTPase-activating protein RanGAP1 between the cytosol and the nuclear pore complex. *The Journal of cell biology,* **135**(6 Pt 1), pp. 1457-1470.

MC INTYRE, J., MULLER, E.G., WEITZER, S., SNYDSMAN, B.E., DAVIS, T.N. and UHLMANN, F., 2007. In vivo analysis of cohesin architecture using FRET in the budding yeast Saccharomyces cerevisiae. *The EMBO journal,* **26**(16), pp. 3783-3793.

MCALEENAN, A., CLEMENTE-BLANCO, A., CORDON-PRECIADO, V., SEN, N., ESTERAS, M., JARMUZ, A. and ARAGON, L., 2013. Post-replicative repair involves separase-dependent removal of the kleisin subunit of cohesin. *Nature,* **493**(7431), pp. 250-254.

MCALEENAN, A., CORDON-PRECIADO, V., CLEMENTE-BLANCO, A., LIU, I., SEN, N., LEONARD, J., JARMUZ, A. and ARAGÓN, L., 2012. SUMOylation of the α-Kleisin Subunit of Cohesin Is Required for DNA Damage-Induced Cohesion. *Current Biology,* **22**(17), pp. 1564-1575.

MCKAY, M.J., TROELSTRA, C., VAN DER SPEK, P., KANAAR, R., SMIT, B., HAGEMEIJER, A., BOOTSMA, D. and HOEIJMAKERS, J.H., 1996. Sequence

conservation of the rad21 Schizosaccharomyces pombe DNA double-strand break repair gene in human and mouse. *Genomics,* **36**(2), pp. 305-315.

MELBY, T.E., CIAMPAGLIO, C.N., BRISCOE, G. and ERICKSON, H.P., 1998. The symmetrical structure of structural maintenance of chromosomes (SMC) and MukB proteins: long, antiparallel coiled coils, folded at a flexible hinge. *The Journal of cell biology,* **142**(6), pp. 1595-1604.

MELCHIOR, F., 2000. SUMO--nonclassical ubiquitin. *Annual Review of Cell and Developmental Biology,* **16**, pp. 591-626.

MICHAELIS, C., CIOSK, R. and NASMYTH, K., 1997. Cohesins: Chromosomal Proteins that Prevent Premature Separation of Sister Chromatids. *Cell,* **91**(1), pp. 35 - 45.

MISHRA, A., HU, B., KURZE, A., BECKOUET, F., FARCAS, A.M., DIXON, S.E., KATOU, Y., KHALID, S., SHIRAHIGE, K. and NASMYTH, K., 2010. Both interaction surfaces within cohesin's hinge domain are essential for its stable chromosomal association. *Current biology : CB,* **20**(4), pp. 279-289.

MOLDOVAN, G.L., PFANDER, B. and JENTSCH, S., 2006. PCNA controls establishment of sister chromatid cohesion during S phase. *Molecular cell,* **23**(5), pp. 723-732.

MORGAN, D.O., 2007. *Cell cycle: Priciples of Control.* New Science Press.

MOSSESSOVA, E. and LIMA, C.D., 2000. Ulp1-SUMO crystal structure and genetic analysis reveal conserved interactions and a regulatory element essential for cell growth in yeast. *Molecular cell,* **5**(5), pp. 865-876.

MUKHOPADHYAY, D. and DASSO, M., 2007. Modification in reverse: the SUMO proteases. *Trends in biochemical sciences,* **32**(6), pp. 286-295.

NACERDDINE, K., LEHEMBRE, F., BHAUMIK, M., ARTUS, J., COHEN-TANNOUDJI, M., BABINET, C., PANDOLFI, P.P. and DEJEAN, A., 2005. The SUMO pathway is essential for nuclear integrity and chromosome segregation in mice. *Developmental cell,* **9**(6), pp. 769-779.

NASMYTH, K., 2011. Cohesin: a catenase with separate entry and exit gates? *Nature cell biology,* **13**(10), pp. 1170-1177.

NASMYTH, K. and HAERING, C.H., 2009. Cohesin: its roles and mechanisms. *Annual Review of Genetics,* **43**, pp. 525-558.

NASMYTH, K. and HAERING, C.H., 2005. The structure and function of SMC and kleisin complexes. *Annual Review of Biochemistry,* **74**, pp. 595-648.

NISHIMURA, K., FUKAGAWA, T., TAKISAWA, H., KAKIMOTO, T. and KANEMAKI, M., 2009. An auxin-based degron system for the rapid depletion of proteins in nonplant cells. *Nature methods,* **6**(12), pp. 917-922.

NISHIYAMA, T., LADURNER, R., SCHMITZ, J., KREIDL, E., SCHLEIFFER, A., BHASKARA, V., BANDO, M., SHIRAHIGE, K., HYMAN, A.A., MECHTLER, K. and PETERS, J.M., 2010. Sororin mediates sister chromatid cohesion by antagonizing Wapl. *Cell,* **143**(5), pp. 737-749.

NITISS, J.L., 2009. DNA topoisomerase II and its growing repertoire of biological functions. *Nature reviews.Cancer,* **9**(5), pp. 327-337.

ONO, T., LOSADA, A., HIRANO, M., MYERS, M.P., NEUWALD, A.F. and HIRANO, T., 2003. Differential contributions of condensin I and condensin II to mitotic chromosome architecture in vertebrate cells. *Cell,* **115**(1), pp. 109-121.

OWERBACH, D., MCKAY, E.M., YEH, E.T., GABBAY, K.H. and BOHREN, K.M., 2005. A proline-90 residue unique to SUMO-4 prevents maturation and sumoylation. *Biochemical and biophysical research communications,* **337**(2), pp. 517-520.

PALECEK, J., VIDOT, S., FENG, M., DOHERTY, A.J. and LEHMANN, A.R., 2006. The Smc5-Smc6 DNA repair complex. bridging of the Smc5-Smc6 heads by the KLEISIN, Nse4, and non-Kleisin subunits. *The Journal of biological chemistry,* **281**(48), pp. 36952-36959.

PALVIMO, J.J., 2007. PIAS proteins as regulators of small ubiquitin-related modifier (SUMO) modifications and transcription. *Biochemical Society transactions,* **35**(Pt 6), pp. 1405-1408.

PANIZZA, S., TANAKA, T., HOCHWAGEN, A., EISENHABER, F. and NASMYTH, K., 2000. Pds5 cooperates with cohesin in maintaining sister chromatid cohesion. *Current biology : CB,* **10**(24), pp. 1557-1564.

PANSE, V.G., HARDELAND, U., WERNER, T., KUSTER, B. and HURT, E., 2004. A proteome-wide approach identifies sumoylated substrate proteins in yeast. *The Journal of biological chemistry,* **279**(40), pp. 41346-41351.

PARKER, J.L. and ULRICH, H.D., 2012. A SUMO-interacting motif activates budding yeast ubiquitin ligase Rad18 towards SUMO-modified PCNA. *Nucleic acids research,* **40**(22), pp. 11380-11388.

PEBERNARD, S., MCDONALD, W.H., PAVLOVA, Y., YATES, J.R.,3rd and BODDY, M.N., 2004. Nse1, Nse2, and a novel subunit of the Smc5-Smc6 complex, Nse3, play a crucial role in meiosis. *Molecular biology of the cell,* **15**(11), pp. 4866-4876.

PEBERNARD, S., WOHLSCHLEGEL, J., MCDONALD, W.H., YATES, J.R.,3rd and BODDY, M.N., 2006. The Nse5-Nse6 dimer mediates DNA repair roles of the Smc5-Smc6 complex. *Molecular and cellular biology,* **26**(5), pp. 1617-1630.

PELCZAR, M.J., CHAN, E.C.S. and KRIEG, N.R., 1993. *Microbiology: Concepts and applications.* McGRAW-HILL, INC., pp. 283.

PETERS, J.M., 2006. The anaphase promoting complex/cyclosome: a machine designed to destroy. *Nature reviews.Molecular cell biology,* **7**(9), pp. 644-656.

PFANDER, B., MOLDOVAN, G.L., SACHER, M., HOEGE, C. and JENTSCH, S., 2005. SUMO-modified PCNA recruits Srs2 to prevent recombination during S phase. *Nature,* **436**(7049), pp. 428-433.

PIAZZA, I., HAERING, C.H. and RUTKOWSKA, A., 2013. Condensin: crafting the chromosome landscape. *Chromosoma,* **122**(3), pp 175-90.

POTTS, P.R., PORTEUS, M.H. and YU, H., 2006. Human SMC5/6 complex promotes sister chromatid homologous recombination by recruiting the SMC1/3 cohesin complex to double-strand breaks. *The EMBO journal,* **25**(14), pp. 3377-3388.

POTTS, P.R. and YU, H., 2005. Human MMS21/NSE2 is a SUMO ligase required for DNA repair. *Molecular and cellular biology,* **25**(16), pp. 7021-7032.

PSAKHYE, I. and JENTSCH, S., 2012. Protein group modification and synergy in the SUMO pathway as exemplified in DNA repair. *Cell,* **151**(4), pp. 807-820.

REMESEIRO, S. and LOSADA, A., 2012. Cohesin, a chromatin engagement ring. *Current opinion in cell biology,* **25(**1), pp. 63-71.

RENSHAW, M.J., WARD, J.J., KANEMAKI, M., NATSUME, K., NEDELEC, F.J. and TANAKA, T.U., 2010. Condensins promote chromosome recoiling during early anaphase to complete sister chromatid separation. *Developmental cell,* **19**(2), pp. 232-244.

ROLEF BEN-SHAHAR, T., HEEGER, S., LEHANE, C., EAST, P., FLYNN, H., SKEHEL, M. and UHLMANN, F., 2008. Eco1-dependent cohesin acetylation during establishment of sister chromatid cohesion. *Science (New York, N.Y.),* **321**(5888), pp. 563-566.

ROWLAND, B.D., ROIG, M.B., NISHINO, T., KURZE, A., ULUOCAK, P., MISHRA, A., BECKOUET, F., UNDERWOOD, P., METSON, J., IMRE, R., MECHTLER, K., KATIS, V.L. and NASMYTH, K., 2009. Building sister chromatid cohesion: smc3 acetylation counteracts an antiestablishment activity. *Molecular cell,* **33**(6), pp. 763-774.

SACHER, M., PFANDER, B., HOEGE, C. and JENTSCH, S., 2006. Control of Rad52 recombination activity by double-strand break-induced SUMO modification. *Nature cell biology,* **8**(11), pp. 1284-1290.

SACHER, M., PFANDER, B. and JENTSCH, S., 2005. Identification of SUMO-protein conjugates. *Methods in enzymology,* **399**, pp. 392-404.

SAITOH, H. and HINCHEY, J., 2000. Functional heterogeneity of small ubiquitin-related protein modifiers SUMO-1 versus SUMO-2/3. *The Journal of biological chemistry,* **275**(9), pp. 6252-6258.

SAPETSCHNIG, A., RISCHITOR, G., BRAUN, H., DOLL, A., SCHERGAUT, M., MELCHIOR, F. and SUSKE, G., 2002. Transcription factor Sp3 is silenced through SUMO modification by PIAS1. *The EMBO journal,* **21**(19), pp. 5206-5215.

SCHMIESING, J.A., BALL, A.R.,Jr, GREGSON, H.C., ALDERTON, J.M., ZHOU, S. and YOKOMORI, K., 1998. Identification of two distinct human SMC protein complexes involved in mitotic chromosome dynamics. *Proceedings of the National Academy of Sciences of the United States of America,* **95**(22), pp. 12906-12911.

SHEN, L., TATHAM, M.H., DONG, C., ZAGORSKA, A., NAISMITH, J.H. and HAY, R.T., 2006. SUMO protease SENP1 induces isomerization of the scissile peptide bond. *Nature structural & molecular biology,* **13**(12), pp. 1069-1077.

SHINTOMI, K. and HIRANO, T., 2010. Sister chromatid resolution: a cohesin releasing network and beyond. *Chromosoma,* **119**(5), pp. 459-467.

SIMPSON, D.P., 1977. ***Cassell's Latin Dictionary: Latin-English, English-Latin***. MACMILLAN, pp. 840.

SKIBBENS, R.V., CORSON, L.B., KOSHLAND, D. and HIETER, P., 1999. Ctf7p is essential for sister chromatid cohesion and links mitotic chromosome structure to the DNA replication machinery. *Genes & development,* **13**(3), pp. 307-319.

SLATER, M.L., 1973. Effect of reversible inhibition of deoxyribonucleic acid synthesis on the yeast cell cycle. *Journal of Bacteriology,* **113**(1), pp. 263-270.

SONG, J., DURRIN, L.K., WILKINSON, T.A., KRONTIRIS, T.G. and CHEN, Y., 2004. Identification of a SUMO-binding motif that recognizes SUMO-modified proteins.

Proceedings of the National Academy of Sciences of the United States of America, **101**(40), pp. 14373-14378.

SONODA, E., MATSUSAKA, T., MORRISON, C., VAGNARELLI, P., HOSHI, O., USHIKI, T., NOJIMA, K., FUKAGAWA, T., WAIZENEGGER, I.C., PETERS, J.M., EARNSHAW, W.C. and TAKEDA, S., 2001. Scc1/Rad21/Mcd1 is required for sister chromatid cohesion and kinetochore function in vertebrate cells. *Developmental cell,* **1**(6), pp. 759-770.

SRIKUMAR, T., LEWICKI, M.C., COSTANZO, M., TKACH, J.M., VAN BAKEL, H., TSUI, K., JOHNSON, E.S., BROWN, G.W., ANDREWS, B.J., BOONE, C., GIAEVER, G., NISLOW, C. and RAUGHT, B., 2013. Global analysis of SUMO chain function reveals multiple roles in chromatin regulation. *The Journal of cell biology,* **201**(1), pp. 145-163.

STANKOVIC-VALENTIN, N., DELTOUR, S., SEELER, J., PINTE, S., VERGOTEN, G., GUERARDEL, C., DEJEAN, A. and LEPRINCE, D., 2007. An acetylation/deacetylation-SUMOylation switch through a phylogenetically conserved psiKXEP motif in the tumor suppressor HIC1 regulates transcriptional repression activity. *Molecular and cellular biology,* **27**(7), pp. 2661-2675.

STEAD, K., AGUILAR, C., HARTMAN, T., DREXEL, M., MELUH, P. and GUACCI, V., 2003. Pds5p regulates the maintenance of sister chromatid cohesion and is sumoylated to promote the dissolution of cohesion. *The Journal of cell biology,* **163**(4), pp. 729-741.

STEPHAN, A.K., KLISZCZAK, M., DODSON, H., COOLEY, C. and MORRISON, C.G., 2011. Roles of vertebrate Smc5 in sister chromatid cohesion and homologous recombinational repair. *Molecular and cellular biology,* **31**(7), pp. 1369-1381.

STERN, B.M. and MURRAY, A.W., 2001. Lack of tension at kinetochores activates the spindle checkpoint in budding yeast. *Current biology : CB,* **11**(18), pp. 1462-1467.

STROM, L., KARLSSON, C., LINDROOS, H.B., WEDAHL, S., KATOU, Y., SHIRAHIGE, K. and SJOGREN, C., 2007. Postreplicative formation of cohesion is required for repair and induced by a single DNA break. *Science (New York, N.Y.),* **317**(5835), pp. 242-245.

SUN, T.T. and GREEN, H., 1976. Differentiation of the epidermal keratinocyte in cell culture: formation of the cornified envelope. *Cell,* **9**(4 Pt 1), pp. 511-521.

SUTANI, T., KAWAGUCHI, T., KANNO, R., ITOH, T. and SHIRAHIGE, K., 2009. Budding yeast Wpl1(Rad61)-Pds5 complex counteracts sister chromatid cohesion-establishing reaction. *Current biology : CB,* **19**(6), pp. 492-497.

TAKAHASHI, Y., DULEV, S., LIU, X., HILLER, N.J., ZHAO, X. and STRUNNIKOV, A., 2008. Cooperation of sumoylated chromosomal proteins in rDNA maintenance. *PLoS genetics,* **4**(10), pp. e1000215.

TAKAHASHI, Y., KAHYO, T., TOH-E, A., YASUDA, H. and KIKUCHI, Y., 2001. Yeast Ull1/Siz1 is a novel SUMO1/Smt3 ligase for septin components and functions as an adaptor between conjugating enzyme and substrates. *The Journal of biological chemistry,* **276**(52), pp. 48973-48977.

TANAKA, K., NISHIDE, J., OKAZAKI, K., KATO, H., NIWA, O., NAKAGAWA, T., MATSUDA, H., KAWAMUKAI, M. and MURAKAMI, Y., 1999. Characterization of a fission yeast SUMO-1 homologue, pmt3p, required for multiple nuclear events, including the control of telomere length and chromosome segregation. *Molecular and cellular biology,* **19**(12), pp. 8660-8672.

TATHAM, M.H., JAFFRAY, E., VAUGHAN, O.A., DESTERRO, J.M., BOTTING, C.H., NAISMITH, J.H. and HAY, R.T., 2001. Polymeric chains of SUMO-2 and SUMO-3 are conjugated to protein substrates by SAE1/SAE2 and Ubc9. *The Journal of biological chemistry,* **276**(38), pp. 35368-35374.

TITTEL-ELMER, M., LENGRONNE, A., DAVIDSON, M.B., BACAL, J., FRANCOIS, P., HOHL, M., PETRINI, J.H., PASERO, P. and COBB, J.A., 2012. Cohesin association to replication sites depends on rad50 and promotes fork restart. *Molecular cell,* **48**(1), pp. 98-108.

TORRES-ROSELL, J., MACHIN, F., FARMER, S., JARMUZ, A., EYDMANN, T., DALGAARD, J.Z. and ARAGON, L., 2005. SMC5 and SMC6 genes are required for the segregation of repetitive chromosome regions. *Nature cell biology,* **7**(4), pp. 412-419.

TORRES-ROSELL, J., SUNJEVARIC, I., DE PICCOLI, G., SACHER, M., ECKERT-BOULET, N., REID, R., JENTSCH, S., ROTHSTEIN, R., ARAGON, L. and LISBY, M., 2007. The Smc5-Smc6 complex and SUMO modification of Rad52 regulates recombinational repair at the ribosomal gene locus. *Nature cell biology,* **9**(8), pp. 923-931.

TOTH, A., CIOSK, R., UHLMANN, F., GALOVA, M., SCHLEIFFER, A. and NASMYTH, K., 1999. Yeast cohesin complex requires a conserved protein, Eco1p(Ctf7), to establish cohesion between sister chromatids during DNA replication. *Genes & development,* **13**(3), pp. 320-333.

UNAL, E., ARBEL-EDEN, A., SATTLER, U., SHROFF, R., LICHTEN, M., HABER, J.E. and KOSHLAND, D., 2004. DNA damage response pathway uses histone

modification to assemble a double-strand break-specific cohesin domain. *Molecular cell,* **16**(6), pp. 991-1002.

UNAL, E., HEIDINGER-PAULI, J.M. and KOSHLAND, D., 2007. DNA double-strand breaks trigger genome-wide sister-chromatid cohesion through Eco1 (Ctf7). *Science (New York, N.Y.),* **317**(5835), pp. 245-248.

WAN, J., SUBRAMONIAN, D. and ZHANG, X., 2012. SUMOylation in Control of Accurate Chromosome Segregation during Mitosis. *Current Protein & Peptide Science,* **13**(5), pp. 467 <last_page> 481.

WANG, S.W., READ, R.L. and NORBURY, C.J., 2002. Fission yeast Pds5 is required for accurate chromosome segregation and for survival after DNA damage or metaphase arrest. *Journal of cell science,* **115**(Pt 3), pp. 587-598.

WATRIN, E., SCHLEIFFER, A., TANAKA, K., EISENHABER, F., NASMYTH, K. and PETERS, J.M., 2006. Human Scc4 is required for cohesin binding to chromatin, sister-chromatid cohesion, and mitotic progression. *Current biology : CB,* **16**(9), pp. 863-874.

WHELAN, G., KREIDL, E., PETERS, J.M. and EICHELE, G., 2012. The non-redundant function of cohesin acetyltransferase Esco2: some answers and new questions. *Nucleus (Austin, Tex.),* **3**(4), pp. 330-334.

WOHLSCHLEGEL, J.A., JOHNSON, E.S., REED, S.I. and YATES, J.R.,3rd, 2004. Global analysis of protein sumoylation in Saccharomyces cerevisiae. *The Journal of biological chemistry,* **279**(44), pp. 45662-45668.

WU, L. and HICKSON, I.D., 2003. The Bloom's syndrome helicase suppresses crossing over during homologous recombination. *Nature,* **426**(6968), pp. 870-874.

WU, N., KONG, X., JI, Z., ZENG, W., POTTS, P.R., YOKOMORI, K. and YU, H., 2012. Scc1 sumoylation by Mms21 promotes sister chromatid recombination through counteracting Wapl. *Genes & development,* **26**(13), pp. 1473-1485.

WYATT, M.D. and PITTMAN, D.L., 2006. Methylating agents and DNA repair responses: Methylated bases and sources of strand breaks. *Chemical research in toxicology,* **19**(12), pp. 1580-1594.

XU, H., TOMASZEWSKI, J.M. and MCKAY, M.J., 2011. Can corruption of chromosome cohesion create a conduit to cancer? *Nature reviews.Cancer,* **11**(3), pp. 199-210.

ZHANG, N., KUZNETSOV, S.G., SHARAN, S.K., LI, K., RAO, P.H. and PATI, D., 2008. A handcuff model for the cohesin complex. *The Journal of cell biology,* **183**(6), pp. 1019-1031.

ZHANG, N. and PATI, D., 2009. Handcuff for sisters: a new model for sister chromatid cohesion. *Cell cycle (Georgetown, Tex.),* **8**(3), pp. 399-402.

ZHAO, X. and BLOBEL, G., 2005. A SUMO ligase is part of a nuclear multiprotein complex that affects DNA repair and chromosomal organization. *Proceedings of the National Academy of Sciences of the United States of America,* **102**(13), pp. 4777-4782.

ZHAO, Y., KWON, S.W., ANSELMO, A., KAUR, K. and WHITE, M.A., 2004. Broad spectrum identification of cellular small ubiquitin-related modifier (SUMO) substrate proteins. *The Journal of biological chemistry,* **279**(20), pp. 20999-21002.

ZHENG, G. and YANG, Y.C., 2004. ZNF76, a novel transcriptional repressor targeting TATA-binding protein, is modulated by sumoylation. *The Journal of biological chemistry,* **279**(41), pp. 42410-42421.

"All the highs, all the lows, as the room is spinning goes..We'll run riot.. We'll be glowing in the dark"

Charlie Brown, Coldplay

Supplementary Article